

Doctor Thesis

**Top quark pair production near the  
threshold in  $e^+e^-$  collisions**

Takaaki NAGANO

*Department of Physics, Tohoku University, Sendai 980-8578, Japan*

## Abstract

The mass  $m_t$  of the top quark  $t$  is now measured to be  $174 \pm 5$  GeV. Improvement of the present error  $\Delta m_t = 5$  GeV is important not only for its own sake. For example with  $\Delta m_t \sim 0.2$  GeV, the Higgs mass  $m_H$  is predicted from electroweak precision measurements with an error of  $\Delta m_H/m_H \sim 20\%$ , which is now  $\sim 60\%$ . There is a consensus that  $m_t$  is best measured at future  $e^+e^-$  Linear Colliders (LC) by using the line shape of the total cross section  $\sigma_{\text{tot}}(\sqrt{s} \sim 2m_t; e^+e^- \rightarrow t\bar{t})$  near the  $t\bar{t}$  threshold. However, it was reported recently that the Next-to-Next-to-Leading-Order (NNLO) correction to  $\sigma_{\text{tot}}$  is as large as the NLO correction to it. This implies that the convergence of the series is not good, and this theoretical uncertainty affects the precision of the determination of  $m_t$  at LC. In the thesis, we improve the convergence of the perturbative series of  $\sigma_{\text{tot}}$  by choosing appropriate expansion parameters for both  $m_t$  and the strong gauge coupling  $\alpha_s$ . As for the mass parameter, the pole mass was used in the previous studies. However, because of the infrared (IR) structure of QCD, the pole mass of a quark is defined only with an ambiguity of  $\mathcal{O}(\Lambda_{\text{QCD}}) \sim 1$  GeV. Instead, we use another mass parameter called potential-subtracted mass, which is less affected by the IR region of QCD. As for the gauge coupling, we resum a certain class of higher order corrections by using renormalization group. With these two prescriptions, the perturbative convergence of  $\sigma_{\text{tot}}$  is much improved. Correspondingly, the resulting ambiguity for the determination of  $m_t$  is estimated to be  $\sim 0.1$  GeV, which is not larger than the expected statistical error at future LC. We also study the top-quark momentum distribution  $d\sigma/dp_t$ . The NNLO correction for the line-shape of  $d\sigma/dp_t$  turns out to be fairly small compared to that for  $\sigma_{\text{tot}}$ .

Aside from the contribution of Standard Model (SM), we also study that of new physics. Since Cabibbo-Kobayashi-Maskawa matrix elements for the top quark are almost diagonal ( $|V_{tb}| \simeq 1$ ), CP-violating effect in top-quark sector is highly suppressed in SM. In the thesis, we study the effect of all types of anomalous CP violating top-quark Electric Dipole Moment (EDM) interactions near the threshold for the first time. If they are measured to be non-zero, it would immediately imply new physics. We show that one can disentangle  $t\bar{t}g$ -,  $t\bar{t}\gamma$ - and  $t\bar{t}Z$ -EDMs by the dependence of CP-odd observables on the CM-energy and on the degree of initial state polarization. The sensitivity to chromo-EDM at LC turns out to be better than that at LC in the open top region ( $\sqrt{s} \gg 2m_t$ ), but to be worse than that at LHC by a factor  $\mathcal{O}(1/10)$ . The sensitivities to electroweak-EDMs near the threshold are similar to those in the open top region at LC.

# Contents

<b>1</b>	<b>Introduction</b>	<b>1</b>
1.1	Top quark . . . . .	1
1.1.1	Top quark pair production in $e^+e^-$ collisions near threshold . . . . .	2
1.2	Overview of $t\bar{t}$ production cross section . . . . .	2
1.2.1	LO and NLO calculations of $\sigma_{\text{tot}}$ and $d\sigma/dp$ . . . . .	3
1.2.2	NNLO calculations of $\sigma_{\text{tot}}$ . . . . .	4
1.2.3	Theoretical progress related to $\sigma_{\text{tot}}$ . . . . .	4
1.2.4	Our contributions . . . . .	5
1.3	Overview of top-quark anomalous EDMs . . . . .	6
1.3.1	Previous studies . . . . .	6
1.3.2	Our contributions . . . . .	6
1.4	Organization of the thesis . . . . .	7
<b>2</b>	<b>Total Production Cross Section</b>	<b>9</b>
2.1	Overview . . . . .	9
2.2	Non-relativistic description of $t\bar{t}$ system . . . . .	10
2.2.1	Optical Theorem . . . . .	10
2.2.2	Order counting . . . . .	12
2.2.3	Complications at $\mathcal{O}(1/c^2)$ . . . . .	13
2.2.4	Non-relativistic NNLO Hamiltonian $H$ . . . . .	15
2.2.5	Soft corrections and hard corrections . . . . .	16
2.3	Non-relativistic $t\bar{t}$ potential $V$ to NNLO . . . . .	16
2.3.1	Normalization of wave functions . . . . .	16
2.3.2	Breit-Fermi potential $V_{\text{BF}}$ . . . . .	17
2.3.3	Non-Abelian effect $V_{\text{NA}}$ . . . . .	19
2.3.4	Radiative corrections $V_1$ for Coulomb potential . . . . .	20
2.4	Reduced Green function $G'$ . . . . .	22
2.4.1	$G$ in terms of $G'$ . . . . .	22
2.4.2	Green function for Coulomb plus $1/r^2$ potentials . . . . .	26
2.4.3	Explicit expression for $G'$ . . . . .	28
2.5	Matching of NRQCD with QCD . . . . .	29
2.6	Previously obtained results for $R$ ratio . . . . .	31
2.6.1	Analytic results . . . . .	31
2.6.2	Numerical results . . . . .	32
2.7	Renormalon ambiguity and PS mass . . . . .	36
2.7.1	Perturbative convergence . . . . .	36
2.7.2	IR gluon contributions to self-energy $\Sigma$ and potential $V(r)$ . . . . .	36

2.7.3	Borel sum and IR renormalon pole . . . . .	38
2.7.4	Potential-Subtracted mass $m_{\text{PS}}(\mu_f)$ . . . . .	40
2.7.5	Results for $R$ ratio with $m_{\text{PS}}(\mu_f)$ . . . . .	41
2.8	Results for $R$ ratio with RG improved $V_{\text{C}}$ and $m_{\text{PS}}$ . . . . .	42
2.8.1	Theoretical uncertainties for NNLO calculation of $R$ ratio . . . . .	44
<b>3</b>	<b>Top-Quark Momentum Distribution</b> . . . . .	<b>53</b>
3.1	Derivation of the distribution . . . . .	53
3.2	Unitarity relation . . . . .	55
3.3	Results for $d\sigma/dp$ . . . . .	58
<b>4</b>	<b>Anomalous Electric Dipole Moments of Top Quark</b> . . . . .	<b>61</b>
4.1	Electric Dipole Moment (EDM) . . . . .	61
4.2	Predictions of EDMs in various models . . . . .	64
4.3	CP violating observables . . . . .	65
4.3.1	P, C and $\tilde{T}$ for $ \mathcal{M} ^2$ . . . . .	66
4.3.2	Expectation values . . . . .	67
4.3.3	Several CP violating observables . . . . .	68
4.4	Studies of EDMs at open top region . . . . .	69
4.4.1	Present bounds for EDMs . . . . .	69
4.4.2	Expected future bounds on EDMs (Open top region) . . . . .	70
4.5	Polarizations . . . . .	73
4.5.1	Polarizations of $e^+e^-$ . . . . .	73
4.5.2	Polarizations of $t\bar{t}$ . . . . .	75
4.5.3	Spin direction of top quark . . . . .	76
4.6	Corrections due to Coulomb rescattering . . . . .	77
4.6.1	Relevant Lagrangian . . . . .	77
4.6.2	Corrections to vertices . . . . .	78
4.6.3	Sketch of the calculation . . . . .	79
4.6.4	Polarization vector of top and antitop . . . . .	81
4.7	Results for EDMs . . . . .	86
4.7.1	Sensitivity . . . . .	87
<b>5</b>	<b>Summary and Discussions</b> . . . . .	<b>97</b>
<b>A</b>	<b></b> . . . . .	<b>99</b>
A.1	Notes on group theory . . . . .	99
A.1.1	Group theoretic factors . . . . .	99
A.1.2	Color charge summation for color-singlet state . . . . .	99
A.2	Notes on non-relativistic quantum mechanics . . . . .	100
A.2.1	Relative coordinate . . . . .	100
A.2.2	Radial momentum $p_r$ . . . . .	100
A.2.3	Operators in momentum and coordinate space . . . . .	102
A.2.4	$S$ -wave projection . . . . .	103
A.3	Formulas for Dirac spinors . . . . .	105
A.3.1	Mode expansions . . . . .	105
A.3.2	Several conjugations: $\Gamma^\dagger$ , $\bar{\Gamma}$ , $\Gamma^c$ and $\Gamma^b$ . . . . .	105
A.3.3	Antiparticle field $\psi^c$ . . . . .	106

A.3.4	Dirac representation . . . . .	107
A.3.5	Pauli spin spinors $\chi^{\pm s}$ and helicity $h$ . . . . .	109
A.3.6	Lorentz transformation for $\gamma$ -matrices . . . . .	110
A.3.7	Projection operators for energy $\Lambda_{\pm}(p)$ and spin $\Sigma(s)$ . . . . .	111
A.4	Gordon identities . . . . .	112
A.5	Merging the effects of $\gamma$ and $Z$ exchange . . . . .	114
A.6	Propagators . . . . .	115
A.6.1	Fermion propagator . . . . .	115
A.6.2	Gluon propagator . . . . .	115
A.7	Parity, Charge Conjugation and Time Reversal . . . . .	116
A.7.1	$\mathcal{P}$ , $\mathcal{C}$ and $\mathcal{T}$ for field operators . . . . .	116
A.7.2	$\mathcal{CPT}$ symmetry . . . . .	119
A.7.3	$\mathcal{P}$ , $\mathcal{C}$ and $\mathcal{T}$ for currents . . . . .	119
A.7.4	$P$ , $C$ and $T$ for amplitudes or currents . . . . .	119
A.7.5	Absorptive parts and $\mathcal{CPT}$ . . . . .	123
A.7.6	$\mathcal{CP}$ violation . . . . .	125
<b>B</b>		<b>129</b>
B.1	Top quark decay width $\Gamma_t$ . . . . .	129
B.2	Coulomb plus $1/r^2$ potential: explicit calculation . . . . .	129
B.3	Results for Coulomb potential . . . . .	133
B.4	Expressions needed for matching . . . . .	134
B.4.1	NRQCD calculation of $R$ ratio . . . . .	135
B.4.2	Perturbative QCD calculation of $R$ ratio . . . . .	137
B.5	Top quark polarization . . . . .	138



# Chapter 1

## Introduction

### 1.1 Top quark

As more experimental data is accumulated, it has become clearer that the Standard Model (SM) describes the physics around and below the ElectroWeak (EW) scale very well. One of the great triumphs of the SM is that the top quark  $t$  is discovered at Tevatron [1] within the range predicted from EW precision measurements. Currently [2]

$$\begin{array}{ll} m_t = 174.3 \pm 5.1 \text{ GeV} & \text{from direct measurement,} \\ m_t = 170 \pm 7(+14) \text{ GeV} & \text{from indirect SM EW fit.} \end{array}$$

For the indirect fit, the central value and the first uncertainty are for  $m_H = m_Z$ , and the second is the shift from changing  $m_H$  to 300 GeV. Here  $m_H$  is the Higgs mass.

Despite of its success, few people consider the SM as the ultimate theory because of its “un-naturalness”. There are several issues and possible solutions to them. First, the gauge symmetry of SM is a direct product of three distinct groups, and gauge anomaly cancellation is highly non-trivial. These “un-natural” aspects are explained if physics at higher energies is governed by a Grand Unified Theory (GUT). In fact, the three gauge couplings unify around  $10^{16}$  GeV in the minimal supersymmetric SM, if the soft SUSY breaking scale is around 1 TeV. Weak-scale Super Symmetry (SUSY) itself is motivated to stabilize the EW scale against radiative corrections, which is also an “un-natural” aspect of the SM.

Another one is flavor repetition, which seems redundant, and its breaking by masses and mixings. In this respect, top quark is highly exceptional, since the mass of the next heaviest fermion  $b$  is  $m_b = 4.1\text{--}4.4$  GeV [2], which is 40 times smaller than  $m_t$ . Thus one can expect that top quark may play an important role for the physics around TeV scale, especially for flavor and Higgs physics. In fact, among the ingredients of the SM, the mechanism that breaks the electroweak symmetry is the only one that is not verified experimentally. The situation is similar also for top quark. Except its mass  $m_t$ , almost no property of the top quark is known experimentally. Thus there are still possibilities of its “anomalous” property. For example, it might not be merely a “heavy quark”, which means that the generation is not repeating in fact; it might be a composite of subquarks, or it might condensate to trigger EW symmetry breaking [5], which means that there is a certain strong attractive force between  $t\bar{t}$ . Or there might be a substantial mixing with a “fourth generation quark”, which can be vector-like. On the other hand, even if top quark itself were merely a “heavy quark”, it is expected to be sensitive to the mechanism of  $SU(2)_L \times U(1)_Y$  breaking, because of its large mass and the large mass difference between  $t$  and  $b$  quarks.

Some properties of top quark will be measured at LHC, which operates before  $e^+e^-$  linear colliders does. With its high CM energy and high luminosity, it is expected that certain clue to new physics will be discovered at LHC. However precise measurement at hadron colliders may not be possible, since the CM energy of each elementary process is not fixed. Thus it is lepton colliders that can measure the properties of top quark etc. precisely, after the discovery at Tevatron, or hadron colliders in general.

### 1.1.1 Top quark pair production in $e^+e^-$ collisions near threshold

Studies on top quark at  $e^+e^-$  colliders can be classified into two groups depending on the CM energy  $\sqrt{s}$ ; one is at the threshold region ( $\sqrt{s} \sim 2m_t$ ), and the other is at the open top region ( $\sqrt{s} \gg 2m_t$ ). One prominent feature of the threshold region, which makes the distinction above, is multiple gluon rescattering between  $t$  and  $\bar{t}$ , which is effectively not suppressed by powers of  $\alpha_s$ . In fact, top quark is an ideal probe of the short distance behavior of QCD. This is because of its large mass  $m_t$  and its large decay width  $\Gamma_t$ , which are related [6,7]<sup>1</sup> as follows:

$$\Gamma_t = \frac{G_F m_t^3}{8\pi\sqrt{2}} \simeq 1.5 \text{ GeV} .$$

This expression holds at tree level in the limit  $m_W/m_t \rightarrow 0$ , and is for the SM, where almost every  $t$  decays into  $bW^+$ . Here  $|V_{tb}| \simeq 1$  is used, which is indeed the case when the unitarity of  $V_{\text{CKM}}$  among the first three generations is assumed. When the distance between  $t$  and  $\bar{t}$  is shorter than the typical non-perturbative scale  $\sim 1/\Lambda_{\text{QCD}} \sim 1/(1 \text{ GeV})$ , gluon exchanges between them can be approximated by the Coulomb potential<sup>2</sup>  $V = -C_F\alpha_s/r$ , where  $C_F = 4/3$  is the quadratic Casimir for the fundamental representation of SU(3). Due to the large mass, the Bohr radius<sup>3</sup>  $r_B$  of the  $t\bar{t}$  pair is much smaller than the typical non-perturbative scale:  $r_B = 1/(C_F\alpha_s m_t/2) \simeq 1/(20 \text{ GeV}) \ll 1/\Lambda_{\text{QCD}}$ . This means that the QCD potential between  $t$  and  $\bar{t}$  is surely well within the perturbative region. And due to the large decay width, a  $t\bar{t}$  pair decays before it hadronizes [6]; that is, the fluctuation of top quark momentum<sup>4</sup>  $\sqrt{m_t\Gamma_t} \simeq 15 \text{ GeV} \gg \Lambda_{\text{QCD}}$  due to the off-shell effect acts as an IR cut-off. Thus a  $t\bar{t}$  pair produced in  $e^+e^-$  collisions can be treated perturbatively from the production to the decay, even near the threshold, where the QCD effect is enhanced. Thus the threshold region is one of the best places for the study of perturbative QCD.

There are many studies on  $t\bar{t}$  pair production near the threshold in  $e^+e^-$  collisions [3,9–32], including ours. Some of them are reviewed briefly in the next two sections, and in the former halves of Chapters 2 and 4 at some length. Concisely speaking, we (i) reduce the theoretical uncertainty for the determination of the top-quark mass using the process  $e^+e^- \rightarrow t\bar{t}$  near the threshold, and (ii) study the sensitivity of  $e^+e^-$  colliders with  $\sqrt{s} \simeq 2m_t$  to all the anomalous Electric Dipole Moments in  $t\bar{t}$ -gauge boson interactions for the first time.

## 1.2 Overview of $t\bar{t}$ production cross section

<sup>1</sup> More detailed expression is shown in Section B.1.

<sup>2</sup> This expression is for a color-singlet  $q\bar{q}$ . For a color-octet state, it is  $V = (C_A/2 - C_F)\alpha_s/r$ , where  $C_A = 3$ .

<sup>3</sup> It is defined in Section B.3. See also Figure 2.4.

<sup>4</sup> The peak momentum of the top quark is  $\sim |\sqrt{m_t(\sqrt{s} - 2m_t + 1 \text{ GeV} + i\Gamma_t)}|$ . See Figure 4.9. The fluctuation given here is for near the threshold.



### 1.2.1 LO and NLO calculations of $\sigma_{\text{tot}}$ and $d\sigma/dp$

In  $e^+e^-$  collisions with  $\sqrt{s} \simeq 2m_q$  where  $q = c, b$ , there are sharp resonances in the total production cross section  $\sigma_{\text{tot}}(s)$  due to the  $q\bar{q}$  bound states such as  $J/\Psi$  or  $\Upsilon$ . The locations of those bound state poles are used to probe the QCD potential at  $r \sim 1/(\alpha_s m_q)$ , which is near the boundary of the perturbative description of QCD [8]. On the other hand, due to the large decay width of top quark  $\Gamma_t$ , (would-be)  $t\bar{t}$  bound-states merge into a single slight rise of  $\sigma_{\text{tot}}(s)$  near the  $1S$  resonance. Thus in order to calculate  $\sigma_{\text{tot}}(s)$  just below the threshold ( $\sqrt{s} \lesssim 2m_t$ ) reliably<sup>5</sup>, one needs to sum over a host of resonances. This summation is conveniently done using the Green function for a  $t\bar{t}$  pair [9]:

$$G(\mathbf{r}, \mathbf{r}') \equiv \left\langle \mathbf{r} \left| \frac{1}{H - (E + i\Gamma_t)} \right| \mathbf{r}' \right\rangle \\ = \sum_n \frac{\psi_n(\mathbf{r}) \psi_n^*(\mathbf{r}')}{E_n - (E + i\Gamma_t)} + \int \frac{d^3k}{(2\pi)^3} \frac{\psi_{\vec{k}}(\mathbf{r}) \psi_{\vec{k}}^*(\mathbf{r}')}{E_{\vec{k}} - (E + i\Gamma_t)},$$

where  $H$  is the Non-Relativistic (NR) Hamiltonian for  $t\bar{t}$ ,  $E \equiv \sqrt{s} - 2m_t$  is the NR energy, and  $\psi_n$  and  $\psi_{\vec{k}}$  are energy eigenfunctions for  $E_n (< 0)$  and  $E_{\vec{k}} \equiv \vec{k}^2/m_t (> 0)$ , respectively. Since top quarks are non-relativistic near the threshold, it is convenient to use a non-relativistic approximation at the leading order. There is another advantage for the NR Green-function treatment. Near the threshold, it is known that the naive perturbative expansion in  $\alpha_s$  breaks down (“threshold singularity”). In fact,  $n$ -th power of  $\alpha_s$  is accompanied by  $1/\beta_t^m$  ( $m \leq n$ ), where  $\beta_t$  is the velocity of  $t$  and  $\bar{t}$  at their CM frame. The situation is similar to certain perturbation series where powers of  $\alpha_s$  are accompanied by powers of  $\log(q/\mu)$ ; a stable perturbative expansion is obtained by summing up (potentially large) leading log’s. In other words, one should identify  $\sum_n (\alpha_s(\mu) \ln(q/\mu))^n$  to be the leading order. Likewise, one should identify  $\sum_n (\alpha_s/\beta_t)^n$  to be the leading order near the threshold. On the other hand, this summation is realized<sup>6</sup> automatically in the Green function for Coulomb potential between  $t$  and  $\bar{t}$ . Thus the Green function method provides an efficient way (i) to sum up infinite number of broad resonances, and (ii) to sum up powers of  $\alpha_s/\beta_t$ . After these summations, the cross section is finite<sup>7</sup> even at the threshold, which corresponds<sup>8</sup> to  $\beta_t = 0$ . Order counting becomes easier by noting  $\alpha_s = g_s^2/(4\pi\hbar c) = \mathcal{O}(1/c)$  and  $\beta_t = v_t/c = \mathcal{O}(1/c)$ , which means  $\alpha_s/\beta_t = \mathcal{O}(1)$ . This is the Leading Order (LO). Likewise the Next-to-Leading Order (NLO) is  $\mathcal{O}(1/c)$ , and so on.

The total cross section at the leading order was calculated in [11] with the QCD potential  $V(r)$  that is Renormalization Group (RG) improved in the coordinate space. It triggered several studies both by experimentalists and by theorists [13–15]. A part of NLO corrections was taken into account in their analysis. After a while, complete NLO corrections to  $t\bar{t}$  production and their decay cross section were calculated [16, 17]. They included the Final-State Interactions (FSIs), by which we mean gluon exchange between  $t$  and  $\bar{b}$ ,  $\bar{t}$  and  $b$ , and  $b$  and  $\bar{b}$ . It was also

<sup>5</sup> The production cross section grows rapidly near the threshold, because the leading contribution is  $S$ -wave. The mass of top quark is determined by measuring this rise of  $\sigma_{\text{tot}}$ . Thus the precise calculation of  $\sigma_{\text{tot}}$  near the threshold is required for this reason. Note also that the “binding energy” for the  $1S$  state is  $\sim p_B^2/m_t \sim 2 \text{ GeV}$ , where  $p_B = 1/r_B$  is Bohr momentum. See Section B.3.

<sup>6</sup> The explicit expression is given in Eq. (2.46). Note that  $\sqrt{E/m_t} = \beta_t + \mathcal{O}(\beta_t^3)$ .

<sup>7</sup> See Figure 2.6.

<sup>8</sup> Due to finite decay width  $\Gamma_t$ , velocity  $\beta_t$  of top quark is not determined by the energy. Its typical fluctuation is  $\beta_t \sim \sqrt{\Gamma_t/m_t} \simeq 0.1 \sim \alpha_s$ . See just below Eq. (2.12). This is consistent with our order counting. The symbol  $c$  is speed of light.

shown that although these FSIs modify the momentum distribution of  $t$ , their corrections to the total cross section cancel to NLO.

Top–anti-top pair production near the threshold in  $e^+e^-$  collisions not only provides the place for a precise study of perturbative QCD, but also was known to be the best environment to determine the top quark mass  $m_t$ . This is because Monte Carlo detector simulations [3, 4, 18] based on NLO calculations [14–16] showed that  $m_t$  can be determined with statistical error<sup>9</sup>  $(\Delta m_t)^{\text{stat}} \simeq 0.2 \text{ GeV}$  using the energy dependence of  $R$ -ratio and the top quark momentum distribution  $d\sigma/dp$ . It was also shown that QCD gauge coupling  $\alpha_s(m_Z)$  can be measured with statistical error 0.005. It was assumed that 11 energy points are sampled with  $1 \text{ fb}^{-1}$  for each point. A similar MC study is shown in [4]. These MC studies are based on Next-to-Leading Order (NLO =  $\mathcal{O}(1/c)$ ) theoretical calculations and assume no theoretical uncertainties.

### 1.2.2 NNLO calculations of $\sigma_{\text{tot}}$

However recently the NNLO corrections to the total cross section  $\sigma_{\text{tot}}$  has been calculated by several groups [26–28]<sup>10</sup>, and it turned out to be unexpectedly large. In fact the magnitude of the NNLO correction is similar to that of the NLO correction. This is problematic since it is desirable to determine the top-quark mass in high precision in order to pin down contributions from new physics (and/or Higgs). For example [4] for wide range of Higgs mass  $m_H$ , the uncertainty  $(\Delta m_H/m_H)$  of Higgs mass extracted from radiative corrections depends on the uncertainty of  $m_t$ , and is 57% for the present precision, while it reduces to 17% for Linear Colliders (LCs) assuming  $(\Delta m_t)^{\text{stat}} \simeq 0.4 \text{ GeV}$ .

### 1.2.3 Theoretical progress related to $\sigma_{\text{tot}}$

After the calculations of the NLO corrections to  $\sigma_{\text{tot}}$ , several pieces of theoretical progress have been made with the precise calculation for heavy quark-antiquark system [65]. One is the use of low energy effective theories called NRQCD [34, 35] and pNRQCD [36, 37], which enabled the calculations of the NNLO corrections explained above, and the other is the cancellation of the ambiguities in the pole mass of a quark and in the coordinate space QCD potential; those ambiguities are due to the infrared structure of QCD, which is called “renormalon ambiguity” [55–60]. The latter enables us to improve the perturbative convergence of  $\sigma_{\text{tot}}$ , which is made in [29], on which a part of the thesis is based. Here we explain these two topics briefly.

At NNLO and beyond, non-relativistic calculations become complicated. There are several reasons. Typical one is that the normalization of the  $t\bar{t}$  current  $j_{t\bar{t}}$  depends on the momentum transfer; in other words, anomalous dimension of  $j_{t\bar{t}}$  is non-zero. This makes the use of low-energy effective theories particularly powerful. Schematically, the reduction goes as follows. The starting point is QCD, which is fully relativistic. By expanding the fields for non-relativistic particles in  $1/c$ , one obtains NRQCD [34, 35]. At NNLO (and lower orders) further reduction is possible, since no real gluon is emitted<sup>11</sup> at these orders. Thus “soft” gluons can be integrated out to result in a  $t\bar{t}$  potential [36, 37]. It is known that this formalism, called potential NRQCD or pNRQCD, reproduces correctly the energy shift of the hydrogen atom and positronium to

<sup>9</sup> On the other hand, LHC may give  $(\Delta m_t)^{\text{stat}} \sim 2 \text{ GeV}$ .

<sup>10</sup> Their results are reproduced in Section 2.6.2. Comprehensive summary (including our work) to the end of 1999 is available in [33].

<sup>11</sup> This may be understood by the fact that the vertex for transverse gluon  $g_T$  in Coulomb gauge is suppressed by  $\mathcal{O}(1/c)$  compared to the vertex for Coulomb gluon  $g_C$ .

$m\alpha^2 \times \alpha^3$  [38]. For actual calculations, one does not need to know the precise “normalization”, or the matching coefficients, of the each operator in pNRQCD Lagrangian, a priori. Only a combination of them is relevant for, say, a total production cross section  $\sigma_{\text{tot}}$ . It can be determined by calculating  $\sigma_{\text{tot}}$  in both perturbative QCD and pNRQCD, and by demanding those two results coincide. This procedure called “direct matching” [39] is possible<sup>12</sup> since for  $\alpha_s \ll \beta_t \ll 1$  both perturbative QCD and pNRQCD are applicable.

On the other hand, “renormalon ambiguity” [55–58] is related to the convergence of a perturbative expansion in QFT, which is in fact an asymptotic expansion. One of the techniques to sum up an asymptotic series  $S(a)$  with respect to  $a$  is Borel summation<sup>13</sup>, where the sum is expressed in terms of integration of  $e^{-t/a} \tilde{S}(t)$  from  $t = 0$  to  $t = \infty$ . Here  $\tilde{S}(t)$  is the function related to  $S(a)$ . The fact that  $S(a)$  diverges is expressed by the poles of  $\tilde{S}(t)$  on the integration path  $t = 0-\infty$ , which are called “renormalon poles”. One can step aside those poles by modifying the integration path; there may be two ways for each pole. Ambiguities due to those poles may be estimated by the difference between the two choices of the modification. Due to the factor  $e^{-t/a}$ , the severest ambiguity comes from the “renormalon pole” nearest to the origin ( $t = 0$ ). Now, it is known that the pole mass  $m_{\text{pole}}$  suffers from the renormalon poles [51–54], which originate from the IR structure of QCD. However it was shown [59, 60] that in the combination  $2m_{\text{pole}} + V(r)$ , where  $V(r)$  is the coordinate space QCD potential, the severest renormalon pole is cancelled; this means  $V(r)$  also suffer from the renormalon pole, and the location of the pole is the same as for  $m_{\text{pole}}$  and the residue is twice and the sign is opposite. This suggests that one should not attempt to determine pole mass. Instead another mass scheme that do not sensitive to IR physics of QCD, such as  $\overline{\text{MS}}$  mass, should be used. Several such “short-distance” mass schemes are proposed in literature; potential-subtracted mass [59],  $1S$  mass [61], and kinetic mass [62].

### 1.2.4 Our contributions

As was explained above, the previous NNLO calculations of  $\sigma_{\text{tot}}$  showed large corrections. However, since the convergence of a perturbative series changes depending on the renormalization scheme<sup>14</sup>, there is a possibility for finding a scheme where  $\sigma_{\text{tot}}$  converges better. This is the subject of the latter half of Chapter 2. There we implement two prescriptions; one is to use the mass scheme that do not suffer from IR renormalon ambiguity; and the other is to sum up (potentially large) leading logarithms by using renormalization group. Both of these reduce the theoretical uncertainty of  $\sigma_{\text{tot}}$ . With this improvement, we estimate the theoretical uncertainty  $(\Delta m_t)^{\text{th}}$  of the top quark mass determination is reduced to  $\sim 0.1$  GeV, which is smaller than the expected statistical error.

We also calculate the NNLO correction for  $d\sigma/dp$  from the rescattering between  $t$  and  $\bar{t}$ . However it is not considered that the rescattering between  $t$  and  $\bar{b}$  etc., which may modify the distribution to the similar extent.

<sup>12</sup> Of course one needs the result for perturbative QCD. For the case we deal,  $\mathcal{O}(\alpha_s^2)$  corrections to  $\sigma(e^+e^- \rightarrow \gamma^* \rightarrow t\bar{t})$  are calculated in [40].

<sup>13</sup> Here  $a$  may be considered as a coupling. Asymptotic behavior of  $S(a)$  can be inferred by using renormalization group, for example. See Section 2.7.3 for detail.

<sup>14</sup> A different renormalization scheme (and renormalization scale) corresponds to a different way of summing up a perturbation series.

### 1.3 Overview of top-quark anomalous EDMs

Of course top quark is (potentially) sensitive not only to the SM dynamics but also to the physics beyond the SM. One particularly clear signal is  $CP$  violation in top-quark sector. This is because the SM contribution is suppressed to many orders below the current or near-future experimental reach<sup>15</sup>. Thus a non-zero expectation value of a  $CP$ -odd observable means contribution from new physics immediately<sup>16</sup>. In fact there are plenty of new sources for  $CP$  violation once the particle content of the SM is extended. Many models, including Minimal SuperSymmetric SM (MSSM) or multi Higgs-doublets model in general, induce  $CP$  violating  $t\bar{t}$ -gauge boson interactions at one-loop level. In the CM frame of  $t\bar{t}$  pair, or a particle-anti-particle system in general, a  $CP$ -odd observable related to them is odd under  $\mathbf{s}_t \leftrightarrow \bar{\mathbf{s}}_t$ , and vice versa, since  $CP$  transformation exchanges their spins  $\mathbf{s}$  at the frame. Also in this respect top quark is excellent since the polarization  $\mathbf{P}_t$  of  $t$  is not disturbed by hadronization, and the information of  $\mathbf{P}_t$  is inherited to its decay products; especially, the charged lepton  $\ell^+$  is emitted with the angular distribution<sup>17</sup>  $\propto 1 + |\mathbf{P}_t| \cos \theta$ , where  $\theta$  is the angle between the polarization of  $t$  and the momentum of  $\ell^+$ . Thus the  $CP$  violations in the top-quark sector can be measured by the difference  $\mathbf{P}_t - \bar{\mathbf{P}}_t$  between the polarizations of  $t$  and  $\bar{t}$ , which can be measured statistically from the directions of the charged leptons.

Since many extensions of the SM contain new sources of  $CP$  violation, we parameterize their effects by effective couplings in a model independent way. Among  $CP$  violating interactions of  $t$ , Electric Dipole Moment (EDM) interaction is the lowest dimensional operator<sup>18</sup>. Thus in terms of an effective Lagrangian,  $CP$  violating effects in the top quark sector are parameterized by several anomalous EDMs of top quark at the first approximation. There are several of them:  $t\bar{t}g$ -,  $t\bar{t}\gamma$ -,  $t\bar{t}Z$ -, and  $t\bar{t}W$ -EDM. The first three affect the production (and rescattering) process of  $t\bar{t}$ , while the last one the decay process.

#### 1.3.1 Previous studies

Many studies<sup>19</sup> have been done for the anomalous EDMs of top quarks. One major topic is how well those EDMs are measured in future colliders. Some study for  $e^+e^-$  colliders with  $\sqrt{s} \gg 2m_t$ , and the others for hadron colliders. The former is suited for the study of EW-EDMs,  $t\bar{t}\gamma$  and  $t\bar{t}Z$ , while the latter for Chromo-EDM,  $t\bar{t}g$ . Both of these results are summarized in Section 4.4.

#### 1.3.2 Our contributions

Although many studies have done for  $e^+e^-$  colliders with  $\sqrt{s} \gg 2m_t$  and for hadron colliders, there was no one for  $e^+e^-$  colliders near the threshold to date. Thus we study this case. We concentrate on the anomalous EDMs in the production process ( $t\bar{t}$ -gauge bosons) here, and leave  $t\bar{t}W$ -EDM for a future study. Among the three flavor-diagonal EDMs, our prime concern is on Chromo Electric Dipole Moment (CEDM):  $t\bar{t}g$ -EDM. The reason is as follows. As shall be shown in Section 4.6, two ElectroWeak EDMs,  $t\bar{t}\gamma$ - and  $t\bar{t}Z$ -EDM, directly modify

<sup>15</sup> This is because the CKM matrix elements for the third generation are almost diagonal:  $|V_{tb}| \simeq 1$ . See Section 4.2 for more quantitative statements.

<sup>16</sup> Provided that the initial state is a  $CP$  eigenstate.

<sup>17</sup> See Section 4.5.3.

<sup>18</sup> See Section A.4.

<sup>19</sup> See Sections 4.2 and 4.4 for the references.

the  $t\bar{t}$  production vertex, and their interactions are proportional to the relative momentum  $|\mathbf{p}| \simeq \sqrt{m_t E}$  between  $t\bar{t}$ . This means open top region ( $\sqrt{s} \gg 2m_t$ ) is more appropriate to study them. On the other hand CEDM modifies the rescattering of  $t\bar{t}$ , which can be suppressed when  $\sqrt{s} \gg 2m_t$ . Thus in open top region at lepton colliders, it can be studied only by real gluon emissions. We find that the threshold region is more sensitive to CEDM than the open top region. As for hadron colliders, they are sensitive to the existence of a non-zero CEDM, since  $t\bar{t}$  pairs are copiously produced in gluon fusions. In fact our result for CEDM is that the sensitivity of  $e^+e^-$  colliders at the threshold are worse than that of hadron colliders. However precise measurement of CEDM may be difficult in hadron colliders. Moreover, while detailed detector simulation seems to be indispensable for the serious study of the sensitivity at hadron colliders, it has not been done so far<sup>20</sup>. On the other hand, a full detector simulation with realistic experimental setup is in progress [125] based on our study presented here. Thanks to the clean environment of  $e^+e^-$  collisions, their first result for the sensitivity is consistent with our naive estimate.

## 1.4 Organization of the thesis

In the thesis I study<sup>21</sup> the physics of  $t\bar{t}$  threshold in  $e^+e^-$  collisions for the study of both in the SM and beyond the SM dynamics.

Chapters 2 and 3 are devoted to the SM dynamics. Total production cross section  $\sigma_{\text{tot}}$  is studied in Chapter 2. By reorganizing perturbation series, we obtain better convergence of  $\sigma_{\text{tot}}$  to NNLO than ever obtained. With this result, theoretical uncertainty to measure  $m_t$  becomes smaller than experimental uncertainties. The chapter also includes a review of previous studies, of theoretical set-up such as the Green function method to calculate  $\sigma_{\text{tot}}$ . A derivation of non-relativistic Hamiltonian to NNLO is also given. Chapter 3 deals with the top-quark momentum distribution. Coulomb rescattering between  $t\bar{t}$  is treated to NNLO.

On the other hand, Chapter 4 is devoted to the contributions from new physics, especially to new sources of  $\mathcal{CP}$  violation. It is explained that, the  $\mathcal{CP}$  violation in top-quark sector within the SM is so small that if it is discovered it would immediately imply new physics.  $\mathcal{CP}$  violation in top-quark sector is parameterized by Electric Dipole Moment (EDM) interactions of top quark, since it is the lowest dimension operator that violates  $\mathcal{CP}$  symmetry. Many studies have been done on EDMs of top quark, but they are all in the open-top region  $\sqrt{s} \gg 2m_t$ . We analyze them in the threshold region  $\sqrt{s} \simeq 2m_t$  for the first time. Due to the multiple Coulomb rescattering near the threshold, differential production cross section is sensitive to  $t\bar{t}$ -gluon anomalous EDM even when  $t\bar{t}$  is produced in  $e^+e^-$  collisions. We find that the sensitivity of future  $e^+e^-$  Linear Colliders (LC) is worse than that at hadron colliders by factor  $\mathcal{O}(1/10)$  or less. Sensitivities for  $t\bar{t}\gamma$ - and  $t\bar{t}Z$ -EDMs are also studied, and are found to be comparable to those in the open-top region at LC.

Summary and discussions are given in Chapter 5.

<sup>20</sup> At least to our knowledge.

<sup>21</sup> This work is based on the collaborations with Y. Sumino and A. Ota [29], and with M. Jezabek and Y. Sumino [66].



# Chapter 2

## Total Production Cross Section

### 2.1 Overview

As was explained in Chapter 1, it was considered that the mass  $m_t$  of top quark  $t$  can be determined most accurately by the energy scan of  $t\bar{t}$  total production cross section near the threshold in  $e^+e^-$  collisions. However there emerge the fear that this way of determination suffer from a large theoretical uncertainty, due to the large NNLO ( $= \mathcal{O}(1/c^2)$ ) correction to the  $t\bar{t}$  production cross section  $\sigma_{\text{tot}}(s)$ , where  $\sqrt{s}$  denotes the CM energy.

In the thesis, we follow closely the procedure used in [27]. There the Green function  $G$  for a  $t\bar{t}$  system is rewritten in a form convenient for numerical calculations. By implementing “renormalon cancellation” and “ $\log(q/\mu)$  resummation”, we improve the convergence of  $\sigma_{\text{tot}}$  obtained in [26–28].

This chapter is organized as follows. In Section 2.2, it is explained that how a non-relativistic (color-singlet)  $t\bar{t}$  pair is described in terms of the Green function of the pair. In particular, the total production cross section is given by the optical theorem, which is explained in Section 2.2.1. In Section 2.2.2, order counting is explained. Also shown is that the Coulomb potential is a part of leading Hamiltonian. At NNLO, there arise several difficulties, which is given in Section 2.2.3. In Section 2.2.4, the Hamiltonian to NNLO is shown. The Hamiltonian is looked at more closely in Section 2.3. We obtain the Green function  $G$  by solving the Schrödinger equation numerically. For this purpose, we express  $G$  in terms of reduced Green function  $G'$ , which satisfies simpler Schrödinger equation than  $G$  itself. This is done in Section 2.4. At that stage, we are equipped to reproduce the previously obtained results for the total cross section, including NNLO ones. They are collected in Section 2.6, and exhibit large correction at NNLO. Hereafter, we try to improve the convergence of the perturbative expansion. It is known that (certain) perturbative expansions involving the pole mass of a quark are less converging than those involving  $\overline{\text{MS}}$  mass, or “short-distance” mass. It is suspected that this is because pole mass suffer from non-perturbative dynamics of QCD. Section 2.7 is devoted to this issue. There we adopt potential-subtracted mass scheme, which is proposed in [59]. This improves the convergence of binding energies. In Section 2.8, certain kind of logarithm in the Coulombic potential is summed up using renormalization group. Tentatively, the convergence of  $R$  ratio is best with these two prescriptions. The section contains the estimate of theoretical uncertainties for this case; in terms of top quark mass, it is  $(\Delta m_t)^{\text{th}} \sim 0.1 \text{ GeV}$ .

## 2.2 Non-relativistic description of $t\bar{t}$ system

### 2.2.1 Optical Theorem

In terms of an amplitude  $\mathcal{M}$ , the unitarity [Eq. (A.55)] of  $S$ -matrix is expressed by optical theorem, which relates the total cross section of a two-body scattering to the imaginary part of the forward scattering amplitude:

$$\sigma_{\text{tot}}(k_1, k_2 \rightarrow \text{anything}) = \frac{1}{s\bar{\beta}_i} \text{Im} \mathcal{M}(k_1, k_2 \rightarrow k_1, k_2) ,$$

where  $\bar{\beta}_i = 2|\mathbf{k}_{\text{CM}}|/\sqrt{s}$ , and  $|\mathbf{k}_{\text{CM}}| \equiv |\mathbf{k}_1| = |\mathbf{k}_2|$  at the CM-frame of two particles with momenta  $k_1$  and  $k_2$ . If we restrict the intermediate states appropriately on the RHS, we have the total cross section for  $k_1, k_2 \rightarrow \text{such-and-such}$ . For the process  $e^+(\bar{p}_e)e^-(p_e) \rightarrow \gamma^* \rightarrow t\bar{t}$ , the total cross section of this process can be obtained from the imaginary part of the amplitude for  $e^+(\bar{p}_e)e^-(p_e) \rightarrow \gamma^* \rightarrow t\bar{t} \rightarrow \gamma^* \rightarrow e^+(\bar{p}_e)e^-(p_e)$ . Let  $(-ieQ_t)^2 \cdot i\Pi^{\mu\nu}(q)$  be the  $t\bar{t}$  contribution to the vacuum polarization of a photon with momentum  $q^\mu$ :

$$\begin{aligned} i\Pi^{\mu\nu}(q) &= i(q^2 g^{\mu\nu} - q^\mu q^\nu) \Pi(q^2) \\ &= \int d^4x e^{iq \cdot x} \langle 0 | \text{T}[j^\mu(x) j^\nu(0)] | 0 \rangle \\ &= \langle 0 | \text{T}[\tilde{j}^\mu(q) \tilde{j}^\nu(-q)] | 0 \rangle \\ &= (-1) N_C \int \frac{d^4p}{(2\pi)^4} \frac{i}{(p - q/2)^2 - m^2 + i\epsilon} \frac{i}{(p + q/2)^2 - m^2 + i\epsilon} \\ &\quad \times \text{tr}[(\not{p} - \not{q}/2 + m)\gamma^\mu(\not{p} + \not{q}/2 + m)\gamma^\nu] , \end{aligned}$$

where  $j^\mu(x) = \bar{t}(x)\gamma^\mu t(x)$ , and the last expression corresponds to one-loop. By contracting indices, we have

$$\Pi(q^2) = \frac{-i}{3q^2} \langle 0 | \text{T}[\tilde{j}^\mu(q) \tilde{j}_\mu(-q)] | 0 \rangle = \frac{1}{3q^2} g_{\mu\nu} \Pi^{\mu\nu}(q) .$$

Thus for unpolarized  $e^+e^-$ ,

$$\begin{aligned} i\mathcal{M}(p_e, \bar{p}_e \rightarrow \cdots \rightarrow p_e, \bar{p}_e) &= (-ieQ_t)^2 \cdot i(q^2 g^{\mu\nu} - q^\mu q^\nu) \Pi(q^2) \left(\frac{-i}{q^2}\right)^2 \times \\ &\quad \times \frac{1}{2^2} \sum_{\text{spins}} \text{tr}[u(p_e)\bar{u}(p_e)\gamma_\mu v(\bar{p}_e)\bar{v}(\bar{p}_e)\gamma_\nu] \\ &= i(4\pi\alpha)^2 Q_e^2 Q_t^2 \Pi(q^2) . \end{aligned}$$

Here we neglect electron mass. Note that the  $q^\mu q^\nu$ -part of  $\Pi^{\mu\nu}$  do not contribute, since  $e^+e^-$ -current is conserved:  $\bar{v}(\bar{p}_e)\not{q}u(p_e) = 0$ , where  $q^\mu = (p_e + \bar{p}_e)^\mu$ . Thus, with  $s = q^2$ ,

$$\begin{aligned} R(s) &\equiv \frac{\sigma_{\text{tot}}(e^+e^- \rightarrow \gamma^* \rightarrow t\bar{t})}{\sigma_{\text{pt}}} \\ &= Q_t^2 12\pi \text{Im} \Pi(q^2) = Q_t^2 \frac{4\pi}{s} \text{Im} \left[ -i \langle 0 | \text{T}[\tilde{j}^\mu(q) \tilde{j}_\mu(-q)] | 0 \rangle \right] , \end{aligned} \tag{2.1}$$



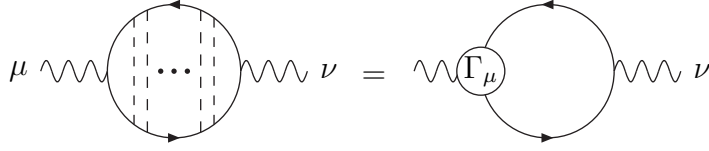


Figure 2.1: Lowest-order ( $=\mathcal{O}(1/c)$ ) contribution of gluon exchange between  $t\bar{t}$  to the total cross section.

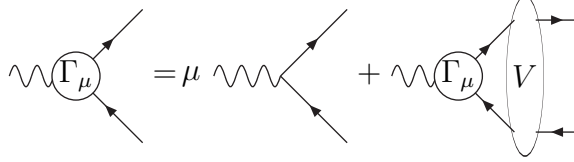


Figure 2.2: Ladder approximation of vertex function  $\Gamma$ . This is sufficient for Coulomb gluon, which is instantaneous.

where

$$\sigma_{\text{pt}}(s) \equiv \frac{4\pi\alpha^2}{3s} = 0.817 \text{ pb} \left( \frac{\sqrt{s}}{2 \times 175 \text{ GeV}} \right)^{-2} \quad (2.2)$$

is “point cross section”, the total cross section for  $e^+e^- \rightarrow \gamma^* \rightarrow \mu^+\mu^-$  with  $\sqrt{s} \gg 2m_\mu$ .

As will be shown in Section 4.6.2, Coulomb rescattering<sup>1</sup> between  $t$  and  $\bar{t}$  can be taken into account<sup>2</sup> by modifying (one of the)  $t\bar{t}\gamma$  vertex as [Figure 2.1]

$$\gamma^\mu \rightarrow [\gamma^\mu]_{\text{rescat}} = \gamma^\mu \tilde{G}(|\mathbf{p}|, E) \left[ \frac{\mathbf{p}^2}{m_t} - (E + i\Gamma) \right],$$

where

$$\tilde{G}(|\mathbf{p}|, E) \equiv \int \frac{d\Omega_{\vec{p}}}{4\pi} \langle \mathbf{p} | G | \mathbf{x}' = 0 \rangle, \quad G \equiv \frac{1}{H - (E + i\Gamma_t)},$$

and  $H$  is a Non-Relativistic Hamiltonian. Thus to the lowest order of  $1/c$ -expansion,

$$\begin{aligned} i\Pi^{\mu\nu}(q) &= (-1)N_C \int \frac{d^4p}{(2\pi)^4} \frac{i}{\left(\frac{E}{2} + p^0 + i\frac{\Gamma_t}{2}\right) - \frac{\mathbf{p}^2}{2m_t}} \frac{i}{\left(\frac{E}{2} - p^0 + i\frac{\Gamma_t}{2}\right) - \frac{\mathbf{p}^2}{2m_t}} \times \\ &\quad \times \text{tr} \left[ \frac{1 + \gamma^0}{2} [\gamma^\mu]_{\text{rescat}} \frac{1 - \gamma^0}{2} \gamma^\nu \right] \\ &= i 2(g^{\mu\nu} - g^{\mu 0} g^{\nu 0}) N_C \int \frac{d^3p}{(2\pi)^3} \tilde{G}(|\mathbf{p}|, E) \\ &= i 2(g^{\mu\nu} - g^{\mu 0} g^{\nu 0}) N_C G(\mathbf{x} = 0, E), \end{aligned}$$

or

$$\Pi(q^2) = \frac{2N_C}{q^2} G(\mathbf{x} = 0, E), \quad \text{Im} \left[ -i \langle 0 | T[\tilde{j}^\mu(q) \tilde{j}_\mu(-q)] | 0 \rangle \right] = 6N_C G(\mathbf{x} = 0, E),$$

<sup>1</sup> We have in mind the rescattering due to the exchange of Coulomb gluons.

<sup>2</sup> Only the effect of “soft” gluons can be taken into account by the Green function  $G$ . See Section 2.2.5.

where  $G(\mathbf{x}, E) \equiv \langle \mathbf{x} | G | \mathbf{x}' = 0 \rangle$ . Thus up to short distance corrections and relativistic corrections,  $R$  ratio near the threshold is given as follows:

$$R(s) = \frac{3}{2} N_C Q_t^2 \frac{4m^2}{s} \cdot \frac{4\pi}{m^2 c} \text{Im} G(\mathbf{x} = 0, E) . \quad (2.3)$$

Note that the velocity  $\beta$  of  $t$  at  $t\bar{t}$  CM frame is

$$\beta = \sqrt{1 - \frac{4m_t^2}{s}} , \quad \text{or,} \quad \frac{4m_t^2}{s} = 1 - \beta^2 = \frac{1}{\gamma^2} . \quad (2.4)$$

If one expands as amplitude  $\mathcal{M}$  into eigenstates of orbital angular momentum  $L$ ,  $\mathcal{M} = \sum_L \mathcal{M}^{(L)}$ , then  $|\mathcal{M}^{(L)}| \propto \beta^L$ . Thus  $S$  wave ( $L = 0$ ) is the leading contribution near the threshold. We sometimes use  $S$ -wave projected notation of Green function  $G(r, r')$  defined in Section A.2.4:

$$G(r = 0, r' = 0) = G(\mathbf{x} = 0, E) . \quad (2.5)$$

Here the energy dependence is implicit.

### 2.2.2 Order counting

The non-relativistic expression of a quantity is obtained by expanding it with respect to  $1/c$ . Noting that

$$\alpha_s = \frac{g_s^2}{4\pi\hbar c} = \mathcal{O}\left(\frac{1}{c}\right) ,$$

it is useful to introduce a dimensionful (but order unity) coupling  $a_s \equiv \alpha_s^{\overline{\text{MS}}}(\mu_s)c$  for order counting; here  $\mu_s$  is a ‘‘soft scale’’, which means the typical scale for the  $t\bar{t}$  potential. Thus the QCD correction  $\alpha_s$  is the same order to the relativistic correction  $\beta$ , where  $\beta = \sqrt{1 - 4m_t^2/s}$  is the velocity of  $t$  and  $\bar{t}$  at their CM-frame:

$$\beta = \frac{v}{c} , \quad \alpha_s(\mu_s) = \frac{a_s}{c} , \quad \frac{\alpha_s(\mu_s)}{\beta} = \frac{a_s}{v} = \mathcal{O}(1) . \quad (2.6)$$

In fact as we shall see near Eq. (2.12),  $\beta_t \sim \sqrt{\Gamma_t/m_t} \simeq 0.1 \sim \alpha_s$  near the threshold. One can clearly see that one need to sum up  $\alpha_s(\mu_s)/\beta$  to all order. The Leading Order (LO) is  $\mathcal{O}(1)$ , the Next-to-Leading Order (NLO) is  $\mathcal{O}(1/c)$ , and the Next-to-Next-to-Leading Order (NNLO) is  $\mathcal{O}(1/c^2)$ .

The following relations may be useful to count the order of  $1/c$ :

$$\dim[mrc] = \dim[rp] = \dim[\hbar] = \dim[1] , \quad \dim[1/r] = \dim[p] .$$

Since  $\dim[a_s] = \dim[c]$  or  $\dim[a_s/r] = \dim[E]$ , the Coulomb potential is the same order to the kinetic term. Thus it is a part of the leading-order Hamiltonian  $H_0$ .

### 2.2.3 Complications at $\mathcal{O}(1/c^2)$

There are several complications at  $\mathcal{O}(1/c^2)$  and beyond. Some are already in freely-propagating  $t\bar{t}$  pairs, some are in the  $t\bar{t}$  potential  $V$ , and some are especially in the Non-Abelian part  $V_{\text{NA}}$  of  $V$ .

For the free  $t\bar{t}$  propagation, (i-1) the Hamiltonian contains  $p^4$  term besides  $p^2$  term, which is the standard kinetic term. (i-2) The wave-function normalization of the production  $t\bar{t}$  current  $j_{t\bar{t}}$  depends on the momentum transfer  $q^2$ , or in other words, anomalous dimension of  $j_{t\bar{t}}$  is non-zero. (i-3) At  $\mathcal{O}(1/c)$  and below, the decay width  $\Gamma_t$  of  $t$  quark can be incorporated by replacing  $H \rightarrow H - i\Gamma$  [9, 16]. At  $\mathcal{O}(1/c^2)$  and higher, this is no longer justified. These three issues are discussed just below.

For the  $t\bar{t}$  potential  $V$ , there are  $\log(q^2/\mu_s^2)$  corrections [43–45]. This is the only correction to  $\mathcal{O}(1/c)$  aside from a finite term. However to  $\mathcal{O}(1/c^2)$ , besides the log corrections, (ii-1) there are also corrections called Breit-Fermi potential  $V_{\text{BF}}$  [41]. These corrections are common to the potential due to both Abelian ( $\gamma$ ) and non-Abelian gauge ( $g$ ) boson exchange. (ii-2) There is also a correction [42] especially due to non-Abelian nature of a gluon, which is absent at  $\mathcal{O}(1/c)$  and below. These two issues are discussed in Section 2.3.

#### Current normalization $C_1^{(\text{cur})}$ , $C_2^{(\text{cur})}$

For  $R$ -ratio, the lowest in both  $\beta$  and  $\alpha_s$  expansion is  $\mathcal{O}(\beta^1, \alpha_s^0)$ . There are several corrections beyond the lowest order. Only relativistic corrections are considered here<sup>3</sup>. For  $\alpha_s = 0$  and to all-order in  $\beta$ , the  $t\bar{t}$  production cross section is

$$R = \frac{3}{2} N_C Q_t^2 \beta \left( 1 - \frac{\beta^2}{3} \right), \quad (2.7)$$

where  $\beta$  is velocity of  $t$  at  $t\bar{t}$  CM frame [Eq. (2.4)]. The Green function formalism [Eq. (2.3)] should reproduce this result. The Non-Relativistic Hamiltonian  $H_{\text{free}}^{(\text{NR})}$  for free  $t\bar{t}$  is

$$\begin{aligned} H_{\text{free}}^{(\text{NR})} &= H_{\text{free}}^{(\text{R})} - 2mc^2 \\ &= \frac{\mathbf{p}^2}{m} - \frac{\mathbf{p}^4}{4m^3c^2} + \mathcal{O}\left(\frac{1}{c^4}\right), \end{aligned}$$

where  $H_{\text{free}}^{(\text{R})}$  is defined in Eq. (2.17). A form factor depends on the momentum-transfer in general, and so does the wave-function normalization for  $t\bar{t}$  vector current  $j^\mu(q)$ . A Taylor expansion, or derivative expansion in coordinate space, of  $R(s)$  reads

$$\begin{aligned} R(s) &= Q_t^2 \frac{4\pi}{s} \text{Im} \left[ -i \langle 0 | T[j^\mu(q) \tilde{j}_\mu(-q)] | 0 \rangle \right] \\ &= \frac{3}{2} N_C Q_t^2 \frac{4m^2}{s} \frac{4\pi}{m^2c} \left\{ C_1^{(\text{cur})} + C_2^{(\text{cur})} \frac{\Delta_r + \Delta_{r'}}{2m^2c^2} \right\} \text{Im} G(r, r') \Big|_{r, r' \rightarrow r_0} + \mathcal{O}\left(\frac{1}{c^3}\right), \end{aligned} \quad (2.8)$$

where  $C_1^{(\text{cur})} = 1 + \mathcal{O}(\alpha_s)$  and  $C_2^{(\text{cur})} = \text{const.} + \mathcal{O}(\alpha_s)$ ; the constant of  $C_2^{(\text{cur})}$  is determined below in this section. The reason for introducing the cutoff parameter  $r_0 (\neq 0)$  shall be explained also

<sup>3</sup> Others are considered in Section 2.5.

below in this section. If the potential between  $t\bar{t}$  is neglected, a part of the expression above can be rewritten as follows:

$$\begin{aligned}
& \text{Im} \left[ \left\{ C_1^{(\text{cur})} + C_2^{(\text{cur})} \frac{\Delta_r + \Delta_{r'}}{2m^2c^2} + \mathcal{O}\left(\frac{1}{c^4}\right) \right\} \langle r | \frac{1}{\frac{\mathbf{p}^2}{m} - \frac{\mathbf{p}^4}{4m^3c^2} + \mathcal{O}\left(\frac{1}{c^4}\right) - (E + i\Gamma_t)} | r' \rangle \right] \\
&= \text{Im} \left[ \left( 1 - C_2^{(\text{cur})} \frac{E + i\Gamma_t}{mc^2} \right) \langle r | \frac{1}{\frac{\mathbf{p}^2}{m} - (E + i\Gamma_t)} | r' \rangle \right] \\
&\quad + \text{Im} \langle r | \frac{1}{\frac{\mathbf{p}^2}{m} - (E + i\Gamma_t)} \frac{\mathbf{p}^4}{4m^3c^2} \frac{1}{\frac{\mathbf{p}^2}{m} - (E + i\Gamma_t)} | r' \rangle + \mathcal{O}\left(\frac{1}{c^4}\right) . \tag{2.9}
\end{aligned}$$

Here we used

$$(\Delta_r + \Delta_{r'}) \langle \mathbf{r} | G | \mathbf{r}' \rangle = - \langle \mathbf{r} | (\mathbf{p}^2 G + G \mathbf{p}^2) | \mathbf{r}' \rangle . \tag{2.10}$$

First, consider the case  $\Gamma_t = 0$ . With the explicit analytic calculations<sup>4</sup> of the Green functions in Section B.4.1, the  $\beta$ -dependence of  $R$  in Green function method is

$$\begin{aligned}
R / \left( \frac{3}{2} N_C Q_t^2 \right) &= (1 - \beta^2) \cdot \frac{u}{c} \left\{ \left( 1 - C_2^{(\text{cur})} \left( \frac{u}{c} \right)^2 \right) + \frac{5}{8} \left( \frac{u}{c} \right)^2 + \mathcal{O}\left(\frac{1}{c^4}\right) \right\} \\
&= \beta \left( 1 - C_2^{(\text{cur})} \beta^2 + \mathcal{O}(\beta^4) \right) ,
\end{aligned}$$

while relativistic QFT says [Eq. (2.7)] it is  $\beta(1 - \beta^2/3)$ . Note that  $u = \beta + \mathcal{O}(\beta^3)$  is defined in Section B.4. Thus we obtain

$$C_2^{(\text{cur})} = \frac{1}{3} + \mathcal{O}(\alpha_s) . \tag{2.11}$$

As shall be seen in Section 2.2.2, soft gluon corrections are suppressed by  $\alpha_s(\mu_s) = \mathcal{O}(1/c)$ , the lowest matching coefficient is sufficient for the  $\mathcal{O}(1/c^2)$  calculations, since  $C_2^{(\text{cur})}$  is a coefficient of  $\mathcal{O}(1/c^2)$  correction.

### Treatment of the finite width $\Gamma_t$

Concentrating on freely-propagating  $t\bar{t}$ , the Green function<sup>5</sup> at the origin is

$$\text{Im} G(0, 0) = \frac{m_t^2}{4\pi} \text{Re} \sqrt{\frac{E + i\Gamma_t}{m_t}} + \mathcal{O}\left(\frac{1}{c}\right) . \tag{2.12}$$

Note that  $\sqrt{E/m_t} = \beta + \mathcal{O}(\beta^3)$ . Thus effectively  $\beta \sim \sqrt{\Gamma_t/m_t} \simeq 0.1$  near the threshold. By using

$$\sqrt{E + i\Gamma_t} = \left[ \frac{\sqrt{E^2 + \Gamma_t^2} + E}{2} \right]^{1/2} + i \left[ \frac{\sqrt{E^2 + \Gamma_t^2} - E}{2} \right]^{1/2} \times \text{sgn}[\Gamma_t] ,$$

<sup>4</sup> The relevant are  $\text{Im} G_0$  and  $\text{Im} G_2$ .

<sup>5</sup> This is derived in Section B.4.1. The relevant one is  $\text{Im} G_0$ .

in general, we have

$$R = \frac{3}{2} N_C Q_t^2 \left[ \frac{\sqrt{E^2 + \Gamma_t^2} + E}{2m_t} \right]^{1/2} + \mathcal{O}\left(\frac{1}{c}\right). \quad (2.13)$$

It is known that the effect of finite decay width  $\Gamma_t$  can be taken into account by the replacement  $E \rightarrow E + i\Gamma_t$  to LO [9] and NLO [16]. However to NNLO with non-zero  $\Gamma_t$ , imaginary part of the Green function is no longer finite when one takes the limit  $r = r' \rightarrow 0$ , which is required by the optical theorem:

$$\text{Eq. (2.9)} = \left( -C_2^{(\text{cur})} + \frac{1}{2} \right) \frac{\Gamma_t}{4\pi c^2 r} + \mathcal{O}\left(r^0 = 1, r'^0 = 1, \frac{1}{c^4}\right),$$

for  $r > r'$ . This means that the effect of the finite width  $\Gamma_t$  is not properly treated by the replacement  $E \rightarrow E + i\Gamma_t$  at  $\mathcal{O}(1/c^2)$ . Here following [27], we regulate this singularity by putting  $r = r' \rightarrow r_0 \neq 0$ , as shown in Eq. (2.8).

### 2.2.4 Non-relativistic NNLO Hamiltonian $H$

The NNLO Hamiltonian<sup>6</sup>  $H$ , which is relevant to us, is

$$H = H_0 + V_1(r) + U(\mathbf{p}, \mathbf{r}), \quad H_0 = \frac{\mathbf{p}^2}{m_t} - \frac{C_F a_s}{r}, \quad (2.14)$$

where  $H_0$  is the leading-order Hamiltonian,  $V_1(r)$  is radiative corrections to the Coulomb potential<sup>7</sup>,

$$V_1(r) = -\frac{C_F a_s}{r} \left[ \frac{a_s}{4\pi c} \{2\beta_0 \ln(\mu' r) + a_1\} + \left( \frac{a_s}{4\pi c} \right)^2 \left\{ \beta_0^2 \left( 4 \ln^2(\mu' r) + \frac{\pi^2}{3} \right) + 2(\beta_1 + 2\beta_0 a_1) \ln(\mu' r) + a_2 \right\} \right], \quad (2.15)$$

and  $U(\mathbf{p}, \mathbf{r})$  is a momentum-dependent potential, which includes only  $\mathcal{O}(1/c^2)$  terms:

$$\begin{aligned} U(\mathbf{p}, \mathbf{r}) &= -\frac{\mathbf{p}^4}{4m_t^3 c^2} - \frac{C_A C_F a_s^2}{2m_t r^2 c^2} \\ &\quad - \frac{C_F a_s}{2m_t^2 c^2} \left\{ \frac{1}{r}, \mathbf{p}^2 \right\} + \frac{C_F a_s}{2m_t^2 c^2} \frac{\mathbf{L}^2}{r^3} + \frac{\pi C_F a_s}{m_t^2 c^2} \left( 1 + \frac{4}{3} \mathbf{S}^2 \right) \delta^{(3)}(\mathbf{r}) \\ &\quad + \frac{3C_F a_s}{2m_t^2 c^2} \frac{\mathbf{L} \cdot \mathbf{S}}{r^3} - \frac{C_F a_s}{2m_t^2 c^2} \frac{1}{r^3} \left( \mathbf{S}^2 - 3 \frac{(\mathbf{S} \cdot \mathbf{r})^2}{r^2} \right) \\ &= -\frac{\mathbf{p}^4}{4m_t^3 c^2} - \frac{C_A C_F a_s^2}{2m_t r^2 c^2} - \frac{C_F a_s}{2m_t^2 c^2} \left\{ \frac{1}{r}, \mathbf{p}^2 \right\} + \frac{11\pi C_F a_s}{3m_t^2 c^2} \delta^{(3)}(\mathbf{r}), \end{aligned}$$

<sup>6</sup> When we say simply ‘‘Hamiltonian’’  $H$ , it means ‘‘Non-Relativistic Hamiltonian’’  $H^{(\text{NR})}$ .

<sup>7</sup> We may sometimes use the word ‘‘Coulombic potential’’  $V_C$  for the Coulomb potential with radiative corrections:

$$V_C(r) = \frac{-C_F a_s}{r} + V_1(r).$$

Coefficients  $a_2$  etc. are defined in Section 2.3.4.

where  $\{ , \}$  means anticommutator, and the last expression is for the  $S$ -wave state,  $L = 0$ ,  $\mathbf{S}^2 = 2$ ,  $r^i r^j = \delta^{ij} r^2/3$ . The first term in  $U(\mathbf{p}, \mathbf{r})$  is the relativistic correction to the free Hamiltonian, and the second term  $V_{\text{NA}}(r)$  is due to Non-Abelian nature of a gluon. The rest is Breit-Fermi potential  $V_{\text{BF}}(\mathbf{p}, \mathbf{r})$ . In the next section, we shall see each of them more closely.

We need to calculate the Green function  $G(r, r')$  for the Hamiltonian  $H$ . Because of the logarithmic corrections to Coulomb potential,  $G(r, r')$  cannot be obtained analytically<sup>8</sup>. For numerical calculations, there are two obvious complications for the  $H$  above. One is  $p^4$ , which makes the Schrödinger equation a fourth-rank differential equation, and the other is the  $\delta$ -function. These two difficulties can be circumvented by rewriting  $H$  appropriately. We do this in Section 2.4.

### 2.2.5 Soft corrections and hard corrections

It is known that the matrix element  $|\mathcal{M}|^2$  is singular near the threshold due to “soft” gluons, if one calculate to a fixed order of  $\alpha_s$ . This is called “threshold singularity”. Here the “soft” gluon means that its momentum is  $\sim \alpha_s m_t$ . However it is also known that this singularity is absent once the terms of  $(\alpha_s/\beta)^n$  are summed over, and this summation is achieved in Non-Relativistic Green function  $G$  with Coulomb potential<sup>9</sup>  $V$ . Thus Green function method [Eq. (2.8)] is convenient for the threshold physics.

On the other hand, if the gluon, exchanged between  $t\bar{t}$ , is “hard”, which means its momentum is  $\sim m_t$ , it is not treated by the non-relativistic potential, but by the matching coefficients of  $t\bar{t}$  production current. It is called “hard vertex correction” [48], which is the same as usual radiative correction to the vector vertex:

$$\gamma^\mu \rightarrow \gamma^\mu \left( 1 - 2C_F \frac{\alpha_s(\mu_h)}{\pi} + \mathcal{O}(\alpha_s^2) \right) \quad (2.16)$$

for each vertex. Here  $\mu_h \simeq m_t$  is a “hard scale” which is a typical scale for short distance physics. We limit ourselves to the contributions from the “soft” gluons for the moment. The matching coefficients, which represent the contributions from the “hard” gluons, are determined in Section 2.5.

## 2.3 Non-relativistic $t\bar{t}$ potential $V$ to NNLO

### 2.3.1 Normalization of wave functions

In QFT, fields of spin-0 are dim-1, while those of spin-1/2 are dim-3/2. Thus if one uses the convention<sup>10</sup> that the dimensions of the creation-annihilation operators are the same for spin-0 fields and spin-1/2 fields, the dimension of c-number wave functions for spin-1/2 fields is higher by 1/2 than that for spin-0. Since the dimensions of states with different spins are the same<sup>11</sup>

<sup>8</sup> Actually, the Green function without  $V_1$  can be obtained analytically. See Section 2.4.2.

<sup>9</sup> Note that  $V$  represents gluons of its momentum is  $\sim \alpha_s m_t$ . The relevant scale for these soft gluons (or for the potential) is denoted by  $mu_s$ .

<sup>10</sup> This is the convention that is usually used in (modern) relativistic calculations.

<sup>11</sup> Since  $\langle \psi | \psi \rangle$  is probability,  $|\psi\rangle$  is dimensionless. While the dimensions of bases are determined by orthonormality relations. For momentum,  $\langle \mathbf{p} | \mathbf{p}' \rangle = (2\pi)^3 \delta^{(3)}(\mathbf{p} - \mathbf{p}')$  means  $\dim[|\mathbf{p}\rangle] = \dim[p^{-3/2}]$ . For spins,  $|\mathbf{s}\rangle$  is dimensionless in usual convention.

in NR-Quantum Mechanics, one has to rescale the wave functions for spin-1/2 fields by hand. We may proceed as follows. Free Relativistic Hamiltonian  $H_{\text{free}}^{(R)}$  of  $t\bar{t}$  pair is

$$\begin{aligned} H_{\text{free}}^{(R)} &= \sqrt{(mc^2)^2 + (\mathbf{p}c)^2} \times 2 \\ &= 2mc^2 + \frac{\mathbf{p}^2}{m} - \frac{\mathbf{p}^4}{4m^3c^2} + \mathcal{O}\left(\frac{1}{c^4}\right). \end{aligned} \quad (2.17)$$

Thus, the propagator for one-particle state in a non-Lorentz-covariant QM is

$$\frac{i}{p^0 - \sqrt{(mc^2)^2 + (\mathbf{p}c)^2}} = \frac{i}{p^0 - mc^2 - \frac{\mathbf{p}^2}{2m} + \frac{\mathbf{p}^4}{8m^3c^2} + \mathcal{O}\left(\frac{1}{c^4}\right)}.$$

On the other hand, in Lorentz-covariant QFT, it is

$$\frac{1}{p^2 - m^2 + i\epsilon} = \frac{1}{2p^0} \left[ \frac{1}{p^0 - \sqrt{\mathbf{p}^2 + m^2} + i\epsilon} + \frac{1}{p^0 + \sqrt{\mathbf{p}^2 + m^2} - i\epsilon} \right]$$

or

$$\begin{aligned} \frac{i(\not{p} + m)}{p^2 - m^2 + i\epsilon} &\simeq \frac{i}{p^0 - \sqrt{\mathbf{p}^2 + m^2} + i\epsilon} \frac{\not{p} + m}{2p^0}, \\ \frac{i(\not{p} - m)}{p^2 - m^2 + i\epsilon} &\simeq \frac{i}{p^0 - \sqrt{\mathbf{p}^2 + m^2} + i\epsilon} \frac{\not{p} - m}{2p^0}. \end{aligned}$$

Thus the non-covariant normalization of spinors, which is used for non-relativistic calculations hereafter, is

$$\sum_s u(p, s) \bar{u}(p, s) = \frac{\not{p} + m}{2p^0}, \quad \sum_s v(p, s) \bar{v}(p, s) = \frac{\not{p} - m}{2p^0},$$

or in Dirac representation,

$$u(p, s) = \sqrt{\frac{p^0 + m}{2p^0}} \begin{pmatrix} \chi^s \\ \frac{\mathbf{p} \cdot \boldsymbol{\sigma}}{p^0 + m} \chi^s \end{pmatrix}, \quad v(p, s) = u^c(p, s) = C \bar{u}(p, s)^\top,$$

where  $C$  is charge conjugation matrix defined in Section A.3.2.

### 2.3.2 Breit-Fermi potential $V_{\text{BF}}$

The potential  $\tilde{V}$  (in momentum space) between  $t\bar{t}$  can be obtained by calculating the matrix element  $\mathcal{M}$  for the elastic scattering of  $t\bar{t}$ ,  $t(p)\bar{t}(\bar{p}) \rightarrow t(p')\bar{t}(\bar{p}')$ , in QFT and comparing this with the formula in Born approximation, which is proportional to  $\tilde{V}(\mathbf{k})$ , where  $\mathbf{k}$  is the momentum transfer. Working in the CM frame of  $t\bar{t}$ , the system can be dealt with one particle QM [Section A.2.1]. Let us define<sup>12</sup>  $k \equiv p' - p$ ,  $K \equiv (p' + p)/2$ , or  $p' = K + \frac{1}{2}k$ ,  $p = K - \frac{1}{2}k$ .

<sup>12</sup> Note that  $k$  is not relative momentum but momentum transfer; likewise  $K$  is not total momentum.

Using  $p^0 = mc^2 + \mathbf{p}^2/(2m) + \mathcal{O}(1/c^2)$  etc.,

$$\begin{aligned}\bar{u}(p')\gamma^0 u(p) &= \chi_t'^{\dagger} \left[ 1 + \frac{1}{c^2} \frac{-\mathbf{k}^2 + 2i\boldsymbol{\sigma}_t \cdot (\mathbf{k} \times \mathbf{K})}{8m^2} + \mathcal{O}\left(\frac{1}{c^4}\right) \right] \chi_t, \\ \bar{u}(p')\gamma^i u(p) &= \chi_t'^{\dagger} \left[ \frac{1}{c} \frac{2K^i - i\epsilon^{ijk} k^j \sigma_t^k}{2m} + \mathcal{O}\left(\frac{1}{c^3}\right) \right] \chi_t.\end{aligned}$$

The corresponding expressions for

$$\bar{v}(\bar{p})\gamma^\mu v(\bar{p}') = -\bar{v}^c(\bar{p}')(\gamma^\mu)^c v^c(\bar{p}) = +\bar{u}(\bar{p}')\gamma^\mu u(\bar{p})$$

can be obtained by replacing  $\mathbf{k} \rightarrow -\mathbf{k}$ ,  $\mathbf{K} \rightarrow -\mathbf{K}$ ,  $\boldsymbol{\sigma}_t \rightarrow \boldsymbol{\sigma}_{\bar{t}}$ ,  $\chi_t^{(\prime)} \rightarrow \chi_{\bar{t}}^{(\prime)}$ . Thus in Coulomb gauge<sup>13</sup> [Section A.6.2],

$$\begin{aligned}i\mathcal{M} &= (-C_F)(-ig_s)^2 \left[ \bar{u}(p')\gamma^0 u(p) \cdot \bar{u}(\bar{p}')\gamma^0 u(\bar{p}) \cdot D^{00} + \bar{u}(p')\gamma^i u(p) \cdot \bar{u}(\bar{p}')\gamma^j u(\bar{p}) \cdot D^{ij} \right] \\ &= (-i)\chi_t'^{\dagger} \chi_{\bar{t}}'^{\dagger} \tilde{V}_{\text{BF}}(\mathbf{p}', \mathbf{p}) \chi_t \chi_{\bar{t}},\end{aligned}$$

where  $V_{\text{BF}}$  is the Breit-Fermi potential [41]:

$$\begin{aligned}\tilde{V}_{\text{BF}}(\mathbf{p}', \mathbf{p}) &= \langle \mathbf{p}' | V_{\text{BF}} | \mathbf{p} \rangle \\ &= -4\pi C_F \alpha_s \left[ \frac{1}{\mathbf{k}^2} + \frac{1}{2m^2 c^2} \left( \frac{\mathbf{p}'^2}{\mathbf{k}^2} + \frac{\mathbf{p}^2}{\mathbf{k}^2} \right) - \frac{1}{2m^2 c^2} \left( \frac{(\mathbf{p}' \cdot \mathbf{k})^2}{(\mathbf{k}^2)^2} + \frac{(\mathbf{k} \cdot \mathbf{p})^2}{(\mathbf{k}^2)^2} \right) + \frac{1}{4m^2 c^2} \right. \\ &\quad \left. + \frac{3i}{4m^2 c^2} \left( \frac{\mathbf{k} \times \mathbf{p}'}{\mathbf{k}^2} \cdot \mathbf{S} + \frac{\mathbf{k} \times \mathbf{p}}{\mathbf{k}^2} \cdot \mathbf{S} \right) - \frac{1}{2m^2 c^2} \left( \mathbf{S}^2 - \frac{(\mathbf{S} \cdot \mathbf{k})^2}{\mathbf{k}^2} \right) + \mathcal{O}\left(\frac{1}{c^4}\right) \right],\end{aligned}$$

where  $\mathbf{k} = \mathbf{p}' - \mathbf{p}$ ,  $\mathbf{S} = \mathbf{S}_t + \mathbf{S}_{\bar{t}}$  and  $\mathbf{S}_t = \boldsymbol{\sigma}_t/2$ ,  $\mathbf{S}_{\bar{t}} = \boldsymbol{\sigma}_{\bar{t}}/2$ . There are several remarks. Since the overall phase of  $\mathcal{M}$  is unphysical, relation between  $i\mathcal{M}$  and  $\tilde{V}$  is determined so as to reproduce the Coulomb potential at the leading order. We rewrote  $\mathbf{K}$  with  $\mathbf{p}, \mathbf{p}', \mathbf{k}$  in a symmetric way:

$$\begin{aligned}4\mathbf{K}^2 &= 2\mathbf{p}'^2 + 2\mathbf{p}^2 - \mathbf{k}^2, \\ 4(\mathbf{k} \cdot \mathbf{K})^2 &= 2(\mathbf{p}' \cdot \mathbf{k})^2 + (\mathbf{k} \cdot \mathbf{p})^2 - (\mathbf{k}^2)^2, \\ \mathbf{k} \times \mathbf{K} &= \frac{1}{2}(-\mathbf{p}' \times \mathbf{k} + \mathbf{k} \times \mathbf{p}).\end{aligned}$$

This makes the hermiticity of  $V_{\text{BF}}$  transparent. Due to  $\mathcal{CP}$  invariance of QCD,  $V_{\text{BF}}$  is symmetric under  $\mathbf{S}_t \leftrightarrow \mathbf{S}_{\bar{t}}$  [Equations 4.5 and A.52]. They are conveniently expressed in terms of the total spin  $\mathbf{S}$ :

$$\mathbf{S}_t \cdot \mathbf{S}_{\bar{t}} = \frac{1}{2} \left( \mathbf{S}^2 - \frac{3}{2} \right), \quad (\mathbf{S}_t \cdot \mathbf{k})(\mathbf{S}_{\bar{t}} \cdot \mathbf{k}) = \frac{1}{2} \left( (\mathbf{S} \cdot \mathbf{k})^2 - \frac{\mathbf{k}^2}{2} \right).$$

The  $\tilde{V}_{\text{BF}}$  depends not only on  $\mathbf{k}$  but also on  $\mathbf{K}$ . This means the potential is momentum dependent [Section A.2.3]. This can be seen clearly in the coordinate-space representation given below.

<sup>13</sup> In fact  $V_{\text{BF}}$  depends on the choice of gauge, and is not hermitian in general. However Coulomb gauge gives hermitian result.



The Breit-Fermi potential  $V_{\text{BF}}(r)$  in coordinate-space can be obtained by Fourier transform:

$$V_{\text{BF}}(\mathbf{r}) \delta^{(3)}(\mathbf{r}' - \mathbf{r}) = \langle \mathbf{r}' | V_{\text{BF}} | \mathbf{r} \rangle = \int \frac{d^3 p'}{(2\pi)^3} \frac{d^3 p}{(2\pi)^3} e^{i(\vec{p}' \cdot \mathbf{r}' - \vec{p} \cdot \mathbf{r})} \tilde{V}_{\text{BF}}(\mathbf{p}', \mathbf{p}),$$

where  $\mathbf{r}$  ( $\mathbf{r}'$ ) is the relative coordinate for the initial (final) state. With

$$\begin{aligned} & d^3 p' d^3 p && \mathbf{p}' \cdot \mathbf{r}' - \mathbf{p} \cdot \mathbf{r} \\ = & d^3 k d^3 p && = \mathbf{k} \cdot \mathbf{r}' + \mathbf{p} \cdot (\mathbf{r}' - \mathbf{r}) \\ = & d^3 p' d^3 k && = \mathbf{p}' \cdot (\mathbf{r}' - \mathbf{r}) + \mathbf{k} \cdot \mathbf{r} \\ = & d^3 K d^3 k, && = \mathbf{K} \cdot (\mathbf{r}' + \mathbf{r})/2 + \mathbf{k} \cdot (\mathbf{r}' - \mathbf{r}), \end{aligned}$$

and

$$\begin{aligned} & \int \frac{d^3 k}{(2\pi)^3} e^{i\vec{k} \cdot \vec{r}} 4\pi \left\{ 1, \frac{k^i k^j}{\mathbf{k}^2}; \frac{1}{|\mathbf{k}|}, \frac{k^i}{\mathbf{k}^2}; \frac{1}{\mathbf{k}^2}, \frac{k^i k^j}{(\mathbf{k}^2)^2} \right\} \\ = & \left\{ 4\pi \delta^{(3)}(\mathbf{r}), \frac{1}{r^3} \left( \delta^{ij} - 3 \frac{r^i r^j}{r^2} \right) + \frac{4\pi}{3} \delta^{ij} \delta^{(3)}(\mathbf{r}); \frac{2}{\pi} \frac{1}{r^2}, \frac{i r^i}{r^3}; \frac{1}{r}, \frac{1}{2r} \left( \delta^{ij} - \frac{r^i r^j}{r^2} \right) \right\}, \end{aligned}$$

we have

$$\begin{aligned} V_{\text{BF}}(\mathbf{r}) = & -\frac{C_F \alpha_s}{r} - \frac{C_F \alpha_s}{2m^2 c^2} \left\{ \frac{1}{r}, \mathbf{p}^2 \right\} + \frac{C_F \alpha_s}{2m^2 c^2} \frac{\mathbf{L}^2}{r^3} + \frac{\pi C_F \alpha_s}{m^2 c^2} \left( 1 + \frac{4}{3} \mathbf{S}^2 \right) \delta^{(3)}(\mathbf{r}) \\ & + \frac{3C_F \alpha_s}{2m^2 c^2} \frac{\mathbf{L} \cdot \mathbf{S}}{r^3} - \frac{C_F \alpha_s}{2m^2 c^2} \frac{1}{r^3} \left( \mathbf{S}^2 - 3 \frac{(\mathbf{S} \cdot \mathbf{r})^2}{r^2} \right) + \mathcal{O}\left(\frac{1}{c^4}\right), \end{aligned} \quad (2.18)$$

where  $\{ , \}$  means anti-commutator, and  $\mathbf{p}$  and  $\mathbf{L} = \mathbf{r} \times \mathbf{p}$  are differential operators that correspond to linear and orbital-angular momentum, respectively. Note that  $\mathbf{L}$  and  $r$  commutes [Section A.2.2]. In this form, one can clearly see that  $V_{\text{BF}}(\mathbf{r})$  is hermitian. The following relations may be useful to compare with the formulas in other literatures:

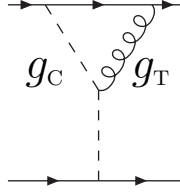
$$\begin{aligned} & \mathbf{S}_t \cdot \mathbf{S}_{\bar{t}} - 3 \frac{(\mathbf{S}_t \cdot \mathbf{r})(\mathbf{S}_{\bar{t}} \cdot \mathbf{r})}{r^2} = \frac{1}{2} \left( \mathbf{S}^2 - 3 \frac{(\mathbf{S} \cdot \mathbf{r})^2}{r^2} \right), \\ - \left\{ \frac{1}{r}, \mathbf{p}^2 \right\} + \frac{\mathbf{L}^2}{r^3} + 4\pi \delta^{(3)}(\mathbf{r}) = & \frac{-1}{r} \left( \mathbf{p}^2 + \frac{1}{r} \mathbf{r} \cdot (\mathbf{r} \cdot \mathbf{p}) \mathbf{p} \right), \\ \left\{ p^i p^j, \frac{1}{2r} \left( \delta^{ij} - \frac{r^i r^j}{r^2} \right) \right\} = & \frac{\mathbf{L}^2}{r^3} + 4\pi \delta^{(3)}(\mathbf{r}). \end{aligned}$$

### 2.3.3 Non-Abelian effect $V_{\text{NA}}$

There is also a potential [42] proportional to  $C_A$ , which is zero for Abelian gauge group (like QED) [Figure 2.3]:

$$\tilde{V}_{\text{NA}}(k) = -\frac{\pi^2 C_A C_F a_s^2}{m_t |\mathbf{k}| c^2}, \quad V_{\text{NA}}(r) = -\frac{C_A C_F a_s^2}{2m_t r^2 c^2}. \quad (2.19)$$

One can see that the potential in momentum space is non-analytic, and in coordinate space it is a strong attractive potential near the origin.

Figure 2.3: Feynman diagram that contributes to  $V_{\text{NA}}$ .

### 2.3.4 Radiative corrections $V_1$ for Coulomb potential

There are also radiative corrections to Coulomb potential. We call this potential Coulombic potential  $V_C$ :

$$V_C(\mathbf{k}^2) = -C_F \frac{4\pi\alpha_s^V(\mathbf{k}^2; \mu^2)}{\mathbf{k}^2}, \quad (2.20)$$

where the coupling in  $V$ -scheme is [43–45]

$$\begin{aligned} \alpha_s^V(\mathbf{k}^2; \mu^2) &= \alpha_s^{\overline{\text{MS}}}(\mu^2) \left[ 1 + \frac{\alpha_s^{\overline{\text{MS}}}(\mu^2)}{4\pi} \left( -\beta_0 \ln \frac{\mathbf{k}^2}{\mu^2} + a_1 \right) \right. \\ &\quad \left. + \left( \frac{\alpha_s^{\overline{\text{MS}}}(\mu^2)}{4\pi} \right)^2 \left( \left( \beta_0 \ln \frac{\mathbf{k}^2}{\mu^2} \right)^2 - (2\beta_0 a_1 + \beta_1) \ln \frac{\mathbf{k}^2}{\mu^2} + a_2 \right) + \dots \right] \\ &= \alpha_s^{\overline{\text{MS}}}(\mathbf{k}^2) \left[ 1 + \frac{\alpha_s^{\overline{\text{MS}}}(\mathbf{k}^2)}{4\pi} a_1 + \left( \frac{\alpha_s^{\overline{\text{MS}}}(\mathbf{k}^2)}{4\pi} \right)^2 a_2 + \dots \right], \quad \text{for } \mu^2 = \mathbf{k}^2. \end{aligned} \quad (2.21)$$

Here the first expression is for fixed order series, and the second for Renormalization-Group (RG) improved series,  $\mu^2 = \mathbf{k}^2$ . In Section 2.2.4 we wrote the log corrections as  $V_1$ :

$$V_C(\mathbf{k}^2) = -C_F \frac{4\pi\alpha_s^{\overline{\text{MS}}}}{\mathbf{k}^2} + V_1(\mathbf{k}^2).$$

The potential  $V_C(r)$  for coordinate space can be obtained analytically only for the fixed-order series:

$$V_C(r) = -C_F \frac{\bar{\alpha}_s^V(1/r; \mu)}{r} = -\frac{C_F \alpha_s^{\overline{\text{MS}}}}{r} + V_1(r), \quad (2.22)$$

where

$$\begin{aligned} \bar{\alpha}_s^V(1/r; \mu) &= \alpha_s^{\overline{\text{MS}}}(\mu^2) \left[ 1 + \frac{\alpha_s^{\overline{\text{MS}}}(\mu^2)}{4\pi} \{ 2\beta_0 \ln(\mu r e^{\gamma_E}) + a_1 \} \right. \\ &\quad \left. + \left( \frac{\alpha_s^{\overline{\text{MS}}}(\mu^2)}{4\pi} \right)^2 \left\{ \beta_0^2 \left( 4 \ln^2(\mu r e^{\gamma_E}) + \frac{\pi^2}{3} \right) + 2(\beta_1 + 2\beta_0 a_1) \ln(\mu r e^{\gamma_E}) + a_2 \right\} \right]. \end{aligned} \quad (2.23)$$

We can see

$$\bar{\alpha}_s^V(1/r; \mu) \simeq \alpha_s^V(\mathbf{k}^2 = 1/r'^2; \mu^2), \quad r' \equiv r e^{\gamma_E}$$

aside from  $\pi^2/3$ . Here  $\gamma_E = 0.5772\dots$  is Euler-Mascheroni constant, and originates from the Fourier transform:

$$\int \frac{d^3k}{(2\pi)^3} \frac{\ln(\mathbf{k}^2) e^{i\vec{k}\cdot\vec{r}}}{\mathbf{k}^2} = \frac{-1}{4\pi r} [\ln(r^2) + 2\gamma_E] .$$

Coefficients  $a_1$  and  $a_2$  are coefficients for  $\mathcal{O}(1/c)$  and  $\mathcal{O}(1/c^2)$  corrections, respectively:

$$\begin{aligned} a_1 &= \frac{31}{9}C_A - \frac{20}{9}T_F n_f = \frac{31}{3} - \frac{10}{9}n_f = 4.77778\dots , \\ a_2 &= \left( \frac{4343}{162} + 4\pi^2 - \frac{\pi^4}{4} + \frac{22}{3}\zeta_3 \right) C_A^2 - \left( \frac{1798}{81} + \frac{56}{3}\zeta_3 \right) C_A T_F n_f \\ &\quad - \left( \frac{55}{3} - 16\zeta_3 \right) C_F T_F n_f + \left( \frac{20}{9}T_F n_f \right)^2 \\ &= 456.749 - 66.3542 n_f + 1.23457 n_f^2 = 155.842\dots . \end{aligned} \quad (2.24)$$

Group theoretic factors  $C_F$  etc. are given in Section A.1.1. In the first calculation of  $\mathcal{O}(\alpha_s^2)$  correction [44], the  $4\pi^2$  in  $C_A^2$  term of  $a_2$  was incorrectly calculated to be  $6\pi^2$ . With this,

$$a_2^{(\text{old})} = 634.402 - 66.3542 n_f + 1.23457 n_f^2 = 333.495\dots .$$

Thus the correct value [45] of  $a_2$  is less than half of  $a_2^{(\text{old})}$ .

Since  $a_2$  is a coefficient of  $\mathcal{O}(1/c^2)$  correction, one can expect better convergence with the correction to  $a_2$ . However for fixed order calculation,  $\ln(k/\mu_s)$  term disturbs this naive expectation. While for RG improved calculation, the size of  $\mathcal{O}(1/c^2)$  correction is diminished by 2.

Coefficients  $\beta_0$  and  $\beta_1$  determine the RG flow of QCD coupling  $\alpha_s(\mu)$ . These first two coefficients are independent to renormalization scheme:

$$\begin{aligned} \frac{\partial}{\partial \ln \mu^2} \left( \frac{4\pi}{\alpha_s(\mu^2)} \right) &= \beta_0 + \beta_1 \frac{\alpha_s(\mu^2)}{4\pi} + \beta_2 \left( \frac{\alpha_s(\mu^2)}{4\pi} \right)^2 + \dots , \quad \text{or} \\ \mu \frac{\partial \alpha_s}{\partial \mu} &= -\frac{\beta_0}{2\pi} \alpha_s^2 - \frac{\beta_1}{8\pi^2} \alpha_s^3 - \frac{\beta_2}{32\pi^3} \alpha_s^4 - \dots , \end{aligned}$$

where

$$\begin{aligned} \beta_0 &= \frac{11}{3}C_A - \frac{4}{3}T_F n_f = 11 - \frac{2}{3}n_f = 7.66667\dots , \\ \beta_1 &= \frac{34}{3}C_A^2 - \frac{20}{3}C_A T_F n_f - 4C_F T_F n_f = 2 \left( 51 - \frac{19}{3}n_f \right) = 38.6667\dots . \end{aligned} \quad (2.25)$$

At the leading order of running, one have

$$\alpha_s(\mu^2) = \frac{\alpha_s(M^2)}{1 + \frac{\beta_0 \alpha_s(M^2)}{4\pi} \log \frac{\mu^2}{M^2}} = \frac{4\pi}{\beta_0 \log \frac{\mu^2}{\Lambda^2}} ,$$

where  $\Lambda^2 = M^2 \exp\left(\frac{-4\pi}{\beta_0 \alpha_s(M^2)}\right)$ . If we identify  $\alpha_s(\mu)/\pi$  and  $(\alpha_s(\mu)/\pi) \ln(\mu^2/k^2)$  to be the expansion parameters, then the coefficients are

$$\begin{aligned} \frac{\beta_0}{4} &= 1.91667\dots , & \frac{\beta_1}{16} &= 2.41667\dots , \\ \frac{a_1}{4} &= 1.19444\dots , & \frac{a_2}{16} &= 9.74014\dots . \end{aligned}$$

One can see that the finite term of  $\mathcal{O}(\alpha_s^2)$  correction  $a_2/16$  is large compared to the other.

## RG improved Coulombic potential

As can be seen in Eqs. (2.21) and (2.23), leading log's,  $\sum(\alpha_s \ln)^n$ , in  $V_C$  can be summed up either in momentum space ( $\mu = k$ ) or in coordinate space ( $\mu = 1/r'$ ). However as we saw above, there is an extra term  $\pi^2/3$  in  $\alpha_s^2$  term for the coordinate space potential. Thus it seems that RG improvement in momentum space is better. The potential in coordinate space is obtained by numerical Fourier transform. There is another advantage<sup>14</sup> for this prescription, which is related to the “renormalon cancellation”, where the infrared part of  $\tilde{V}_C(k)$  plays an important role. However let us postpone this subject until Section 2.7.

Scale dependence of  $\alpha_V(q, \mu_s)$  and  $\alpha_s^{\overline{\text{MS}}}(\mu_s)$  are shown in Figure 2.4 for  $\mu_s = 20$  GeV, 75 GeV, and  $q$ . One can see that perturbative convergence is improved by the RG prescription  $\mu_s = q$  over the whole relevant momentum scale. Since the coupling becomes stronger as higher orders are taken into account, it is expected that the binding energy becomes larger with higher order corrections. Scaling behavior of  $\overline{\text{MS}}$  coupling is also shown for comparison. It is similar but higher order corrections are much smaller. In fact one can hardly distinguish 2-loop and 3-loop running. This is because  $a_2$  (and  $a_1$ ) is large. See the relation of V-scheme coupling to  $\overline{\text{MS}}$ -scheme coupling [Eq. (2.21)]. Also shown is the straight line  $q/(C_F m_t/2)$ . The solution  $q/(C_F m_t/2) = \alpha_V(q)$ , or

$$\mu_s = C_F \alpha_V(\mu_s) m_t / 2$$

gives Bohr momentum  $p_B = \mu_s$ . We can see that  $p_B \simeq 20$  GeV and  $\alpha_V(p_B) \simeq 0.16$ .

As shall be explained in Section 2.6.1, the normalization of the total cross section is determined by the strength of the attractive force  $dV/dr$  between  $t\bar{t}$ . This is shown in Figure 2.5. One can see that the perturbative convergence is worse for  $\mu_s = 20$  GeV  $\simeq p_B$  than for  $\mu_s = 75$  GeV or  $\mu_s = q$ .

## 2.4 Reduced Green function $G'$

### 2.4.1 $G$ in terms of $G'$

As was explained above, the Hamiltonian  $H$  to NNLO ( $= \mathcal{O}(1/c^2)$ ) [Eq. (2.14)] is not convenient for numerical calculation. Thus following [27], we rewrite the Green function  $G$  for  $H$  in this section.

We are interested in a Green function  $G(r, r')$  that is projected to the  $S$ -wave. In operator language, it is defined as follows [Section A.2.4]:

$$G \equiv \frac{1}{H - \omega}, \quad \omega \equiv E + i\Gamma_t, \quad (2.26)$$

$$G(\mathbf{r}, \mathbf{r}') \equiv \langle \mathbf{r} | G | \mathbf{r}' \rangle, \quad G(r, r') \equiv \int \frac{d\Omega_r}{4\pi} \frac{d\Omega_{r'}}{4\pi} G(\mathbf{r}, \mathbf{r}').$$

Here  $H$  is defined in Eq. (2.14). Using operator identities derived in Section A.2.2

$$[\mathbf{p}^2, ip_r] = 4\pi\delta^{(3)}(\mathbf{r}) + \frac{2\mathbf{L}^2}{r^3}, \quad \left[\frac{1}{r}, ip_r\right] = \frac{1}{r^2},$$

<sup>14</sup> It was argued in [46] that large theoretical uncertainty remains even after the RG improvement of  $V_C$ . This claim was based on a large discrepancy between results of renormalization-group improvements in momentum space and in coordinate space. However in view of “renormalon cancellation”, momentum space is better.

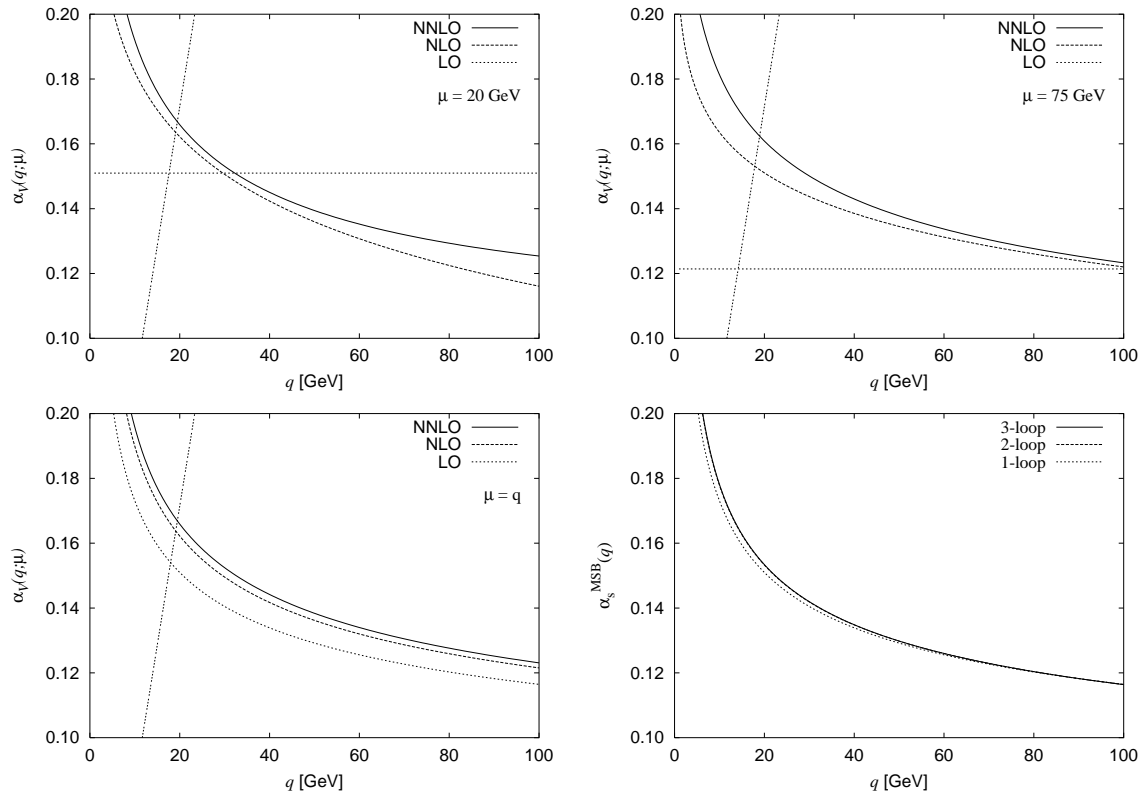


Figure 2.4: The momentum-space couplings  $\alpha_V$  vs. momentum transfer  $q$  at LO (dot-dashed), NLO (dashed), and NNLO (solid). Two are fixed order ( $\mu_s = 20$  GeV, 75 GeV), and one is RG improved ( $\mu_s = q$ ). Intersection of  $\alpha_V$  and the straight line  $q/(C_F m_t/2)$ , which is also shown, gives Bohr momentum  $p_B$  and the coupling  $\alpha_V(p_B)$  at the scale  $p_B$  [Section B.3]. Running of  $\overline{\text{MS}}$  coupling is also shown for reference.

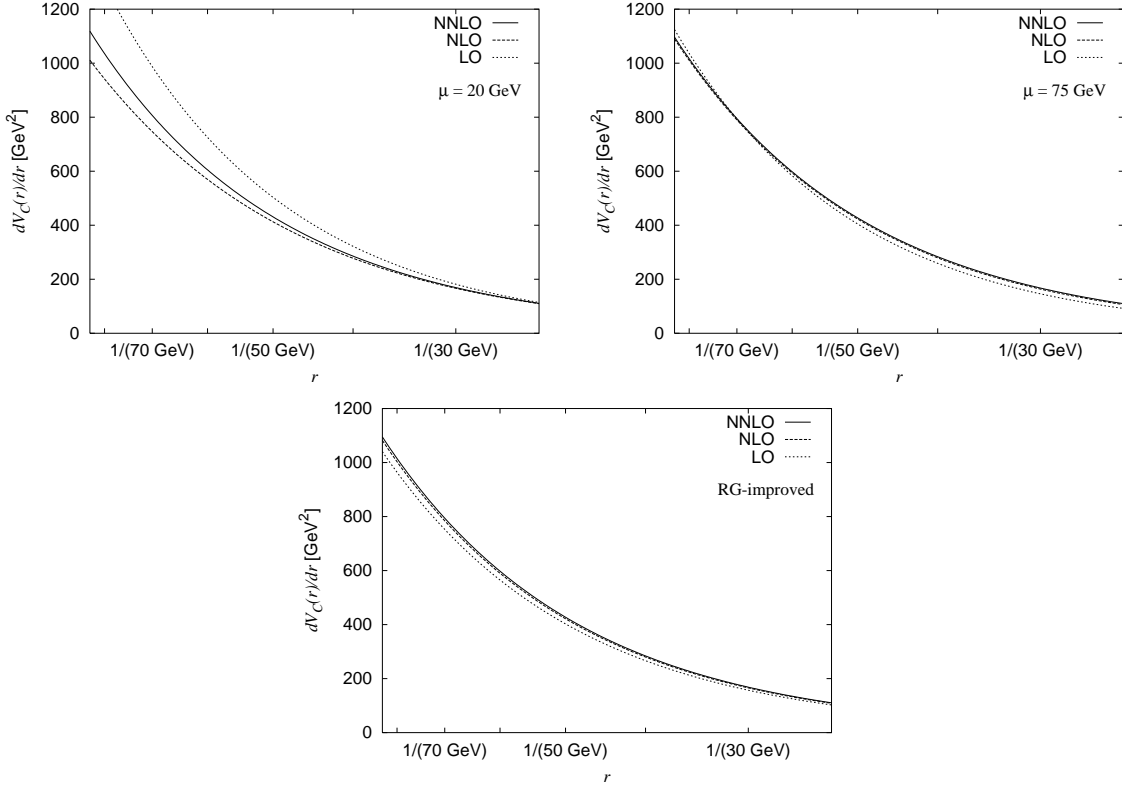


Figure 2.5: Attractive force  $dV/dr$  due to Coulombic potential  $V_C$ , with  $\mu_s = 20 \text{ GeV}$ ,  $75 \text{ GeV}$ ,  $q$ .

or

$$\frac{4\pi}{m_t} \delta^{(3)}(\mathbf{r}) = [H_0, ip_r] - \frac{2\mathbf{L}^2}{m_t r^3} + \frac{C_F a_s}{r^2},$$

$$\left(\frac{\mathbf{p}^2}{m_t}\right)^2 = H_0^2 + \left\{ H_0, \frac{C_F a_s}{r} \right\} + \frac{C_F^2 a_s^2}{r^2},$$

the momentum dependent  $\mathcal{O}(1/c^2)$  potential  $U(\mathbf{p}, \mathbf{r})$  can be rewritten as follows:

$$\begin{aligned} U(\mathbf{p}, \mathbf{r}) &= -\frac{1}{4m_t c^2} H_0^2 - \frac{C_F^2 a_s^2}{2m_t c^2} \left( \frac{2}{3}(3 - \mathbf{S}^2) + \frac{C_A}{C_F} \right) \frac{1}{r^2} \\ &\quad - \frac{3C_F a_s}{4m_t c^2} \left\{ H_0, \frac{1}{r} \right\} + \frac{3 + 4\mathbf{S}^2}{12} \frac{C_F a_s}{m_t c^2} [H_0, ip_r] \\ &\quad - \frac{2C_F a_s}{3m_t^2 c^2} \frac{\mathbf{L}^2 \mathbf{S}^2}{r^3} + \frac{3C_F a_s}{2m_t^2 c^2} \frac{\mathbf{L} \cdot \mathbf{S}}{r^3} - \frac{C_F a_s}{2m_t^2 c^2} \frac{1}{r^3} \left( \mathbf{S}^2 - 3 \frac{(\mathbf{S} \cdot \mathbf{r})^2}{r^2} \right) \\ &= -\frac{1}{4m_t c^2} H_0^2 - \frac{C_F^2 a_s^2}{2m_t c^2} \left( \frac{2}{3} + \frac{C_A}{C_F} \right) \frac{1}{r^2} \\ &\quad - \frac{3C_F a_s}{4m_t c^2} \left\{ H_0, \frac{1}{r} \right\} + \frac{11C_F a_s}{12m_t c^2} [H_0, ip_r], \end{aligned}$$

where the last expression is for the  $S$ -wave. We concentrate on the  $S$ -wave hereafter. To

summarize,

$$\begin{aligned}
H &= H_0 + V_1 + U , \\
U &= bH_0^2 + \{H_0, \mathcal{O}_E\} + [H_0, \mathcal{O}_O] + W , \\
b &\equiv \frac{-1}{4m_t c^2} , \quad \mathcal{O}_E \equiv \frac{-3C_F a_s}{4m_t c^2} \frac{1}{r} , \quad \mathcal{O}_O \equiv \frac{11C_F a_s}{12m_t c^2} i p_r , \\
W &\equiv -\frac{C_F^2 a_s^2}{2m_t c^2} \left( \frac{2}{3} + \frac{C_A}{C_F} \right) \frac{1}{r^2} \equiv -\frac{\kappa}{m_t r^2 c^2} .
\end{aligned} \tag{2.27}$$

Note that  $\mathcal{O}_O$  is anti-hermitian, and thus  $U$  is hermitian. Using this expression for  $U$ , we can rewrite  $G$  up to  $\mathcal{O}(1/c^3)$ :

$$\begin{aligned}
G &= \frac{1}{H_0 + V_1 + U - \omega} \\
&\simeq \frac{1}{H_0 - \omega} - \frac{1}{H_0 - \omega} (V_1 + U) \frac{1}{H_0 - \omega} + \frac{1}{H_0 - \omega} V_1 \frac{1}{H_0 - \omega} V_1 \frac{1}{H_0 - \omega} \\
&\simeq -b + (1 - b\omega - \mathcal{O}_E - \mathcal{O}_O) \frac{1}{H_0 - \omega} (1 - b\omega - \mathcal{O}_E + \mathcal{O}_O) \\
&\quad - \frac{1}{H_0 - \omega} (V_1 + b\omega^2 + 2\omega\mathcal{O}_E + W) \frac{1}{H_0 - \omega} + \frac{1}{H_0 - \omega} V_1 \frac{1}{H_0 - \omega} V_1 \frac{1}{H_0 - \omega} \\
&\simeq -b + (1 - b\omega - \mathcal{O}_E - \mathcal{O}_O) \frac{1}{H_0 + V_1 + b\omega^2 + 2\omega\mathcal{O}_E + W - \omega} (1 - b\omega - \mathcal{O}_E + \mathcal{O}_O) ,
\end{aligned}$$

or

$$\begin{aligned}
G &= G' - \{b\omega + \mathcal{O}_E, G'\} - [\mathcal{O}_O, G'] - b + \mathcal{O}\left(\frac{1}{c^3}\right) , \\
G' &\equiv \frac{1}{H' - \mathcal{E}} , \quad H' \equiv H_0 + V_1 + 2\omega\mathcal{O}_E + W , \quad \mathcal{E} \equiv \omega - b\omega^2 .
\end{aligned} \tag{2.28}$$

Note that  $H'$  does not contain neither  $p^4$  nor  $\delta(\mathbf{r})$ :

$$H' = \frac{p^2}{m} - \frac{C_F \bar{a}_s}{r} + V_1(r) - \frac{\kappa}{m r^2 c^2} , \tag{2.29}$$

where

$$\bar{a}_s \equiv a_s \left( 1 + \frac{3}{2} \frac{E + i\Gamma}{m c^2} \right) , \quad \mathcal{E} \equiv (E + i\Gamma) \left( 1 + \frac{E + i\Gamma}{4m c^2} \right) ,$$

and

$$\begin{aligned}
\kappa &\equiv \frac{C_F^2}{2} \left( \frac{2}{3} + \frac{C_A}{C_F} \right) \left( \frac{a_s}{c} \right)^2 \\
&= 2.5926 a_s^2 = 0.06637 \times \left( \frac{a_s}{0.16} \right)^2 .
\end{aligned} \tag{2.30}$$

Thus numerical calculation of Green function is much easier for  $G'$  than  $G$  itself. In terms of

c-number functions, they are related as

$$\begin{aligned}
G(r, r') &= \left[ 1 + \frac{E + i\Gamma}{2mc^2} + \frac{3C_F}{4} \left(\frac{a_s}{c}\right)^2 \left( \frac{1}{ma_s r} + \frac{1}{ma_s r'} \right) \right. \\
&\quad \left. - \frac{11C_F}{12} \left(\frac{a_s}{c}\right)^2 \left( \frac{1}{ma_s r} \frac{d}{dr} r + \frac{1}{ma_s r'} \frac{d}{dr'} r' \right) \right] G'(r, r') \\
&\quad + \frac{1}{4mc^2} \frac{1}{4\pi r r'} \delta(r - r') + \mathcal{O}\left(\frac{1}{c^3}\right) \\
&= \left[ 1 + \frac{E + i\Gamma}{2mc^2} - \frac{C_F}{6} \left(\frac{a_s}{c}\right)^2 \left( \frac{1}{ma_s r} + \frac{1}{ma_s r'} \right) + \frac{11C_F^2}{12} \left(\frac{a_s}{c}\right)^2 \right] G'(r, r') \\
&\quad + \frac{1}{4mc^2} \frac{1}{4\pi r r'} \delta(r - r') + \mathcal{O}\left(r, r' \frac{1}{c^3}\right), \tag{2.31}
\end{aligned}$$

where we used the relation Eq. (B.9) for the Coulomb Green function. Note that the difference is higher order. Thus,

$$\begin{aligned}
&\text{Im } G(r_0, r_0) \\
&= \left[ 1 + \left(\frac{a_s}{c}\right)^2 \left( \frac{-C_F}{3ma_s r_0} + \frac{11C_F^2}{12} \right) \right] \text{Im} \left[ \left( 1 + \frac{E + i\Gamma}{2m^2 c^2} \right) G'(r_0, r_0) \right] + \mathcal{O}\left(r_0, \frac{1}{c^3}\right). \tag{2.32}
\end{aligned}$$

## 2.4.2 Green function for Coulomb plus $1/r^2$ potentials

In this section, we consider the Hamiltonian,

$$H = \frac{p^2}{m} - \frac{C_F a_s}{r} - \frac{\kappa}{mr^2 c^2}, \tag{2.33}$$

because (i) the Green function  $G$  (projected to  $S$ -wave) can be obtained analytically; and (ii) the Green function  $G'$  for  $H'$  in Eq. (2.29) without log corrections  $V_1(r)$  can be obtained by replacing  $a_s \rightarrow \bar{a}_s$ ,  $E \rightarrow \mathcal{E}$ . The results for pure Coulomb potential, which we shall use several times, are also obtained by expanding in  $\kappa$ .

The Schrödinger equation for  $G(\vec{r}, \vec{r}')$  is

$$\left[ E - \left( -\frac{\Delta_{\vec{r}}}{m} - \frac{C_F \alpha_s}{r} - \frac{\kappa}{mr^2} \right) \right] G(\vec{r}, \vec{r}') = -\delta^{(3)}(\vec{r} - \vec{r}'),$$

where  $r = |\vec{r}|$ . We are interested in the Green function  $G(r, r')$  projected to  $S$ -wave:

$$\left[ E - \left( \frac{-1}{mr} \frac{\partial^2}{\partial r^2} r - \frac{C_F \alpha_s}{r} - \frac{\kappa}{mr^2} \right) \right] G(r, r') = \frac{-1}{4\pi r r'} \delta(r - r').$$

To simplify the equation, we introduce the following notations:

$$G(r, r') = \frac{g(r, r')}{r r'}, \quad z = C_F \alpha_s m r, \quad \nu^2 = \frac{(C_F \alpha_s)^2 m}{4E}. \tag{2.34}$$

Here  $z$  is  $r$  measured in unit of (twice) the Bohr radius  $p_B$ , and  $1/\nu^2$  is  $E$  in the unit of the Bohr energy  $E_B$  [Eq. (B.7)]. Thus by dividing by  $(C_F \alpha_s)^2 m$ , we have

$$\left( \frac{1}{4\nu^2} + \frac{\partial^2}{\partial z^2} + \frac{1}{z} + \frac{\kappa}{z^2} \right) g(z, z') = \frac{-1}{4\pi C_F \alpha_s} \delta(z - z'),$$



where  $g(z, z')$  is just  $g(r, r')$  without rescaling:

$$g(z, z') = g\left(r = z/(C_F \alpha_s m), r' = z'/(C_F \alpha_s m)\right) ,$$

while the normalization of  $\delta$ -function changes according to  $\pi\delta(z) = \text{Im}[1/(z - i\epsilon)]$ . Solutions with  $\delta$ -function source can be obtained by the solutions without  $\delta$ -functions:

$$g(z, z') = \frac{1}{4\pi C_F \alpha_s W} [g_{<}(z)g_{>}(z')\theta(z' - z) + g_{<}(z')g_{>}(z)\theta(z - z')] , \quad (2.35)$$

where  $W$  is the Wronskian<sup>15</sup>,

$$W \equiv W(g_{>}, g_{<}; z) \equiv \begin{vmatrix} g_{>}(z) & g_{<}(z) \\ g'_{>}(z) & g'_{<}(z) \end{vmatrix} = g_{>}(z)g'_{<}(z) - g_{<}(z)g'_{>}(z) ,$$

and the function  $g_{>}(z)$  ( $g_{<}(z)$ ) is the solution to the homogeneous differential equation:

$$\left( \frac{1}{4\nu^2} + \frac{d^2}{dz^2} + \frac{1}{z} + \frac{\kappa}{z^2} \right) g(z) = 0 , \quad (2.36)$$

which is “well-behaved” at  $z \rightarrow \infty$  ( $z \rightarrow 0$ ). Since we use the value of the Green function near the origin, it is important to know its behavior around there. For  $\kappa > 0$ , which is the case, the potential is dominated by  $1/z^2$  near the origin. Assuming a solution of power behavior,

$$\left( \frac{d^2}{dz^2} + \frac{\kappa}{z^2} \right) z^d \simeq 0 ,$$

one obtains

$$d = \frac{1 \pm \sqrt{1 - 4\kappa}}{2} \equiv d_{\pm} , \quad d_+ + d_- = 1 , \quad d_+ d_- = \kappa . \quad (2.37)$$

This may indicate that the wave function is collapsed into the origin when the attractive force is as strong as  $\kappa > 1/4$ . However we don't have to worry about this because  $\kappa \sim 0.06$  for our case. For small  $\kappa$ ,  $d_+ \simeq 1 - \kappa$ ,  $d_- \simeq \kappa$ . Thus in order to obtain the results for Coulomb potential, it is convenient to write  $d_+$  ( $= 1 - d_-$ ) in terms of  $d_-$ . For both choice of  $d_{\pm}$ ,  $g(z)/z$  diverges at the origin, but it's milder for  $d_+$ . Thus  $g_{<}(z) \sim z^{d_+}$  near the origin. For Coulomb ( $\kappa = 0$ ), two independent solutions are

$$z - \frac{1}{2}z^2 + \mathcal{O}(z^3) , \quad 1 - z \ln z + \mathcal{O}(z^2 \ln z) .$$

In order for  $g(z)/z$  to be finite at the origin,  $g_{<}(z) \sim z - \frac{1}{2}z^2$ .

Further calculations are done in Section B.2. Especially, results for pure Coulomb potential, which we frequently refer to, is collected in Section B.3.

<sup>15</sup> One can easily show that the Wronskian  $W$  for the two solutions of a 2nd-rank homogeneous ordinary differential equation without 1st-derivative term, is independent of  $z$ :

$$\frac{dW}{dz} = 0 .$$

Thus one can calculate  $W$  wherever he/she wants.

### 2.4.3 Explicit expression for $G'$

The optical theorem shows that all we have to do is to calculate the Green function  $G$ , or  $G'$ , near the origin. The reduced Green function  $G'$  is defined in Eqs. (2.28) and (2.29). Thus we numerically solve the Schrödinger equation

$$\left[ \mathcal{E} - \left( -\frac{\Delta}{m} - \frac{C_F \bar{a}_s}{r} + V_1(r) - \frac{\kappa}{mr^2} \right) \right] \frac{g(r)}{r} = 0, \quad (2.38)$$

or, equivalently,

$$\left( \frac{1}{4\nu^2} + \frac{d^2}{dz^2} + \frac{\kappa}{z^2} + \frac{1}{z} [\ell_2 \ln^2(\tilde{\mu}'z) + \ell_1 \ln(\tilde{\mu}'z) + \ell_0] \right) g(z) = 0,$$

where

$$z = C_F \alpha_s m r, \quad \nu^2 = \frac{(C_F \alpha_s)^2 m}{4\mathcal{E}}, \quad \tilde{\mu}'z = \mu r e^{\gamma_E},$$

and

$$\begin{aligned} \ell_2 &= \left( \frac{a_s}{4\pi} \right)^2 4\beta_0^2, \\ \ell_1 &= \frac{a_s}{4\pi} 2\beta_0 + \left( \frac{a_s}{4\pi} \right)^2 2(\beta_1 + 2\beta_0 a_1), \\ \ell_0 &= 1 + \frac{3(E + i\Gamma)}{2m} + \frac{a_s}{4\pi} a_1 + \left( \frac{a_s}{4\pi} \right)^2 \left( \frac{\pi^2}{3} \beta_0^2 + a_2 \right). \end{aligned}$$

There are two independent solutions for this differential equation. Assuming their form near the origin as

$$g_{\pm}(z) = z^{d_{\pm}} \left[ 1 + z (L_2^{\pm} \ln^2(\tilde{\mu}'z) + L_1^{\pm} \ln(\tilde{\mu}'z) + L_0^{\pm}) + \mathcal{O}(z^2) \right], \quad (2.39)$$

we have

$$\begin{aligned} L_2^{\pm} &= -\frac{\ell_2}{2d_{\pm}}, \\ L_1^{\pm} &= \frac{2d_{\pm} + 1}{2d_{\pm}^2} \ell_2 - \frac{1}{2d_{\pm}} \ell_1, \\ L_0^{\pm} &= -\frac{4d_{\pm}^2 + 2d_{\pm} + 1}{4d_{\pm}^3} \ell_2 + \frac{2d_{\pm} + 1}{4d_{\pm}^2} \ell_1 - \frac{1}{2d_{\pm}} \ell_0. \end{aligned}$$

With these two solutions, solutions (nearly) regular for  $z \rightarrow \infty$  and  $z \rightarrow 0$ , respectively, are

$$g_{>}(r) = g_{-}(z) + B g_{+}(z), \quad g_{<}(r) = g_{+}(z).$$

With the normalization in Eq. (2.39), the Wronskian  $W$  with respect to  $z$  is the same as Eq. (B.6):  $W = \sqrt{1 - 4\kappa}$ . Thus we have

$$\begin{aligned}
\frac{4\pi}{m^2c} G'(r, r') &= \frac{4\pi}{m^2c} \frac{1}{4\pi C_F a_s W} \frac{g_>(z)g_<(z')}{rr'}, \quad (z > z') \\
&= \frac{C_F a_s}{\sqrt{1 - 4\kappa}} \left[ \frac{g_+(z)g_-(z')}{zz'} + B \frac{g_+(z)g_+(z')}{zz'} \right] \\
&\rightarrow \frac{C_F a_s}{\sqrt{1 - 4\kappa}} \left[ \frac{1}{z} \left\{ 1 + z \sum_{i=\pm} \left( L_2^{(i)} \ln^2(\tilde{\mu}'z) + L_1^{(i)} \ln(\tilde{\mu}'z) + L_0^{(i)} \right) + \dots \right\} \right. \\
&\quad \left. + B z^{-2d_-} \left\{ 1 + 2z \left( L_2^{(+)} \ln^2(\tilde{\mu}'z) + L_1^{(+)} \ln(\tilde{\mu}'z) + L_0^{(+)} \right) + \dots \right\} \right] \\
&= \frac{C_F a_s}{\sqrt{1 - 4\kappa}} \left[ \frac{1}{z} + \sum_{i=\pm} \left( L_2^{(i)} \ln^2(\tilde{\mu}'z) + L_1^{(i)} \ln(\tilde{\mu}'z) + L_0^{(i)} \right) + B z^{-2d_-} \right] \\
&\quad + (\text{vanish when } z \rightarrow 0). \tag{2.40}
\end{aligned}$$

where  $\rightarrow$  means  $r = r' = r_0 \rightarrow 0$ .

## 2.5 Matching of NRQCD with QCD

Having taken into account the ‘‘soft’’ gluon contributions, next we consider the effect of ‘‘hard’’ gluons. It is determined by matching the NRQCD calculation to QCD one. Short distance coefficients  $C_1^{(\text{cur})}$ ,  $C_2^{(\text{cur})}$  for  $t\bar{t}$  production current, defined in Eq. (2.8), are determined in the same section to the lowest order of  $\alpha_s$ . Higher orders can be determined by matching the result for Green function method with that for usual perturbative QCD. The Green function method, or NRQCD, can be applied when  $\beta \ll 1$ , while pQCD can be applied when  $\alpha_s/\beta \ll 1$ . Thus both formalism is valid when  $\alpha_s \ll \beta \ll 1$ . For this energy region, Green functions can be calculated perturbatively. While relativistic pQCD calculation was done in [40]. Both of these results are summarized in Section B.4. By demanding these two results to coincide, we obtain  $C_1^{(\text{cur})}$  and  $C_2^{(\text{cur})}$ . Actually for  $C_2^{(\text{cur})}$ , we need only to the leading order, which was obtained already in free-propagating limit [Eq. (2.11)]. With  $C_2^{(\text{cur})} = 1/3$ ,

$$\begin{aligned}
&\left\{ C_1^{(\text{cur})} + C_2^{(\text{cur})} \frac{\Delta_r + \Delta_{r'}}{2m^2c^2} \right\} \text{Im} G(r, r') \Big|_{r, r' \rightarrow r_0} \tag{2.41} \\
&= \left\{ C_1^{(\text{cur})} - \left( \frac{a_s}{c} \right)^2 \frac{C_F}{3ma_s r_0} \right\} \text{Im} \left[ \left( 1 - \frac{E + i\Gamma}{3mc^2} \right) G(r_0, r_0) \right] \\
&= \left\{ C_1^{(\text{cur})} + \left( \frac{a_s}{c} \right)^2 \left( \frac{-2C_F}{3ma_s r_0} + \frac{11}{12} C_F^2 \right) \right\} \text{Im} \left[ \left( 1 + \frac{E + i\Gamma}{6mc^2} \right) G'(r_0, r_0) \right]
\end{aligned}$$

where the equalities are up to  $\mathcal{O}(1/c^3)$ . Here we used Eqs. (2.10) and (2.26), or

$$\begin{aligned}
\left[ -\frac{\Delta_r}{m} - \frac{C_F a_s}{r} - (E + i\Gamma) + \mathcal{O}\left(\frac{1}{c}\right) \right] G(r, r') &= \frac{1}{4\pi r r'} \delta(r - r'), \text{ or} \\
\frac{\Delta_r}{m} \text{Im} G(r, r') &= -\text{Im} \left[ \left( \frac{C_F a_s}{r} + E + i\Gamma \right) G(r, r') \right] + \mathcal{O}\left(\frac{1}{c}\right).
\end{aligned}$$

The same relation holds also for  $G'(r, r')$  since their difference is  $\mathcal{O}(1/c^2)$ . With the definition

$$\begin{aligned} & \left\{ 1 + \left( \frac{\alpha_s(\mu_h)}{\pi} \right) C_F C_1 + \left( \frac{\alpha_s(\mu_h)}{\pi} \right)^2 C_F C_2(r_0) \right\} \\ & \equiv \left\{ C_1^{(\text{cur})} + \left( \frac{a_s}{c} \right)^2 \left( \frac{-2C_F}{3m_t a_s r_0} + \frac{11}{12} C_F^2 \right) \right\} , \end{aligned} \quad (2.42)$$

we have [27]

$$\begin{aligned} C_1 &= -4 , \\ C_2(r_0) &= C_F C_2^A + C_A C_2^{NA} + T_F n_f C_2^L + T_F n_H C_2^H \\ &+ \pi^2 \left( \frac{2}{3} C_F + C_A \right) \ln \left( \frac{r_0}{r_0^{(\text{ref})}} \right) + 2\beta_0 \ln \left( \frac{m_t}{\mu_h} \right) \\ &= -19.17 + 0.611111 n_f + 0.251199 n_H \\ &+ 38.3818 \ln \left( \frac{r_0}{r_0^{(\text{ref})}} \right) + \left( 22 - \frac{4}{3} n_f \right) \ln \left( \frac{m_t}{\mu_h} \right) \\ &= -18.3077 + 38.3818 \ln \left( \frac{r_0}{r_0^{(\text{ref})}} \right) + 15.3333 \ln \left( \frac{m_t}{\mu_h} \right) , \end{aligned} \quad (2.43)$$

$$r_0^{(\text{ref})} \equiv \frac{e^{2-\gamma_E}}{2m_t c} = \frac{2.07433}{m_t c} \quad (2.44)$$

where

$$\begin{aligned} C_2^A &= \frac{39}{4} - \zeta_3 + \pi^2 \left( \frac{4}{3} \ln 2 - \frac{35}{18} \right) = -1.5215 \dots , \\ C_2^{NA} &= -\frac{151}{36} - \frac{13}{2} \zeta_3 + \pi^2 \left( \frac{179}{72} - \frac{8}{3} \ln 2 \right) = -5.71378 \dots , \\ C_2^L &= \frac{11}{9} = 1.22222 \dots , \\ C_2^H &= \frac{44}{9} - \frac{4}{9} \pi^2 = 0.502398 \dots . \end{aligned}$$

Note that the velocity dependence of the matching coefficient is determined by single number:  $C_2^{(\text{cur})} = 1/3$ . Thus it is highly non-trivial that the matching is surely possible.

Let us consider the  $r_0$  dependence of  $R$  ratio for the case  $\Gamma_t = 0$ . Since only  $\ell_0$  and  $L_0^\pm$ , among  $\ell_i$  and  $L_i^\pm$ , have imaginary part, we see from Eq. (2.40),

$$\begin{aligned} \frac{4\pi}{m^2 c} \text{Im} G'(r_0, r_0) &= \frac{C_F a_s}{\sqrt{1-4\kappa}} \left\{ \text{Im} [B] z_0^{-2d_-} + \text{Im} [L_0^+ + L_0^-] \right\} \\ &= \frac{C_F a_s}{\sqrt{1-4\kappa}} \left\{ \text{Im} [B] z_0^{-2d_-} - \frac{3\Gamma_t}{4\kappa m_t} \right\} . \end{aligned}$$

Here we omit the terms that vanish when  $z_0 \rightarrow 0$ . Since  $\kappa$  is a coefficient of  $\mathcal{O}(1/c^2)$  interaction, we need only the terms with the first (or less) order in  $\kappa$ . Thus

$$\begin{aligned} \text{Im} G' &\sim z_0^{-2d_-} = e^{-2d_- \ln z_0} = 1 - 2d_- \ln(z_0) + \dots \\ &= 1 - 2\kappa \ln(z_0) - 2\kappa^2 \ln(z_0)(1 - \ln(z_0)) + \dots \end{aligned}$$

where  $z_0 = C_F \alpha_s(\mu_s) m_t r_0$ . While  $r_0$  dependence of matching coefficients [Eq. (2.43)] is

$$C \sim 1 + 2\kappa \ln(r_0/r_0^{(\text{ref})}) .$$

Thus we can see that  $\ln r_0$  singularity is cancelled in  $R$  ratio to the order we are concerning<sup>16</sup>. However for finite width  $\Gamma_t$ , the expression for  $R$  diverges with  $1/r_0$  and  $\ln(r_0)$ . This is due to the incomplete treatment of the width  $\Gamma_t$ . Here we follow the treatment of [27]; that is, expand the expression with respect to  $r_0$  as detail as possible, and drop the terms that vanish when  $r_0 \rightarrow 0$ . We choose  $r_0 = r_0^{(\text{ref})}$ .

## 2.6 Previously obtained results for $R$ ratio

In this section, we show  $R$  ratio for freely-propagating  $t\bar{t}$  with and without finite decay width  $\Gamma_t$ , Leading Order (LO) Coulomb rescattering with and without  $\Gamma_t$ , Next-to-Leading Order (NLO =  $\mathcal{O}(1/c)$ ) Coulomb rescattering with  $\Gamma_t$ , and Next-to-Next-to-Leading Order (NNLO =  $\mathcal{O}(1/c^2)$ ) Coulomb rescattering with  $\Gamma_t$ . All of these are for fixed order  $\alpha_s(\mu_s)$  calculations<sup>17</sup>, and are obtained before our work, except those with  $a_2^{\text{new}}$ .

### 2.6.1 Analytic results

Analytic formulas for  $R$  ratios [Eq. (2.1)] are available for the following cases:

$$\begin{aligned} R &= \frac{3}{2} N_C Q_t^2 \sqrt{\frac{E}{m_t}} , & \text{for free; without } \Gamma_t , \\ R &= \frac{3}{2} N_C Q_t^2 \sqrt{\frac{\sqrt{E^2 + \Gamma_t^2} + E}{2m_t}} , & \text{for free; with } \Gamma_t , \\ R &= \frac{3}{2} N_C Q_t^2 \frac{\pi C_F \alpha_s}{1 - e^{-z_E}} , \quad z_E = \pi C_F \alpha_s \sqrt{\frac{m_t}{E}} , & \text{for LO; without } \Gamma_t , \end{aligned} \quad (2.46)$$

where  $E = \sqrt{s} - 2m_t$ . The second one is given in Eq. (2.13), and the last one is in Eq. (B.8). These results are shown in Figure 2.6. We can see several points. Because of non-zero width  $\Gamma_t$ , the production cross section is non-zero also for  $E < 0$ . More prominently, attractive Coulomb interaction between  $t\bar{t}$  enhance  $t\bar{t}$  production cross section by many times. This is because the  $t\bar{t}$  wave function  $|\psi(0)|^2$  at the origin is enhanced by the attractive potential.

### Wave function $\psi(0)$ at the origin and potential $V(r)$

The magnitude of a wave function at the origin is related to (the expectation value of) the attractive force  $dV(r)/dr$  [47]. We are interested only in  $S$  wave. Higher orbital angular momentum states may not contribute to  $\psi(0)$ . Thus we define

$$\psi(\mathbf{r}) = \frac{1}{\sqrt{4\pi}} \frac{y(r)}{r}$$

<sup>16</sup> The  $\kappa$  in  $G'$  is evaluated at the scale  $\mu_s$ , while the  $\kappa$  in  $C$  is evaluated at  $\mu_h$ . However, the difference between  $\alpha_s(\mu_s)^2$  and  $\alpha_s(\mu_h)^2$  is higher order, at least formally.

<sup>17</sup> LO and NLO corrections with RG improvement were also calculated; these are summarized in Figure 2.10.

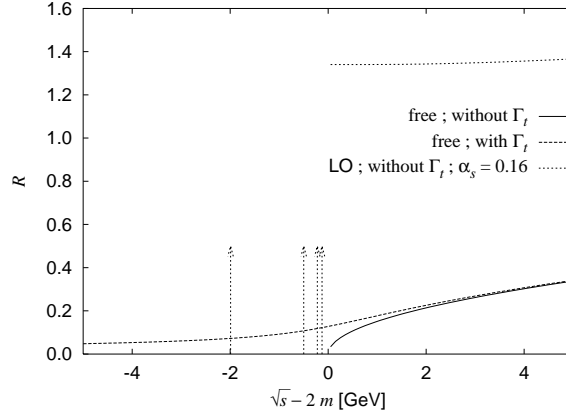


Figure 2.6:  $R$  ratios for the situations that analytic formulas are available. We used  $m_t = 175$  GeV,  $\Gamma_t = 1.43$  GeV,  $\alpha_s(\mu_s) = 0.16$ , which is for  $\mu_s \simeq 20$  GeV. Shown in vertical lines are the first four resonances for Coulomb potential:  $E_n = -E_B/n^2$  where  $E_B \equiv p_B^2/m_t$  and  $p_B \equiv C_F \alpha_s(\mu_s) m_t/2$ . Note that the self-consistent solution for  $p_B = C_F \alpha_s(\mu_s = p_B) m_t/2$  is  $p_B \simeq 20$  GeV.

for  $S$  wave, which means

$$\Delta\psi(\mathbf{r}) = \frac{1}{\sqrt{4\pi}} \frac{y''(r)}{r} .$$

With this and the Schrödinger equation

$$\left[ -\frac{\Delta}{2\mu} + V(\mathbf{r}) \right] \psi(\mathbf{r}) = E\psi(\mathbf{r}) ,$$

where  $\mu = m_t/2$  is the reduced mass, the following quantity can be evaluated in two ways:

$$\begin{aligned} - \int d^3r \frac{y''y'}{4\pi r^2} &= \frac{-1}{2} \int dr (y^2)' = \frac{-1}{2} (y^2)'|_0^\infty = -2\pi (\psi + r\psi')^2|_0^\infty = 2\pi |\psi(0)|^2 , \quad \text{while} \\ &= 2\mu \int d^3r [E - V(r)] \frac{yy'}{4\pi r^2} = \mu \int dr [E - V(r)] (y^2)' = \mu \int dr V'(r) y^2 = \mu \langle V' \rangle . \end{aligned}$$

Thus we have

$$|\psi(0)|^2 = \frac{\mu}{2\pi} \langle V'(r) \rangle . \quad (2.47)$$

On the other hand, constant shift of the potential,  $V(r) \rightarrow V(r) + \delta V$ , can be compensated by the shift of the energy,  $E \rightarrow E + \delta V$ . Thus it is related to the shift of the mass  $m_t$ , since  $E = \sqrt{s} - 2m_t$ . This issue is discussed intensively in Section 2.7 in connection with renormalon ambiguity of both pole mass  $m_t^{\text{pole}}$  of a quark and potential  $V(r)$  in coordinate space.

## 2.6.2 Numerical results

Analytic formulas for  $R$  ratio cannot be obtained with non-zero width  $\Gamma_t$  even for LO. For LO and NLO, the expression for  $R$  ratio is

$$R(s) = \frac{3}{2} N_C Q_t^2 \frac{4\pi}{m^2 c} C_1^{(\text{cur})} \text{Im} G(r=0, r'=0) ,$$

where the ( $S$  wave projected) Green function  $G(r, r')$  is the solution for

$$\left[ (E + i\Gamma_t) - \left( \frac{-1}{m_t} \left[ \frac{d^2}{dr^2} + \frac{2}{r} \frac{d}{dr} \right] - \frac{C_F a_s}{r} + V_1(r) \right) \right] G(r, r') = \frac{-1}{4\pi r r'} \delta(r - r') ,$$

with  $E = \sqrt{s} - 2m_t^{(\text{pole})}$ . Note that  $V_1(r)$  is zero for LO. For NLO, only  $\mathcal{O}(1/c)$  terms are used in  $V_1(r)$ . The same notice is applied for the short-distance current renormalization  $C_1^{(\text{cur})}$ . It can read from Eqs. (2.42) and (2.43); it is unity for LO, and  $(1 - 2C_F\alpha_s(\mu_h)/\pi)^2 = (1 - 4C_F\alpha_s(\mu_h)/\pi)$  for NLO [Eq. (2.16)].

The situation becomes more complicated for NNLO (and higher). The last expression is the one we actually used:

$$\begin{aligned} R &= \frac{3}{2} N_C Q_t^2 \frac{4m^2}{s} \frac{4\pi}{m^2 c} \left\{ C_1^{(\text{cur})} + C_2^{(\text{cur})} \frac{\Delta_r + \Delta_{r'}}{2m^2 c^2} \right\} \text{Im} G(r, r') \Big|_{r, r' \rightarrow r_0} \\ &= \frac{3}{2} N_C Q_t^2 \frac{4m^2}{s} \frac{4\pi}{m^2 c} \left\{ 1 + \left( \frac{\alpha_s(\mu_h)}{\pi} \right) C_F C_1 + \left( \frac{\alpha_s(\mu_h)}{\pi} \right)^2 C_F C_2(r_0) \right\} \times \\ &\quad \times \text{Im} \left[ \left( 1 + \frac{E + i\Gamma}{6mc^2} \right) G'(r_0, r_0) \right] \tag{2.48} \\ &= \frac{3}{2} N_C Q_t^2 \frac{4m^2}{s} \left\{ 1 + \left( \frac{\alpha_s(\mu_h)}{\pi} \right) C_F C_1 + \left( \frac{\alpha_s(\mu_h)}{\pi} \right)^2 C_F C_2(r_0) \right\} \frac{C_F a_s}{\sqrt{1 - 4\kappa}} \times \\ &\quad \times \text{Im} \left[ \left( 1 + \frac{E + i\Gamma}{6mc^2} \right) \left\{ B z_0^{-2d_-} + \frac{1}{z_0} + \sum_{i=\pm} \left( L_2^{(i)} \ln^2(\tilde{\mu}' z_0) + L_1^{(i)} \ln(\tilde{\mu}' z_0) + L_0^{(i)} \right) \right\} \right] , \end{aligned}$$

where  $z_0 = C_F \alpha_s m r_0$ ,  $\tilde{\mu}' z_0 = \mu r_0 e^{\gamma_E}$ , and  $r_0 = r_0^{(\text{ref})} \equiv e^{2-\gamma_E} / (2m_t)$ . Here we used Eqs. (2.8), (2.41), (2.42) and (2.40). Reduced Green function  $G'(r, r')$  is the solution of

$$\left[ \mathcal{E} - \left( \frac{-1}{m_t} \left[ \frac{d^2}{dr^2} + \frac{2}{r} \frac{d}{dr} \right] - \frac{C_F \bar{a}_s}{r} + V_1(r) - \frac{\kappa}{m_t r^2} \right) \right] G'(r, r') = \frac{-1}{4\pi r r'} \delta(r - r') ,$$

where

$$\bar{a}_s \equiv a_s \left( 1 + \frac{3}{2} \frac{E + i\Gamma}{mc^2} \right) , \quad \kappa = \frac{C_F^2}{2} \left( \frac{2}{3} + \frac{C_A}{C_F} \right) \left( \frac{a_s}{c} \right)^2 , \quad \mathcal{E} = (E + i\Gamma) \left( 1 + \frac{E + i\Gamma}{4mc^2} \right) .$$

The coefficient  $B$  is determined as

$$B = - \frac{g_-(r)}{g_+(r)} \Big|_{r \rightarrow \infty} ,$$

where  $g_{\pm}(r)$  are the solutions of homogeneous differential equation for  $G'(r, r')$  with the boundary condition

$$g_{\pm}(z) = z^{d_{\pm}} \left[ 1 + z \left( L_2^{\pm} \ln^2(\tilde{\mu}' z) + L_1^{\pm} \ln(\tilde{\mu}' z) + L_0^{\pm} \right) + \mathcal{O}(z^2) \right] .$$

Our input is

$$m_t = 175 \text{ GeV} , \quad \Gamma_t = 1.43 \text{ GeV} , \quad \alpha_s^{\overline{\text{MS}}}(m_Z) = 0.118 .$$

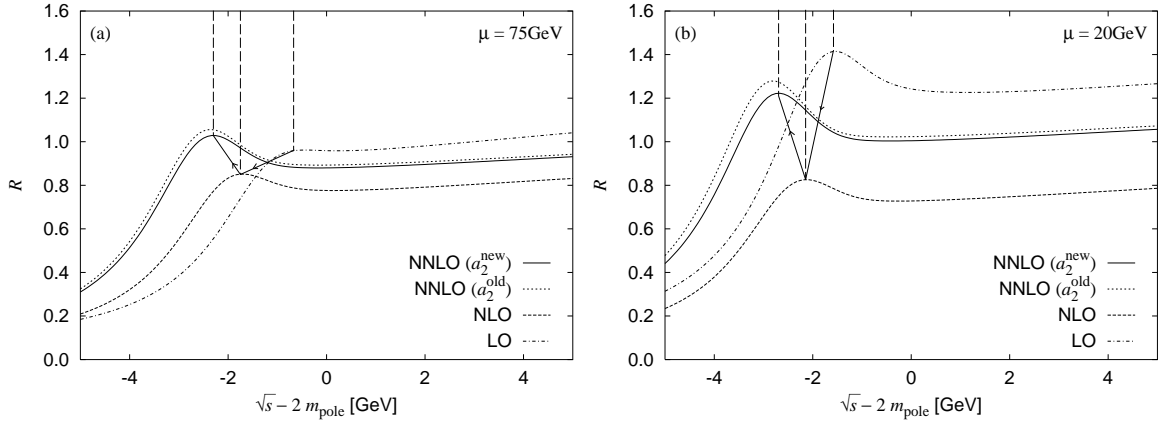


Figure 2.7:  $R$ -ratios for  $e^+e^- \rightarrow \gamma^* \rightarrow t\bar{t}$  at LO (dot-dashed), NLO (dashed), and NNLO (solid) as functions of the energy measured from twice the pole mass,  $E = \sqrt{s} - 2m_{\text{pole}}$ . Arrows indicate dislocations of the maximum point of  $R$  as the  $\mathcal{O}(1/c)$  and  $\mathcal{O}(1/c^2)$  corrections are included, respectively. We put  $m_{\text{pole}} = m_t = 175$  GeV,  $\Gamma_t = 1.43$  GeV, and  $\alpha_s(m_Z) = 0.118$ . Dotted lines show NNLO  $R$ -ratios calculated with an old value of  $a_2$  [44], which is one of the coefficients in the two-loop perturbative QCD potential  $V_1(r)$ . Figure (a) is for  $\mu_s = 75$  GeV and (b) is for  $\mu_s = 20$  GeV.

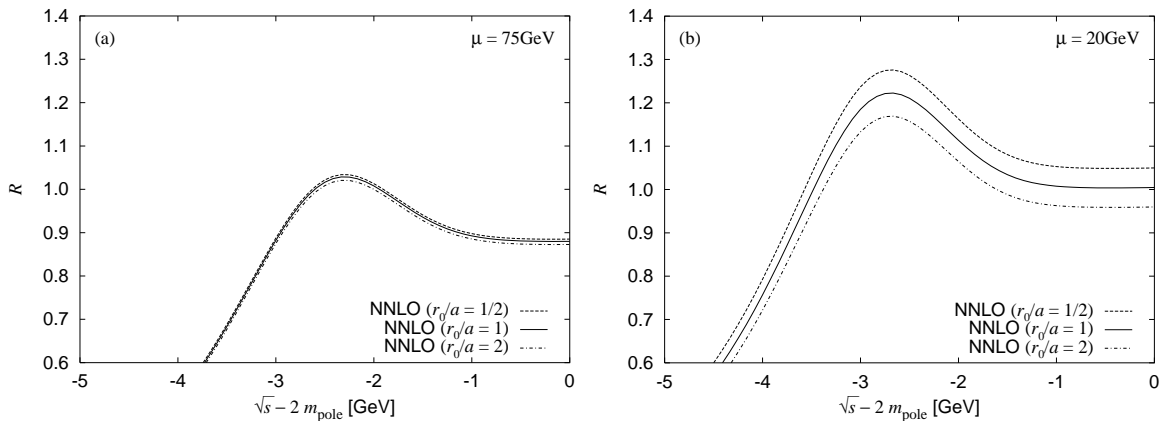


Figure 2.8:  $R$ -ratios for  $e^+e^- \rightarrow \gamma^* \rightarrow t\bar{t}$  at NNLO for several values of  $r_0$ :  $r_0 = a/2$  (dashed),  $r_0 = a$  (solid), and  $r_0 = 2a$  (dot-dashed), where  $a \equiv r_0^{(\text{ref})} \equiv e^{2-\gamma_E}/2m_t$ . Figure (a) is for  $\mu_s = 75$  GeV, and (b) is for  $\mu_s = 20$  GeV. Other notations and parameters are same as in Figure 2.7.



There are also another inputs. One is the “hard scale”  $\mu_h = m_t$ , which is for  $\alpha_s$  in matching coefficients, and the “soft scale”  $\mu_s = 20 \text{ GeV}, 75 \text{ GeV}$ , which is for  $\alpha_s$  in potential. The other is regulator  $r_0 = r_0^{(\text{ref})}$  for the incomplete treatment of  $\Gamma_t$ .

Shown in Figure 2.7 is the  $R$ -ratios for LO, NLO ( $= \mathcal{O}(1/c)$ ) and NNLO ( $= \mathcal{O}(1/c^2)$ ), where the last one is calculated in [26–28] for  $\mu_s = 75 \text{ GeV}$ . Our numerical results are consistent with them. As was already pointed in [26–28],  $\mathcal{O}(1/c)$  and  $\mathcal{O}(1/c^2)$  corrections for  $R$  ratio are not small at all. In fact this is the motivation for us to study this issue: how well can we improve the perturbative convergence of  $R$ . There are three possible sources of this bad convergence: (i) after the calculations in [26–28], it was found [45] that the previous calculation [44] of a coefficient  $a_2$  in  $V_1$ , which is one of the  $\mathcal{O}(1/c^2)$  corrections, turn out to wrong. In fact the original value of  $a_2$  is so huge that it was suspected to be wrong before the calculation in [45]. We see the effect of this modification just below in this section. (ii) One can see that the soft-scale ( $\mu_s$ ) dependence of  $R$  is also large. This suggests the necessity of Renormalization-Group (RG) improvement. We do this in Section 2.8. (iii) Yet another possible source is renormalon ambiguity of pole mass and potential. We pursue this issue in Section 2.7.

Before studying suspects (ii) and (iii) above, let us look at more closely these fixed order results for now. In Figures 2.7, the difference of those two figures are the choice of the soft scale  $\mu_s$ , which is written simply as  $\mu$ . One choice is  $\mu_s = 20 \text{ GeV} \simeq p_B$  and the other is  $75 \text{ GeV}$ . The latter is chosen somewhat arbitrary. Naively, the natural scale for Coulomb potential is Bohr momentum  $p_B \simeq 20 \text{ GeV}$  [Eq. (B.7)]. However one can see that the convergence of the normalization is better for  $\mu_s = 75 \text{ GeV}$  than that for  $\mu_s = 20 \text{ GeV}$ , although the convergence of the peak position ( $\simeq$  mass of the  $1S$  resonance) is better for  $\mu_s = 20 \text{ GeV}$  than that for  $\mu_s = 75 \text{ GeV}$ . This maybe because the normalization is determined by the wave function at the origin, which is much shorter than  $1/p_B$ ;  $|\psi(0)|^2(\propto \langle V'(r) \rangle)$ . More explicitly, from Figure 2.5 one can see that the convergence of the attractive force due to Coulombic potential  $V_C$  is worse for  $\mu = 20 \text{ GeV}$ . There is another attractive force due to  $V_{NA}$  for NNLO. This also increases the normalization<sup>18</sup>. On the other hand, the position of  $1S$  peak is determined by Bohr momentum  $p_B$ . However corrections to the potential  $V_1(r)$  are minimized near<sup>19</sup>  $1/r \simeq \mu'_s = \mu_s e^{\gamma_E}$ . Interplay of these factors makes the estimate of the optimal scale for  $\mu_s$  complicated. We consider this issue once more in Section 2.8.1, where the theoretical ambiguities of our calculations are examined.

Also shown in the same figures are the effects of correcting  $a_2$  [44, 45], which is a coefficient of NNLO correction to Coulomb potential. Numerically, the difference between  $a_2^{(\text{old})} \simeq 333$  and  $a_2^{(\text{new})} \simeq 156$  is large, but the effect of correcting it to  $R$  turns out to be small. This is because log term in  $V_1(r)$  [Eq. (2.15)] are also large. In the following section, we give the results for RG improved potential, where large log’s are summed. For those cases, NNLO corrections diminishes by factor two when the correct value for  $a_2$  is used.

Shown in Figures 2.8 are the  $r_0$  dependence of  $R$  ratio. Both vertical and horizontal directions are magnified by two, compared to Figures 2.7. The value of  $r_0$  is varied by factors 2 and  $1/2$ . As was explained in Section 2.4.3, the variation in  $R$  is due to not only  $\mathcal{O}(1/c^3)$  corrections but also  $\mathcal{O}(\Gamma_t/m_t)$  terms in Eq. (2.48). The size of this variation is a measure of one of the uncertainties of our theoretical prediction. We can see it is rather small compared to the  $\mathcal{O}(1/c^2)$  correction itself. Especially, side-ward shift is very small.

<sup>18</sup> Short distance vertex corrections  $C_1$  etc. also affects the overall normalization. For example, with  $\alpha_s^{\overline{\text{MS}}}(m_t) = 0.107$ , it is  $1 - 4C_F\alpha_s^{\overline{\text{MS}}}(\mu_h = m_t)/\pi = 0.818$  to NLO.

<sup>19</sup> For reference,  $e^{\gamma_E} = 1.781 \dots$ .

## 2.7 Renormalon ambiguity and PS mass

### 2.7.1 Perturbative convergence

It is known that the perturbative expansion in QFT is an asymptotic expansion. The ambiguity due to this is called “renormalon ambiguity” [55–58]. This is the subject of this section.

For some quantities  $Q$ , explicit calculations show that perturbative convergence of  $Q$  is much better when  $Q$  are expressed in terms of  $\overline{\text{MS}}$ -mass  $m_t^{\overline{\text{MS}}}$  than in pole-mass  $m_t^{\text{pole}}$ . One example is the leading fermionic correction  $(\Delta\rho)_f$  to the  $\rho$ -parameter [49]:

$$\begin{aligned}\Delta\rho^{\text{on-shell}} &\simeq N_C \frac{G_F M_t^2}{8\sqrt{2}\pi^2} \left[ 1 - \frac{\alpha_s(\mu)}{\pi} \times 2.9 - \left( \frac{\alpha_s(\mu)}{\pi} \right)^2 \left( 5.0 \ln \frac{\mu^2}{M_t^2} + 15. \right) \right], \\ \Delta\rho^{\overline{\text{MS}}} &\simeq N_C \frac{G_F \bar{m}_t(\mu)^2}{8\sqrt{2}\pi^2} \left[ 1 + \frac{\alpha_s(\mu)}{\pi} (2\ell - 0.19) + \left( \frac{\alpha_s(\mu)}{\pi} \right)^2 \left( \frac{15}{4} \ell^2 + 2.0\ell - 4.0 \right) \right],\end{aligned}$$

where<sup>20</sup>  $M_t \equiv m_t^{\text{pole}}$ ,  $\bar{m}_t(\mu) \equiv m_t^{\overline{\text{MS}}}(\mu)$ , and  $\ell \equiv \ln[\mu^2/\bar{m}_t(\mu)^2] = 0$  for  $\mu = \mu_t \equiv \bar{m}_t(\mu_t)$ . One can see that with  $\mu = \mu_t$ , the coefficient of  $\alpha_s/\pi$  is smaller by factor 15 for  $\overline{\text{MS}}$ -mass, and factor 4 in the case  $(\alpha_s/\pi)^2$ . A similar behavior can also be seen in the QCD corrections to the interactions  $\ell^+\ell^-H$ ,  $W^+W^-H$ , and  $ZZH$  [50]. It is suspected that these worse convergence may be a signal of renormalon contributions.

Likewise, as we shall see below, the pole mass  $m_t^{\text{pole}}$  of a quark itself suffers from “renormalon ambiguity” of  $\mathcal{O}(\Lambda_{\text{QCD}})$  even if  $\Gamma_t > \Lambda_{\text{QCD}}$  [51–54]. For example, the invariant mass  $m_{jW}$  of the jet and  $W$ , which are the decay products of  $t$ , distributes around  $m_t$ . However since  $b$  is not color-singlet, the  $m_{jW}$ -distribution do not directly represent  $m_t^{\text{pole}}$ .

On the other hand, there is also “renormalon ambiguity” for quark-antiquark potential  $V(r)$  in coordinate space, and it can be shown [59, 60] that the severest ambiguity cancel in the combination  $2m_t^{\text{pole}} + V(r)$ . We shall see this just below.

### 2.7.2 IR gluon contributions to self-energy $\Sigma$ and potential $V(r)$

The mass  $m$  of a particle  $f$  is renormalized due to the self-energy  $\Sigma$  of  $f$  by  $\delta m = m\Sigma_1$ , since

$$\begin{aligned}\frac{i}{\not{p} - m - \Sigma} &= \frac{i}{\not{p} - m - m\Sigma_1 - (\not{p} - m)\Sigma_2} \\ &\simeq \frac{1}{1 - \Sigma_2} \frac{i}{\not{p} - m(1 + \Sigma_1)},\end{aligned}$$

where

$$\begin{aligned}\Sigma(p, m) &\equiv m\Sigma_1(p^2, m) + (\not{p} - m)\Sigma_2(p^2, m) \\ &= \not{p}\Sigma_2 + m(\Sigma_1 - \Sigma_2).\end{aligned}$$

<sup>20</sup>See also [50].

Let us consider the one-loop gluon contribution to  $\Sigma$  of a quark. Since gluon is strongly coupled in IR region, we concentrate on those region. For a static quark  $p^\mu \simeq (m, \vec{0})$  [54],

$$\begin{aligned}
-i\Sigma_{\text{IR}} &= (-ig_s)^2 T^a T^a \int_{\vec{k}=\text{soft}} \frac{d^4 k}{(2\pi)^4} \gamma^0 \frac{i(\not{p} + \not{k} + m)}{(p+k)^2 - m^2 + i\epsilon} \gamma^0 \frac{-i}{-|\mathbf{k}|^2 + i\epsilon} \Big|_{p^2 \simeq m^2} \\
&\simeq \frac{1 + \gamma^0}{2} C_F g_s^2 \int_{\vec{k}=\text{soft}} \frac{d^4 k}{(2\pi)^4} \frac{1}{(k^0 + i\epsilon)(|\mathbf{k}|^2 - i\epsilon)} \\
&= \frac{1 + \gamma^0}{2} \frac{-i}{2} \int_{\vec{k}=\text{soft}} \frac{d^3 k}{(2\pi)^3} \frac{4\pi C_F \alpha_s}{|\mathbf{k}|^2} \\
&\simeq (-i) \frac{1 + \gamma^0}{2} \frac{1}{2} \int_{\vec{k}=\text{soft}} \frac{d^3 k}{(2\pi)^3} \frac{4\pi C_F \alpha_s (|\mathbf{k}|^2)}{|\mathbf{k}|^2},
\end{aligned}$$

where we used  $k^i \sim 0$  in the denominator, and  $\frac{1}{k^0 + i\epsilon} = \text{P} \frac{1}{k^0} - i\pi\delta(k^0)$ . Fermion bubbles in the gluon propagation alter the  $|\mathbf{k}|$ -dependence with the coefficient  $n_f$ , the number of (light) fermion flavor. By naively non-abelianizing  $n_f$  to  $\beta_0$ , we have the last expression. Thus we have  $\Sigma_2 = \Sigma_1 - \Sigma_2$ , or

$$\begin{aligned}
\delta m_{\text{IR}} &= m\Sigma_1 = m \cdot 2\Sigma_2 \\
&= \frac{1}{2} \int_{\vec{k}=\text{soft}} \frac{d^3 k}{(2\pi)^3} \frac{4\pi C_F \alpha_s (|\mathbf{k}|^2)}{|\mathbf{k}|^2},
\end{aligned}$$

where  $\delta m_{\text{IR}}$  means the contribution from IR gluons. This expression is ill-defined due to the IR-pole of the QCD coupling  $\alpha_s(\mu)$ . On the other hand, the QCD-potential  $V(r)$  in coordinate space is also ill-defined due to just the same reason:

$$\delta V(r)_{\text{IR}} = \int_{\vec{k}=\text{soft}} \frac{d^3 k}{(2\pi)^3} e^{i\vec{k}\cdot\vec{r}} \frac{-4\pi C_F \alpha_s (|\mathbf{k}|^2)}{|\mathbf{k}|^2}.$$

However we can see that [59, 60] the “severest IR renormalon pole” is canceled in the combination  $2m_{\text{pole}} + V(r)$ . The precise meaning of this statement is explained in the next section. The origin of the difference of the sign can be understood as follows. Consider an Abelian gauge group for simplicity. For the self-energy  $\Sigma$ , both end of a “gluon” couple to the “quarks” of the same charge; thus  $\Sigma \propto +C_F \alpha_s$ , where  $C_F \sim Q^2$  ( $Q$  is Abelian charge). For the potential  $V$ , one end of a “gluon” couples to a “quark” while the other to a “anti-quark”; thus  $V \propto -C_F \alpha_s$ .

### 2.7.3 Borel sum and IR renormalon pole

IR renormalon in  $m_{\text{pole}}$  is discussed in [37, 52, 53]. IR gluon contribution for a quark mass is

$$\begin{aligned} \delta m_{\text{IR}}(\mu) &\equiv \frac{1}{2} \int_{|\vec{k}| < \mu} \frac{d^3k}{(2\pi)^3} \frac{4\pi C_F \alpha_s(|\mathbf{k}|^2)}{|\mathbf{k}|^2} = \frac{C_F}{\pi} \int_0^\mu dk \alpha_s(k^2) \\ &= \frac{C_F \alpha_s(\mu)}{\pi} \mu \sum_{n=0}^{\infty} n! \left( 2 \frac{\beta_0 \alpha_s(\mu)}{4\pi} \right)^n \end{aligned} \quad (2.49)$$

$$= \frac{C_F}{\pi} \mu \int_0^\infty dt e^{-t/\alpha_s(\mu)} \frac{1}{1 - 2 \frac{\beta_0 t}{4\pi}}. \quad (2.50)$$

We can see several points. With the expression in the second line<sup>21</sup>, which is written in series, the coefficients grows with  $n!$ , thus the series is asymptotic one, which means it does not converge at all. The procedure that leads to the final expression is called ‘‘Borel resummation’’. One can easily check that this expression is the same as the above one at least formally, by expanding the denominator and integrating each term, which gives simply  $\Gamma$ -function or  $n!$ . The integration parameter  $t$  is called the ‘‘Borel parameter’’ conjugate to  $\alpha_s(\mu)$ . It is sometimes convenient to use the rescaled Borel parameter  $u \equiv \frac{\beta_0 t}{4\pi}$  conjugate to  $\frac{\beta_0 \alpha_s(\mu)}{4\pi}$ . The complex plane of the Borel parameter  $t$  or  $u$  is called ‘‘Borel plane’’. With the Borel-sum representation of  $\delta m_{\text{IR}}$ , there is a pole on the path of integration, since  $\beta_0 > 0$ . The pole in the Borel plane that originates from the asymptotic behavior of a perturbative expansion is called a renormalon pole. We can see that the pole mass has a IR renormalon pole at  $u = \frac{1}{2}$ . The following expressions may be useful to follow some of the calculations here:

$$\begin{aligned} \alpha_s(k) &= \frac{\alpha_s(\mu)}{1 - \frac{\beta_0 \alpha_s(\mu)}{4\pi} \ln \frac{\mu^2}{k^2}} = \alpha_s(\mu) \cdot \sum_{n=0}^{\infty} \left( \frac{\beta_0 \alpha_s(\mu)}{4\pi} \ln \frac{\mu^2}{k^2} \right)^n, \\ \alpha_s(\mu) &= \frac{4\pi}{\beta_0 \ln \left( \frac{\mu^2}{\Lambda^2} \right)} = \int_0^\infty dt \left( \frac{\mu^2}{\Lambda^2} \right)^{-\frac{\beta_0}{4\pi} t}, \\ \exp \left( \frac{-4\pi}{\beta_0 \alpha_s(\mu)} \right) &= \frac{\Lambda^2}{\mu^2}, \quad e^{-t/\alpha_s(\mu)} = \left( \frac{\mu^2}{\Lambda^2} \right)^{-\frac{\beta_0}{4\pi} t}. \end{aligned}$$

where  $\Lambda = \Lambda_{\text{QCD}}$ . The most RHS of the second equation may be called Borel representation for the running coupling [57].

#### Short distance mass and long distance mass

IR renormalon pole disturbs pole mass  $m_{\text{pole}}$  but not  $\overline{\text{MS}}$  mass  $m_{\overline{\text{MS}}}$ . This is because  $\overline{\text{MS}}$  scheme subtracts only the pole that originates from UV divergence. Such a mass scheme may be called ‘‘short distance mass’’. On the other hand, a mass scheme sensitive to IR physics may be called ‘‘long distance mass’’. For example, the peak of the invariant mass  $m_{jW}$  of the jet and  $W$  that are decay products of  $t$ , may be a kind of long distance mass of top quark. Those mass schemes suffer from IR renormalon ambiguity.

<sup>21</sup> Here we used  $\int_0^1 dx \left( \ln \frac{1}{x^2} \right)^n = 2^n n!$ .

### Ambiguity due to IR renormalon pole

There are several ways to estimate the ambiguity of  $m_{\text{pole}}$  due to IR physics. We show three ways here. It may be useful to see that both the Borel-summed expression and the asymptotic-series one give almost the same result. The symbol  $\Delta$  denotes ambiguity.

(i) In the Borel-summed expression Eq. (2.50), there is a pole on the path of integration. There may be two choices to step aside this singularity; one is to around upper side of the pole, and the other is lower side. The ambiguity may be estimated by the difference of these two [51]:

$$\begin{aligned}\Delta(\delta m_{\text{IR}}(\mu)) &\simeq \frac{1}{2} \text{Im} \left[ \frac{C_F}{\pi} \mu \oint_C dt e^{-t/\alpha_s(\mu)} \frac{1}{1 - 2\frac{\beta_0 t}{4\pi}} \right] \\ &= \frac{-1}{2} \frac{4\pi C_F}{\beta_0} \mu \left( \frac{\Lambda_{\text{QCD}}^2}{\mu^2} \right)^{1/2} = \frac{-1}{2} \frac{4\pi C_F}{\beta_0} \Lambda_{\text{QCD}} .\end{aligned}$$

Note that the power 1/2 of  $\Lambda^2/\mu^2$  reflects the position of the renormalon pole  $u = 1/2$ . Because of the exponential dumping factor  $\exp[-t/\alpha_s(\mu)]$ , the severest ambiguity is due to the renormalon pole that is closest to the origin. For the case of  $m_{\text{pole}}$ , it is  $u = 1/2$ . However in the combination  $2m_{\text{pole}} + V(r)$ , this severest pole is cancelled each other. The next severest pole, which may not be cancelled in the combination above, may be  $u = 1$ . The ambiguity due to this renormalon pole is

$$\Delta(\delta m_{\text{IR}}) \sim \mu \left( \frac{\Lambda^2}{\mu^2} \right)^1 = \Lambda \cdot \frac{\Lambda}{\mu} \quad \text{for } u = 1 ,$$

thus suppressed by factor  $\Lambda/\mu \sim 1/175$  for  $\mu \sim m_t$ . Precise determination of the residue may be difficult.

(ii) Let us consider a asymptotic series  $\sum_{n=0}^{\infty} x^n n!$  [52]. The best approximation may be obtained when one sums up until the ratio of a term and the next term becomes greater than unity:  $[x^{n+1}(n+1)!]/[x^n n!] = xn < 1$ , or  $n \lesssim n_{\text{crit}} \equiv 1/x$ . The ambiguity may be estimated by the magnitude to the last term:

$$\begin{aligned}\Delta \left( \sum_{n=0}^{n_{\text{crit}}} x^n n! \right) &\simeq x^n n! \Big|_{n=n_{\text{crit}}} \simeq \frac{n!}{n^n} \Big|_{n=n_{\text{crit}}} \\ &\simeq \sqrt{2\pi n_{\text{crit}}} e^{-n_{\text{crit}}} .\end{aligned}$$

For the case we deal,

$$n_{\text{crit}} = \frac{1}{2} \frac{4\pi}{\beta_0 \alpha_s(\mu)} \simeq 6 \text{ to } 7 .$$

Note that if the severest IR renormalon pole is not  $u = 1/2$  but  $u = 1$ , then  $n_{\text{crit}} = 4\pi/(\beta_0 \alpha_s)$ . Thus from Eq. (2.49) we have

$$\begin{aligned}\Delta(\delta m_{\text{IR}}) &\simeq \frac{C_F}{\pi} \mu \alpha_s(\mu) \cdot \sqrt{2\pi n_{\text{crit}}} e^{-n_{\text{crit}}} \\ &= \frac{C_F \alpha_s(\mu)}{\pi} \frac{2\pi}{\sqrt{\beta_0 \alpha_s(\mu)}} \Lambda_{\text{QCD}} .\end{aligned}$$

(iii) There is also another way to estimate. It gives small imaginary part directly to the denominator of the integrand of momentum integration [52]:

$$\begin{aligned}\Delta(\delta m_{\text{IR}}(\mu)) &\simeq \text{Im}[\delta m_{\text{IR}}(\mu)] = \text{Im}\left[\frac{C_F}{\pi}\frac{4\pi}{\beta_0}\int_0^\mu dk\frac{1}{\ln\frac{k^2}{\Lambda^2}+i\epsilon}\right] \\ &= \frac{-1}{2}\frac{4\pi C_F}{\beta_0}\Lambda_{\text{QCD}}.\end{aligned}$$

For an asymptotic slavery theory  $\beta_0 < 0$  such as QED, the IR renormalon pole is not on the path of integration, thus it may not be big problem. In terms of an asymptotic series, each term is sign altering, thus the singularity is less than the case for  $\beta_0 > 0$ . There are also UV renormalon poles in QCD (and in QED as well). However, they are situated at the negative region of the real axis (for  $\beta_0 > 0$ ), thus cause no ambiguity at least with regard to the Borel resum.

#### 2.7.4 Potential-Subtracted mass $m_{\text{PS}}(\mu_f)$

Arguments by now indicate that one should attempt to extract the  $\overline{\text{MS}}$  mass  $m_{\overline{\text{MS}}}$  directly, not the pole mass  $m_{\text{pole}}$ , from experiments. However one crucial point is that  $\overline{\text{MS}}$  mass is not calculated to the order we need. This is because the binding energy ( $\sim -E_{\text{B}}$ ) is already  $\mathcal{O}(m\alpha_s^2)$  to the leading order [Eq. (B.7)]. Thus to NNLO, one needs  $\mathcal{O}(m\alpha_s^4)$  term, which is N<sup>4</sup>LO correction to the quark mass. Recently N<sup>3</sup>LO correction to the quark mass was calculated [64]. But one more higher order may be very hard to calculate. One way to circumvent this dilemma is to introduce another “short-distance” mass scheme. There may be a host of schemes, but one scheme which is convenient to our problem is Potential-Subtracted (PS) mass  $m_{\text{PS}}$  proposed in [59]. The argument goes as follows. As we showed above, the combination  $2m_{\text{pole}} + V(r)$  is free from the (severest) IR renormalon pole, but each of  $m_{\text{pole}}$  and  $V(r)$  are not. The problematic part is the IR part of  $\tilde{V}(|\mathbf{k}|)$ . The idea is to add that part to the mass. Then the new potential is free from (severest) IR renormalon ambiguity. Thus so is the new mass scheme, since the sum is so:

$$2m_{\text{pole}} + V_{\text{C}}(r) = 2m_{\text{PS}}(\mu_f) + V_{\text{C}}(r; \mu_f), \quad (2.51)$$

where<sup>22</sup>

$$m_{\text{PS}}(\mu_f) \equiv m_{\text{pole}} + \Delta m(\mu_f), \quad V_{\text{C}}(r; \mu_f) \equiv V_{\text{C}}(r) - 2\Delta m(\mu_f)$$

and

$$\begin{aligned}\Delta m(\mu_f) &\equiv \frac{1}{2}\int_{|\vec{q}|<\mu_f}\frac{d^3q}{(2\pi)^3}\tilde{V}_{\text{C}}(q) \\ &= \frac{-C_F a_s}{\pi}\mu_f\left[1 + \frac{a_s}{4\pi}\left\{a_1 - \beta_0\left(\ln\frac{\mu_f^2}{\mu_s^2} - 2\right)\right\}\right. \\ &\quad \left.+ \left(\frac{a_s}{4\pi}\right)^2\left\{a_2 - (2a_1\beta_0 + \beta_1)\left(\ln\frac{\mu_f^2}{\mu_s^2} - 2\right) + \beta_0^2\left(\ln^2\frac{\mu_f^2}{\mu_s^2} - 4\ln\frac{\mu_f^2}{\mu_s^2} + 8\right)\right\}\right],\end{aligned}\quad (2.52)$$

<sup>22</sup> Note that our  $\Delta m(\mu_f)$  is related to a corresponding quantity in [59] by  $\Delta m(\mu_f) = -\delta m(\mu_f)$ , and is negative.

$\Delta m(\mu_f)$	$\mu_f = 3 \text{ GeV}$		$\mu_f = 10 \text{ GeV}$	
	$\mu_s = 20 \text{ GeV}$	$\mu_s = 75 \text{ GeV}$	$\mu_s = 20 \text{ GeV}$	$\mu_s = 75 \text{ GeV}$
LO	-0.1922 GeV	-0.1546 GeV	-0.6408 GeV	-0.5153 GeV
NLO	-0.3123 GeV	-0.2589 GeV	-0.8945 GeV	-0.7707 GeV
NNLO	-0.4003 GeV	-0.3389 GeV	-1.035 GeV	-0.9255 GeV

Table 2.1: The difference  $\Delta m(\mu_f) = m_{\text{PS}}(\mu_f) - m_{\text{pole}}$  of PS mass and pole mass, defined in Eq. (2.52). Although we use  $\mu_f = 3 \text{ GeV}$  in the study, we also show  $\Delta m(\mu_f = 10 \text{ GeV})$  for reference.

where  $\tilde{V}_C(q)$  is the Fourier transform of the Coulombic potential  $V_C(r)$  defined in Eq. (2.20), and  $a_s = \alpha_s^{\overline{\text{MS}}}(\mu_s)$ . The scale  $\mu_f$  for factorization should be larger than  $\Lambda_{\text{QCD}}$  in order to remove the IR ambiguity. On the other hand it seems that  $\mu_f$  should not be as large as Bohr momentum  $p_B$  in order not to disturb the Coulombic potential near Bohr radius. Following the original paper [59] for PS mass, we choose  $\mu_f = 3 \text{ GeV}$ . Explicit values are given in Table 2.1. For reference,  $\Delta m(\mu_f = 10 \text{ GeV})$  is also shown. Note that in the definition above, we dropped the  $r$ -dependence of  $\Delta m(\mu_f)$ . Thus the equality in Eq. (2.51) is up to  $\mathcal{O}(\Lambda_{\text{QCD}}^3 r^2)$  at least perturbatively<sup>23</sup>. There may be renormalon ambiguity also in this  $r$ -dependent term. This ambiguity can not be cancelled in the combination  $2m_{\text{pole}} + V(r)$  since the pole mass is  $r$ -independent. However the ambiguity in this term may not be serious, because the typical scale  $r$  for (would-be)  $t\bar{t}$  bound state is  $1/p_B \simeq 1/(20 \text{ GeV})$ , which means the ambiguity is of order  $\Lambda_{\text{QCD}}^2 r \sim 0.05 \text{ GeV}$ . It is known that  $V(r) \propto r$  outside the perturbative region. However as we shall see in Section 2.8.1, this ambiguity is negligible in our case due to the large mass and decay width of the top quark [9, 11, 12, 14]. Thus the next-severest renormalon ambiguity above may also be negligible.

Recently, the relation between  $\overline{\text{MS}}$ - and pole-mass was calculated to  $\mathcal{O}(\alpha_s^3)$  [63]. With this, PS-mass can be related more accurately to  $\overline{\text{MS}}$ -mass than to pole-mass<sup>24</sup>.

### 2.7.5 Results for $R$ ratio with $m_{\text{PS}}(\mu_f)$

Following the arguments above, it is PS mass (or a short-distance mass, in general) that is well determined from experiments. Thus we fix PS mass but not pole mass. With the choice  $\mu_f = 3 \text{ GeV}$ , the difference  $\Delta m(\mu_f) \simeq -0.4 \text{ GeV}$  of pole mass  $m_{\text{pole}}$  and PS mass  $m_{\text{PS}}$  is tiny compared to  $m_{\text{pole}} \simeq 175 \text{ GeV}$ . Thus the Schrödinger equation barely changes except the origin of non-relativistic energy  $E$ , since it is now  $E = \sqrt{s} - 2m_{\text{PS}}$ . Note that, as explained in Section 2.6.1, constant shift of potential  $V$  simply means the shift of the origin of  $E$ . Shown in Figure 2.9 are almost the same as those in Figure 2.7 except we fixed  $m_{\text{PS}}(\mu_f = 3 \text{ GeV}) = 175 \text{ GeV}$  rather than  $m_{\text{pole}}$ . Since  $|\Delta m(\mu_f)|$  is larger for higher order, the position of  $1S$  peak moves more for higher order. We can see the sideward convergence becomes better by the difference  $|(\Delta m)^{\text{NNLO}} - (\Delta m)^{\text{NLO}}| \simeq 0.1 \text{ GeV}$  and  $|(\Delta m)^{\text{NLO}} - (\Delta m)^{\text{LO}}| \simeq 0.1 \text{ GeV}$ , respectively. On the other hand the normalization barely changes, as is anticipated. In the next section we study RG improvement of the potential, which is expected to be effective to this problem.

<sup>23</sup> There is no  $\mathcal{O}(\Lambda_{\text{QCD}}^2 r)$  term due to rotational symmetry. However I'm not sure if this is true also non-perturbatively.

<sup>24</sup> See the reference above for details.

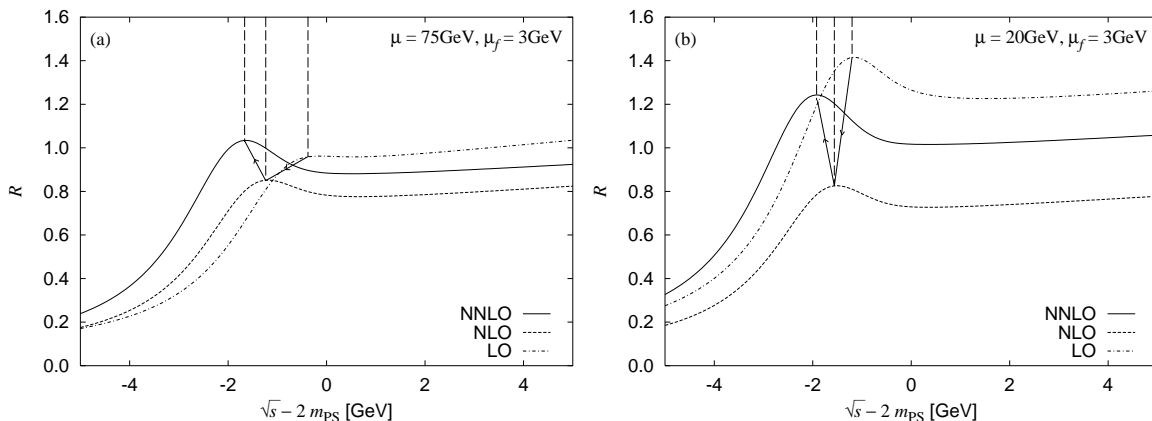


Figure 2.9:  $R$ -ratios for  $e^+e^- \rightarrow \gamma^* \rightarrow t\bar{t}$  at LO (dot-dashed), NLO (dashed), and NNLO (solid) as functions of the energy measured from twice the potential-subtracted mass,  $\sqrt{s} - 2m_{\text{PS}}$ . We set  $\mu_f = 3 \text{ GeV}$  and  $m_{\text{PS}}(\mu_f) = 175 \text{ GeV}$ . Figure (a) is for  $\mu_s = 75 \text{ GeV}$ , and (b) is for  $\mu_s = 20 \text{ GeV}$ . Other notations and parameters are same as in Figure 2.7.

## 2.8 Results for $R$ ratio with RG improved $V_C$ and $m_{\text{PS}}$

As mentioned in Section 2.6.2, large renormalization-scale  $\mu_s$  dependence of  $R$  ratio indicates the necessity of  $\log(\mu_s)$  resummation. As first step<sup>25</sup>, we sum up  $\log(\mu_s)$  in the Coulombic potential  $V_C(r)$ . Thus our results here still depends on the soft scale  $\mu_s$ , which is in  $V_{\text{BF}}$  and  $V_{\text{NA}}$ . As we saw in Figure 2.4, couplings converge much better for RG-improved case than for fixed order, all over the relevant momentum scale  $C_F a_s m_t \lesssim 1/r < m_t$ . Thus it is expected that the convergence is improved by the use of  $V_C^{(\text{RG})}(r)$  that is RG improved ( $\mu_s = q$ ) in the momentum space and Fourier transformed to the coordinate space.

PS mass  $m_{\text{PS}}(\mu_f)$  with RG improved potential is ambiguous, since  $\tilde{V}_C^{(\text{RG})}$  diverges at IR region. Here we define as follows:

$$m_{\text{PS}}(\mu_f) \equiv m_{\text{pole}} + \Delta m(\mu_f), \quad V_C^{(\text{RG})}(r; \mu_f) \equiv \int_{|\vec{q}| > \mu_f} \frac{d^3 q}{(2\pi)^3} e^{i\vec{q}\cdot\vec{r}} \tilde{V}_C^{(\text{RG})}(q),$$

$$\Delta m(\mu_f) \equiv \frac{1}{2} \int_{|\vec{q}| < \mu_f} \frac{d^3 q}{(2\pi)^3} \tilde{V}_C^{(\text{fixed})}(q).$$

Our final result for  $R$ -ratio in this paper is shown in Figure 2.10. For comparison,  $R$ -ratios both with and without the RG improvement for  $V_C$  are given. We can see that convergence of both the normalization and the peak position is improved slightly. The latter is listed in Table 2.2 as the “binding energies” of the  $1S$  resonance state  $2m_{\text{PS}}(\mu_f) - M_{1S}$ . They are determined by reducing the decay width  $\Gamma_t$  tentatively.

Why is the convergence not improved much better? Let us drop the corrections other than those for  $V_C(r)$ , for the moment. The  $R$  ratio for this case is shown in Figure 2.11. The relevant

<sup>25</sup> A full resummation of logarithms up to NNLO requires a significant modification of the formula Eq. (2.48); we will study its incorporation in our future work.



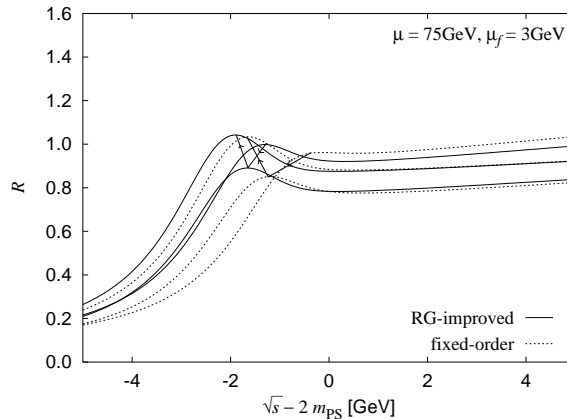


Figure 2.10: Our final result for  $R$ -ratios in this paper for  $e^+e^- \rightarrow \gamma^* \rightarrow t\bar{t}$  at LO, NLO, and NNLO. Solid lines show those with renormalization-group improved Coulombic potentials,  $V_C^{(\text{RG})}(r; \mu_f)$ . Dashed lines are those with fixed-order Coulombic potentials  $V_C(r)$ . Arrows indicate dislocations of the maximum point of  $R$  as the  $\mathcal{O}(1/c)$  and  $\mathcal{O}(1/c^2)$  corrections are included, respectively. We set  $\mu_f = 3 \text{ GeV}$ ,  $m_{\text{PS}}(\mu_f) = 175 \text{ GeV}$ ,  $\mu_s = 75 \text{ GeV}$ ,  $\Gamma_t = 1.43 \text{ GeV}$ , and  $\alpha_s(m_Z) = 0.118$ .

	(fixed-order)		(RG-improved)	
	$\mu_s = 20 \text{ GeV}$	$\mu_s = 75 \text{ GeV}$	$\mu_s = 20 \text{ GeV}$	$\mu_s = 75 \text{ GeV}$
LO	1.390 GeV	0.838 GeV	1.573 GeV	1.573 GeV
NLO	1.716 GeV	1.453 GeV	1.861 GeV	1.861 GeV
NNLO	2.062 GeV	1.817 GeV	2.136 GeV	2.058 GeV

Table 2.2: “Binding energies” of the  $1S$  resonance state defined as  $2m_{\text{PS}}(\mu_f) - M_{1S}$  at LO, NLO, and NNLO calculated with  $V_C(r)$  (fixed-order) and with  $V_C^{(\text{RG})}(r; \mu_f)$  (RG-improved). These are determined by reducing the decay width  $\Gamma_t$  tentatively. We set  $\mu_f = 3 \text{ GeV}$ ,  $m_{\text{PS}}(\mu_f) = 175 \text{ GeV}$ ,  $\Gamma_t = 1.43 \text{ GeV}$ , and  $\alpha_s(m_Z) = 0.118$ .

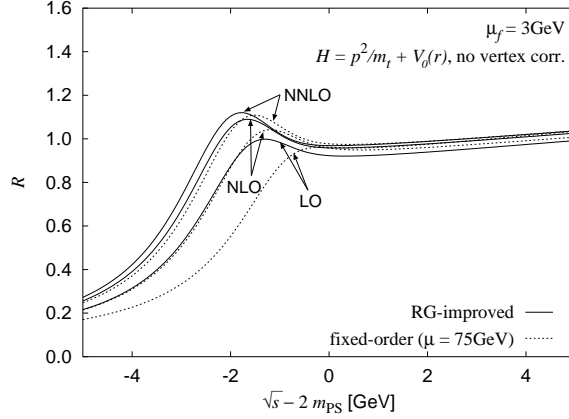


Figure 2.11:  $R$ -ratios for  $e^+e^- \rightarrow \gamma^* \rightarrow t\bar{t}$  calculated with a Hamiltonian  $H = p^2/m_t + V_0(r)$ , where  $V_0(r)$  includes only the Coulombic part of the  $t\bar{t}$  potential. Other corrections (hard vertex corrections, relativistic corrections, etc.) are not included. Solid and dashed lines, respectively, show  $R$ -ratios with ( $V_0(r) = V_C^{(\text{RG})}(r; \mu_f)$ ) and without ( $V_0(r) = V_C^{(\text{fixed})}(r; \mu_f)$ ,  $\mu_s = 75 \text{ GeV}$ ) a renormalization-group improvement of the Coulombic potential. We set  $\mu_f = 3 \text{ GeV}$ ,  $m_{\text{PS}}(\mu_f) = 175 \text{ GeV}$ ,  $\Gamma_t = 1.43 \text{ GeV}$ , and  $\alpha_s(m_Z) = 0.118$ .

formula is

$$R(s) = \frac{6\pi N_c Q_t^2}{m_t^2} \text{Im} G(0, 0)$$

with

$$\left\{ \frac{-1}{m_t} \left[ \frac{d^2}{dr^2} + \frac{2}{r} \frac{d}{dr} \right] + V_0(r) - \omega \right\} G(r, r') = \frac{1}{4\pi r r'} \delta(r - r'),$$

both for fixed order  $V_0(r) = V_C^{(\text{fixed})}(r; \mu_f)$  and RG-improved  $V_0(r) = V_C^{(\text{RG})}(r; \mu_f)$ . We can see clearly that the convergence is much improved by the  $\log(\mu_s)$  resummations. Thus it is other corrections that disturb the perturbative convergence of  $R$  ratio. Among them the  $1/r^2$  potential  $V_{\text{NA}}(r)$ , which is a strong attractive potential near the origin, is suspected to be the worst. It remains as our future task to gain better understandings of these residual large corrections.

Shown in Figure 2.12 is  $\alpha_s^{\overline{\text{MS}}}(m_Z)$ -dependence of  $R$  ratio. The peak position moves  $0.12 \text{ GeV} \times 2$  with the variation of  $\alpha_s^{\overline{\text{MS}}}(m_Z) = 0.119 \pm 0.002$ , which is the current uncertainty [2].

### 2.8.1 Theoretical uncertainties for NNLO calculation of $R$ ratio

There are several uncertainties in our NNLO calculation of  $R$  ratio. In this section we study the size of them and estimate the theoretical uncertainty  $(\Delta m_t^{\text{PS}})^{\text{th}}$  of top mass determination. Since the perturbative convergence of  $R$  ratio is the best with the RG-improved potential and the Potential-Subtracted mass, we study the uncertainties for this case.

Leading  $\log(q/\mu_s)$ 's of  $\tilde{V}_C(q)$  can be summed over not only with the choice  $\mu_s = q$ , but also  $\mu_s = 2q$  etc. Their difference is related to the summation of the next-to-leading log's (and higher). Shown in Figure 2.13 are the uncertainties due to this freedom. One can see that it

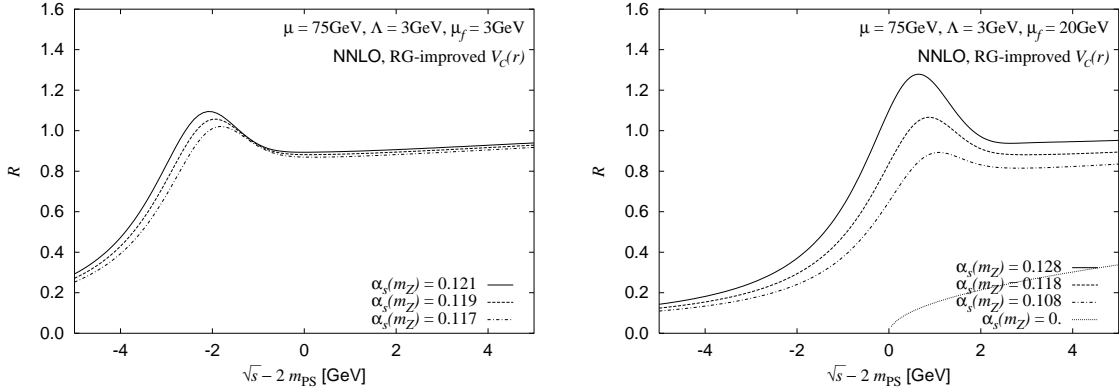


Figure 2.12: Dependence of  $R$  ratio with the variation of  $\alpha_s^{\overline{\text{MS}}}(m_Z)$ : 0.117, 0.119, and 0.121 for the left, and 0.108, 0.118, and 0.128 for the right. For both figures, IR part  $k < \Lambda = 3 \text{ GeV}$  of Coulombic potential  $\tilde{V}_C(k)$  is not taken into account for the Fourier transform to  $V_C(r)$ . For the figure on the right, twice the  $\Delta m(\mu_f = 20 \text{ GeV}) - \Delta m(\Lambda = 3 \text{ GeV})$  is further subtracted from  $V_C(r)$  and added to  $m_{\text{PS}}$ . No width is included for  $\alpha_s(m_Z) = 0$ . We set  $\mu_s = 75 \text{ GeV}$ ,  $m_{\text{PS}}(\mu_f) = 175 \text{ GeV}$ ,  $\Gamma_t = 1.43 \text{ GeV}$ .

is fairly small for both NLO and NNLO. The dependence is large for LO, since there is no log that compensates the log dependence of the coupling.

The soft-scale dependence still remains in the potential, since we RG improve only the Coulombic part. It is shown in the left-half of Figure 2.14. A physical quantity  $Q$  do not depend on the choice of renormalization scale  $\mu$  provided  $Q$  is calculated to all order. If perturbative expansion is terminated to certain order,  $Q$  depends on  $\mu$  since the discarded higher order terms depend on  $\mu$ . Thus it is expected that the truncated perturbative expansion is a “good” approximation when  $\mu$  dependence is small, and the magnitude of  $\mu$  dependence around there is a measure of (uncalculated) higher order corrections. With this view, one can see that the choice  $\mu_s \simeq p_B \simeq 20 \text{ GeV}$  is not “good” for  $R$  ratio. The right-half of Figure 2.14 shows cut-off  $r_0$  dependence, which is absent for NLO and LO, and also for NNLO if one treats the effect of top decay width  $\Gamma_t$  properly. One can see that the dependence on  $r_0$  is small for  $r_0 \simeq r_0^{(\text{ref})}$ . Thus one can see both  $\mu_s$  and  $r_0$  dependence is small compared to the difference of NNLO  $R$  ratio and NLO  $R$  ratio. Besides the shifts are only horizontal, thus do not disturb the determination of top mass  $m_t^{\text{PS}}(\mu_f)$ .

More quantitatively, the variation of the peak position of  $\sigma_{\text{tot}}^{\text{NNLO}}$  is  $0.08 \text{ GeV} \times 2$  both for  $\mu_s = 20 \text{ GeV} - 150 \text{ GeV}$  and  $\mu_s/q = 1/2 - 2$ .

### Estimate of $(\Delta m_t)^{\text{th}}$

Now let us estimate the theoretical uncertainty of top quark mass  $m_t^{\text{PS}}(\mu_f)$  with  $\mu_f = 3 \text{ GeV}$  based on our NNLO calculations. Since both  $\mu_s$ - and  $r_0$ -dependence are fairly small in the side-ward direction, we can forget about them. RG-improve prescription dependence [Figure 2.13] may serve as a measure of theoretical uncertainty. One can see that the sideward NLO correction to LO  $R$ -ratio is similar to the uncertainty of LO  $R$ -ratio due to the choice of  $\mu_s/q$ . Likewise, NNLO correction of NLO  $R$  is also similar to the uncertainty of NLO, but it is a little smaller. This may be because there are sources of NNLO correction other than those log’s; that

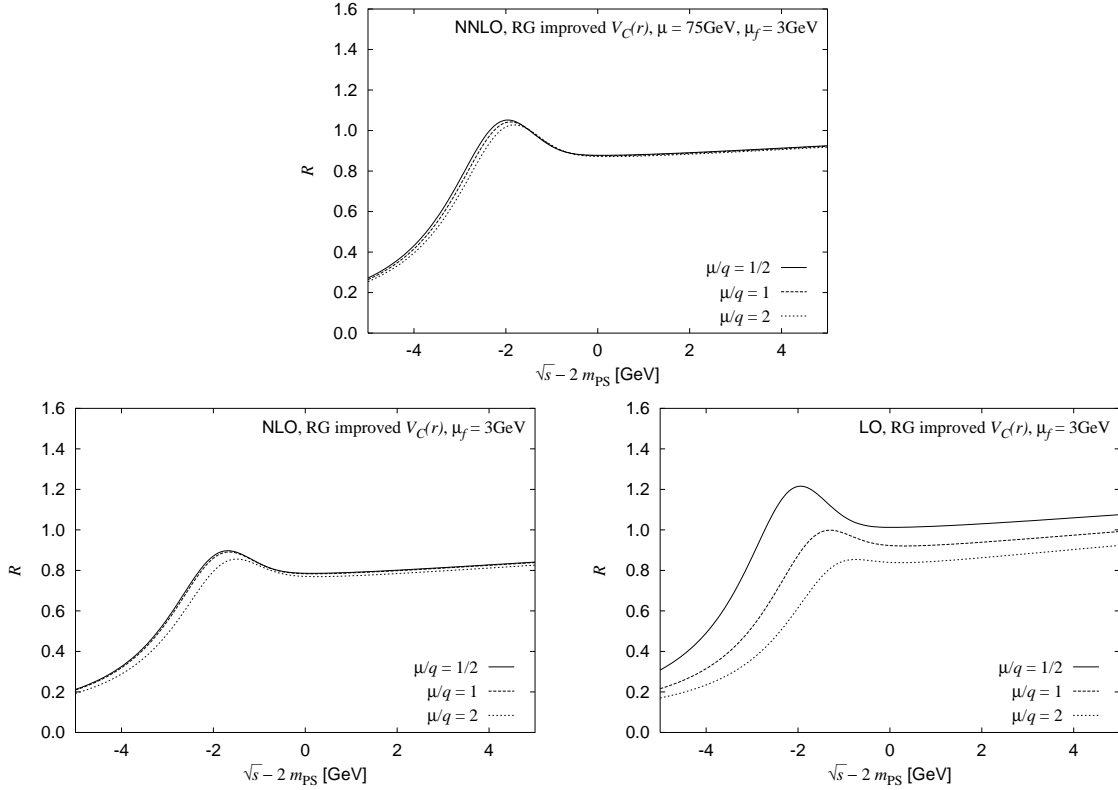


Figure 2.13: Dependence of  $R$  ratio on the prescription to sum-over leading  $\log(\mu_s/q)$ 's of  $\tilde{V}_C(q)$ . Three choices are given for each with NNLO (top), NLO (bottom-left), and LO (bottom-right) corrections:  $\mu_s = q/2, q, 2q$ . We set  $\mu_f = 3 \text{ GeV}$ ,  $m_{\text{PS}}(\mu_f) = 175 \text{ GeV}$ ,  $\Gamma_t = 1.43 \text{ GeV}$ , and  $\alpha_s(m_Z) = 0.118$ . For NNLO  $\mu_s = 75 \text{ GeV}$ .

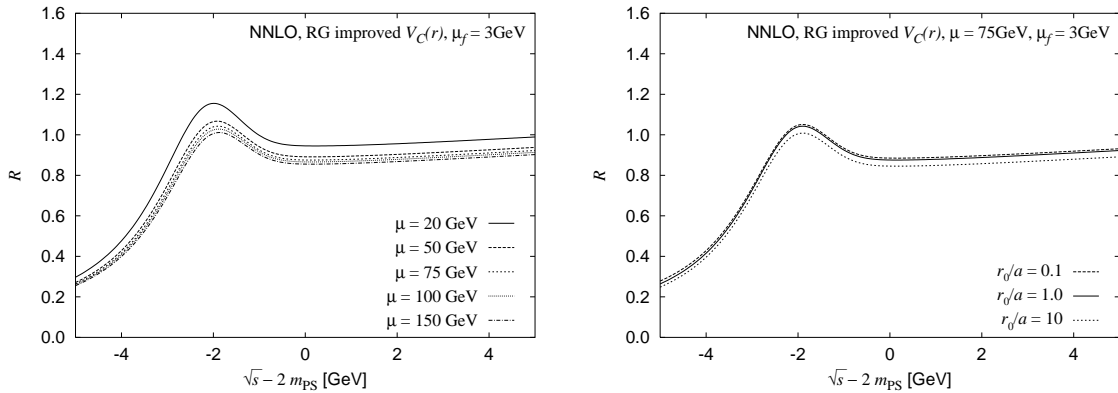


Figure 2.14: (Left) The soft-scale ( $\mu_s$ ) dependence of  $R$  ratio with NNLO corrections.  $\mu_s$  is written as  $\mu$  for simplicity. The normalization changes monotonically in the choice of  $\mu_s$  shown in the figure:  $\mu_s = 20 \text{ GeV}$  for highest and  $\mu_s = 150 \text{ GeV}$  for the lowest. (Right) The cut-off ( $r_0$ ) dependence of  $R$  ratio with NNLO corrections.  $r_0^{(\text{ref})}$  is written as  $a$  for simplicity. In both figures, we set  $\mu_f = 3 \text{ GeV}$ ,  $m_{\text{PS}}(\mu_f) = 175 \text{ GeV}$ ,  $\Gamma_t = 1.43 \text{ GeV}$ , and  $\alpha_s(m_Z) = 0.118$ .

is,  $V_{\text{BF}}$  and  $V_{\text{NA}}$ . Thus we estimate the NNLO theoretical ambiguity to be  $(\Delta m_t)^{\text{th}} \sim 0.1 \text{ GeV}$ . Here we are conservative, since there are corrections aside from log's, such as  $V_{\text{VA}}$ .

As for  $\text{N}^3\text{LO} = \mathcal{O}(1/c^3)$  corrections, those terms for  $V_{\text{BF}}$  is  $\sim C_F a_s / (m^3 c^3 r^4)$ , since  $mcr$  is dimensionless. Here only the dimension is considered. Thus translations like  $1/r^2 \sim p^2$ ,  $1/r^3 \sim \delta^{(3)}(\mathbf{r})$ ,  $1/r \sim d/dr$  are possible. Likewise,  $\mathcal{O}(1/c^3)$  correction to  $V_{\text{NA}}$  may be  $\sim C_A C_F a_s^2 / (m^2 r^3 c^3)$ , since  $a_s^4$  may be  $\mathcal{O}(1/c^4)$ . Another significant modification is that real gluon emission is possible to  $\mathcal{O}(1/c^3)$ .

In our calculations, leading log's in  $V_C$  are summed with RG. Recently next-to-leading log's corrections of  $\text{N}^3\text{LO}$ ,  $\alpha_s^3 \ln^2(1/\alpha_s)$ , to  $R$  ratio is calculated in [32]. One can read that the size of  $\text{N}^3\text{LO}$  corrections to the peak position is  $\sim 2 \times 0.1 \text{ GeV}$ , which is consistent with the estimate above.

### Non-perturbative effect

Non-perturbative corrections modify QCD potential at  $r \sim 1/(1 \text{ GeV})$  and far. Thus their effects can be estimated by the dependence of Green function  $G$  with respect to the variation of the potential around  $r \sim 1/(1 \text{ GeV})$ ; and it turns out to be small. For  $r > r'$ ,

$$G'(r, r') = \frac{1}{4\pi C_F a_s W} \frac{g_>(r)g_<(r')}{rr'},$$

where  $g_>(r)/r$  and  $g_<(r)/r$  are the solutions of (reduced) Schrödinger equation [Eq. (2.38)] with the boundary conditions  $\lim_{r \rightarrow \infty} g_>(r) = 0$  and  $\lim_{r \rightarrow 0} g_<(r) \simeq (C_F a_s m_t r)^{d_+}$ , respectively. Since only  $G'(r, r')|_{r=r' \simeq 0}$  is relevant for  $R$  ratio, it is  $g_>(r)$  near the origin that determines  $R$  ratio. It may be affected by non-perturbative effect ( $r \gtrsim 1/(1 \text{ GeV})$ ) through the boundary condition. However we can see in Figure 2.16 that  $g_>(r)$  dumps well within perturbative region  $r/r_B \lesssim 20$  with  $r \sim 1/(1 \text{ GeV})$ . Thus non-perturbative effect (to the QCD potential) do not alter the Green function for  $t\bar{t}$ . We also show  $g_<(r)$  in Figures 2.17 and 2.18, for reference.

### Effect of $Z$ exchange

To  $\mathcal{O}(1/c^2)$ , axial-vector current  $j_A^\mu$  also contributes since it is suppressed by  $\mathcal{O}(1/c)$ . Note that the ‘‘cross term’’  $j_A^* j_V$  of axial-vector and vector ( $j_V^\mu$ ) current do not contribute to total cross section Section 4.3.2. The effect of  $Z$  exchange between  $e^+e^-$  current and  $t\bar{t}$  current is incorporated by rescaling the vector–vector coupling and by adding the effect of axial-vector–axial-vector coupling. With the notation defined in Eq. (A.33), the former changes only overall normalization by the ratio  $|[v^e v^t]|^2 + |[a^e v^t]|^2$  to  $Q_t^2$ . The effective couplings  $[v^e v^t]$  etc. are defined in Section A.5. Numerically it is  $0.480/0.444 = 1.080$  on the threshold. Especially, theoretical uncertainty  $(\Delta m_t)^{\text{th}}$  for determination of  $m_t$  is not altered by this inclusion, since it is energy independent. While in [30] it is shown that the effect of  $j_A^* j_A$  is small and flat with respect to  $E$  near the threshold<sup>26</sup>, since it is suppressed by  $\beta^2$  compared to  $j_V^* j_V$ . Note that only the leading order calculation of  $j_A^* j_A$  is sufficient for the NNLO calculation of  $R$  ratio. Thus  $R$  ratio near the threshold is not altered when the effect of  $Z$  exchange is taken into account, and so is  $(\Delta m_t)^{\text{th}}$ .

<sup>26</sup> Note that the corresponding coupling is  $|[v^e a^t]|^2 + |[a^e a^t]|^2 = 0.1430$  on the threshold.

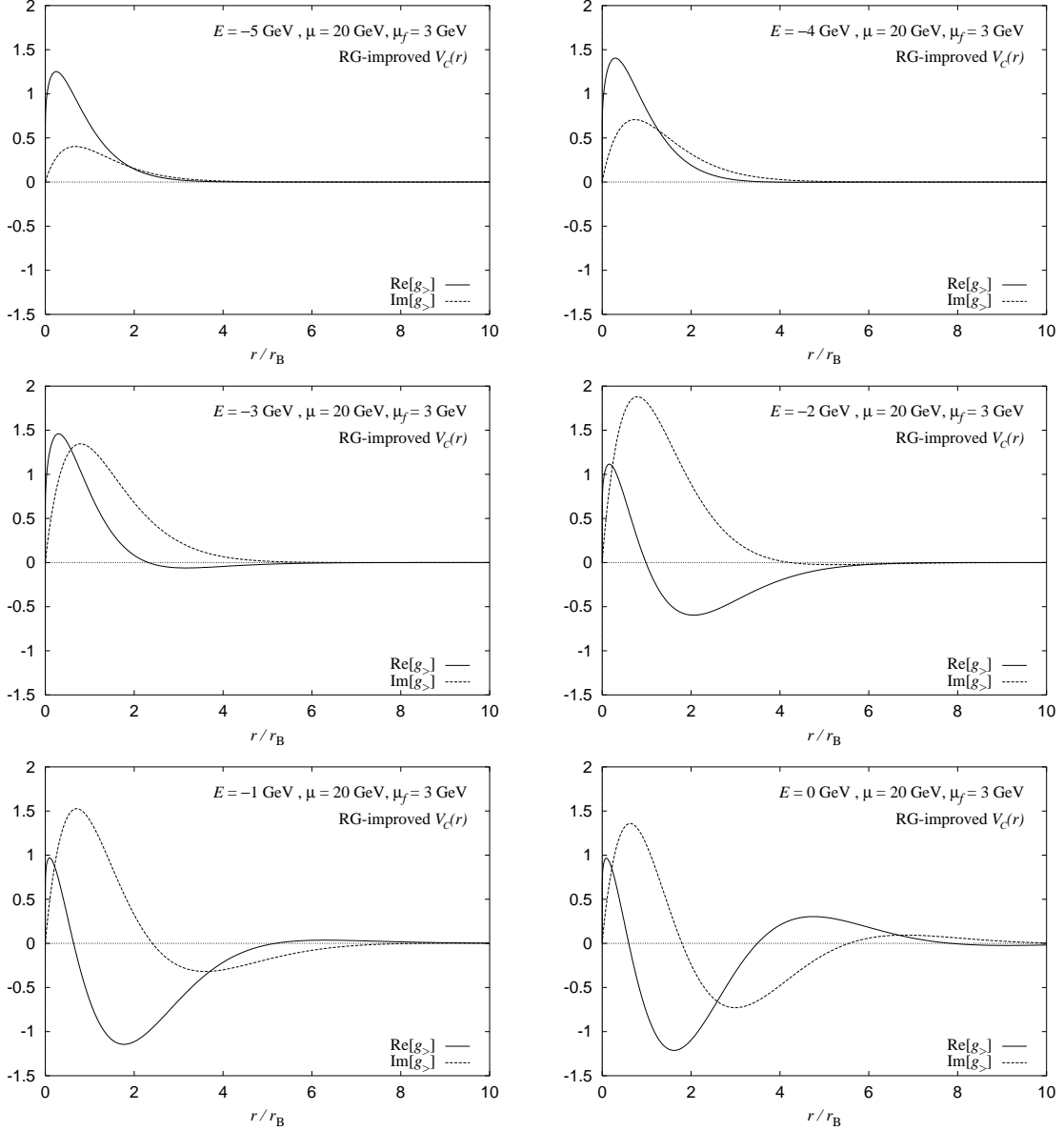


Figure 2.15: The function  $g_{>}(r)/r$  is a solution of the (reduced) Schrödinger equation to NNLO [Eq. (2.38)] that dumps at  $r \rightarrow \infty$ . CM energy is changed from  $E = -5$  GeV to 0 GeV. They are plotted vs.  $r/r_B = p_B r$ , where  $1/r_B = p_B = C_F \alpha_s m_t / 2 = 17.94$  GeV for  $\alpha_s = \alpha_s^{\overline{\text{MS}}}(\mu_s = 20 \text{ GeV}) = 0.1534$ . Perturbative potential description is valid within the hard scale  $\sim p_B/m_t = 0.1023$  and the  $\Lambda_{\text{QCD}}$  scale  $\sim p_B/(1 \text{ GeV}) = 17.94$ . We set  $\mu_s = 20$  GeV,  $\mu_f = 3$  GeV,  $m_{\text{PS}}(\mu_f) = 175$  GeV,  $\Gamma_t = 1.43$  GeV, and  $\alpha_s(m_Z) = 0.118$ .

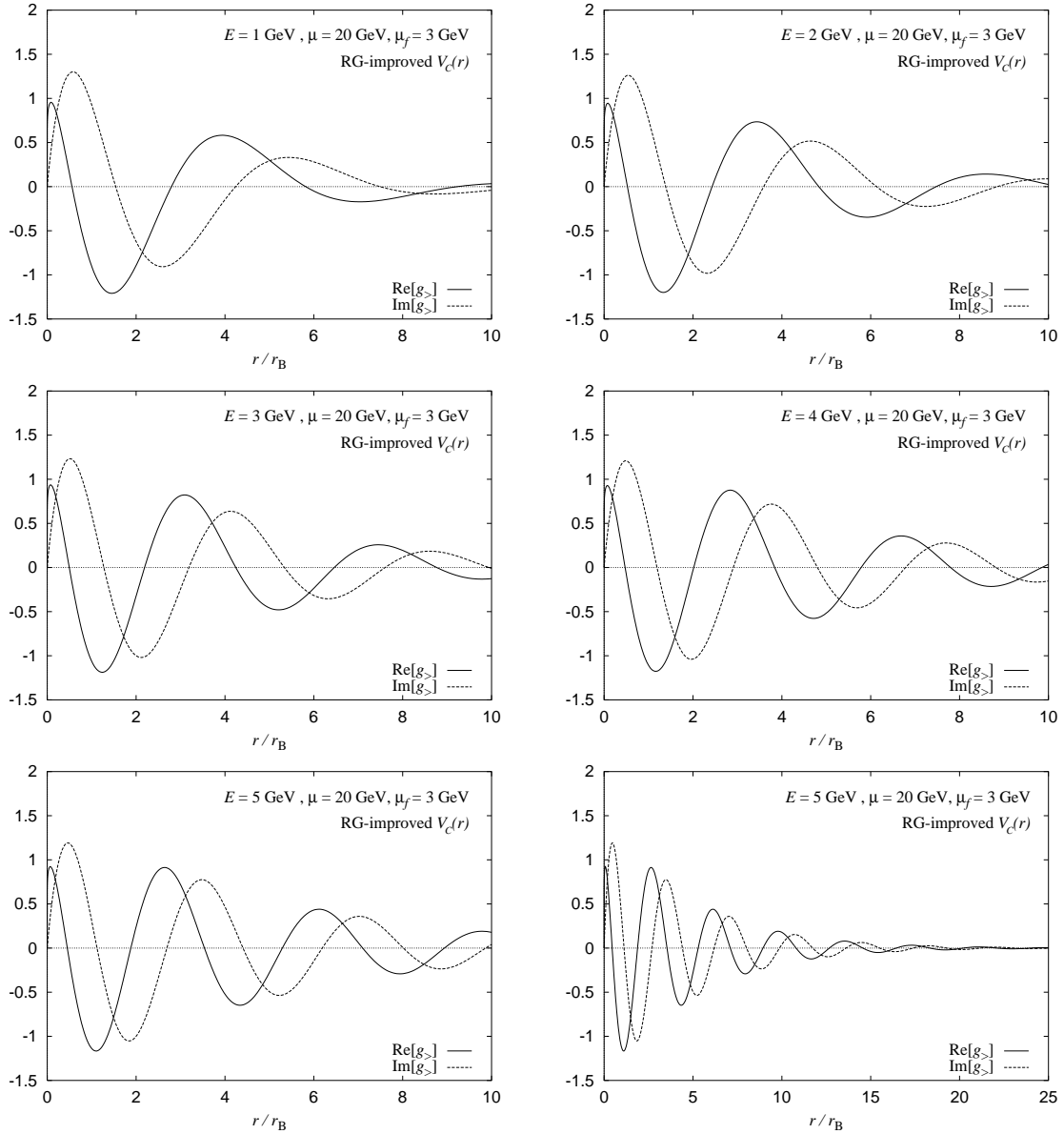


Figure 2.16: The same as Figure 2.15. CM energy is changed from  $E = 1 \text{ GeV}$  to  $5 \text{ GeV}$ . The last two figures are both for  $E = 5 \text{ GeV}$ ; only the range of  $r$  differs.

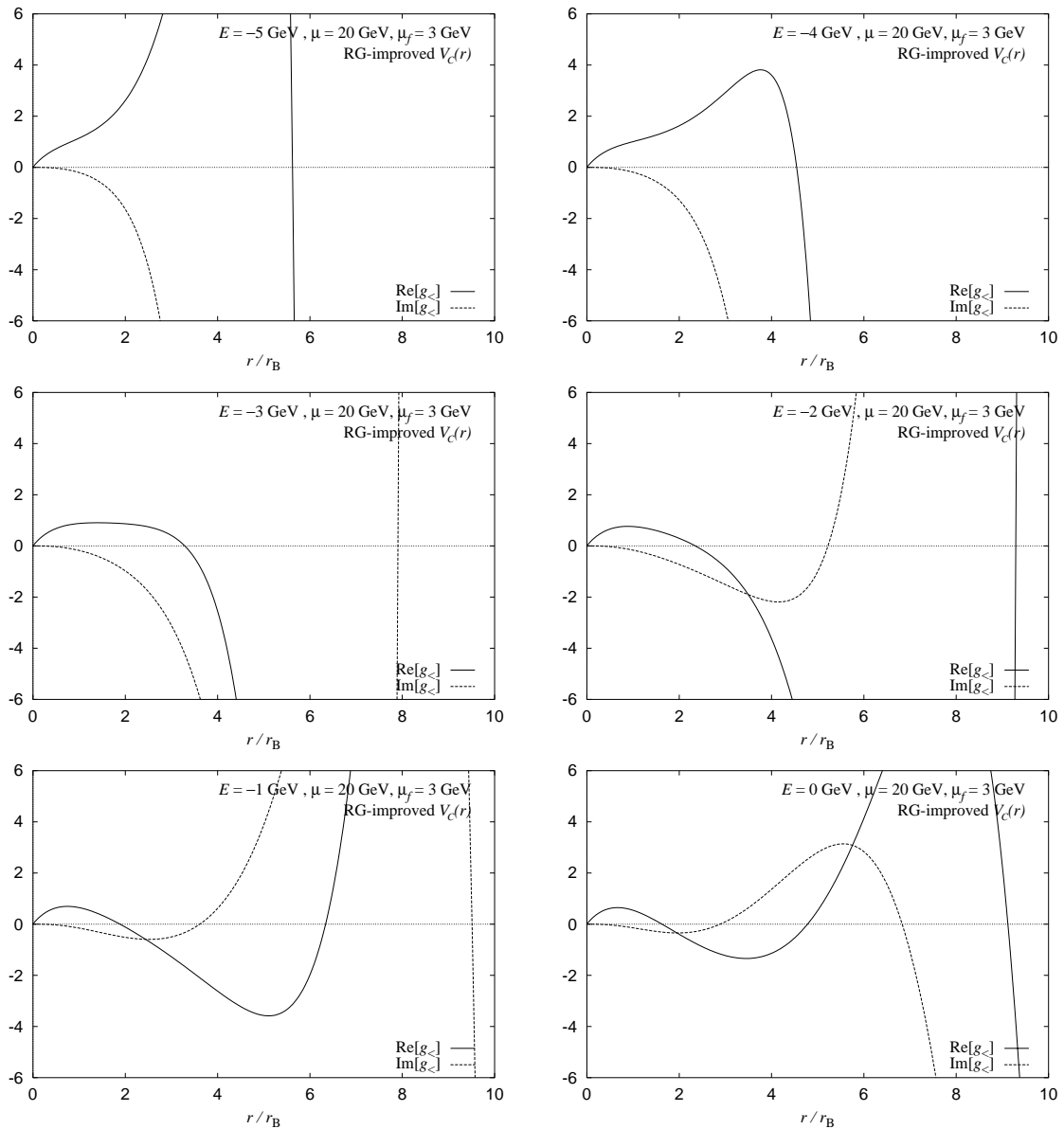


Figure 2.17: The function  $g_{<}(r)/r$  is a solution of the (reduced) Schrödinger equation to NNLO [Eq. (2.38)] that dumps at  $r \rightarrow 0$ . Other situations are just the same as Figure 2.15.



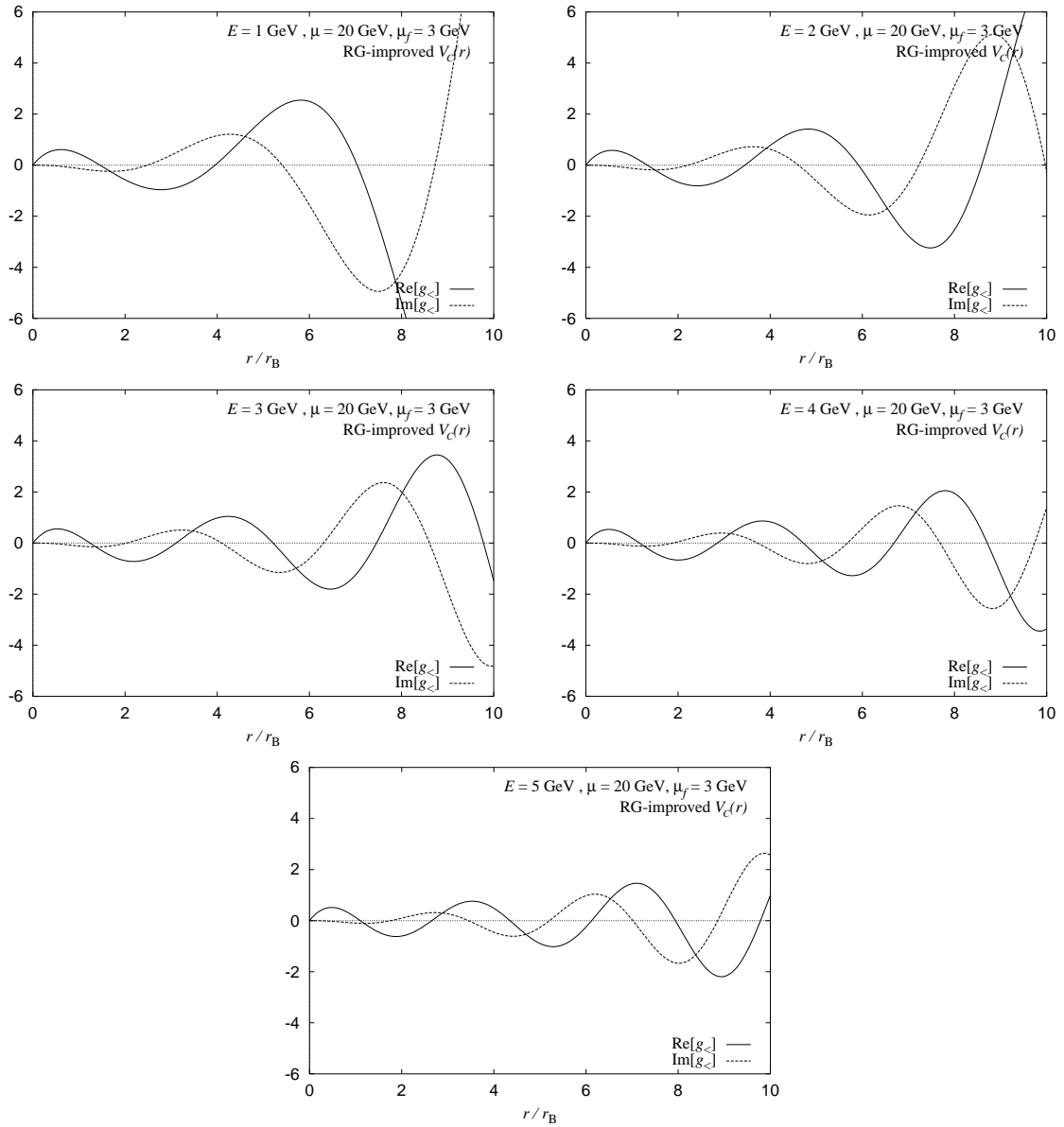


Figure 2.18: Solutions of the (reduced) Schrödinger equation to NNLO [Eq. (2.38)] that dumps at  $r \rightarrow 0$ . Other situations are just the same as Figure 2.16.

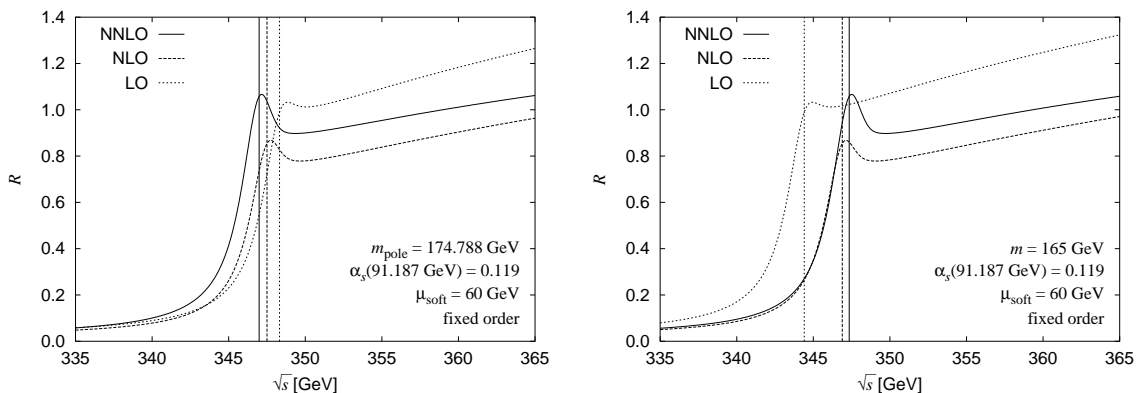


Figure 2.19:  $R$  ratio in  $m_{\text{pole}}$  scheme (left) and  $m_{\overline{\text{MS}}}$  scheme. See text for detail.

### Effect of using $m_{\overline{\text{MS}}}$ instead of $m_{\text{pole}}$

Shown in Figure 2.19 is the effect of using different mass schemes. In the left figure, pole-mass is fixed to  $m_{\text{pole}} = 174.788 \text{ GeV}$ ; while in the right one,  $\overline{\text{MS}}$ -mass is fixed to  $\bar{m}(\bar{m}) = 165 \text{ GeV}$ , which corresponds to  $m_{\text{pole}} = 174.788 \text{ GeV}$  at NNNLO. In both figures,  $\alpha_s^{\overline{\text{MS}}}(m_Z) = 0.119$  is used; this corresponds to  $\alpha_s^{\overline{\text{MS}}}(165 \text{ GeV}) = 0.109$ . Note that the used potential is one in fixed-order; also PS-mass scheme is not used. By letting  $\Gamma_t \rightarrow 0$ , one can investigate the position of  $1S$  peak. These positions are also shown in the figures by vertical lines. Numerically, they are (348.321 GeV, 347.504 GeV, 346.986 GeV) for (LO, NLO, NNLO) when  $m_{\text{pole}}$  is fixed, while (344.408 GeV, 346.892 GeV, 347.340 GeV) when  $\bar{m}(\bar{m})$  is fixed.

# Chapter 3

## Top-Quark Momentum Distribution

Due to the large decay width  $\Gamma_t$ , the momentum  $|\mathbf{p}_t|$  of top quark is not determined by the CM energy  $\sqrt{s} = 2m_t + E$ , but distributes around  $|\sqrt{m_t(E + 1 \text{ GeV} + i\Gamma_t)}|$ , where  $1 \text{ GeV} \sim$  binding energy. Momentum distribution  $d\sigma/dp$  of top quark in  $e^+e^- \rightarrow t\bar{t}$  near the threshold is calculated in [13] to LO, and in [15] to NLO. In this section we calculate a part of NNLO correction; that is, only gluon exchange between  $t\bar{t}$  is considered. Gluon exchange between  $t$  and  $\bar{b}$  etc. are not considered.

### 3.1 Derivation of the distribution

Differential cross section of  $t\bar{t}$  pair production can be written as follows:

$$\begin{aligned} d\sigma(e^+e^- \rightarrow t\bar{t} \rightarrow bW^+\bar{b}W^-) &= \frac{N_C}{2s} \sum_{X,Y=\gamma,Z} \frac{(2m_t)^4}{(s - m_X^2)(s - m_Y^2)} (E_{XY})^{\mu\nu} (H_{XY})^{\mu\nu} \\ &\times \left| \frac{1}{p_t^2 - m_t^2 + im_t\Gamma_t} \frac{1}{\bar{p}_t^2 - m_t^2 + im_t\Gamma_t} \right|^2 d\Phi_4(bW^+\bar{b}W^-), \end{aligned}$$

where

$$\begin{aligned} (E_{XY})^{\mu\nu} &= \text{tr} \left[ \Lambda_X^\mu \frac{(1 - P_{e^+} P_{e^-}) - (P_{e^+} - P_{e^-}) \not{p}'_e \bar{\Lambda}_Y^\nu \not{p}'_e}{4} \right], \\ (H_{XY})^{\mu\nu} &= \left( \frac{g_W}{\sqrt{2}} \right)^4 \text{tr} \left[ \frac{\not{p}'_t + m_t}{2m_t} \Gamma_X^\mu \frac{-\not{p}'_t + m_t}{2m_t} \gamma^\alpha \frac{1 - \gamma_5}{2} \not{p}'_b \gamma^\beta \frac{1 - \gamma_5}{2} \times \right. \\ &\times \left. \frac{-\not{p}'_t + m_t}{2m_t} \bar{\Gamma}_Y^\nu \frac{\not{p}'_t + m_t}{2m_t} \gamma^\rho \frac{1 - \gamma_5}{2} \not{p}'_b \gamma^\sigma \frac{1 - \gamma_5}{2} \right] \times \\ &\times \left[ -g_{\alpha\beta} + \frac{(\bar{p}_W)_\alpha (\bar{p}_W)_\beta}{m_W^2} \right] \left[ -g_{\rho\sigma} + \frac{(p_W)_\rho (p_W)_\sigma}{m_W^2} \right], \end{aligned}$$

and

$$\begin{aligned}\Lambda_X^\mu &= g_X (v^{eX} \gamma^\mu - a^{eX} \gamma^\mu \gamma_5) , \\ \Gamma_X^\mu &= (|\mathbf{p}_t|^2/m_t - (E + i\Gamma_t)) \times \\ &\quad \times g_X \left[ v^{tX} (1 + \delta_V) \tilde{G}(E, \mathbf{p}_t) \gamma^\mu - a^{tX} (1 + \delta_A) \tilde{F}(E, \mathbf{p}_t) \gamma^\mu \gamma_5 \right] , \\ \delta_V &= -\frac{8\alpha_s}{3\pi} , \quad \delta_A = -\frac{4\alpha_s}{3\pi} .\end{aligned}$$

This can be obtain by usual Feynman rules with the modification of the  $t\bar{t}$  production vertex  $\Gamma^\mu$  due to the Coulomb rescattering. The formula above can be reduced more by approximating the momenta of top and anti-top by their on-shell values<sup>1</sup>. By decomposing the phase space of  $bW^+\bar{b}W^-$  into  $t\bar{t}$

$$d\Phi_4(bW^+\bar{b}W^-) = \frac{d^4p}{(2\pi)^4} d\Phi_2(t^* \rightarrow bW^+) d\Phi_2(\bar{t}^* \rightarrow \bar{b}W^-) ,$$

where  $p_t = q/2 + p$  and  $\bar{p}_t = q/2 - p$  ( $q$  is the total momentum), both  $bW^+$  and  $\bar{b}W^-$  can integrated out:

$$\begin{aligned}\int d\Phi_2(\bar{t} \rightarrow \bar{b}W^-) &\left( \frac{g_W}{\sqrt{2}} \right)^2 \gamma^\alpha \frac{1 - \gamma_5}{2} \not{p}_b \gamma^\beta \frac{1 - \gamma_5}{2} \left[ -g_{\alpha\beta} + \frac{(\bar{p}_W)_\alpha (\bar{p}_W)_\beta}{m_W^2} \right] \\ &= \frac{\Gamma_t}{m_t} \not{p}_t (1 - \gamma_5) .\end{aligned}$$

As for the remaining phase space  $d^4p/(2\pi)^4$ , the time-component can be integrated with the formulas

$$\begin{aligned}\int \frac{dz}{2\pi} \frac{1}{z - (x + iy)} \frac{1}{z + (x + iy)} &= \frac{i}{2(x + iy)} , \\ \int \frac{dz}{2\pi} \left| \frac{1}{z - (x + iy)} \frac{1}{z + (x + iy)} \right|^2 &= \left| \frac{i}{2(x + iy)} \right|^2 \frac{1}{y} ,\end{aligned}$$

since we put  $p_t^0 = \sqrt{\mathbf{p}_t^2 + m_t^2}$  everywhere aside from at the denominators of propagators. Thus we have

$$\begin{aligned}\frac{d\sigma(e^+e^- \rightarrow t\bar{t})}{d^3p} &= \frac{1}{(2\pi)^3} \frac{N_C}{2s} \sum_{X,Y=\gamma,Z} \frac{2\Gamma_t}{(s - m_X^2)(s - m_Y^2)} \left| \frac{1}{E - \mathbf{p}^2/m_t + i\Gamma_t} \right|^2 \times \\ &\quad \times \text{tr} \left[ \Gamma_X^\mu \frac{\not{p}_t - m_t}{2m_t} \bar{\Gamma}_Y^\nu \frac{\not{p}_t + m_t}{2m_t} \right] (E_{XY})_{\mu\nu} .\end{aligned}$$

The momentum distributions of the decay products of  $W$ 's depend on the polarization of top-quark. For such calculations, the following relations may be useful:

$$\frac{\not{p} + m}{2m} G \frac{\not{p} + m}{2m} = \frac{\not{p} + m}{2m} \frac{1 - \not{P} \gamma_5}{2} C , \quad \frac{\not{p} - m}{2m} \bar{G} \frac{\not{p} - m}{2m} = \frac{\not{p} - m}{2m} \frac{1 - \bar{P} \gamma_5}{2} \bar{C} ,$$

<sup>1</sup> Except at the denominators of the top and anti-top propagators.

where

$$\frac{1 - \mathbf{P} \cdot \mathbf{s}}{2} C = \text{tr} \left[ G \frac{\not{p} + m}{2m} \frac{1 - \not{s} \gamma_5}{2} \right], \quad \frac{1 - \bar{\mathbf{P}} \cdot \bar{\mathbf{s}}}{2} \bar{C} = \text{tr} \left[ \bar{G} \frac{\not{\bar{p}} - m}{2m} \frac{1 - \bar{\not{s}} \gamma_5}{2} \right].$$

These relations hold when  $p^2 = m^2$ ,  $\mathbf{P} \cdot \mathbf{p} = \mathbf{s} \cdot \mathbf{p} = 0$ , and the likewise for  $\bar{p}$ . These relations can be easily verified at the rest frame of  $p$ . Note that although  $G$  is a general  $4 \times 4$  matrix, only  $2 \times 2$  sub-matrix contributes because of the projection operators  $\not{p} + m/(2m)$  etc. Those four degrees of freedom are expressed by one scalar  $C$  and one 4-vector  $\mathbf{P}$  with one constraint  $\mathbf{P} \cdot \mathbf{p} = 0$ .

For the case of  $\gamma$ -mediated  $t\bar{t}$  production, the distribution  $d\sigma/dp$  can be calculated in usual way with the vertices

$$\Lambda^\mu = e Q_e \gamma^\mu, \quad \Gamma^\mu = (|\mathbf{p}_t|^2/m_t - (E + i\Gamma_t)) e Q_t \tilde{G}(E, \mathbf{p}_t) \gamma^\mu.$$

At the leading order, the distribution can be written as

$$\frac{1}{\sigma_{\text{pt}}} \frac{d\sigma}{dp} = \frac{4\pi p^2}{(2\pi)^3} \cdot \frac{3}{2} N_C Q_t^2 \frac{4m^2}{s} \frac{4\pi}{m^2 c} \Gamma_t \left| \tilde{G}(r=0, p) \right|^2.$$

For  $\Gamma_t \rightarrow 0$ , this is zero unless  $\tilde{G}(r=0, p)$  diverges. This is consistent with

$$\frac{1}{\sigma_{\text{tot}}} \frac{d\sigma}{dp} = \delta(p - \sqrt{m_t E}), \quad \text{for } \Gamma_t = 0.$$

## 3.2 Unitarity relation

Momentum integration of the differential cross section  $d\sigma/dp$  should coincide to the total cross section  $\sigma_{\text{tot}}$ . This relation is called unitarity. It is important to confirm oneself that unitarity holds both theoretically and numerically within the accuracy considered.

For a Green function

$$G = \frac{1}{H - \omega}, \quad \omega = E + i\Gamma,$$

its imaginary part can be expressed as

$$\begin{aligned} \text{Im } G &\equiv \frac{1}{2i} (G - G^\dagger) = G^\dagger \frac{(G^{-1})^\dagger - G^{-1}}{2i} G = G \frac{(G^{-1})^\dagger - G^{-1}}{2i} G^\dagger \\ &= G^\dagger \text{Im} [(G^{-1})^\dagger] G = G^\dagger \text{Im} [H - E + i\Gamma] G \\ &= G^\dagger G \Gamma = G G^\dagger \Gamma, \end{aligned}$$

or

$$\int \frac{d^3p}{(2\pi)^3} \Gamma_t \left| \tilde{G}(|\mathbf{p}|, E) \right|^2 = \text{Im } G(\mathbf{x} = 0, E).$$

Thus the relation

$$\frac{d\sigma}{d^3p} = \sigma_{\text{pt}} N_C Q_t^2 \frac{3}{4\pi^2 m_t^2} \Gamma_t \left| \tilde{G}(|\mathbf{p}|, E) \right|^2, \quad \text{or} \quad \frac{d\sigma}{dp} = \sigma_{\text{pt}} N_C Q_t^2 \frac{3}{\pi m_t^2} p^2 \Gamma_t \left| \tilde{G}(|\mathbf{p}|, E) \right|^2$$

is consistent with the expression for the  $R$  ratio in Eq. (2.3).

Including the higher order corrections for  $t\bar{t}$  current, the unitarity relation above becomes

$$\begin{aligned} & \text{Im} \left[ \left\{ C_1^{(\text{cur})} + C_2^{(\text{cur})} \frac{\Delta_r + \Delta_{r'}}{2m^2 c^2} \right\} G(r, r') \right] \\ &= \int \frac{d^3 p}{(2\pi)^2} \left\{ C_1^{(\text{cur})} + C_2^{(\text{cur})} \frac{\Delta_r + \Delta_{r'}}{2m^2 c^2} \right\} \tilde{G}^*(p, r) \tilde{G}(p, r') \Gamma \\ &= \int \frac{d^3 p}{(2\pi)^2} \left\{ C_1^{(\text{cur})} + C_2^{(\text{cur})} \frac{\Delta_r + \Delta_{r'}}{2m^2 c^2} \right\} \tilde{G}(r, p) \tilde{G}^*(r', p) \Gamma . \end{aligned}$$

Thus the momentum distribution is expected to be expressed as follows:

$$\frac{1}{\sigma_{\text{pt}}} \frac{d\sigma}{dp} = \frac{4\pi p^2}{(2\pi)^3} \cdot \frac{3}{2} N_C Q_t^2 \frac{4m^2}{s} \frac{4\pi}{m^2 c} \Gamma \left\{ C_1^{(\text{cur})} + C_2^{(\text{cur})} \frac{\Delta_r + \Delta_{r'}}{2m^2 c^2} \right\} \tilde{G}(r, p) \tilde{G}^*(r', p) \Big|_{r, r' \rightarrow r_0} ,$$

With the relation

$$\frac{\Delta_r}{m} \tilde{G}(r, p) = - \left[ \frac{C_F a_s}{r} + (E + i\Gamma) \right] \tilde{G}(r, p) - \frac{\sin(pr)}{pr} + \mathcal{O}\left(\frac{1}{c}\right) ,$$

which is just the Schrödinger equation with the Coulomb potential, the derivatives can be removed:

$$\begin{aligned} & \left\{ C_1^{(\text{cur})} + C_2^{(\text{cur})} \frac{\Delta_r + \Delta_{r'}}{2m^2 c^2} \right\} \tilde{G}(r, p) \tilde{G}^*(r', p) \Big|_{r, r' \rightarrow r_0} \\ &= \left\{ C_1^{(\text{cur})} - \frac{C_F}{3} \left(\frac{a_s}{c}\right)^2 \frac{1}{ma_s r_0} - \frac{E}{3m^2 c^2} \right\} \left| \tilde{G}(r_0, p) \right|^2 \\ & \quad - \frac{1}{3mc^2} \frac{\sin(pr_0)}{pr_0} \text{Re} \left[ \tilde{G}(r_0, p) \right] . \end{aligned} \quad (3.1)$$

Here the equality is up to  $\mathcal{O}(1/c^3)$ . We want to express the unitary relation in terms of the reduced Green function  $G'$ :

$$G = G' + \delta G' + \mathcal{O}\left(\frac{1}{c^3}\right) , \quad \text{where} \quad \delta G' = - \{ b\omega + \mathcal{O}_E, G' \} - [\mathcal{O}_O, G'] - b .$$

Thus with

$$\tilde{G}(r, p) = \tilde{G}'(r, p) + \delta \tilde{G}'(r, p) + \mathcal{O}\left(\frac{1}{c^3}\right) ,$$

where  $\tilde{G}(r, p) = \langle r | G | p \rangle$ , we have

$$\left| \tilde{G}(r, p) \right|^2 = \left| \tilde{G}'(r, p) \right|^2 + 2 \text{Re} \left[ \delta \tilde{G}'(r, p) \tilde{G}'^*(r', p) \right] + \mathcal{O}\left(\frac{1}{c^3}\right) .$$

Differential operators can be rewritten in terms of c-numbers as we did for the total cross section:

$$\frac{1}{ma_s r} \frac{d}{dr} r \tilde{G}'(r, p) = \left( \frac{1}{ma_s r} - \frac{C_F}{2} \right) \tilde{G}'(r, p) + \mathcal{O}\left(r, \frac{1}{c}\right) .$$

Thus with the definitions

$$\begin{aligned}\tilde{G}'_E(r, p) &\equiv \langle r | G' \frac{1}{ma_s r} | p \rangle = \frac{4\pi}{ma_s p} \int_0^\infty dr' \sin(pr') G'(r, r') , \\ \tilde{G}'_O(r, p) &\equiv \langle r | G' \frac{1}{ma_s} i p_r | p \rangle = \frac{-4\pi}{ma_s} \int_0^\infty dr' \cos(pr') r' G'(r, r') ,\end{aligned}$$

we have, up to  $\mathcal{O}(1/c^3)$ ,

$$\begin{aligned}\delta\tilde{G}'(r, p) &= \left( \frac{E + i\Gamma}{2mc^2} + \frac{3C_F a_s}{4mc^2 r} \right) \tilde{G}'(r, p) + \frac{3C_F}{4} \left( \frac{a_s}{c} \right)^2 \tilde{G}'_E(r, p) \\ &\quad - \frac{11C_F a_s}{12mc^2} \frac{1}{r} \frac{d}{dr} r \tilde{G}'(r, p) - \frac{11C_F}{12} \left( \frac{a_s}{c} \right)^2 \tilde{G}'_O(r, p) + \frac{1}{4mc^2} \frac{\sin(pr)}{pr} \\ &= \left\{ \frac{E + i\Gamma}{2mc^2} + \frac{3C_F}{4} \left( \frac{a_s}{c} \right)^2 \frac{1}{ma_s r} - \frac{11C_F}{12} \left( \frac{a_s}{c} \right)^2 \left( \frac{1}{ma_s r} - \frac{C_F}{2} \right) \right\} \tilde{G}'(r, p) \\ &\quad + \frac{3C_F}{4} \left( \frac{a_s}{c} \right)^2 \tilde{G}'_E(r, p) - \frac{11C_F}{12} \left( \frac{a_s}{c} \right)^2 \tilde{G}'_O(r, p) + \frac{1}{4mc^2} \frac{\sin(pr)}{pr} ,\end{aligned}$$

$$\begin{aligned}2 \operatorname{Re} \left[ \delta\tilde{G}'(r_0, p) \tilde{G}'(r_0, p)^* \right] \\ = \left\{ \frac{E}{mc^2} + \left( \frac{a_s}{c} \right)^2 \left( -\frac{C_F}{3ma_s r_0} + \frac{11C_F^2}{12} \right) \right\} \left| \tilde{G}'(r_0, p) \right|^2 \\ + \frac{3C_F}{2} \left( \frac{a_s}{c} \right)^2 \operatorname{Re} \left[ \tilde{G}'_E(r_0, p) \tilde{G}'(r_0, p)^* \right] - \frac{11C_F}{6} \left( \frac{a_s}{c} \right)^2 \operatorname{Re} \left[ \tilde{G}'_O(r_0, p) \tilde{G}'(r_0, p)^* \right] \\ + \frac{1}{2mc^2} \frac{\sin(pr_0)}{pr_0} \operatorname{Re} \left[ \tilde{G}'(r_0, p) \right] .\end{aligned}$$

Thus

$$\begin{aligned}\text{Eq. (3.1)} \\ = \left\{ 1 + \left( \frac{\alpha_s(\mu_h)}{\pi} \right) C_F C_1 + \left( \frac{\alpha_s(\mu_h)}{\pi} \right)^2 C_F C_2(r_0) \right\} \left[ \left( 1 + \frac{2E}{3mc^2} \right) \left| \tilde{G}'(r_0, p) \right|^2 \right. \\ \left. + \frac{3C_F}{2} \left( \frac{a_s}{c} \right)^2 \operatorname{Re} \left[ \tilde{G}'_E(r_0, p) \tilde{G}'(r_0, p)^* \right] - \frac{11C_F}{6} \left( \frac{a_s}{c} \right)^2 \operatorname{Re} \left[ \tilde{G}'_O(r_0, p) \tilde{G}'(r_0, p)^* \right] \right. \\ \left. + \frac{1}{6mc^2} \frac{\sin(pr_0)}{pr_0} \operatorname{Re} \left[ \tilde{G}'(r_0, p) \right] \right]\end{aligned}$$

Here we used Eq. (2.42). Up to the terms that vanish when  $r_0 \rightarrow 0$ ,

$$\begin{aligned}\tilde{G}'(r_0, p) &= \frac{1}{4\pi C_F a_s \sqrt{1-4\kappa}} \frac{4\pi}{p} r_0^{-d_-} \int_0^\infty dr \sin(pr) g_>(r) , \\ \tilde{G}'_E(r_0, p) &= \frac{1}{4\pi C_F a_s \sqrt{1-4\kappa}} \frac{4\pi}{ma_s p} r_0^{-d_-} \int_0^\infty dr \frac{\sin(pr)}{r} g_>(r) , \\ \tilde{G}'_O(r_0, p) &= \frac{1}{4\pi C_F a_s \sqrt{1-4\kappa}} \frac{-4\pi}{ma_s} r_0^{-d_-} \int_0^\infty dr \cos(pr) g_>(r)\end{aligned}$$

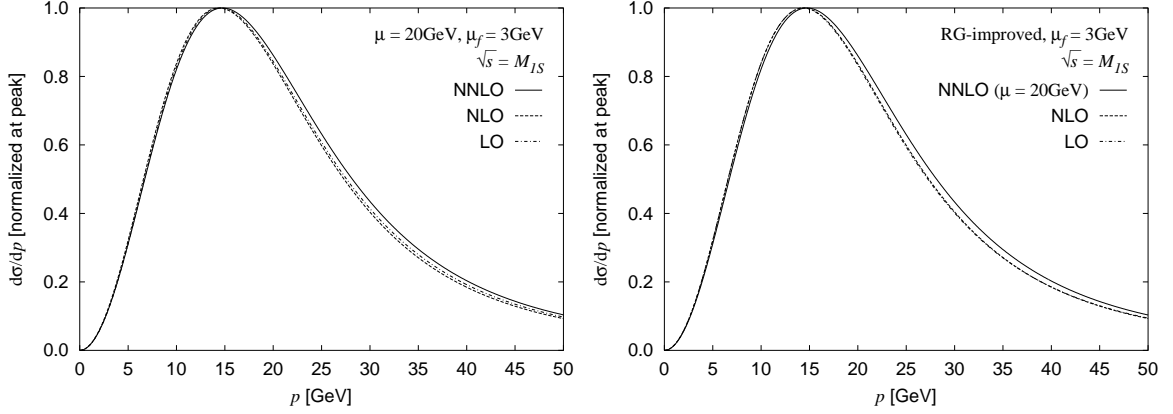


Figure 3.1: Top quark momentum distributions at LO (dot-dashed), NLO (dashed), and NNLO (solid) for  $\mu_s = 20$  GeV (left) and  $\mu_s = 3$  GeV (right). For each curve, we set the c.m. energy on the  $1S$  resonance state,  $\sqrt{s} = M_{1S}$ .

### 3.3 Results for $d\sigma/dp$

To summarize, the momentum distribution of top quark near the threshold can be written as follows:

$$\frac{d\sigma}{dp} = \frac{16\alpha^2}{s^2} N_c Q_q^2 \left\{ 1 + \left( \frac{\alpha_s(\mu_h)}{\pi} \right) C_F C_1 + \left( \frac{\alpha_s(\mu_h)}{\pi} \right)^2 C_F C_2(r_0) \right\} \times p^2 \Gamma_t f(p, r_0) ,$$

where

$$f(p, r_0) = \left\{ \left( 1 + \frac{2E}{3m_t} \right) |\tilde{G}'(p, r_0)|^2 + \frac{3}{2} C_F \alpha_s(\mu_s)^2 \operatorname{Re} \left[ \tilde{G}'_{1/r}(p, r_0) \tilde{G}'(p, r_0)^* \right] - \frac{11}{6} C_F \alpha_s(\mu_s)^2 \operatorname{Re} \left[ \tilde{G}'_{ipr}(p, r_0) \tilde{G}'(p, r_0)^* \right] + \frac{1}{6m_t} \frac{\sin(pr_0)}{pr_0} \operatorname{Re} \left[ \tilde{G}'(p, r_0) \right] \right\} .$$

Here  $p = |\mathbf{p}_t|$ . We changed a notation of momentum-space Green functions a little bit:

$$\begin{aligned} \tilde{G}(p, r_0) &= \int d^3r e^{i\vec{p}\cdot\vec{r}} G(r, r_0) , \\ \tilde{G}'_{1/r}(p, r_0) &= \int d^3r e^{i\vec{p}\cdot\vec{r}} \frac{1}{\alpha_s(\mu)m_t r} G(r, r_0) , \\ \tilde{G}'_{ipr}(p, r_0) &= \int d^3r e^{i\vec{p}\cdot\vec{r}} \frac{ip_r}{\alpha_s(\mu)m_t} G(r, r_0) . \end{aligned}$$

The unitarity relation holds numerically, to the degree we are concerning.

Our choice for the soft scale is  $\mu_s = 20$  GeV since a relevant scale around the distribution peak is the scale of Bohr momentum  $p_B$ .

Shown in Figures 3.1 and 3.2 are the top quark momentum distributions. We normalize the distribution to unity at each distribution peak, because overall normalization do not have extra information other than the total cross section  $R$  has. This distribution depends on CM energy. The Figure 3.1 is on  $1S$  resonance and Figure 3.2 is 4 GeV above the  $1S$ . We use the notation  $\Delta E = \sqrt{s} - M_{1S}$ . One can see that corrections are fairly small compared to those for



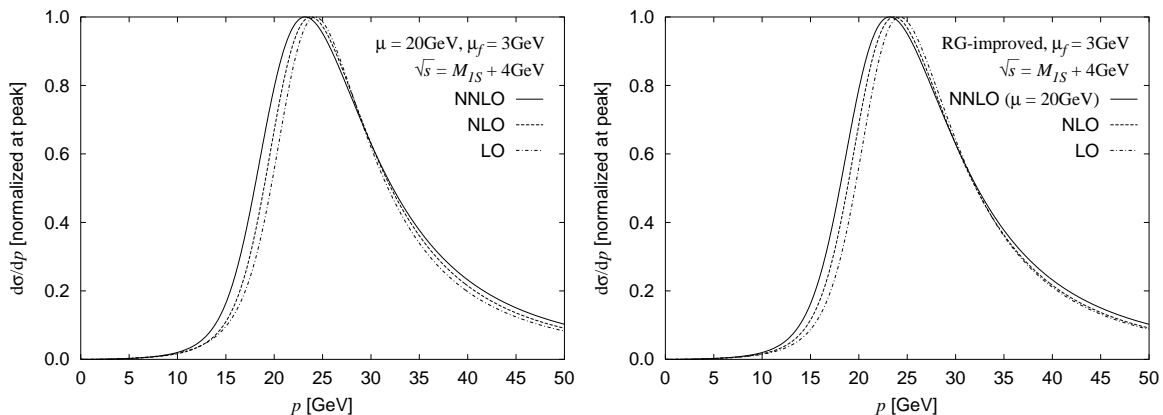


Figure 3.2: Top quark momentum distributions at LO (dot-dashed), NLO (dashed), and NNLO (solid) for  $\mu_s = 20$  GeV (left) and  $mu_s = q$  (right). For each curve, we set the c.m. energy at 4 GeV above the  $1S$  resonance mass.

total cross section  $R$ . Using RG improved Coulombic potential also do not change qualitative feature. Both  $\mathcal{O}(1/c)$  and  $\mathcal{O}(1/c^2)$  corrections are similar qualitatively, while quantitatively, the latter is larger. The most prominent correction is the shifts of peak momenta  $p_{\text{peak}}$  for  $\Delta E = 4$  GeV Figure 3.2. However this is mainly due to the shift of  $1S$  resonance, which is already visible in  $R$  ratio. That is, for energies  $\Delta E > 1-2$  GeV, the peak momentum of the distribution tends to be determined only by kinematics,  $p_{\text{peak}} \simeq \frac{1}{2}\sqrt{s - 4m_t^2}$ . Note that binding energy becomes deeper with higher order correction Table 2.2. Correspondingly, the peak momentum in Figure 3.2 lower with higher corrections. On the other hand, this kind of correction is small on the  $1S$  resonance ( $\Delta E = 0$ , Figure 3.1). Quantitatively,  $\mathcal{O}(1/c)$  and  $\mathcal{O}(1/c^2)$  corrections shift  $p_{\text{peak}}$  is  $\delta p_{\text{peak}}/p_{\text{peak}} = -0.8\%$  and  $+2.5\%$ , respectively, for fixed order, while  $+0.5\%$  and  $+2.2\%$  for RG improved. Behavior in intermediate energy is as follows. At  $\Delta E = 0$  the corrections are positive  $\sim +\text{few}\%$ ; between  $\Delta E = 0$  and  $\Delta E = 1-2$  GeV, the corrections decrease and change sign from  $+\text{few}\%$  to  $-\text{few}\%$ ; at higher energies,  $\Delta E > 1-2$  GeV, the corrections stay negative, but their magnitude  $|\delta p_{\text{peak}}/p_{\text{peak}}|$  decrease with energy.

Aside from the correction mentioned above, the next prominent correction is for higher momentum region. This is because higher order corrections in  $1/c$ -expansion are less suppressed for higher energy and momentum.

### Other corrections

Although the momentum distributions above are calculated with  $\mathcal{O}(1/c^2)$  corrections, they are not complete. This is mainly because we do not treat the decay process of  $t$  and  $\bar{t}$  properly. In Section 2.2.3 we mentioned that treating the decay width  $\Gamma_t$  with the replacement  $E \rightarrow E + i\Gamma$  is valid for  $\mathcal{O}(1/c)$  and below. In fact, this is only for total cross section  $R$ . Final-State Interactions (FSI) between the decay products of  $t$  and  $\bar{t}$  modify the momentum distribution of  $t$  already at  $\mathcal{O}(1/c)$ . In the analysis above, we dropped this effect. The effect of FSI to  $\mathcal{O}(1/c^2)$  is not calculated yet. Shown in Figure 3.3 are  $\mathcal{O}(1/c)$  momentum distributions with and without FSI. We can see that the effect of NLO FSI is somewhat larger than that of NNLO potential modifications etc. Quantitatively, the final-state interactions reduce the peak momentum about 5% almost independent to the energy [18]. Note that the energy dependence of the corrections are different for NLO FSI and NNLO potential modifications etc.

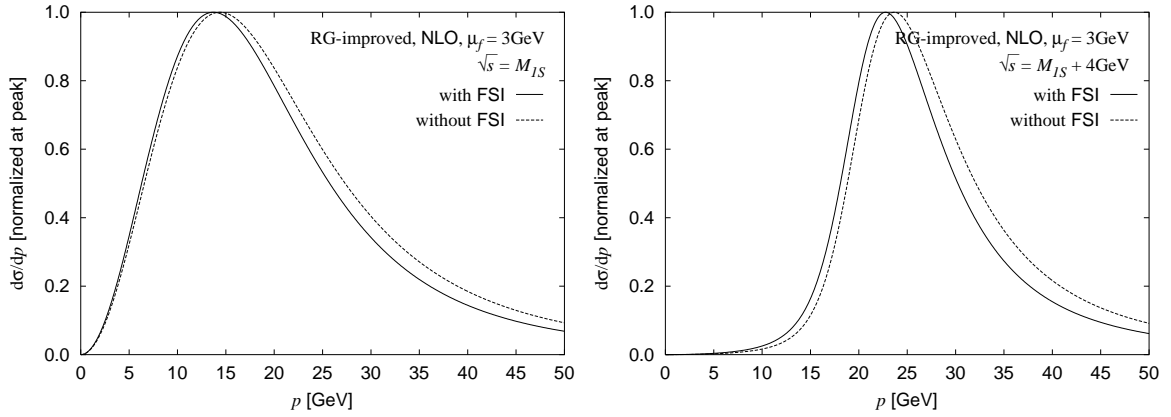


Figure 3.3: Top quark momentum distributions at NLO with the renormalization group improvement for the Coulomb part of the potential. The c.m. energy is set on the  $1S$  resonance state (left) and 4 GeV above it (right). The solid (dashed) line is calculated with (without) the  $\mathcal{O}(1/c)$  final-state interaction corrections.

# Chapter 4

## Anomalous Electric Dipole Moments of Top Quark

In the early stage of studies on  $e^+e^- \rightarrow t\bar{t}$  near the threshold, the effects of a Higgs exchange between  $t\bar{t}$  were also examined [11]. It showed that the mass  $m_H$  and the coupling  $g_{\bar{t}tH}$  of the Higgs can be probed, if the Higgs is light. Many of extensions of the Standard Model (SM), including Supersymmetric SM (SSM), contain extra Higgs multiplets. They in general introduce complex couplings that are unremovable by field redefinitions, or “physical”, thus provide sources of  $CP$  violation other than those in CKM matrix. Not only in extra Higgs multiplets, but also in other extensions, there are plenty of sources for  $CP$  violation in general, once we expand the particle content of a model. For example in SSM, mass matrices for squarks and sleptons can have complex phases. These extra sources for  $CP$  violation induce EDM for various particles to one-loop level, while the leading SM contribution is three-loop. The magnitude of EDM of a fermion is proportional to its mass, in general. Thus we study the EDMs of top quark in this section. Because EDMs are  $CP$  violating, their effect can be seen in the difference of the polarization of  $t$  and  $\bar{t}$ , which is zero if all the relevant interaction is  $CP$  conserving.

In Section 4.1 it is explained that a non-zero value of (intrinsic) EDM violates both  $P$  and  $T$ . Field theoretic description of EDM is also given. In Section 4.2 expected values of EDMs in various models are summarized.

### 4.1 Electric Dipole Moment (EDM)

Total angular momentum is a sum of orbital angular momentum and (intrinsic) spin. Just the same situation holds for Electric Dipole Moment (EDM)  $\boldsymbol{\mu}_E$  and Magnetic Dipole Moment (MDM)  $\boldsymbol{\mu}_B$ :

$$\boldsymbol{\mu}_E = \boldsymbol{\mu}_{\text{EDM}} + \boldsymbol{D} , \quad \boldsymbol{\mu}_B = \boldsymbol{\mu}_{\text{MDM}} + \boldsymbol{M} . \quad (4.1)$$

Here we mean intrinsic dipole moments by  $\boldsymbol{\mu}_{\text{EDM}}$  and  $\boldsymbol{\mu}_{\text{MDM}}$ , and “orbital” ones by  $\boldsymbol{D}$  and  $\boldsymbol{M}$ . As is well known, the transformation properties of electric field  $\boldsymbol{E}$  etc. under, say, parity can be defined so that the classical electromagnetism is invariant under any combinations of Parity  $P$ , Charge conjugation  $C$ , and Time reversal  $T$ . However this is not the case for quantum field theories, as we shall see below.

	$\rho$	$\mathbf{j}$	$\mathbf{E}$	$\mathbf{B}$	$\mathbf{D}$	$\mathbf{M}$	$\mathbf{s}$	$\mathbf{x}$	$\mathbf{p}$
P	+	-	-	+	-	+	+	-	-
C	-	-	-	-	-	-			
T	+	-	+	-	+	-	-	+	-

Table 4.1: Transformation properties under Parity  $P$  etc. of the quantities related to classical electromagnetism;  $\rho$  is charge density,  $\mathbf{j}$  current density,  $\mathbf{E}$  electric field,  $\mathbf{B}$  magnetic field,  $\mathbf{D}$  “orbital” part of electric dipole moment,  $\mathbf{M}$  “orbital” part of magnetic dipole moment. These are fields.  $\mathbf{s}$  is spin (or angular momentum, in general),  $\mathbf{x}$  is coordinate,  $\mathbf{p}$  is linear momentum. P etc. mean the eigenvalues under  $P$  etc. For  $P$  and  $T$ , arguments of fields are changed from  $(\mathbf{x}, t)$  to  $(-\mathbf{x}, t)$  and  $(\mathbf{x}, -t)$ , respectively.

The EDM  $\boldsymbol{\mu}_E$  and MDM  $\boldsymbol{\mu}_B$  are defined by the following interactions:

$$V = -\boldsymbol{\mu}_E \cdot \mathbf{E} - \boldsymbol{\mu}_B \cdot \mathbf{B} . \quad (4.2)$$

Within the classical electromagnetism, only the “orbital” contributions  $(\mathbf{D}, \mathbf{M})$  to the dipole moments can be calculated:

$$\mathbf{D}(t) = \int d^3x \mathbf{x} \rho(\mathbf{x}, t) , \quad \mathbf{M}(t) = \frac{1}{2} \int d^3x \mathbf{x} \times \mathbf{j}(\mathbf{x}, t) ,$$

where

$$\rho(\mathbf{x}, t) = \sum_i q_i \delta^{(3)}(\mathbf{x} - \mathbf{x}_i(t)) , \quad \mathbf{j}(\mathbf{x}, t) = \sum_i q_i \frac{d\mathbf{x}_i(t)}{dt} \delta^{(3)}(\mathbf{x} - \mathbf{x}_i(t)) ,$$

are charge density and current density, respectively. From these definitions, we can see the transformation properties under Parity and Time reversal. For example,

$$\rho(\mathbf{x}, t) \xrightarrow{P} \sum_i q_i \delta^{(3)}(\mathbf{x} - (-\mathbf{x}_i(t))) = +\rho(-\mathbf{x}, t) ,$$

because  $\delta$ -function is an even function, and then

$$\mathbf{D}(t) \xrightarrow{P} \int d^3x \cdot (-\mathbf{x}) \rho(-\mathbf{x}, t) = -\mathbf{D}(t) .$$

Here we changed the integration variable  $\mathbf{x} \rightarrow \mathbf{x}' = -\mathbf{x}$ . The transformation properties of other quantities are given in Table 4.1.

Within the framework of QFT, spin  $\mathbf{s}$  is the only vector available for a particle at rest, thus

$$\boldsymbol{\mu}_{\text{EDM}} , \boldsymbol{\mu}_{\text{MDM}} // \mathbf{s} .$$

Thus  $\boldsymbol{\mu}_{\text{MDM}} \cdot \mathbf{B}$  is  $(P, T) = (+, +)$  while  $\boldsymbol{\mu}_{\text{EDM}} \cdot \mathbf{E}$  is  $(P, T) = (-, -)$ , which means non-zero value of (intrinsic) EDM  $\boldsymbol{\mu}_{\text{EDM}}$  is allowed only when both  $P$  and  $T$  (or  $CP$ ) are violated.

As is well known, when the interaction of fermion-fermion-gauge boson has the form of

$$\Gamma^\mu = \gamma^\mu F_1(q^2) + \frac{i}{2m} \sigma^{\mu\nu} q_\nu F_2(q^2) ,$$

MDM is expressed as

$$\boldsymbol{\mu}_{\text{MDM}} = \frac{e}{m} [F_1(q^2) + F_2(q^2)] \frac{\boldsymbol{\sigma}}{2} \stackrel{q^2 \rightarrow 0}{=} \frac{e}{m} \frac{g}{2} \frac{\boldsymbol{\sigma}}{2} ,$$

where  $m$  is the mass of the fermion,  $F_1(q^2)$  and  $F_2(q^2)$  are form factors<sup>1</sup>, which depend on the momentum of the gauge boson  $q_\mu$  (flows into the fermion current), and  $g$  is Landé  $g$ -factor:  $(g - 2)/2 = \alpha/(2\pi) + \dots$ . Thus anomalous MDM is expressed by the second term of the following effective Lagrangian:

$$\mathcal{L} = -eF_1(q^2) \bar{\psi} \gamma^\mu \psi A_\mu - \frac{e}{2m} F_2(q^2) \bar{\psi} \sigma^{\mu\nu} \psi \partial_\mu A_\nu .$$

From this we can obtain the corresponding term for EDM by replacing  $\mathbf{B}$  by  $\mathbf{E}$ . This can be done by using dual field strength:

$$F_{\mu\nu} = (F_{0i}, \frac{-1}{2} \epsilon_{ijk} F_{jk}) = (\mathbf{E}, \mathbf{B}) , \quad \frac{1}{2!} \epsilon_{\mu\nu\rho\sigma} F^{\rho\sigma} = (-\mathbf{B}, \mathbf{E}) .$$

Our convention for the totally antisymmetric tensor is  $\epsilon_{0123} = +1$ . Thus with

$$\sigma^{\mu\nu} \partial_\mu A_\nu = \frac{1}{2} \sigma^{\mu\nu} F_{\mu\nu} \longrightarrow \frac{1}{2} \sigma^{\mu\nu} \cdot \frac{1}{2} \epsilon_{\mu\nu\rho\sigma} F^{\rho\sigma} = \frac{i}{2} \sigma^{\mu\nu} \gamma_5 F_{\mu\nu} = i \sigma^{\mu\nu} \gamma_5 \partial_\mu A_\nu ,$$

we have

$$\Gamma^\mu = \gamma^\mu F_1(q^2) + \frac{i}{2m} \sigma^{\mu\nu} q_\nu [F_2(q^2) + i \gamma_5 d(q^2)] ,$$

or the following effective Lagrangian for EDM:

$$\begin{aligned} \mathcal{L} &= -eF_1(q^2) \bar{\psi} \gamma^\mu \psi A_\mu - \frac{ed(q^2)}{2m} \bar{\psi} i \sigma^{\mu\nu} \gamma_5 \psi \partial_\mu A_\nu \\ &\simeq -eF_1(q^2) \bar{\psi} \gamma^\mu \psi A_\mu + \frac{ed(q^2)}{2m} (\bar{\psi} i \gamma_5 i \overleftrightarrow{\partial}^\mu \psi) A_\mu , \end{aligned} \quad (4.3)$$

where  $d(q^2)$  is a dimensionless form factor for anomalous EDM:

$$\boldsymbol{\mu}_{\text{EDM}} = \frac{ed}{m} \frac{\boldsymbol{\sigma}}{2} .$$

The “ $\simeq$ ” in the last step means they coincide with the use of the eqs. of motion [Section A.4]. The operator  $\frac{1}{2} \bar{\psi} i \sigma^{\mu\nu} \gamma_5 \psi F_{\mu\nu} \simeq -(\bar{\psi} i \gamma_5 i \overleftrightarrow{\partial}^\mu \psi) A_\mu$  has  $(\mathbf{P}, \mathbf{T}) = (-, -)$  [Tables A.2, A.3]. The anomalous EDM interactions with  $Z$  and gluon  $g$  are defined in the same way. Since the interactions are flavor-diagonal, its existence immediately means  $CP$  violation.

In fact, as shall be shown in Section A.4, the EDM-interaction above, which is dim-5, is the lowest dimension operator for  $t$ - $\bar{t}$ -gauge boson that violates  $CP$  invariance. Thus  $CP$ -violating effect is taken into account by the EDM to the leading order. The form factors  $d(q^2)$  depend on

<sup>1</sup>  $F_1(q^2 = 0)$  is the electric charge of the relevant particle.

the momentum transfer  $q^2$  in general. However to the lowest order of derivative expansion, it is constant. To our knowledge, all studies to date concerning sensitivities of collider experiments to the EDMs assumed that the momentum dependence of  $d(q^2)$  can be neglected. Also, as we shall see in the following section, the  $q^2$ -dependence is shown to be moderate, by explicit calculations of EDMs based on specific models like Minimum Supersymmetric Standard Model (MSSM). Thus we also follow this assumption. The magnitude of EDMs are

$$\begin{aligned} t\bar{t}\gamma\text{-EDM} &= \frac{ed_{t\gamma}}{m_t} = d_{t\gamma} \times 1.13 \times 10^{-16} e \text{ cm} , \\ t\bar{t}Z\text{-EDM} &= \frac{g_Z d_{tZ}}{m_t} = d_{tZ} \times 1.13 \times 10^{-16} g_Z \text{ cm} , \\ t\bar{t}g\text{-EDM} &= \frac{g_s d_{tg}}{m_t} = d_{tg} \times 1.13 \times 10^{-16} g_s \text{ cm} . \end{aligned} \quad (4.4)$$

Note that  $g_Z/e = (g/\cos\theta_W)/(g\sin\theta_W) = 1/(\cos\theta_W \sin\theta_W) = 2.372\dots$ .

As can easily be checked, the term  $d\bar{\psi}i\sigma^{\mu\nu}\gamma_5\psi F_{\mu\nu}$  is hermitian only if the EDM-coupling  $d$  is real. However as explained in Section A.7.5, an effective Lagrangian need not be hermitian; its anti-hermitian part simply parameterizes an absorptive part  $T - T^\dagger$ , where  $T = (S - 1)/i$  is a  $T$ -matrix defined from the  $S$ -matrix. Thus we assume  $d$ 's are complex.

## 4.2 Predictions of EDMs in various models

In all models with  $CP$  violation, EDMs of top quark may not be zero. For example in the Standard Model,  $t\bar{t}\gamma$ -EDM is estimated to be  $\sim 10^{-30} e \text{ cm}$  [69, 70]. Those for  $t\bar{t}Z$ - and  $t\bar{t}g$ -EDM are obtained by changing the unit to  $g_Z \text{ cm}$  and  $g_s \text{ cm}$ , respectively<sup>2</sup>. Compared with the ‘‘ $\mathcal{O}(1)$ -coupling’’ result [Eq. (4.4)]  $e/m_t \simeq 10^{-16} e \text{ cm}$ , it is very small. This is because in the SM, the lowest contribution arises from three-loop diagrams, which is proportional to  $G_F^2 \alpha_s$  [69, 70].

Since the operator  $\bar{\psi}i\sigma^{\mu\nu}\gamma_5\psi$  responsible for EDM is chirality flipping, one need to pick up a mass of a fermion at least once. Large mass may be advantageous to obtain large EDM, but it may also be a suppression factor when the relevant fermion is in a loop. Thus in various models, EDM of a fermion is typically proportional to its mass. This makes the EDM of top quark very interesting.

There are several models that induce EDM at 1-loop. These include models with extra-Higgs multiples and supersymmetry, which are natural candidates for beyond the SM. See [67] for reviews on early studies. Here we summarize studies made after these reviews<sup>3</sup>. The conclusion of this section is as follows: the size of EDMs are expected to be

$$t\bar{t}g\text{-EDM} \sim 10^{-19} - 10^{-20} g_s \text{ cm} ,$$

and the same for other EDMs with appropriate changes of the unit, if  $CP$ -violating parameters in the models are  $\mathcal{O}(1)$ .

In a model with two Higgs doublets, it is estimated by W. Bernreuther, T. Schröder and T. N. Pham (1992) [71] that

$$t\bar{t}\gamma\text{-EDM} \sim \frac{eG_F m_t^3}{4\pi^2 m_\phi^2} = 3.1 \times 10^{-18} e \text{ cm} \left( \frac{m_\phi}{100 \text{ GeV}} \right)^{-2} ,$$

<sup>2</sup> These can be obtained by assuming that the result for  $d_{u\bar{u}\gamma}$  in [70] can be applied also for  $d_{t\bar{t}\gamma}$  etc.

<sup>3</sup> See also [68].

where the extra  $m_t^2$  comes from the Higgs-fermion couplings. Numerical calculations show the real part and the imaginary part of the ElectroWeak-EDMs are the similar order each other. For  $t\bar{t}\gamma$ -EDM it is  $\sim 2 \times 10^{-19} e \text{ cm}$  for  $m_t = 150 \text{ GeV}$ ,  $m_H = 200 \text{ GeV}$ ,  $\sqrt{s} = 400 \text{ GeV}$ ; and  $t\bar{t}Z$ -EDM  $\sim 0.2 \times t\bar{t}\gamma$ -EDM. They assumed  $CP$ -violating parameters in the model to be of order unity. EDMs induced by neutral Higgs boson exchange are considered also in A. Soni and R. M. Xu (1992) [72]. They estimated

$$\begin{aligned} t\bar{t}\gamma\text{-EDM} &\simeq 4 \times 10^{-20} e \text{ cm} , \\ t\bar{t}g\text{-EDM} &\simeq \frac{g_s}{Q_t e} \times t\bar{t}\gamma\text{-EDM} \simeq 6 \times 10^{-20} g_s \text{ cm} , \end{aligned}$$

for  $m_H = 2m_t$  and  $m_t = 125 \text{ GeV}$ .  $CP$ -violating parameters in the model are assumed to be of order unity. They argued that the effects due to charged-Higgs-boson exchange may be suppressed by a factor  $m_b^2/M^2$ , where  $M^2$  is a linear combination of  $m_t^2$  and  $m_H^2$ . Thus the charged Higgs boson contribution is likely to be subleading to the neutral Higgs boson exchange. They also calculated the  $q^2$  dependence of the EDM form factors, which turn out to be moderate. The  $t\bar{t}\gamma$ - and  $t\bar{t}Z$ -EDM induced by Higgs exchange are calculated also in [76, 92, 93].

In the MSSM, one can introduce (unremovable) complex couplings with only one generation [74]. Induced EDMs in MSSM is considered in [73]. They find that both  $t\bar{t}\gamma$ - and  $t\bar{t}Z$ -EDM can reach  $10^{-20} e \text{ cm}$ . Exchanged particles are gluino, charginos, neutralinos and squarks. In most cases gluino  $\tilde{g}$  gives the leading contribution. However when  $m_{\tilde{g}} \gtrsim 500 \text{ GeV}$ , they find that chargino contribution can be larger than that from gluino due to the large Yukawa coupling of top quark. They assume the unification of gauge couplings and gaugino masses but others. In particular, they do not assume unification of the scalar mass parameters and the trilinear scalar coupling parameter  $A_q$  of the different generations. Their reference set of parameters are such that squark are lighter than  $400 \text{ GeV}$ , and complex phases in squark mixing matrices and in higgsino mixing parameter  $\mu$  are of order unity. They vary one parameter while others are fixed to the reference values. The  $t\bar{t}\gamma$ - and  $t\bar{t}Z$ -EDMs in Supersymmetric Standard Model (SSM) was studied also in [118, 119]. The  $t\bar{b}W$ -EDM in SSM was studied in [111, 118].

There are also other models. For example in the model [75] with  $SU(3)_C \times SU(3)_L \times U(1)_X$ , contribution of charged and neutral Higgs exchange at one-loop is estimated to  $10^{-19} e \text{ cm}$  and  $10^{-19} g_s \text{ cm}$  for the values of relative phases of the vev's such that  $CP$  violation is maximal. See also [77–80] for works related to top-quark EDM, [81] for EDMs of  $b$ -quark etc. in supersymmetric models, and [82] for EDMs of  $b$ -quark etc. in leptoquark model.

### 4.3 CP violating observables

At the Lagrangian level,  $CP$ -symmetry is violated if the field-dependent phases  $\eta_C \eta_P$  in Eq. (A.44) cannot be tuned so that the all term in  $\mathcal{L}$  transform with the same phase<sup>4</sup>. Since kinetic terms are invariant, or “even”, under any combinations of  $\mathcal{P}$ ,  $\mathcal{C}$ , and  $\mathcal{T}$ , a  $CP$ -odd interaction is synonymous with  $CP$ -violating one. We are concerned with  $CP$ -odd observables, which needs the interference of  $CP$ -even and  $CP$ -odd amplitudes:  $\mathcal{M}_{CP\text{-even}} \mathcal{M}_{CP\text{-odd}}^*$ . Transformation properties of  $\mathcal{M}$  or  $\mathcal{L}$  are discussed in Section A.7. Here we apply it to  $|\mathcal{M}|^2$ , or  $d\sigma$ . As we shall see in Section A.7.5, observables are classified into  $CPT$ -even and -odd ones. The latter can be non-zero if and only if there is a finite absorptive part, which is defined as the anti-hermitian

<sup>4</sup> One usually redefines the fields to include  $(\eta_C \eta_P)^{-1/2}$ . See Section A.7.6.

	$E - \bar{E}$	$E + \bar{E}$	$\mathbf{p} - \bar{\mathbf{p}}$	$\mathbf{p} + \bar{\mathbf{p}}$	$\mathbf{p} \times \bar{\mathbf{p}}$	$\mathbf{p} \cdot \bar{\mathbf{p}}$	$\mathbf{s} - \bar{\mathbf{s}}$	$\mathbf{s} + \bar{\mathbf{s}}$	$\mathbf{s} \times \bar{\mathbf{s}}$	$\mathbf{s} \cdot \bar{\mathbf{s}}$
CP	-	+	+	-	-	+	-	+	-	+
CPT $\tilde{\text{T}}$	-	+	-	+	-	+	+	-	-	+
P	+	+	-	-	+	+	+	+	+	+
C	-	+	-	+	-	+	-	+	-	+
$\tilde{\text{T}}$	+	+	-	-	+	+	-	-	+	+

Table 4.2: Transformation properties of the energies, the momenta and the spins of particle-antiparticle system. In their CM frame,  $E - \bar{E} = 0$ ,  $E + \bar{E} = 2E$ ,  $\mathbf{p} - \bar{\mathbf{p}} = 2\mathbf{p}$ ,  $\mathbf{p} + \bar{\mathbf{p}} = 0$ ,  $\mathbf{p} \times \bar{\mathbf{p}} = 0$  and  $\mathbf{p} \cdot \bar{\mathbf{p}} = -|\mathbf{p}|^2$ .

part  $T - T^\dagger$  of  $T$ -matrix,  $S = 1 + iT$ . Sources for an absorptive part are, for example, decay width and final- and initial-state rescattering. For the case we are considering,  $e^+e^- \rightarrow t\bar{t}$  near the threshold, there is plenty of Coulomb rescattering between  $t\bar{t}$ . Thus we can probe both CP $\tilde{\text{T}}$ -even and -odd observables simultaneously.

A word for notation may be in order.  $\mathcal{P}$  is a field-theoretic operator acting on creation-annihilation operators [Eq. (A.44)];  $P$  is an operation for  $\mathcal{M}$  defined by  $\gamma$ -matrices, which is c-number [Eq. (A.46)];  $\mathbf{P}$  is an eigenvalue with respect to  $\mathcal{P}$  or  $P$  [Tables 4.1, A.2, A.3];  $\mathbf{P}$  is an operation for quantities such as spin  $\mathbf{s}$  or momentum  $\mathbf{p}$  [Eq. (4.5), Table 4.2]. However there may be no confusion even if these distinctions are not made, aside from Time Reversal.

### 4.3.1 $\mathbf{P}$ , $\mathbf{C}$ and $\tilde{\text{T}}$ for $|\mathcal{M}|^2$

Basic discrete symmetry operations in QFT are  $\mathcal{P}$ ,  $\mathcal{C}$  and  $\mathcal{T}$ . These operate on creation-annihilation operators, and are summarized in Section A.7.1. We can define corresponding operations  $P$ ,  $C$  and  $T$  for (a part of) an amplitude  $\mathcal{M}$ . These are represented not by operators of QFT, but by combinations of  $\gamma$  matrices. These operations are summarized in Section A.7.4. We can also define related operations  $\mathbf{P}$ ,  $\mathbf{C}$  and  $\tilde{\text{T}}$  for the each term of  $|\mathcal{M}|^2$ , or  $d\sigma$ . For definiteness, we limit ourselves to the case we are considering:  $e^-(\mathbf{p}_e, \mathbf{s}_e) e^+(\bar{\mathbf{p}}_e, \bar{\mathbf{s}}_e) \rightarrow \gamma^*/Z^* \rightarrow t(\mathbf{p}_t, \mathbf{s}_t) \bar{t}(\bar{\mathbf{p}}_t, \bar{\mathbf{s}}_t)$ , followed by  $t \rightarrow bW^+$  ( $\bar{t} \rightarrow \bar{b}W^-$ ) etc. For particle-antiparticle pair, these operations are defined by

$$\begin{aligned}
\mathbf{P} &\cdots (\mathbf{p}, \mathbf{s}, \bar{\mathbf{p}}, \bar{\mathbf{s}}) \rightarrow (-\mathbf{p}, \mathbf{s}, -\bar{\mathbf{p}}, \bar{\mathbf{s}}) \\
\mathbf{C} &\cdots (\mathbf{p}, \mathbf{s}, \bar{\mathbf{p}}, \bar{\mathbf{s}}) \rightarrow (\bar{\mathbf{p}}, \bar{\mathbf{s}}, \mathbf{p}, \mathbf{s}) = (-\mathbf{p}, \bar{\mathbf{s}}, -\bar{\mathbf{p}}, \mathbf{s}) \\
\tilde{\text{T}} &\cdots (\mathbf{p}, \mathbf{s}, \bar{\mathbf{p}}, \bar{\mathbf{s}}) \rightarrow (-\mathbf{p}, -\mathbf{s}, -\bar{\mathbf{p}}, -\bar{\mathbf{s}}) \\
\text{CP} &\cdots (\mathbf{p}, \mathbf{s}, \bar{\mathbf{p}}, \bar{\mathbf{s}}) \rightarrow (-\bar{\mathbf{p}}, \bar{\mathbf{s}}, -\mathbf{p}, \mathbf{s}) = (\mathbf{p}, \bar{\mathbf{s}}, \bar{\mathbf{p}}, \mathbf{s}) \\
\text{CPT}\tilde{\text{T}} &\cdots (\mathbf{p}, \mathbf{s}, \bar{\mathbf{p}}, \bar{\mathbf{s}}) \rightarrow (\bar{\mathbf{p}}, -\bar{\mathbf{s}}, \mathbf{p}, -\mathbf{s}) = (-\mathbf{p}, -\bar{\mathbf{s}}, -\bar{\mathbf{p}}, -\mathbf{s}) .
\end{aligned} \tag{4.5}$$

The equalities are for the case  $\mathbf{p} + \bar{\mathbf{p}} = 0$ . Some combinations are given in Table 4.2, whose contents can also be organized as follows:

$$\begin{aligned}
(\text{CP}, \text{CPT}\tilde{\text{T}}) &= (-, +) \cdots \mathbf{s} - \bar{\mathbf{s}}, \quad \mathbf{p} + \bar{\mathbf{p}}, \\
(\text{CP}, \text{CPT}\tilde{\text{T}}) &= (-, -) \cdots \mathbf{s} \times \bar{\mathbf{s}}, \quad \mathbf{p} \times \bar{\mathbf{p}}, \quad E - \bar{E}, \\
(\text{CP}, \text{CPT}\tilde{\text{T}}) &= (+, +) \cdots \mathbf{s} \cdot \bar{\mathbf{s}}, \quad \mathbf{p} \cdot \bar{\mathbf{p}}, \quad E + \bar{E}, \\
(\text{CP}, \text{CPT}\tilde{\text{T}}) &= (+, -) \cdots \mathbf{s} + \bar{\mathbf{s}}, \quad \mathbf{p} - \bar{\mathbf{p}} .
\end{aligned} \tag{4.6}$$



Candidates of the particle-antiparticle pair are  $(e^-, e^+)$ ,  $(t, \bar{t})$ ,  $(\ell^-, \ell^+)$  and  $(b, \bar{b})$ . The last two originate from the decays of  $t$  and  $\bar{t}$ .

Note that the operation  $\tilde{T}$  do not interchange initial and final states. The tilde  $\sim$  on  $T$  emphasis this point. This operation  $\tilde{T}$  is sometimes called “naive  $T$ ”<sup>5</sup>. It may be difficult, if not impossible, to built the field theoretic operator  $\tilde{\mathcal{T}}$  for  $\tilde{T}$ . For example, the operator with the same properties as  $\mathcal{T}$  but without the anti-unitarity nature does not do the job. This is because the transformation for creation-annihilation operators  $\tilde{\mathcal{T}}a(\mathbf{p}, \mathbf{s})\tilde{\mathcal{T}}^\dagger = a(-\mathbf{p}, -\mathbf{s})$  etc. with an unitary operator  $\tilde{\mathcal{T}}$ , do not lead to the same transformation for  $\psi$  and  $\bar{\psi}$  as  $\mathcal{T}$ , since  $\psi$  (and  $\bar{\psi}$ ) contains  $u$  and  $v$ , which are c-numbers.

With the knowledge of Section A.7.4, it is sensible to operate P and/or C to a part of a process when all relevant Feynman diagrams are topologically the same. In our case, we can apply P etc. separately to the final or the initial current. On the other hand, one should operate  $\tilde{T}$  to the whole process.

Symmetry property of  $|\mathcal{M}|^2$  is directly related to that of the expectation values of observables, which we now turn to.

### 4.3.2 Expectation values

Since an expectation value is obtained by integration over the phase space, not all terms in  $|\mathcal{M}|^2$  contribute to it. The transformation properties under Parity etc. can be used to determine a relevant combination of interactions.

Consider for example, an expectation value

$$\langle (\mathbf{p}_e - \bar{\mathbf{p}}_e) \cdot (\mathbf{p}_t - \bar{\mathbf{p}}_t) \rangle = 4 \langle \mathbf{p}_e \cdot \mathbf{p}_t \rangle = \frac{4}{\sigma_{\text{tot}}} \int d\Phi \mathbf{p}_e \cdot \mathbf{p}_t \frac{d\sigma(\mathbf{p}_e, \mathbf{p}_t)}{d\Phi},$$

which is P-odd with respect to both the final and the initial currents. Thus only a part of  $d\sigma$  contributes to the expectation value; that is, which have the same transformation property to the relevant observable. There are four combinations for the SM vertices:

$$\begin{aligned} & [v^e v^t]^* \cdot [a^e a^t] \times ((\bar{v}\gamma_\mu u)_e (\bar{u}\gamma^\mu v)_t)^* \cdot ((\bar{v}\gamma_\nu \gamma_5 u)_e (\bar{u}\gamma^\nu \gamma_5 v)_t) + \text{c.c.} \\ & + [v^e a^t]^* \cdot [a^e v^t] \times ((\bar{v}\gamma_\nu u)_e (\bar{u}\gamma^\nu \gamma_5 v)_t)^* \cdot ((\bar{v}\gamma_\mu \gamma_5 u)_e (\bar{u}\gamma^\mu v)_t) + \text{c.c.} \end{aligned}$$

Here  $[v^e v^t]$  etc. are (energy dependent) couplings that combine both  $\gamma$  and  $Z$  contributions. These are defined in Eq. (A.33). Note that P of both initial and final current should be opposite. Thus only the combination  $a_3 \equiv [v^e v^t]^* [a^e a^t] + [a^e v^t]^* [v^e a^t]$  contributes to the forward-backward asymmetry (after one sum over spins)<sup>6</sup>. The effective couplings  $[v^e v^t]$  etc. are defined in Section A.5, and the combinations  $a_3$  etc. are defined in Eq. (4.26).

Another example is the total cross section  $\sigma_{\text{tot}}$ . After summing over spins, momenta are the only vectors. Thus each term in  $|\mathcal{M}|^2$  should be composed of even number of momenta. From Eq. (A.51), we know that the product of the Parity of the final-currents should be even, which means even number of momenta of final state. Thus the number of momenta of initial state should also be even, which means the product of the Parity eigenvalues of the initial-current should be even. To summarize, an interference of amplitudes  $\mathcal{M}_1 \mathcal{M}_2^*$  contributes to

<sup>5</sup>In my opinion, “naive time reversal” seems to mean “just flip initial and final states”; just the opposite.

<sup>6</sup>Before summing the spin  $\mathbf{s}_t$  of  $t$ ,  $(\mathbf{s}_t \cdot \mathbf{p}_e) (\mathbf{p}_e \cdot \mathbf{p}_t) \propto \cos \theta_{te}$  contributes to “spin-direction-specified FB asymmetry”. This observable is P-odd w.r.t. the final  $t\bar{t}$  current but P-even w.r.t. the initial  $e^-e^+$  current. Thus the combination  $a_4 \equiv [v^e v^t]^* [v^e a^t] + [a^e v^t]^* [a^e a^t]$  also contributes to this asymmetry. Note that non-zero polarization of initial  $e^+e^-$  effectively mixes the vector vertex and the axial-vector vertex of  $e^+e^-$ .

the total cross section if and only if the Parities of the final-currents in  $\mathcal{M}_1$  and  $\mathcal{M}_2$  are the same, and so are initial-currents.

CP transformation interchanges the spins of a particle and its anti-particle  $(\mathbf{s}_t, \bar{\mathbf{s}}_t) \rightarrow (\bar{\mathbf{s}}_t, \mathbf{s}_t)$  at the CM frame of them. Thus the interference  $(\mathcal{M}_{\text{CP}=\pm} \mathcal{M}_{\text{CP}=\pm}^*)$  of the amplitudes with the same CP contributes in the same sign to the polarizations<sup>7</sup> of a particle and its anti-particle. On the other hand, the interference  $(\mathcal{M}_{\text{CP}=\pm} \mathcal{M}_{\text{CP}=\mp}^*)$  of the amplitudes with the opposite CP contributes in the opposite sign to the polarizations of a particle and its anti-particle. We see the example latter.

### 4.3.3 Several CP violating observables

From Table 4.2 or Eq. (4.6), we can see that  $(\mathbf{s}_t \mp \bar{\mathbf{s}}_t) \cdot (\mathbf{p}_e \times \mathbf{p}_t)$  is  $(\text{CP}, \text{CPT}) = (\mp, \pm)$  and  $(\mathbf{s}_t \mp \bar{\mathbf{s}}_t) \cdot (\mathbf{p}_t - \mathbf{p}_e (\mathbf{p}_e \cdot \mathbf{p}_t) / |\mathbf{p}_e|^2)$  is  $(\text{CP}, \text{CPT}) = (\mp, \mp)$ . Here the CP operation can be limited to the final current. Within the Standard Model, where CP-odd contributions to both  $t\bar{t}$  and  $e^+e^-$  vertices are highly suppressed, we see that

$$\begin{aligned} \langle \mathbf{s}_t \cdot (\mathbf{p}_e \times \mathbf{p}_t) \rangle - \langle \bar{\mathbf{s}}_t \cdot (\mathbf{p}_e \times \mathbf{p}_t) \rangle &= 0, \\ \langle \mathbf{s}_t \cdot (\mathbf{p}_t - \mathbf{p}_e (\mathbf{p}_e \cdot \mathbf{p}_t) / |\mathbf{p}_e|^2) \rangle - \langle \bar{\mathbf{s}}_t \cdot (\mathbf{p}_t - \mathbf{p}_e (\mathbf{p}_e \cdot \mathbf{p}_t) / |\mathbf{p}_e|^2) \rangle &= 0, \end{aligned}$$

because they are CP-odd combinations. The former is suppressed in the open top region, since  $(\mathbf{s}_t + \bar{\mathbf{s}}_t) \cdot (\mathbf{p}_e \times \mathbf{p}_t)$  is CPT-odd, which means the expectation value is proportional to the absorptive part of the amplitude, which come from EW and QCD radiative corrections. It is known [90] that the polarization  $P_N$  ( $\sim \langle \mathbf{s}_t \cdot (\mathbf{p}_e \times \mathbf{p}_t) \rangle$ ) of top quark normal to the  $e^+e^-t\bar{t}$  plane is  $\mathcal{O}(10^{-2})$  for the SM. However for the SM, the difference  $P_N - \bar{P}_N$  is far smaller than the current experimental reach, since it is CP-odd.

The following are some of CP-odd combinations of observables<sup>8</sup> (at the CM frame of  $e^+e^-$ ):

$$\begin{aligned} s_{//} - \bar{s}_{//} &\propto (\mathbf{s}_t - \bar{\mathbf{s}}_t) \cdot \mathbf{p}_e & \text{CPT} &= - \\ s_{\perp} - \bar{s}_{\perp} &\propto (\mathbf{s}_t - \bar{\mathbf{s}}_t) \cdot (\mathbf{p}_t - \mathbf{p}_e (\mathbf{p}_e \cdot \mathbf{p}_t) / |\mathbf{p}_e|^2) & \text{CPT} &= - \\ s_N - \bar{s}_N &\propto (\mathbf{s}_t - \bar{\mathbf{s}}_t) \cdot (\mathbf{p}_e \times \mathbf{p}_t) & \text{CPT} &= + \\ A_E^f &= E_f - E_{\bar{f}} \quad (f = \ell^+, b) & \text{CPT} &= - \\ A_1^f &= \hat{\mathbf{p}}_e \cdot (\mathbf{p}_f \times \mathbf{p}_{\bar{f}}) & \text{CPT} &= + \\ A_2^f &= \hat{\mathbf{p}}_e \cdot (\mathbf{p}_f + \mathbf{p}_{\bar{f}}) & \text{CPT} &= - \\ T_{33}^f &= 2(\mathbf{p}_f - \mathbf{p}_{\bar{f}})_3 (\mathbf{p}_f \times \mathbf{p}_{\bar{f}})_3 & \text{CPT} &= + \\ Q_{33}^f &= 2(\mathbf{p}_f + \mathbf{p}_{\bar{f}})_3 (\mathbf{p}_f - \mathbf{p}_{\bar{f}})_3 - \frac{2}{3}(|\mathbf{p}_f|^2 - |\mathbf{p}_{\bar{f}}|^2) & \text{CPT} &= - \end{aligned} \tag{4.7}$$

Note that  $\mathbf{p}_e = (\mathbf{p}_e - \bar{\mathbf{p}}_e)/2$  and  $\mathbf{p}_t = (\mathbf{p}_t - \bar{\mathbf{p}}_t)/2$ . Also, kinematical cuts should respect CP-invariance.

Expectation values of CP-odd observables are not the only CP-violating observables. Event rate asymmetries also do the job. However, these two kinds of observables may be related closely. For example, Forward-Backward asymmetry  $A_{\text{FB}}$  of top quark is similar to the correlation  $\langle \mathbf{p}_e \cdot \mathbf{p}_t \rangle \propto \langle \cos \theta_{te} \rangle$ . More precisely,  $A_{\text{FB}} = \langle \text{sgn}(\mathbf{p}_e \cdot \mathbf{p}_t) \rangle / \sigma_{\text{tot}}$ . Several kinds of event rate

<sup>7</sup>See Section 4.5 for polarization.

<sup>8</sup>We follow the notations of [24, 115, 122].

asymmetries are considered in literatures. One is the difference of production cross sections for  $t_L \bar{t}_L$  and  $t_R \bar{t}_R$  [76, 93]<sup>9</sup>

$$\sigma(t_L \bar{t}_L) - \sigma(t_R \bar{t}_R) \quad \text{CPT} = - ,$$

where  $\bar{t}_L = \overline{t_R}$ . These are chirality-flipping, and thus are small for relativistic top quarks. Note that from Eq. (4.5),  $\sigma(t_L \bar{t}_L) \leftrightarrow \sigma(t_R \bar{t}_R)$  under  $\text{CPT}$ , while the other two chirality-non-flipping's,  $\sigma(t_L \bar{t}_R)$  and  $\sigma(t_R \bar{t}_L)$ , are self-conjugate under CP. As we shall see in Section 4.5.3, the charged leptons  $\ell^+$  produced in  $t$  (or more directly,  $W^+$ ) decays are emitted preferentially in the direction of top-quark spin. Thus  $\ell^+$  produced in  $t_L$  decay is less energetic than that in  $t_R$  decay. Thus the event asymmetry above is similar to  $A_E^\ell$  defined above, which is also  $\text{CPT}$ -odd. Another event rate asymmetry is up-down asymmetry  $A_{\text{up-down}}$  [93], which is the rate difference between the events with  $\ell^\pm$  above the reaction plane and the events with  $\ell^\pm$  below the  $e^+e^-t\bar{t}$  plane:

$$A_{\text{up-down}}(f) = \frac{N_{\text{up}}(f^\pm) - N_{\text{down}}(f^\pm)}{N_{\text{up}}(f^\pm) + N_{\text{down}}(f^\pm)} \quad \text{CPT} = + ,$$

where  $f = \ell^+, b$ , and  $N_{\text{up}}(f^\pm) = N_{\text{up}}(f) + N_{\text{up}}(\bar{f})$  etc. This quantity is “similar” to the correlation  $\langle (\mathbf{p}_{\ell^+} + \mathbf{p}_{\ell^-}) \cdot (\mathbf{p}_e \times \mathbf{p}_t) \rangle$ , which is  $\text{CPT}$ -even. Yet another one is the particle-antiparticle asymmetry [97, 117]:

$$N(f) - N(\bar{f}) \quad \text{CPT} = - ,$$

where  $f = \ell^+, b$ . Since both momentum and spin are summed<sup>10</sup>, CP-odd means  $\text{CPT}$ -odd. Still another one is [97]

$$A_{\text{FB}}(f) + A_{\text{FB}}(\bar{f}) \propto (N_{\text{F}}(f) - N_{\text{B}}(\bar{f})) + (N_{\text{F}}(\bar{f}) - N_{\text{B}}(f)) \quad \text{CPT} = + ,$$

where  $f = \ell^+, b$ . This quantity is  $(\text{CP}, \text{CPT}) = (-, +)$ , because  $\mathbf{p} \leftrightarrow -\bar{\mathbf{p}}$  for CP and  $\mathbf{p} \leftrightarrow +\bar{\mathbf{p}}$  for  $\text{CPT}$ .

For  $pp$  collisions, there may be non-zero CP-odd asymmetry that is not related to CP-violating interactions, since the initial state is not a CP eigenstate. However such an effect is estimated to be small [76, 103].

## 4.4 Studies of EDMs at open top region

There has been many studies on EDMs of top quark. These exploit “open”  $t$ 's; that is, relativistic  $t$  and  $\bar{t}$ :  $\beta \simeq 1$ . Although our concern is at the threshold region  $\beta \lesssim 0.1$ , we summarize results obtained from the analyses in open top region, for comparison.

### 4.4.1 Present bounds for EDMs

There are several EDMs for top-quark;  $t\bar{t}\gamma$ ,  $t\bar{t}Z$ ,  $t\bar{t}g$ , and  $t\bar{t}W$ . Experimental bounds on these EDMs at present are summarized here. Conclusion is that “ $\mathcal{O}(1)$ ” couplings are allowed:

$$t\bar{t}g\text{-EDM} \lesssim 10^{-16} g_s \text{ cm} \quad \text{etc.}$$

<sup>9</sup> References in this section are not meant to be extensive but only examples.

<sup>10</sup> In this case, both CP and  $\text{CPT}$  just interchange particle and antiparticle.

P. Haberl, O. Nachtmann and A. Wilch (1996) [84] studied the present bound on  $t\bar{t}g$ -EDM and -MDM from the  $p\bar{p} \rightarrow t\bar{t}X$  total production rate at Tevatron  $\sqrt{s} = 1.8$  TeV. They found the coupling of order unity is allowed, which means  $t\bar{t}g$ -EDM =  $10^{-16}g_s$  cm is allowed, and so is for MDM.

K. Cheung and D. Silverman (1997) [85] also studied the present bounds on  $q\bar{q}g$ -EDM and -MDM, and are both calculated to be  $0.89 \times 10^{-16}g_s$  cm. They used the transverse momentum distribution of prompt photon produced in  $qg \rightarrow q\gamma$ ,  $\bar{q}g \rightarrow \bar{q}\gamma$ ,  $q\bar{q} \rightarrow g\gamma$  at Tevatron  $\sqrt{s} = 1.8$  TeV,  $0.1 \text{ fb}^{-1}$  (Run I).

EW-EDMs are constrained indirectly from  $B \rightarrow X_s\gamma$  [86]; it shows that  $\mathcal{O}((1))$  coupling is allowed.

A. De Rújula, M. B. Gavela, O. Pène and F. J. Vegas (1991) [83] studied bounds on EDMs of quarks from neutron  $\gamma$ -EDM:  $|t\bar{t}\gamma\text{-EDM}| < 2.0 \times 10^{-17}e$  cm,  $|t\bar{t}Z\text{-EDM}| < 8.7 \times 10^{-18}g_z$  cm, and  $|t\bar{t}g\text{-EDM}| < 5.8 \times 10^{-20}g_s$  cm. They used  $m_t = 100$  GeV; this may change the limit above. As they themselves pointed out, it is doubtful whether their calculation is applicable to top quark. Thus we don't take these limits seriously.

In [87],  $CP$  conserving anomalous EW couplings of top quark is constrained from LEP/SLC data.

For  $\tau$ , present bound from LEP is obtained in [88].

#### 4.4.2 Expected future bounds on EDMs (Open top region)

There are already several studies on the top quark EDMs. Some are for  $e^+e^-$  colliders, others are for hadron colliders. We choose two representative studies for each of these, and report the results of their analyses. In  $e^+e^-$  collisions,  $t\bar{t}\gamma$ - and  $t\bar{t}Z$ -EDM can be studied in the production process, while in hadron collisions,  $t\bar{t}g$ -EDM can be studied. The summary of this section is,

- Bounds of  $10^{-18}e$  cm on  $t\bar{t}\gamma$ - and  $t\bar{t}Z$ -EDM are possible at a  $e^+e^-$  colliders at  $\sqrt{s} = 500$  GeV. With the use of “optimal observable”, this can be improved by factor 2. However this observable may have larger systematic error than simpler observables.
- Bound of  $10^{-18}$ – $10^{-19}g_s$  cm on  $t\bar{t}g$ -EDM is possible for hadron collisions at  $\sqrt{s} = 14$  TeV.

##### (i) Anomalous ElectroWeak vertices in $e^+e^-$ or $\gamma\gamma$ collisions

(i-0) Detector simulation [113] was performed with  $\int\mathcal{L} = 50 \text{ fb}^{-1}$ ,  $m_t = 180$  GeV,  $\sqrt{s} = 500$  GeV, polarization of  $e^-$  beam =  $\pm 80\%$ . They used the decay chain  $t\bar{t} \rightarrow b\bar{b}WW \rightarrow b\bar{b}q\bar{q}'\ell\nu$ , where  $\ell = e, \mu$ . The relevant branching fraction is  $8/27$ . They obtained overall efficiency of the analysis, including branching fractions, reconstruction efficiency, and acceptance,  $\simeq 18\%$ . Their results is that the sensitivity for EW-EDM is  $\mathcal{O}(0.1)$  with 90% CL.

(i-1) D. Atwood and A. Soni (1992) [91]. They studied the sensitivities for  $t\bar{t}\gamma$ - and  $t\bar{t}Z$ -EDM, (and -MDM) of  $e^+e^- \rightarrow t\bar{t}$  with  $\sqrt{s} = 0.5$  TeV. No specific model is assumed. Assuming that the top decay vertex  $t\bar{t}W$  is the SM one, they claimed  $1\sigma$ -bounds are  $\sim 10^{-18}e$  cm for  $10^4$  events. They introduce the notion of an “optimal observable” that have the maximum sensitivity to the relevant coupling. This observable turn out to be powerful as we shall see. However in general, this observable is rather complicated combination of momenta (and spins, maybe). Thus as themselves noted [103], there may be larger systematic error than that for simple observables. The events they use are that with both  $W$  decay leptonically:  $b\ell^+\nu_e\bar{b}\ell^-\bar{\nu}_e$ .

	Re [ $t\bar{t}\gamma$ -EDM]	Im [ $t\bar{t}\gamma$ -EDM]	Re [ $t\bar{t}Z$ -EDM]	Im [ $t\bar{t}Z$ -EDM]
without $E_W$ , with optimal	$4 \times 10^{-17}$	$1 \times 10^{-17}$	$1 \times 10^{-17}$	$4 \times 10^{-17}$
with $E_W$ , with simple	$4 \times 10^{-18}$	$1 \times 10^{-18}$	$4 \times 10^{-18}$	$4 \times 10^{-18}$
with $E_W$ , with optimal	$4 \times 10^{-19}$	$4 \times 10^{-19}$	$4 \times 10^{-19}$	$4 \times 10^{-19}$

Table 4.3: D. Atwood and A. Soni (1992) [91].  $1\sigma$  sensitivities in units of  $e$  cm. “With  $E_W$ ” means “to use polarization of  $W$ ”. Simple observables are explained in the text. See the original paper for optimal observables.

In this case, one can measure the polarization  $E_W^\mu$  of  $W$ , statistically by the distribution of  $\ell^\pm$ :

$$E_W^\mu = \frac{\text{tr} [\not{\epsilon}_\nu \not{\omega}_0 \not{\epsilon}_\ell \gamma^\mu (1 - \gamma_5)]}{4\sqrt{p_\nu \cdot \omega_0} p_\ell \cdot \omega_0},$$

where its “gauge” is fixed by an arbitrary lightlike vector  $\omega_0$ . As summarized in Table 4.3, the use of  $E_W^\mu$  improves the sensitivity about  $\mathcal{O}(10^2)$ . They propose several observables that are expectation values of certain operators. Explicit formulas of the operators for optimal observables are quite lengthy. They also studied simple operators. Those with best sensitivities are

$$\begin{aligned} \epsilon_{\mu\nu\rho\sigma} P_b^\mu Q_z^\nu H^{+\rho} H^{-\sigma} & \quad \text{for Re}[ $t\bar{t}\gamma$ -EDM] , \\ \epsilon_{\mu\nu\rho\sigma} P_e^\mu Q_z^\nu H^{+\rho} H^{-\sigma} & \quad \text{for Re}[ $t\bar{t}Z$ -EDM] , \\ H^- \cdot Q_z & \quad \text{for both Im}[ $t\bar{t}\gamma$ -EDM] and Im}[ $t\bar{t}Z$ -EDM] , \end{aligned}$$

where  $P_b = p_{\bar{b}} - p_b$ ,  $P_e = p_{e^+} - p_{e^-}$ ,  $Q_z = p_{e^+} + p_{e^-}$ ,  $H^\pm = 2(E_{W^+} \cdot p_t) E_{W^+} \pm 2(E_{W^-} \cdot p_t) E_{W^-}$ .

(i-2) M. S. Baek, S. Y. Choi and C. S. Kim (1997) [92]. They studied the sensitivities for  $t\bar{t}\gamma$ -EDM and  $t\bar{t}Z$ -EDM of  $e^+e^-$  collisions and  $\gamma\gamma$  collisions at NLC with  $\sqrt{s} = 0.5$  TeV,  $\int \mathcal{L}_{ee} = 10 \text{ fb}^{-1}$  for polarized electrons and the twice for unpolarized electrons. No specific model is assumed. The real part of EDMs are bounded by CPT-even observables (when there is no absorptive part). With polarized electrons, the tightest bound is obtained through  $A_1^b$ , defined in Eq. (4.7), in the inclusive top-quark decay mode:

$$|\text{Re}(t\bar{t}\gamma\text{-EDM})| \leq 1.4 \times 10^{-17} e \text{ cm} , \quad |\text{Re}(t\bar{t}Z\text{-EDM})| \leq 2.3 \times 10^{-17} e \text{ cm} .$$

Likewise, the imaginary part is bounded by CPT-odd observables. With polarized electrons, the tightest bound is obtained through  $A_E^b$ , defined in Eq. (4.7), in the inclusive top-quark decay mode:

$$|\text{Im}(t\bar{t}\gamma\text{-EDM})| \leq 1.8 \times 10^{-17} e \text{ cm} , \quad |\text{Im}(t\bar{t}Z\text{-EDM})| \leq 3.1 \times 10^{-17} e \text{ cm} .$$

For polarized  $\gamma\gamma$  collisions,  $|\text{Re}(t\bar{t}\gamma\text{-EDM})| \leq 1.8 \times 10^{-17} e \text{ cm}$  for  $\sqrt{s} = 0.5$  TeV, and  $0.2 \times 10^{-17} e \text{ cm}$  for 1.0 TeV. They argued that the sensitivity is much sensitive to  $\sqrt{s}$  than  $e^+e^-$  collisions.

(i-3) These couplings are also studied in [95–97]. In [93, 94],  $t\bar{t}\gamma$ -EDM and  $t\bar{t}Z$ -EDM are considered within two Higgs doublets model. QCD corrections to this process well above the threshold are considered in [98]. Studies in  $\gamma\gamma$  colliders are given in [99, 100]; sensitivity is  $\sim 10^{-17} e \text{ cm}$  with  $\int \mathcal{L} = 10 \text{ fb}^{-1}$  and  $\sqrt{s} = 500$  GeV.

**(ii) Anomalous Chromomagnetic vertex in hadron collisions**

(ii-1) D. Atwood, A. Aeppli and A. Soni (1992) [103]. It was studied that the sensitivities of  $gg \rightarrow t\bar{t}$  at SSC and LHC for the real part of  $t\bar{t}g$ -EDM.  $1\sigma$  sensitivity is  $0.3 \times 10^{-19} g_s$  cm with optimal observable  $f_{\text{opt}}$ ,  $0.5 \times 10^{-19} g_s$  cm with  $f_1$ , and  $0.6 \times 10^{-19} g_s$  cm with  $f_2$ . We do not reproduce their explicit form. Assumed experimental setup is mainly, SSC,  $\sqrt{s} = 40$  TeV,  $10 \text{ fb}^{-1}$ ,  $10^7$  leptonic  $t\bar{t}$  events. However, they say that the difference is only a few percent by changing SSC  $\sqrt{s} = 40$  TeV to LHC  $\sqrt{s} = 16$  TeV. Correlations between the  $t$  and  $\bar{t}$  polarizations are used:  $f_{\text{opt}}, f_1, f_2, f_3$ . The  $f_{\text{opt}}$  and  $f_1$  are tailored to maximize the sensitivity for  $\text{Re}(t\bar{t}g\text{-EDM})$ , and are fairly complicated combination of momenta and spins. As they pointed out, there may be larger systematic error than simpler observables such as  $f_2$  and  $f_3$ :

$$f_2 = \frac{\epsilon_{\mu\nu\rho\sigma} p_{e1}^\mu p_{e2}^\nu p_{b1}^\rho p_{b2}^\sigma}{(p_{e1} \cdot p_{e2} p_{b1} \cdot p_{b2})^{1/2}}.$$

$f_3$  turn out to be less sensitive than  $f_2$  by  $\mathcal{O}(10)$ .

(ii-2) S. Y. Choi, C. S. Kim and Jake Lee (1997) [104]. The sensitivity of  $gg \rightarrow t\bar{t}$  (LHC) for  $t\bar{t}g$ -EDM was studied. Assumed setup is acceptance efficiency  $\epsilon = 10\%$ ,  $B_\ell = B_{\bar{\ell}} = 20\%$  for  $\ell = e, \mu$ ,  $\sqrt{s} = 14$  TeV, and  $\int \mathcal{L}_{pp} = 10 \text{ fb}^{-1}$ . CP-odd energy and angular correlations are used for unpolarized proton beam.  $1\sigma$  sensitivity is

$$\begin{aligned} |\text{Re}(t\bar{t}g\text{-EDM})| &= 0.899 \times 10^{-17} g_s \text{ cm} & \cdots & T_{33}^\ell, \\ |\text{Im}(t\bar{t}g\text{-EDM})| &= 0.858 \times 10^{-18} g_s \text{ cm} & \cdots & A_E^\ell, \\ |\text{Im}(t\bar{t}g\text{-EDM})| &= 0.205 \times 10^{-17} g_s \text{ cm} & \cdots & Q_{33}^\ell, \end{aligned}$$

where written in the RHS are relevant observables defined in Eq. (4.7). There may be (at least) two more operators that are CP-odd:  $A_1^\ell$  and  $A_2^\ell$ , also defined in Eq. (4.7). However these correlation are zero, since the cross section is symmetric under  $(\mathbf{p}_g, \bar{\mathbf{p}}_g) \rightarrow (\bar{\mathbf{p}}_g, \mathbf{p}_g)$  due to Bose symmetry:  $|\mathbf{p}_g, \bar{\mathbf{p}}_g\rangle = a^\dagger(\mathbf{p}_g) a^\dagger(\bar{\mathbf{p}}_g) |0\rangle = + |\bar{\mathbf{p}}_g, \mathbf{p}_g\rangle$ . For polarized proton beam, one can probe CP-violating effect without detailed reconstruction of the final states. Thus they used CP-odd rate asymmetry,

$$A = \frac{\sigma_+ - \sigma_-}{\sigma_+ + \sigma_-},$$

where  $\sigma_\pm$  is the cross section for  $t\bar{t}$  production in collision of an unpolarized proton to a polarized proton of helicity  $\pm$ . They obtained  $|\text{Im}(t\bar{t}g\text{-EDM})| \leq 10^{-20} g_s$  cm. They found sensitivity depends crucially on the degree of polarization of gluons. Berger-Qiu parameterization [105] for polarized gluon distribution functions was used.

(ii-3) In [76],  $N(t_L \bar{t}_L) - N(t_R \bar{t}_R)$  was studied. In [106] Tevatron Run II ( $\sqrt{s} = 2$  TeV) was considered. In [99],  $\gamma\gamma \rightarrow t\bar{t}$  is also considered; a list of sensitivities is also given. In [108], two-doublets Higgs models was considered. In [107] the process  $gW^+ \rightarrow t\bar{b}$  was studied, and the contribution turned to be small; the reason is also given.

(ii-4) Here are comments for the uncertainties in the theoretical analyses of sensitivity studies at hadron colliders. Some of the existing sensitivity studies make use of some complicated combinations of momenta of leptons and b's; those include "optimal observable". Whether these analyses can be taken seriously was questioned; there are several reasons. Firstly the CM energy of a reaction cannot be measured in hadron collisions. In view of event reconstruction, more questionable is the efficiencies for the assignments of jets to the parent partons. A jet,

which is assigned to a parent parton, must be well separated from other jets in order for it to be used as a signal jet; in other words, not all hadrons are assigned to one of the signal jets, which means the jets used for the analysis. This is in contrast to  $e^+e^-$  collisions, where every hadrons are assigned to one of the jets. Generally certain amount of energy is not correctly assigned but included into other (non-signal) jets. Usually the missing energy will be supplemented artificially by multiplying some factor to the observed energy. Under such circumstances it should be examined carefully, incorporating realistic detector simulations, how well the required parton four-momenta can be reconstructed.

### (iii) Other situations

Anomalous chromo-EDM vertex in  $e^+e^-$  collisions is studied in [101, 102]. In [101], gluon jet energy distribution for the process  $e^+e^- \rightarrow t\bar{t}g$  is studied. They concluded that the sensitivity is  $\mathcal{O}(1)$  with  $\sqrt{s} = 500$  GeV,  $\int \mathcal{L} = 50 \text{ fb}^{-1}$ , identification-efficiency for top-quark pair-production event  $\simeq 100\%$ , and  $E_g^{\text{min}} = 25$  GeV. The last one is the cut for the minimum gluon-jet energy, which is necessary because (1) the cross section is IR singular, and (2) to avoid the contamination due to the gluon radiation from  $b$ -quark; the cross section grows rapidly as  $E_g^{\text{min}}$  is lowered. On the other hand, in [102],  $CP$ -odd spin correlation of  $t$  and  $\bar{t}$  is studied. They concluded that the sensitivity is  $\mathcal{O}(10)$  with  $\sqrt{s} = 500$  GeV,  $\int \mathcal{L} = 50 \text{ fb}^{-1}$ , and top-detection efficiency  $\epsilon = 0.1$ .

Anomalous EW vertices in hadron collisions are studied in [76].

Anomalous decay vertex is studied in [109–112]. Both production and decay anomalous vertices are studied simultaneously in [113–119] for  $e^+e^-$  collisions, and in [120] for hadron collisions.  $CP$  violation in top sector is studied also in [121].  $CP$  violation in other sectors (EDM of  $\tau$  etc.) are studied in [122–124].

## 4.5 Polarizations

In the previous section, we saw that the spin-direction of  $t$  and  $\bar{t}$  may serve as a probe of EDMs. In this section, we see how the effects of polarization can be incorporated to actual calculations, and how the polarizations can be measured.

### 4.5.1 Polarizations of $e^+e^-$

Polarization is a incoherent sum of states with definite spin direction. Thus this can be treated by a density matrix. For spin-1/2 particle, polarization  $\vec{P}$  is defined to twice the expectation value of spin  $\vec{S}$ :  $\vec{P} = 2\langle \vec{S} \rangle$ . Thus the density matrix  $\rho$  is

$$\rho = \frac{1}{2} \left( \mathbf{1} + \sum_i P_i \sigma_i \right) = \frac{1}{2} \begin{pmatrix} 1 + P_z & P_x - iP_y \\ P_x + iP_y & 1 - P_z \end{pmatrix},$$

because  $\text{tr}(\rho) = 1$ ,  $\text{tr}(\rho S_i) = \langle S_i \rangle$ . Then for longitudinal polarization, we just sum “spin-up” and “spin-down” with the weight  $\frac{1+P}{2}$  and  $\frac{1-P}{2}$ , respectively. Since electron mass is negligible, chirality is the same to helicity for electron, and the opposite for positron:  $(\psi_L)^c = (\psi^c)_R$ . Thus the matrix element  $E^{\mu\nu} \simeq \sum_{\text{spins}} j_{ee}^{\mu} j_{ee}^{\nu*}$  for initial  $e^+e^-$  current with incomplete polarizations

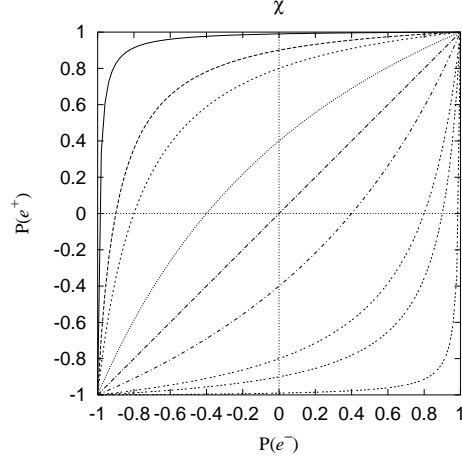


Figure 4.1: Contours of the measure of initial polarization:  $\chi = (\bar{P}_e - P_e)/(1 - P_e\bar{P}_e)$ . In the figure  $P(e^-) = P_e$  and  $P(e^+) = \bar{P}_e$ . From left-top to right-bottom, the contours are for  $\chi = 0.99, 0.9, 0.8, 0.4, 0.0, -0.4, -0.8, -0.9, \text{ and } -0.99$ . For unpolarized positron beam  $\bar{P}_e = 0, \chi = -P_e$ .

can be written as follows:

$$\begin{aligned} E_{\mu\nu} &= \text{tr} \left[ \Lambda_\mu \left( \frac{1 + P_e}{2} \frac{1 + \gamma_5}{2} + \frac{1 - P_e}{2} \frac{1 - \gamma_5}{2} \right) \not{p}_e \times \right. \\ &\quad \left. \times \bar{\Lambda}_\nu \not{p}_e \left( \frac{1 + \bar{P}_e}{2} \frac{1 + \gamma_5}{2} + \frac{1 - \bar{P}_e}{2} \frac{1 - \gamma_5}{2} \right) \right] \\ &= \frac{1 - P_e \bar{P}_e}{4} \text{tr} \left[ \Lambda_\mu (1 - \chi \gamma_5) \not{p}_e \bar{\Lambda}_\nu \not{p}_e \right]. \end{aligned}$$

Here  $P_e = 1$  ( $\bar{P}_e = 1$ ) means the complete polarization with right-handed helicity for electron (positron), and

$$\chi = \frac{\bar{P}_e - P_e}{1 - P_e \bar{P}_e} \quad (4.8)$$

is a measure of initial polarization;  $\chi = \pm 1$  means  $(P_e, \bar{P}_e) = (\mp 1, \pm 1)$ . The contours of  $\chi$  are shown in Figure 4.1. We can see that non-zero polarization effectively mixes vector- and axial-vector-vertices, or  $\chi \neq 0$  means that the initial state is parity violating. Thus when  $\chi \neq 0$ , an expectation value of parity-odd observable can be non-zero, even if all the relevant interactions are parity conserving.

The effect of non-zero  $\chi$  can easily be recovered from the results with  $\chi = 0$ , in the following way. Since we don't assume anomalous vertices for initial  $e^+e^-$  current,

$$\begin{aligned} E_{\mu\nu} &\propto \text{tr} [(v^{eX} \gamma_\mu - a^{eX} \gamma_\mu \gamma_5) (1 - \chi \gamma_5) \not{p}_e (v^{eY*} \gamma_\nu - a^{eY*} \gamma_\nu \gamma_5) \not{p}_e] \\ &= \text{tr} [\gamma_\mu \not{p}_e \gamma_\nu \not{p}_e \{ (v^{eX} v^{eY*} + a^{eX} a^{eY*}) + \chi (v^{eX} a^{eY*} + a^{eX} v^{eY*}) \} \\ &\quad + \gamma_\mu \not{p}_e \gamma_\nu \not{p}_e \gamma_5 \{ (v^{eX} a^{eY*} + a^{eX} v^{eY*}) + \chi (v^{eX} v^{eY*} + a^{eX} a^{eY*}) \}]. \end{aligned}$$

Thus we can recover terms proportional to  $\chi$  from those without  $\chi$  as follows: every terms in  $|\mathcal{M}|^2$  contain two factors of  $v^e$  or  $a^e$ ; exchange each one of them with the rule  $v^e \leftrightarrow a^e$  and divide by two. The product of couplings in Eqs. (4.26) and (4.27) are defined such that each



pair of  $(a_1, a_2)$ ,  $(a_3, a_4)$  and  $(a_5, a_6)$  are “conjugate” with the procedure above. Thus we can recover  $\chi$  dependence simply by replacing  $(a_1, a_2)$  with  $(a_1 + \chi a_2, a_2 + \chi a_1)$  and similarly for  $(a_3, a_4)$  and  $(a_5, a_6)$ .

### 4.5.2 Polarizations of $t\bar{t}$

Although the spin  $\mathbf{s}$  of, say,  $t$  is surely a 3-vector, but one should be careful to its quantum nature. That is, two spins that are orthogonal in a sense of 3-vector, are not “orthogonal”. For a spin-1/2 state,

$$|\langle \theta, \phi | \hat{z} \rangle|^2 = \cos^2 \frac{\theta}{2} = \frac{1 + \cos \theta}{2},$$

where  $\theta$  and  $\phi$  denote polar coordinates, and  $|\hat{z}\rangle = |\theta = 0\rangle$ . Thus, when an amplitude vanishes for some choice of spin  $\vec{s} = -\vec{n}$ , it means the spin-direction is  $+\vec{n}$ , not perpendicular to  $-\vec{n}$ .

Let us look at them more closer. In quantum mechanics, the polarization  $\vec{P}$  along some direction  $\vec{n}$  ( $|\vec{n}|^2 = 1$ ) may be calculated as follows:

$$\begin{aligned} \vec{n} \cdot \vec{P} &= \langle \Psi | \vec{n} \cdot (2\hat{S}) | \Psi \rangle / \langle \Psi | \Psi \rangle \\ &= \sum_{P=\pm 1} P |\langle \vec{s} = P\vec{n} | \Psi \rangle|^2 / \langle \Psi | \Psi \rangle, \end{aligned}$$

Here we used

$$1 = \sum_{P=\pm 1} |\vec{s} = P\vec{n}\rangle \langle \vec{s} = P\vec{n}|, \quad \vec{n} \cdot \hat{S} |P\vec{n}\rangle = \frac{P}{2} |P\vec{n}\rangle.$$

Note that  $\hat{S}_i$  means spin operator, while  $s_i$  means spin-direction:  $|\vec{s}|^2 = 1$ .

With this experience in mind, next we consider the process  $e^+e^- \rightarrow t(s)\bar{t}(\bar{s})$ , where  $s$  ( $\bar{s}$ ) is a 3-vector for the spin-direction of  $t$  ( $\bar{t}$ ) at its rest frame. Let us write the spin dependence of the matrix element  $\mathcal{M}$  as follows:

$$\begin{aligned} |\mathcal{M}(s^i, \bar{s}^j)|^2 &= \frac{C}{4} [1 + s^i P^i + \bar{s}^j \bar{P}^j + s^i \bar{s}^j (P^i \bar{P}^j + M^{ij})] \\ &= C \left[ \left( \frac{1 + s^i P^i}{2} \right) \left( \frac{1 + \bar{s}^j \bar{P}^j}{2} \right) + \frac{1}{4} s^i \bar{s}^j M^{ij} \right]. \end{aligned} \quad (4.9)$$

As the notation indicates,  $P_i$  can be interpreted as the polarization vector for  $t$ . This can be seen as follows. Total cross section  $\sigma$  is

$$\sigma \propto \int d\Omega \sum_{\substack{s^i = \pm n^i \\ \bar{s}^j = \pm \bar{n}^j}} |\mathcal{M}(s^i, \bar{s}^j)|^2 = \int d\Omega C.$$

Note that momentum 3-vectors are summed over all direction, while spin 3-vectors are summed only “up” and “down”, because this is the way they form a complete set. The directions  $\vec{n}, \vec{\bar{n}}$  of quantization-axes are arbitrary, here. While, the polarization vector  $P^i$  of  $t$  for a fixed momentum configuration is

$$\langle n^i \cdot 2S^i \rangle \propto \sum_{\substack{P=\pm 1 \\ \bar{P}=\pm 1}} P |\mathcal{M}(s^i = Pn^i, \bar{s}^j = \bar{P}\bar{n}^j)|^2 = n^i P^i C.$$

The spin quantization-axis  $\vec{n}$  for  $\bar{t}$  is arbitrary. Dividing by  $\sigma$ , we see that  $P^i$  defined at Eq. (4.9) is surely a polarization vector for  $t$ , when one sum over the spin of  $\bar{t}$ . Likewise,

$$\langle n^i \cdot 2S^i \bar{n}^j \cdot 2\bar{S}^j \rangle \propto \sum_{\substack{P=\pm 1 \\ \bar{P}=\pm 1}} P\bar{P} |\mathcal{M}(s^i = Pn^i, \bar{s}^j = \bar{P}\bar{n}^j)|^2 = n^i \bar{n}^j (P^i \bar{P}^j + M^{ij}) C .$$

Thus we see

$$\langle S^i \bar{S}^j \rangle = \frac{P^i \bar{P}^j}{2} + \frac{M^{ij}}{4} \neq \frac{P^i}{2} \frac{\bar{P}^j}{2} = \langle S^i \rangle \langle \bar{S}^j \rangle ,$$

which means the spins of  $t$  and  $\bar{t}$  are correlated when  $M^{ij} \neq 0$ . This can be seen already in the definition Eq. (4.9); when  $M^{ij} = 0$ ,  $|\mathcal{M}(s^i = -P^i, \bar{s}^j)|^2 = 0$  irrespective of  $\bar{s}^j$  (when  $|\vec{P}|^2 = 1$ ). This means the spin-direction  $\vec{s}$  is  $\vec{P}$ , and is determined solely by the momentum configuration, because so is  $\vec{P}$ . In general  $M^{ij} \neq 0$ , because momenta and spins have independent degrees of freedom. However in some cases, the two spin-directions factorize. For example, for the process  $e^-(L) e^+(R) \rightarrow \gamma^* \rightarrow t(s) \bar{t}(\bar{s})$  near the threshold,

$$|\mathcal{M}|^2 \propto \left(1 - \mathbf{s}_t \cdot \frac{\mathbf{p}_{e^-}}{m_t}\right) \left(1 - \bar{\mathbf{s}}_t \cdot \frac{\mathbf{p}_{e^-}}{m_t}\right) + \mathcal{O}(\beta_t^2) ,$$

where  $\beta_t = 2|\mathbf{p}_t|/\sqrt{s}$ . Here  $e^+(R)$  means positron of right-handed helicity, not chirality. This shows that the direction of spins of both  $t$  and  $\bar{t}$  are anti-parallel to the direction of (left-handed) initial electron. This is due to the conservation of total angular momentum; on the threshold, there is no orbital angular momentum.

The polarization vectors  $\vec{P}, \vec{\bar{P}}$  should be composed of odd number of  $\mathbf{p}_t$  and  $\mathbf{p}_e$ , since  $|\mathcal{M}|^2$  is a scalar under 3-dimensional rotation. This means the polarization vectors are odd under ‘‘overall’’ parity transformation [Section A.7.4], which means parity violating. These vectors are non-zero even for zero initial polarization  $\chi$ , because the coupling of  $Z$  to fermion-antifermion is parity violating.

A  $|\mathcal{M}|^2$  for the definite momenta and spin-directions of  $t$  and  $\bar{t}$  can be calculated with the usual Trace technique with spin-projection operators [Section A.3.7]. One can easily see that the general spin structure for  $|\mathcal{M}|^2$  is that given in Eq. (4.9). In the next section, it is given that the simple example of a calculation with a spin-projection.

### 4.5.3 Spin direction of top quark

The direction of the spin of top quark can be measured statistically for the decay process  $t \rightarrow b\bar{\ell}\nu_\ell$ . This is because [90] at the rest frame of  $t$ , the charged lepton  $\bar{\ell}$  is emitted preferentially to the direction of the spin of top quark. This can be seen as follows. Using  $\bar{u}_1 \Gamma v_2 = -\bar{v}_2^c \Gamma^c u_1^c = -\bar{u}_2 \Gamma^c v_1$  for commuting spinors, and Fierz identity,

$$\begin{aligned} \mathcal{M} &\sim \bar{u}(p_b) \gamma^\mu \frac{1-\gamma_5}{2} u(p_t) \bar{u}(p_\nu) \gamma_\mu \frac{1-\gamma_5}{2} v(p_{\bar{\ell}}) \\ &= +\bar{u}(p_b) \gamma^\mu \frac{1-\gamma_5}{2} u(p_t) \bar{u}(p_{\bar{\ell}}) \gamma_\mu \frac{1+\gamma_5}{2} v(p_\nu) \\ &= \frac{1}{2} \bar{u}(p_b) (1 + \gamma_5) v(p_\nu) \bar{u}(p_{\bar{\ell}}) (1 - \gamma_5) u(p_t) , \end{aligned}$$

which means

$$\begin{aligned}
|\mathcal{M}|^2 &\propto \sum_{s_{\bar{\ell}}} |\bar{u}(p_{\bar{\ell}}, s_{\bar{\ell}})(1 - \gamma_5)u(p_t, s_t)|^2 \\
&= \text{tr} \left[ \not{\bar{p}}_{\bar{\ell}}(1 - \gamma_5)(\not{p}_t + m_t)\frac{1 - \not{s}_t \gamma_5}{2}(1 + \gamma_5) \right] \\
&= 4p_{\bar{\ell}} \cdot (p_t - m_t s_t) \\
&= 4m_t E_{\bar{\ell}}(1 + \mathbf{s}_t \cdot \boldsymbol{\beta}_{\bar{\ell}}) \quad \text{at the rest frame of top.}
\end{aligned}$$

That is, roughly speaking,  $\mathbf{s}_t \parallel +\langle \mathbf{p}_{\ell^+} \rangle$  and  $\mathbf{s}_{\bar{t}} \parallel -\langle \mathbf{p}_{\ell^-} \rangle$ . Thus the component  $n \cdot s_t$  of the spin  $s_t$  of top quark parallel to certain direction  $n$  can be obtained statistically by  $\langle n \cdot p_{\bar{\ell}} \rangle$ . Then we treat the spin (or polarization) of top quark as if it were a observable.

## 4.6 Corrections due to Coulomb rescattering

### 4.6.1 Relevant Lagrangian

From now on, we concentrate to the  $t\bar{t}$  production near the threshold. This also means to use  $e^+e^-$  collisions, since for hadron colliders  $\sqrt{s}$  of each subprocess is not fixed. As emphasized in Chapter 2, the most prominent feature of threshold region is leading-order multiple Coulomb rescattering<sup>11</sup>, which means higher orders of  $\alpha_s$  are not suppressed compared to the propagation without gluon exchange. This drastically changes the behavior of  $t\bar{t}$  production cross section, compared to the tree-level expectation. For example, the magnitude of the ‘‘imaginary part’’ (= absorptive part) of the amplitude is similar to the ‘‘real part’’.

The relevant part of the Lagrangian is as follows:

$$\begin{aligned}
\mathcal{L} &= -g_s(\bar{t}\gamma^\mu T^a t)G_\mu^a - \frac{g_s d_{tg}}{2m_t}(\bar{t}i\sigma^{\mu\nu}\gamma_5 T^a t)\partial_\mu G_\nu^a \\
&\quad - g_z(\bar{t}\gamma^\mu(v^{tZ} - a^{tZ}\gamma_5)t)Z_\mu - \frac{g_z d_{tZ}}{2m_t}(\bar{t}i\sigma^{\mu\nu}\gamma_5 t)\partial_\mu Z_\nu \\
&\quad - eQ_t(\bar{t}\gamma^\mu t)A_\mu - \frac{e d_{t\gamma}}{2m_t}(\bar{t}i\sigma^{\mu\nu}\gamma_5 t)\partial_\mu A_\nu \\
&\quad + \text{terms required by gauge invariance} + \dots,
\end{aligned}$$

where the couplings are defined in Eq. (A.32). Feynman rule for, say,  $t\bar{t}\gamma$  vertex is proportional to  $Q_t\gamma^\mu + d_{t\gamma}/(2m_t)\sigma^{\nu\mu}\gamma_5 q_\nu$ , where  $q_\nu$  is a momentum flows into  $t\bar{t}$  current. Note that

$$\frac{d}{2m}(\bar{t}i\sigma^{\mu\nu}\gamma_5 t)\partial_\mu A_\nu \simeq \frac{-d}{2m}(\bar{t}i\gamma_5 i\vec{\partial}^\mu t)A_\mu \simeq -d\frac{(p_t - \bar{p}_t)^\mu}{2m}\bar{u}(p_t)i\gamma_5 v(\bar{p}_t)\epsilon_\mu,$$

where the first ‘‘ $\simeq$ ’’ means they coincide with the use of eqs. of motion, and the second means to sandwich with  $\langle p_t, \bar{p}_t |$  and  $|q\rangle$  and to integrate over  $x$  [Section A.4]. We checked that both of these forms of the interaction give the same result, at least for the case we deal with.

<sup>11</sup> Since the Coulomb rescattering is indispensable for the threshold region, in some case its effect is implicit, and the word ‘‘rescattering’’ is saved for the other corrections; that is, gluon exchange between  $t$  and  $\bar{b}$  for example. However here we do not care about those corrections involving decay products.

As we saw in Section 2.3, the potential  $V_C$  between  $t\bar{t}$  due to  $\mathcal{L}_{\text{int}} = -g_s(\bar{t}\gamma^\mu T^a t)G_\mu^a$  is  $\tilde{V}_C = -C_F g_s^2/|\mathbf{q}|^2$ , where  $\mathbf{q}$  is momentum transfer from  $\bar{t}$  to  $t$ . Likewise, one can show that the potential  $V_{\text{CEDM}}$  due to the  $t\bar{t}g$ -EDM interaction above is [Figure 4.2]

$$\tilde{V}_{\text{CEDM}} = \frac{-C_F g_s^2}{|\mathbf{q}|^2} \frac{-d_{tg}}{m_t} i\mathbf{q} \cdot \left( \frac{\boldsymbol{\sigma}_t}{2} - \frac{\boldsymbol{\sigma}_{\bar{t}}}{2} \right). \quad (4.10)$$

This potential is  $(\text{P}, \text{C}) = (-, +)$ , as it should be.



Figure 4.2: Contribution of anomalous  $t\bar{t}g$ -EDM to  $t\bar{t}$  potential.

Note that the magnitude of the EDM-interactions are proportional to the momentum transfer between  $t\bar{t}$ . This can clearly be seen in the modified vertices Eq. (4.12) in the next section. Thus the effects of two EW-EDMs becomes larger for higher CM energy  $\sqrt{s}$ , because they affect directly the  $t\bar{t}$  production vertex. While the effect of CEDM do not become larger for higher  $\sqrt{s}$ , because<sup>12</sup> it affects the Coulomb rescattering between  $t\bar{t}$ , whose relative significance becomes smaller for  $\sqrt{s}$ . Thus the threshold region does not suit for the measurement of EW-EDMs. On the other hand, CEDM can be measured only near the threshold for lepton colliders. Note that even though the sensitivity to the existence of finite CEDM may be better for hadron colliders, the precise measurement of its magnitude may only be achieved at lepton colliders.

## 4.6.2 Corrections to vertices

In the next section, we show that the effect of Coulomb rescattering between  $t$  and  $\bar{t}$  is to change the vertices for  $t\bar{t}\gamma$  and  $t\bar{t}Z$ . The result is as follows. To the tree-level (and without anomalous vertices), the electroweak  $t\bar{t}$  vertices are

$$(\Gamma^X)^\mu = v^{tX}\Gamma_V^\mu - a^{tX}\Gamma_A^\mu, \quad \text{where} \quad \Gamma_V^\mu = \gamma^\mu, \quad \Gamma_A^\mu = \gamma^\mu\gamma_5 \quad (X = \gamma, Z),$$

times  $-ig_X$ . See Section A.5 for the definition of the couplings. Rescattering and anomalous vertices modify the vertices:

$$(\tilde{\Gamma}^X)^\mu = v^{tX}\tilde{\Gamma}_V^\mu - a^{tX}\tilde{\Gamma}_A^\mu + d_{tX}\Gamma_{\text{EW-EDM}}^\mu, \quad (4.11)$$

where

$$\begin{aligned} \tilde{\Gamma}_V^\mu &= \left[ \gamma^\mu G(E, |\mathbf{p}|) - i\gamma_5 \frac{-p^\mu}{m_t} d_{tg} D(E, |\mathbf{p}|) \right] \times \left( \frac{|\mathbf{p}|^2}{m_t} - (E + i\Gamma_t) \right), \\ \tilde{\Gamma}_A^\mu &= \gamma^\mu\gamma_5 F(E, |\mathbf{p}|) \times \left( \frac{|\mathbf{p}|^2}{m_t} - (E + i\Gamma_t) \right), \\ \Gamma_{\text{EW-EDM}}^\mu &= i\gamma_5 \frac{-p^\mu}{m_t} F(E, |\mathbf{p}|) \times \left( \frac{|\mathbf{p}|^2}{m_t} - (E + i\Gamma_t) \right), \end{aligned} \quad (4.12)$$

<sup>12</sup> More concretely speaking, because the combination of the Green function  $D = F - G$ , which is relevant to CEDM, becomes zero for  $\sqrt{s} \gg 2m_t$ .

where  $\mathbf{p} = (\mathbf{p}_t - \bar{\mathbf{p}}_t)/2$  is the relative momentum of  $t\bar{t}$ , and  $E = \sqrt{s} - 2m_t$  is non-relativistic CM energy;  $G(E, |\mathbf{p}|)$  and  $F(E, |\mathbf{p}|)$  are  $S$ - and  $P$ -wave Green functions, respectively

$$G(E, |\mathbf{p}|) = \langle \mathbf{p} | G | \mathbf{x}' = \vec{0} \rangle, \quad \mathbf{p} F(E, |\mathbf{p}|) = \langle \mathbf{p} | \mathbf{p} F | \mathbf{x}' = \vec{0} \rangle, \quad (4.13)$$

and

$$\left( \frac{|\mathbf{p}|^2}{m_t} - \omega + V_C \right) G = 1, \quad \left( \frac{|\mathbf{p}|^2}{m_t} - \omega + V_C \right) \mathbf{p} F = \mathbf{p}, \quad (4.14)$$

and  $D(E, |\mathbf{p}|) = G(E, |\mathbf{p}|) - F(E, |\mathbf{p}|)$ . We can see from the equations for Green functions that

$$G(E, |\mathbf{p}|) = F(E, |\mathbf{p}|) = 1 / \left( \frac{|\mathbf{p}|^2}{m_t} - (E + i\Gamma_t) \right) \quad \text{for } V \rightarrow 0,$$

and  $D(E, |\mathbf{p}|) = 0$ . Thus in the weak potential limit, or for  $\sqrt{s} \gg 2m_t$  where the effect of Coulomb rescattering is diminished, the vertices reduces the tree-level ones with anomalous EW-EDMs but QCD-EDM.

We can see from Eq. (4.12) that the effects of anomalous  $\mathcal{CP}$ -violating interactions are suppressed<sup>13</sup> only by  $\beta_t = |\mathbf{p}_t|/m_t$ . Thus we take into account  $\mathcal{O}(\beta_t)$  corrections, and neglect the higher orders<sup>14</sup>.

### 4.6.3 Sketch of the calculation

Using Non-Relativistic form of the propagators,

$$\begin{aligned} S_F(k + \frac{q}{2}) &= \frac{1 + \gamma^0}{2} \frac{i}{E/2 + k^0 - |\mathbf{q}|^2/(2m_t) + i\Gamma_t/2} + \mathcal{O}\left(\frac{1}{c}\right), \\ S_F(k - \frac{q}{2}) &= \frac{1 - \gamma^0}{2} \frac{i}{E/2 - k^0 - |\mathbf{q}|^2/(2m_t) + i\Gamma_t/2} + \mathcal{O}\left(\frac{1}{c}\right), \end{aligned} \quad (4.15)$$

Lippmann-Schwinger equation for the vector vertex is written as follows:

$$\begin{aligned} \Gamma_V^i(E, p) &= \gamma^i + C_F(-ig_s)^2 \int \frac{d^4k}{(2\pi)^4} \frac{i}{E/2 + k^0 - |\mathbf{k}|^2/(2m_t) + i\Gamma_t/2} \times \\ &\quad \times \frac{i}{E/2 - k^0 - |\mathbf{k}|^2/(2m_t) + i\Gamma_t/2} \times \\ &\quad \times \left[ \gamma^0 \frac{1 + \gamma^0}{2} \Gamma_V^i(E, k) \frac{1 - \gamma^0}{2} \gamma^0 \right. \\ &\quad \quad + \left( \frac{d_{tg}}{2m_t} \right) \sigma^{j0} \gamma_5 \frac{-(p-k)^j}{c} \frac{1 + \gamma^0}{2} \Gamma_V^i(E, k) \frac{1 - \gamma^0}{2} \gamma^0 \\ &\quad \quad + \left( \frac{d_{tg}}{2m_t} \right) \gamma^0 \frac{1 + \gamma^0}{2} \Gamma_V^i(E, k) \frac{1 - \gamma^0}{2} \sigma^{j0} \gamma_5 \frac{+(p-k)^j}{c} \\ &\quad \left. \right] \times \frac{i}{|\mathbf{p} - \mathbf{k}|^2}. \end{aligned} \quad (4.16)$$

<sup>13</sup> Note that the time-component of the vertex do not contribute to  $|\mathcal{M}|^2$ , since the initial  $e^+e^-$  current  $j_{e^+e^-}^\mu$  is conserved  $q_\mu j_{e^+e^-}^\mu = 0$  (because the mass of  $e^-$  can be neglected). Thus at the CM-frame  $q_\mu = (\sqrt{s}, \vec{0})$ , the time-component of  $e^+e^-$  current is zero  $j_{e^+e^-}^0 = 0$ . Propagators of gauge bosons are proportional to  $g_{\mu\nu}$ , aside from  $q_\mu q_\nu$ . Thus only the space-component of  $t\bar{t}$  current  $j_{t\bar{t}}^\mu$  contributes.

<sup>14</sup> We also neglect the  $\mathcal{O}(\beta_t)$  corrections from FSIs.

A similar equation holds also for the axial vertex. Since there is no  $p^0$ -dependence on the right-hand side, consistency requires  $\Gamma_V^i(E, p) = \Gamma_V^i(E, \mathbf{p})$ . Thus we can trivially integrate  $p^0$ , and obtain

$$\Gamma_V^i(E, \mathbf{p}) = \gamma^i - \int \frac{d^3k}{(2\pi)^3} \frac{-C_F g_s^2}{|\mathbf{p} - \mathbf{k}|^2 |\mathbf{k}|^2 / m_t - (E + i\Gamma_t)} \times \quad (4.17)$$

$$\times \frac{1 + \gamma^0}{2} \left[ \Gamma_V^i(E, \mathbf{k}) - \frac{d_{tg}}{2m_t} \frac{(\mathbf{p} - \mathbf{k})^j}{c} \{ \sigma^{j0} \gamma_5 \Gamma_V^i(E, \mathbf{k}) + \Gamma_V^i(E, \mathbf{k}) \sigma^{j0} \gamma_5 \} \right] \frac{1 - \gamma^0}{2}.$$

In view of the structure of gamma matrix, we decompose the vertex function  $\Gamma_V^i(E, \mathbf{p})$  as follows:

$$\frac{1 + \gamma^0}{2} \Gamma_V^i(E, \mathbf{p}) \frac{1 - \gamma^0}{2} = \frac{1 + \gamma^0}{2} \left[ \gamma^j \left( \delta^{ij} \Gamma_G(E, \mathbf{p}) + \Gamma_B^{ij}(E, \mathbf{p}) \right) + i \sigma^{ij} \gamma_5 \Gamma_F^j(E, \mathbf{p}) - i \gamma_5 \Gamma_D^i(E, \mathbf{p}) \right] \frac{1 - \gamma^0}{2} \quad (4.18)$$

where  $\sum_{ij} \Gamma_B^{ij}(E, \mathbf{p}) = 0$ . By plugging this expression into the integral equation above, one obtains the integral equations for each (reduced) vertex functions  $\Gamma_G(E, \mathbf{p})$  etc. One can see that  $\Gamma_D^i(E, \mathbf{p}) = \mathcal{O}(d_{tg})$ ,  $\Gamma_B^{ij}(E, \mathbf{p}) = \mathcal{O}(d_{tg}^2)$ . Thus we forget about  $\Gamma_B^{ij}(E, \mathbf{p})$  hereafter. One can do just the same procedure for the axial vertex  $\Gamma_A^i(E, \mathbf{p})$ , and finds that anomalous  $ttg$  vertex we inserted do not alter the axial vertex to the order we consider now. We extract Lorentz structure of  $\Gamma_F^i(E, \mathbf{p})$  etc. as follows:

$$\Gamma_G(E, \mathbf{p}) = \left( \frac{|\mathbf{p}|^2}{m_t} - (E + i\Gamma_t) \right) G(E, |\mathbf{p}|),$$

$$\Gamma_F^i(E, \mathbf{p}) = \left( \frac{|\mathbf{p}|^2}{m_t} - (E + i\Gamma_t) \right) \frac{-p^i}{m_t c} F(E, |\mathbf{p}|),$$

$$\Gamma_D^i(E, \mathbf{p}) = \left( \frac{|\mathbf{p}|^2}{m_t} - (E + i\Gamma_t) \right) \frac{-p^i}{m_t c} d_{tg} D(E, |\mathbf{p}|). \quad (4.19)$$

In terms of  $G(E, |\mathbf{p}|)$ , the Lippmann-Schwinger eqs. become NR Schrödinger equations:

$$\left( \frac{|\mathbf{p}|^2}{m_t} - (E + i\Gamma_t) \right) G(E, |\mathbf{p}|) + \int \frac{d^3k}{(2\pi)^3} \left[ \tilde{V}_C(|\mathbf{p} - \mathbf{k}|) G(E, |\mathbf{k}|) \right] = 1,$$

$$\left( \frac{|\mathbf{p}|^2}{m_t} - (E + i\Gamma_t) \right) \mathbf{p}^i F(E, |\mathbf{p}|) + \int \frac{d^3k}{(2\pi)^3} \left[ \tilde{V}_C(|\mathbf{p} - \mathbf{k}|) \mathbf{k}^i F(E, |\mathbf{k}|) \right] = \mathbf{p}^i.$$

$$\left( \frac{|\mathbf{p}|^2}{m_t} - (E + i\Gamma_t) \right) \mathbf{p}^i D(E, |\mathbf{p}|) + \int \frac{d^3k}{(2\pi)^3} \left[ \tilde{V}_C(|\mathbf{p} - \mathbf{k}|) \mathbf{k}^i D(E, |\mathbf{k}|) \right]$$

$$= \int \frac{d^3k}{(2\pi)^3} \left[ \tilde{V}_C(|\mathbf{k} - \mathbf{p}|) (\mathbf{p} - \mathbf{k})^i G(E, |\mathbf{k}|) \right].$$

We find that  $D = G - F$ . As for EW-EDMs, since

$$\frac{1}{2m_t} \sigma^{\lambda\mu} \gamma_5 q_\lambda \simeq \sigma^{0\mu} \gamma_5 \simeq i \gamma_5 \frac{-p^\mu}{m_t c}, \quad (4.20)$$

we can put as

$$\Gamma_{\text{EW-EDM}}^i(E, \mathbf{p}) = i \gamma_5 \frac{-p^i}{m_t c} K(E, |\mathbf{p}|) \left( \frac{|\mathbf{p}|^2}{m_t} - (E + i\Gamma_t) \right). \quad (4.21)$$

By comparing with

$$\gamma^i \gamma_5 \simeq i \sigma^{ij} \gamma_5 \frac{-p^j}{m_t c} ,$$

one can see that  $p^i K(E, |\mathbf{p}|)$  satisfies the same Lippmann-Schwinger eq. as  $p^i F(E, |\mathbf{p}|)$ , thus  $K(E, |\mathbf{p}|) = F(E, |\mathbf{p}|)$ .

Likewise,

$$\Gamma_A^i \simeq i \sigma^{ij} \gamma_5 \Gamma_F^j \simeq \left( \frac{|\mathbf{p}|^2}{m_t} - (E + i\Gamma_t) \right) \gamma^i \gamma_5 F(E, |\mathbf{p}|) .$$

#### 4.6.4 Polarization vector of top and antitop

Including  $\mathcal{O}(\beta_t)$  contribution, the production cross section for  $t\bar{t}$  pair can be written as follows:

$$\frac{d\sigma}{d^3\mathbf{p}_t} = \frac{N_C \alpha^2 \Gamma_t}{2\pi m_t^4} \frac{1 - P_{e^+} P_{e^-}}{2} |G|^2 (a_1 + \chi a_2) \left\{ 1 + 2 \operatorname{Re} \left( C_{\text{FB}} \frac{F}{G} \right) \beta_t \cos \theta_{te} \right\} ,$$

where

$$\beta_t = \frac{|\mathbf{p}_t|}{m_t} , \quad \cos \theta_{te} = \frac{\mathbf{p}_e \cdot \mathbf{p}_t}{|\mathbf{p}_e| |\mathbf{p}_t|} ,$$

and  $\chi$  is a measure of the polarization of initial  $e^+e^-$  defined in Eq. (4.8). The coefficient  $C_{\text{FB}}$  is defined in Eq. (4.23). For unpolarized positron beam ( $\bar{P}_e = 0$ ),  $\chi = -P_e$ , where  $P_e = -1$  for the electron beam that is completely polarized to left-handed helicity. Hard vertex corrections are not included, since we are working with non-renormalizable interactions. In the formula above we summed over spins of  $t$  and  $\bar{t}$ . Before summing over the spins of  $t\bar{t}$ , the production cross section for them can be written as follows:

$$\frac{d\sigma(\mathbf{s}_t, \bar{\mathbf{s}}_t)}{d^3\mathbf{p}_t} = \frac{d\sigma}{d^3\mathbf{p}_t} \frac{1 + \mathbf{P} \cdot \mathbf{s}_t + \bar{\mathbf{P}} \cdot \bar{\mathbf{s}}_t + (\mathbf{s}_t)_i (\bar{\mathbf{s}}_t)_j \mathbf{Q}_{ij}}{4} ,$$

As was explained in Section 4.5.2,  $\mathbf{P}$  and  $\bar{\mathbf{P}}$  can be interpreted as polarization vectors for  $t$  and  $\bar{t}$ , respectively. Both SM and anomalous interactions contribute to the polarizations:

$$\mathbf{P} = \mathbf{P}_{\text{SM}} + \delta\mathbf{P} , \quad \bar{\mathbf{P}} = \bar{\mathbf{P}}_{\text{SM}} + \delta\bar{\mathbf{P}} .$$

With the knowledge of Section 4.3.2, the interference of an anomalous vertex, which is CP-odd, and the standard one, which is CP-even, contributes in the opposite sign to the polarizations of  $t$  and  $\bar{t}$ . On the other hand, the interference among the standard interactions contribute in the same sign:

$$\bar{\mathbf{P}}_{\text{SM}} = \mathbf{P}_{\text{SM}} , \quad \delta\bar{\mathbf{P}} = -\delta\mathbf{P} , \quad (4.22)$$

or

$$\mathbf{P}_{\text{SM}} = (\mathbf{P} + \bar{\mathbf{P}})/2 , \quad \delta\mathbf{P} = (\mathbf{P} - \bar{\mathbf{P}})/2 .$$

Note that we are working to the leading order of the anomalous couplings. Hereafter we express those vector by components:

$$\mathbf{P} = P_{//}\mathbf{n}_{//} + P_{\perp}\mathbf{n}_{\perp} + P_N\mathbf{n}_N, \quad \mathbf{s}_t = s_{//}\mathbf{n}_{//} + s_{\perp}\mathbf{n}_{\perp} + s_N\mathbf{n}_N,$$

where the axes are determined by the beam direction and the production plane:

$$\mathbf{n}_{//} \equiv \frac{\mathbf{p}_e}{|\mathbf{p}_e|}, \quad \mathbf{n}_N \equiv \frac{\mathbf{p}_e \times \mathbf{p}_t}{|\mathbf{p}_e \times \mathbf{p}_t|}, \quad \mathbf{n}_{\perp} \equiv \mathbf{n}_N \times \mathbf{n}_{//}.$$

Now the polarization of  $t$  is as follows<sup>15</sup>:

$$\begin{aligned} (P_{\text{SM}})_{//} &= C_{//}^0 + \text{Re} \left( C_{//}^1 \frac{F}{G} \right) \beta_t \cos \theta_{te}, \\ (P_{\text{SM}})_{\perp} &= \text{Re} \left( C_{\perp} \frac{F}{G} \right) \beta_t \sin \theta_{te}, \\ (P_{\text{SM}})_N &= \text{Im} \left( C_N \frac{F}{G} \right) \beta_t \sin \theta_{te} \end{aligned}$$

for the contributions from the standard interactions<sup>16</sup>, and

$$\begin{aligned} \delta P_{//} &= 0, \\ \delta P_{\perp} &= \left[ \text{Im} \left( B_{\perp}^g d_{tg} \frac{D}{G} \right) + \text{Im} \left( B_{\perp}^{\gamma} d_{t\gamma} \frac{F}{G} \right) + \text{Im} \left( B_{\perp}^Z d_{tZ} \frac{F}{G} \right) \right] \beta_t \sin \theta_{te}, \\ \delta P_N &= \left[ \text{Re} \left( B_N^g d_{tg} \frac{D}{G} \right) + \text{Re} \left( B_N^{\gamma} d_{t\gamma} \frac{F}{G} \right) + \text{Re} \left( B_N^Z d_{tZ} \frac{F}{G} \right) \right] \beta_t \sin \theta_{te} \end{aligned}$$

for the contribution from the anomalous interactions. Coefficients  $C_{//}^0$  etc. are defined below. There is also correlation between  $\mathbf{s}_t$  and  $\bar{\mathbf{s}}_t$ :

$$(\mathbf{s}_t)_i (\bar{\mathbf{s}}_t)_j \mathbf{Q}_{ij} = (\mathbf{s}_t)_i (\bar{\mathbf{s}}_t)_j \mathbf{Q}_{ij\text{SM}} + (\mathbf{s}_t)_i (\bar{\mathbf{s}}_t)_j \delta \mathbf{Q}_{ij},$$

$$\begin{aligned} (\mathbf{s}_t)_i (\bar{\mathbf{s}}_t)_j \mathbf{Q}_{ij\text{SM}} &= s_{//}\bar{s}_{//} + (s_{//}\bar{s}_{\perp} + s_{\perp}\bar{s}_{//}) \text{Re} \left( C_N \frac{F}{G} \right) \beta_t \sin \theta_{te} \\ &\quad + (s_{//}\bar{s}_N + s_N\bar{s}_{//}) \text{Im} \left( C_{\perp} \frac{F}{G} \right) \beta_t \sin \theta_{te}, \end{aligned}$$

$$\begin{aligned} (\mathbf{s}_t)_i (\bar{\mathbf{s}}_t)_j \delta \mathbf{Q}_{ij} &= \\ &+ (s_{//}\bar{s}_{\perp} - s_{\perp}\bar{s}_{//}) \left[ \text{Im} \left( B_N^g d_{tg} \frac{D}{G} \right) + \text{Im} \left( B_N^{\gamma} d_{t\gamma} \frac{F}{G} \right) + \text{Im} \left( B_N^Z d_{tZ} \frac{F}{G} \right) \right] \beta_t \sin \theta_{te} \\ &+ (s_{//}\bar{s}_N - s_N\bar{s}_{//}) \left[ \text{Re} \left( B_{\perp}^g d_{tg} \frac{D}{G} \right) + \text{Re} \left( B_{\perp}^{\gamma} d_{t\gamma} \frac{F}{G} \right) + \text{Re} \left( B_{\perp}^Z d_{tZ} \frac{F}{G} \right) \right] \beta_t \sin \theta_{te}. \end{aligned}$$

<sup>15</sup> We use notation similar to [24]. There are two differences: (i)  $a_3$  and  $a_4$  of them are twice of ours; and (ii)  $C_N$  of them is  $-C_N$  of ours.

<sup>16</sup> These results coincide with those in [24].



We do not use these correlations in this work.

Coefficients of the polarization are defined as follows:

$$\begin{aligned} C_{//}^0(\chi) &= -\frac{a_2 + \chi a_1}{a_1 + \chi a_2}, & C_{//}^1(\chi) &= 2C_{//}^0 C_N + C_{\perp} = 2(1 - \chi^2) \frac{a_2 a_3 - a_1 a_4}{(a_1 + \chi a_2)^2}, \\ C_{\perp}(\chi) &= -\frac{a_4 + \chi a_3}{a_1 + \chi a_2}, & C_N(\chi) &= \frac{a_3 + \chi a_4}{a_1 + \chi a_2} = C_{\text{FB}} \end{aligned} \quad (4.23)$$

for the standard vertices, and

$$\begin{aligned} B_{\perp}^g(\chi) &= -1, & B_N^g(\chi) &= +C_{//}^0(\chi), \\ B_{\perp}^{\text{EW}}(\chi) &= \frac{a_5 + \chi a_6}{a_1 + \chi a_2} = B_{\perp}^{\gamma}(\chi) d_{t\gamma} + B_{\perp}^Z(\chi) d_{tZ}, \\ B_N^{\text{EW}}(\chi) &= \frac{a_6 + \chi a_5}{a_1 + \chi a_2} = B_N^{\gamma}(\chi) d_{t\gamma} + B_N^Z(\chi) d_{tZ}, \end{aligned} \quad (4.24)$$

where

$$\begin{aligned} B_{\perp}^{\gamma}(\chi) &= \frac{1}{a_1 + \chi a_2} \left\{ ([v^e v^t]^* v^{e\gamma} + [a^e v^t]^* a^{e\gamma}) + \chi ([v^e v^t]^* a^{e\gamma} + [a^e v^t]^* v^{e\gamma}) \right\} \\ &= \frac{1}{a_1 + \chi a_2} ([v^e v^t]^* v^{e\gamma} + \chi [a^e v^t]^* v^{e\gamma}), \\ B_{\perp}^Z(\chi) &= \frac{1}{a_1 + \chi a_2} \left\{ ([v^e v^t]^* v^{eZ} + [a^e v^t]^* a^{eZ}) + \chi ([v^e v^t]^* a^{eZ} + [a^e v^t]^* v^{eZ}) \right\} d(s), \\ B_N^{\gamma}(\chi) &= \frac{1}{a_1 + \chi a_2} \left\{ \chi ([v^e v^t]^* v^{e\gamma} + [a^e v^t]^* a^{e\gamma}) + ([v^e v^t]^* a^{e\gamma} + [a^e v^t]^* v^{e\gamma}) \right\} \\ &= \frac{1}{a_1 + \chi a_2} (\chi [v^e v^t]^* v^{e\gamma} + [a^e v^t]^* v^{e\gamma}), \\ B_N^Z(\chi) &= \frac{1}{a_1 + \chi a_2} \left\{ \chi ([v^e v^t]^* v^{eZ} + [a^e v^t]^* a^{eZ}) + ([v^e v^t]^* a^{eZ} + [a^e v^t]^* v^{eZ}) \right\} d(s) \end{aligned} \quad (4.25)$$

for the anomalous vertices. Symbols  $a_{1\sim 6}$  are the combinations of EW couplings:

$$\begin{aligned} a_1 &= |[v^e v^t]|^2 + |[a^e v^t]|^2, & a_2 &= 2 \text{Re}([v^e v^t]^* [a^e v^t]), \\ a_3 &= [v^e v^t]^* [a^e a^t] + [a^e v^t]^* [v^e a^t], & a_4 &= [v^e v^t]^* [v^e a^t] + [a^e v^t]^* [a^e a^t], \end{aligned} \quad (4.26)$$

for the standard vertices and the anomalous  $t\bar{t}g$ -vertex, and

$$\begin{aligned} a_5 &= [v^e v^t]^* [v^e d^t] + [a^e v^t]^* [a^e d^t] \\ &= [v^e v^t]^* v^{e\gamma} d^{t\gamma} + [a^e v^t]^* a^{e\gamma} d^{t\gamma} + [v^e v^t]^* v^{eZ} d(s) d^{tZ} + [a^e v^t]^* a^{eZ} d(s) d^{tZ} \\ &= [v^e v^t]^* v^{e\gamma} d^{t\gamma} + [v^e v^t]^* v^{eZ} d(s) d^{tZ} + [a^e v^t]^* a^{eZ} d(s) d^{tZ}, \\ a_6 &= [v^e v^t]^* [a^e d^t] + [a^e v^t]^* [v^e d^t] \\ &= [v^e v^t]^* a^{e\gamma} d^{t\gamma} + [a^e v^t]^* v^{e\gamma} d^{t\gamma} + [v^e v^t]^* a^{eZ} d(s) d^{tZ} + [a^e v^t]^* v^{eZ} d(s) d^{tZ} \\ &= [a^e v^t]^* v^{e\gamma} d^{t\gamma} + [v^e v^t]^* a^{eZ} d(s) d^{tZ} + [a^e v^t]^* v^{eZ} d(s) d^{tZ} \end{aligned} \quad (4.27)$$

	$ G ^2 (G^*D)$		$G^*F$			
	$a_1$	$a_2$	(SM)*	(SM)	(SM)*	(EW-EDM)
$P_{t\bar{t}}$	$+(-)$	$+(-)$	$-$	$-$	$-$	$-$
$P_{e^-e^+}$	$+$	$-$	$-$	$+$	$+$	$-$

Table 4.4: “Eigenvalues” of the products of couplings  $a_1$  etc., defined in Eqs. (4.26) and (4.27) under Parity transformations P for the final ( $t\bar{t}$ ) and initial ( $e^-e^+$ ) currents. See text for the details.

for the anomalous  $t\bar{t}\gamma$ - and  $t\bar{t}Z$ -vertices. Symbols  $[v^e a^t]$  etc. are defined in Eq. (A.33), and  $d(s)$  is a ratio of  $Z$ -propagator to  $\gamma$ -propagator [Eq. (A.34)]. These combinations  $a_{1\sim 6}$  are chosen so that the dependence on the initial polarization can be seen easily; each pair of  $(a_1, a_2)$ ,  $(a_3, a_4)$ ,  $(a_5, a_6)$  is “conjugate” each other with respect to the exchange  $e^+e^-$  couplings [Section 4.5.1].

Table 4.4 is “eigenvalues” of the products of couplings  $a_1$  etc., defined in Eqs. (4.26) and (4.27) under Parity transformations P for the final ( $t\bar{t}$ ) and initial ( $e^-e^+$ ) currents. It read as follows. For example, the coupling  $a_5 = [v^e v^t]^* [v^e d^t] + [a^e v^t]^* [a^e d^t]$  is a coefficient of the cross term of SM contribution and EW-EDM contribution,  $\mathcal{M}_{\text{SM}}^* \mathcal{M}_{\text{EW-EDM}}$ . Thus in  $|\mathcal{M}|^2$ ,  $a_5$  is accompanied by  $G^*F$ , since

$$\begin{aligned}
\mathcal{M}_{\text{SM}} &\sim G + F = \mathcal{O}(1) + \mathcal{O}(\beta_t) && \dots && \text{CP-even} \\
\mathcal{M}_{\text{C-EDM}} &\sim D = \mathcal{O}(\beta_t) && \dots && \text{CP-odd} \\
\mathcal{M}_{\text{EW-EDM}} &\sim F = \mathcal{O}(\beta_t) && \dots && \text{CP-odd} .
\end{aligned}$$

Note that we are working to  $\mathcal{O}(\beta_t)$ . Under  $P_{t\bar{t}}$ ,  $v^t$ -part of  $\mathcal{M}_{\text{SM}}$  is transformed with the eigenvalue  $+1$ , while  $d^t$ -part of  $\mathcal{M}_{\text{EW-EDM}}$  is  $-1$ ; thus in  $|\mathcal{M}|^2$ , the term with  $a_5$  should be  $-1$  under  $P_{t\bar{t}}$ . A complication occurs for  $a_1$  and  $a_2$ , which contain  $v_t$ , which is a coefficient of both  $\gamma^\mu G$ , which is P-even, and  $i\gamma_5(p^\mu/m)D$ , which is P-odd. The former is  $\mathcal{O}(\beta^0)$ , while the others are  $\mathcal{O}(\beta)$ . Since now we are working to  $\mathcal{O}(\beta)$ , only the interference  $G^*D$  contributes, as far as  $D$  is concerned. Thus  $v^t v^t$  can be  $P_{t\bar{t}} = \pm 1$ , where  $+1$  for  $|G|^2$ , while  $-1$  for  $G^*D$ . Thus denoted in parentheses for  $a_1$  and  $a_2$  are for  $G^*D$ . On the other hand,  $v_t$  in  $a_{3-6}$  should be SM contribution, not chromo-EDM contribution. This is can be seem from the order counting for the velocity  $\beta$ ; all anomalous contributions to  $\mathcal{M}$  are  $\mathcal{O}(\beta)$ , while SM contributions are  $\mathcal{O}(1)$ . This table can be used as follows. For example in  $|\mathcal{M}|^2$ , a term with  $(P_{t\bar{t}}, P_{e^-e^+}) = (+, +)$  should be accompanied by  $a_1|G|^2$ . Likewise, a term with  $(P_{t\bar{t}}, P_{e^-e^+}) = (-, -)$  should be  $a_3G^*F$ , which is SM contribution, or  $a_2G^*D$ , which is the interference between chromo-EDM contribution and SM one.

### Physical considerations

Let us see if our results for  $d\sigma(\mathbf{s}_t, \bar{\mathbf{s}}_t)/d^3\mathbf{p}_t$  is plausible. For this purpose, it is convenient to express it in terms of vectors  $\mathbf{p}$  and  $\mathbf{s}$ , not the components of them; see Section B.5. We already saw in Eq. (4.22) that CP-property of the terms in  $|\mathcal{M}|^2$  relates the  $\mathbf{s}$ -dependence and  $\bar{\mathbf{s}}$ -dependence [See also Eq. (4.5)]. Here we shall see that Parity-property can be used to derive momentum-dependence. As was explained in Section 4.5.1, non-zero polarization  $\chi$  for initial  $e^+e^-$  current mixes the vector and axial vertices, thus it complicates symmetry considerations.

		$(\mathbf{P}_{e^+e^-}, \mathbf{P}_{t\bar{t}})$	(SM)* (SM)	(SM)* (C-EDM)	(SM)* (EW-EDM)
$ \mathbf{p}_e ^2$	$\mathcal{O}(1)$	(+, +)	$a_1 G ^2$		
$\mathbf{p}_e \cdot \mathbf{p}_t$	$\mathcal{O}(\beta_t)$	(-, -)	$\text{Re}[a_3 G^* F]$		
$\mathbf{p}_e$	$\mathcal{O}(1)$	(-, +)	$a_2 G ^2$		
$\mathbf{p}_t, \mathbf{p}_e (\mathbf{p}_e \cdot \mathbf{p}_t)$	$\mathcal{O}(\beta_t)$	(+, -)	$a_4 G^* F$	$a_1 G^* D$	$a_5 G^* F$
$\mathbf{p}_e \times \mathbf{p}_t$	$\mathcal{O}(\beta_t)$	(-, -)	$a_3 G^* F$	$a_2 G^* D$	$a_6 G^* F$
$(\mathbf{p}_e)_i (\mathbf{p}_e)_j$	$\mathcal{O}(1)$	(+, +)	$a_1 G ^2$		
$(\mathbf{p}_e)_i (\mathbf{p}_t)_j$	$\mathcal{O}(\beta_t)$	(-, -)	$a_3 G^* F$	$a_2 G^* D$	$a_6 G^* F$
$(\mathbf{p}_e)_i (\mathbf{p}_e \times \mathbf{p}_t)_j$	$\mathcal{O}(\beta_t)$	(+, -)	$a_4 G^* F$	$a_1 G^* D$	$a_5 G^* F$

Table 4.5: Note that spin ( $\mathbf{s}$ ) is even under P. Thus  $\mathbf{P}_{t\bar{t}}$  etc. is determined solely by momenta  $(\mathbf{p}_e, \mathbf{p}_t)$ . On the other hand,  $\text{CPT}$  depends on  $\mathbf{s}$ .

However as explained in Section 4.5.1, the results for non-zero  $\chi$  can easily be recovered from those for  $\chi = 0$  by replacing couplings appropriately:  $a_1 \rightarrow a_1 + \chi a_2$ , for example. Thus in this section, we consider the case when the spins of  $e^+e^-$  are summed with even weights:  $\chi = 0$ . Before calculating the traces for  $|\mathcal{M}|^2$ , it is easy to see that each momentum<sup>17</sup>  $(\mathbf{p}_t, \mathbf{p}_e)$  can appear only twice or less in  $|\mathcal{M}|^2$ , and each spin-vector  $(\mathbf{s}_t, \bar{\mathbf{s}}_t)$  can appear only once or less. However since we are working to  $\mathcal{O}(\beta_t)$  or less, momenta of  $t$  and  $\bar{t}$  cannot appear twice:  $|\mathbf{p}_t| = \beta_t \gamma_t m_t$ ,

Let us start with the unpolarized part  $d\sigma_{\text{unpol}}$ . As is shown in Eq. (A.53),  $\text{CP}$ -odd part of the (product of the)  $t\bar{t}$  current  $(jj^\dagger)_{t\bar{t}} \equiv j_{t\bar{t}} j_{t\bar{t}}^\dagger$  do not contribute to spin-summed cross section. Since the anomalous interactions are  $\text{CP}$ -odd while the Standard ones are even, the interferences between them are  $\text{CP}$ -odd. This means those interferences  $(\mathcal{M}_{\text{SM}}^* \mathcal{M}_{\text{EDM}})$  do not contribute to  $d\sigma_{\text{unpol}}$ ; the interference among anomalous contributions  $(\mathcal{M}_{\text{EDM}}^* \mathcal{M}_{\text{EDM}})$  is  $\mathcal{O}(\beta_t^2)$ , and thus is beyond our concern here; only  $\mathcal{M}_{\text{SM}}^* \mathcal{M}_{\text{SM}}$  contributes to  $d\sigma_{\text{unpol}}$ . Since  $d\sigma_{\text{unpol}}$  is a scalar,  $(\mathbf{p}_e, \mathbf{p}_t)$ -dependence of it is either  $|\mathbf{p}_e|^2$ ,  $\mathbf{p}_e \cdot \mathbf{p}_t$ , or  $|\mathbf{p}_t|^2$ ; see Table 4.5. Among these,  $|\mathbf{p}_t|^2$  is  $\mathcal{O}(\beta_t^2)$ , and thus is beyond our concern here. ‘‘Eigenvalues’’ under  $\mathbf{P}_{e^+e^-}$  etc. can be easily seen; for example,  $\mathbf{p}_e \cdot \mathbf{p}_t$  has odd number of  $\mathbf{p}_e$  and odd number of  $\mathbf{p}_t$ ; thus it has  $(\mathbf{P}_{e^+e^-}, \mathbf{P}_{t\bar{t}}) = (-, -)$ . Accompanied couplings and Green functions can also be determined from Table 4.4; for example, a term of  $(\mathbf{P}_{e^+e^-}, \mathbf{P}_{t\bar{t}}) = (-, -)$  is accompanied by either  $a_2 G^* D$  or  $a_3 G^* F$ . But the former do not contribute to  $d\sigma_{\text{unpol}}$ , since it is  $\mathcal{M}_{\text{SM}}^* \mathcal{M}_{\text{EDM}}$ . Since  $\mathbf{p}_e \cdot \mathbf{p}_t$  is  $\text{CPT}$ -even, it is accompanied by  $\text{Re}(a_3 G^* F)$ ; note that a  $\text{CPT}$ -even (-odd) term is proportional to ‘‘real’’ (‘‘imaginary’’) part [Section A.7.5]. Among  $d\sigma_{\text{unpol}}$ , only the part with  $\mathbf{P}_{t\bar{t}} = +1$  contributes to the total cross section  $\sigma_{\text{tot}}$  [Eq. (A.51)]; thus  $\sigma_{\text{tot}} \propto a_1 |G|^2$ . On the other hand,  $\mathbf{P}_{t\bar{t}} = -1$  part contributes to the Forward-Backward asymmetry  $A_{\text{FB}} = \langle \text{sgn}(\mathbf{p}_e \cdot \mathbf{p}_t) \rangle / \sigma_{\text{tot}}$  [Section 4.3.2]. Thus the ‘‘coupling’’ of the term  $\mathbf{p}_e \cdot \mathbf{p}_t \propto \beta_t \cos \theta_{te}$  is  $\text{Re}(a_3 G^* F)$ . This completes the analysis of  $d\sigma_{\text{unpol}}$ .

Next we consider the terms proportional to the spin-vectors:  $\mathbf{P}_t \cdot \mathbf{s}_t + \bar{\mathbf{P}}_t \cdot \bar{\mathbf{s}}_t$ . Since the polarization vectors  $\mathbf{P}_t$  and  $\bar{\mathbf{P}}_t$  are 3-vectors, each term of them is proportional to either of  $\mathbf{p}_e$ ,  $\mathbf{p}_t$  or  $\mathbf{p}_e \times \mathbf{p}_t$ . The number of  $\mathbf{p}_t$  should be zero or one, since we are working to  $\mathcal{O}(\beta_t)$ ; note that  $|\mathbf{p}_e|^2 = E^2$ , where  $E$  is beam energy. Thus the momentum dependence of  $\mathbf{P}_t$  and  $\bar{\mathbf{P}}_t$  is either

<sup>17</sup>We are working at the CM-frame of  $e^+e^-$ .

$\mathbf{p}_e$ ,  $\mathbf{p}_t$ ,  $\mathbf{p}_e(\mathbf{p}_e \cdot \mathbf{p}_t)$ , or  $\mathbf{p}_e \times \mathbf{p}_t$ . These<sup>18</sup> are listed in Table 4.5. Also shown is the order of velocity; only the interference among SM contributions are  $\mathcal{O}(1)$ , and the others are  $\mathcal{O}(\beta_t)$ . Note that under  $\text{CPT}$ , “eigenvalues” of  $(\mathbf{p}, \mathbf{s} + \bar{\mathbf{s}}, \mathbf{s} - \bar{\mathbf{s}})$  are  $(-, -, +)$  [Table 4.2]. From this, for example, one can see that the chromo-EDM contribution to the CP-odd term<sup>19</sup>  $(\mathbf{s}_t - \bar{\mathbf{s}}_t) \cdot (\mathbf{p}_e \cdot \mathbf{p}_t)$  in  $d\sigma$  is proportional to  $\text{Re}(a_2 G^* D)$ , since the term is  $\text{CPT}$ -even. This completes the analysis of the term  $\mathbf{P}_t \cdot \mathbf{s}_t + \bar{\mathbf{P}}_t \cdot \bar{\mathbf{s}}_t$  in  $d\sigma_{\text{unpol}}$ , except the relative magnitude of each term, especially of  $\mathbf{p}_t$  and  $\mathbf{p}_e(\mathbf{p}_e \cdot \mathbf{p}_t)$ . Our result for  $\delta\mathbf{P}$  shows that they are proportional to either

$$(\mathbf{s}_t - \bar{\mathbf{s}}_t) \cdot (\mathbf{p}_t - \mathbf{p}_e \frac{\mathbf{p}_e \cdot \mathbf{p}_t}{|\mathbf{p}_e|^2}) \quad \text{or} \quad (\mathbf{s}_t - \bar{\mathbf{s}}_t) \cdot (\mathbf{p}_e \times \mathbf{p}_t),$$

which are both perpendicular to the beam direction  $\mathbf{p}_e$ . It seems that we miss some symmetry. However for the effect of chromo-EDM, it can be understood as follows. For that case,  $t\bar{t}$  is produced in  $(L, S) = (0, 1)$  or  $J^{PC} = 1^{--}$  at first. Note that  $\mathbf{P} = (-1)^{L+1}$  and  $\mathbf{C} = (-1)^{L+S}$  for fermion–anti-fermion pair. Then they are modified by the anomalous  $t\bar{t}g$ -EDM potential [Eq. (4.10)], which has  $(\mathbf{P}, \mathbf{C}) = (-, +)$ ; thus the resulting state is  $J^{PC} = 1^{+-}$  or  $(L, S) = (1, 0)$ . On the other hand,  $\langle \text{spin-1} | (S_i - \bar{S}_i) | \text{spin-0} \rangle$  is zero for  $i = z$ , and non-zero for  $i = x, y$ . Thus there is no contribution to parallel component.

One also see the terms proportional to  $\mathbf{s}_t^i \bar{\mathbf{s}}_t^j$  can be understood in the same manner, except the anomalous contributions:

$$(\mathbf{s}_t \times \bar{\mathbf{s}}_t) \cdot (\mathbf{p}_t - \mathbf{p}_e \frac{\mathbf{p}_e \cdot \mathbf{p}_t}{|\mathbf{p}_e|^2}) \quad \text{or} \quad (\mathbf{s}_t \times \bar{\mathbf{s}}_t) \cdot (\mathbf{p}_e \times \mathbf{p}_t).$$

We can see that neglecting  $\mathcal{O}(\beta_t)$  and higher,

$$\frac{d\sigma(\mathbf{s}_t, \bar{\mathbf{s}}_t)}{d^3\mathbf{p}_t} \propto 1 + C_{//}^0(s_{//} + \bar{s}_{//}) + s_{//}\bar{s}_{//}$$

Thus if  $s_{//} = 1$ , which means the spin of  $t$  is parallel to  $\mathbf{p}_e$ , then  $\bar{s}_{//} \neq -1$ , which means the spin of  $\bar{t}$  cannot be anti-parallel to  $\mathbf{p}_e$ , or should be parallel to  $\mathbf{p}_e$  [Section 4.5.2]. The situation is more clear for the case  $\chi = \pm 1$ , or  $C_{//}^0 = \mp 1$ :

$$\frac{d\sigma(\mathbf{s}_t, \bar{\mathbf{s}}_t)}{d^3\mathbf{p}_t} \propto (1 \mp s_{//})(1 \mp \bar{s}_{//})$$

This factorization shows that when  $\chi = +1$  [ $-1$ ], or when the helicity of initial  $(e^-, e^+)$  is  $(L, R)$  [ $(R, L)$ ], the spins of both  $t$  and  $\bar{t}$  are anti-parallel [parallel] to  $\mathbf{p}_e$ . For other choice of  $\chi$ , the spins of  $t$  and  $\bar{t}$  have no definite direction. Including  $\mathcal{O}(\beta_t)$  corrections, the factorization do not hold even for  $\chi = \pm 1$ .

## 4.7 Results for EDMs

Here comes our numerical results. We shall see that it is possible to disentangle that the effects of each three anomalous interactions  $d_{tg}$ ,  $d_{t\gamma}$ , and  $d_{tZ}$ .

<sup>18</sup> Here  $\mathbf{p}_e(\mathbf{p}_e \cdot \mathbf{p}_t)$  is the vector  $\mathbf{p}_e$  with the coefficient  $\mathbf{p}_e \cdot \mathbf{p}_t$ .

<sup>19</sup> Of course there is no such contribution to the CP-even term such as  $(\mathbf{s}_t + \bar{\mathbf{s}}_t) \cdot (\mathbf{p}_e \cdot \mathbf{p}_t)$ .

If all the couplings  $d_{tg}$  etc. are real and the decay width  $\Gamma_Z$  of  $Z$  is neglected, the effects of anomalous interactions for polarization are

$$\begin{aligned}\delta P_{\perp} &= \left( -B_{\perp}^g d_{tg} + B_{\perp}^{\gamma} d_{t\gamma} + B_{\perp}^Z d_{tZ} \right) \text{Im} \left( \frac{F}{G} \right) \beta_t \sin \theta_{te} , \\ \delta P_{\text{N}} &= \left[ \left( -B_{\text{N}}^g d_{tg} + B_{\text{N}}^{\gamma} d_{t\gamma} + B_{\text{N}}^Z d_{tZ} \right) \text{Re} \left( \frac{F}{G} \right) + B_{\text{N}}^g d_{tg} \right] \beta_t \sin \theta_{te} .\end{aligned}$$

This assumption is realistic, since the imaginary part is generated by physical threshold in loop diagram. From Figures 4.11 and 4.9, we can see that Chromo-EDM  $d_{tg}$  and EW-EDMs  $d_{t\gamma}, d_{tZ}$  can be separated through their energy dependence, since typical  $\beta_t$  become larger for larger energy. The  $\text{Re}[(F - G)/G] \beta_t$  becomes smaller for larger energy, because  $F = G$  for the case  $V = 0$ ; note that the effect of rescattering becomes smaller as one leaves from the threshold. On the other hand, from Figure 4.3, we can see that the two EW-EDMs,  $d_{t\gamma}$  and  $d_{tZ}$ , can be separated through the response with respect to the initial polarization  $\chi$ . This is also pointed out some time ago [96] in the context of open top analysis. Note also that from the definitions,  $B_{\perp} = \pm B_{\text{N}}$  for  $\chi = \pm 1$ .

The relation

$$p_{\text{peak}} \simeq \left| \sqrt{m_t (E + 1 \text{ GeV} + i\Gamma_t)} \right| \quad (4.28)$$

agrees qualitatively with Figure 4.9. Here  $1 \text{ GeV} \simeq 2m_t - M_{1S} = \text{binding energy}$ . Note that with  $V \rightarrow 0$ , the relation  $p_{\text{peak}} = \left| \sqrt{m_t (E + i\Gamma_t)} \right|$  holds<sup>20</sup>.

For stable quark under LO Coulomb rescattering,  $G$  and  $F$  can be obtained analytically [24]:

$$\begin{aligned}\lim_{\substack{\Gamma_t \rightarrow 0 \\ E \rightarrow p^2/m_t}} \left( E - \frac{\mathbf{p}^2}{m_t} + i\Gamma_t \right) G(\mathbf{p}, E) &= \exp\left(\frac{\pi p_{\text{B}}}{2p}\right) \Gamma\left(1 + i\frac{p_{\text{B}}}{p}\right) , \\ \lim_{\substack{\Gamma_t \rightarrow 0 \\ E \rightarrow p^2/m_t}} \left( E - \frac{\mathbf{p}^2}{m_t} + i\Gamma_t \right) F(\mathbf{p}, E) &= \left(1 - i\frac{p_{\text{B}}}{p}\right) \exp\left(\frac{\pi p_{\text{B}}}{2p}\right) \Gamma\left(1 + i\frac{p_{\text{B}}}{p}\right) ,\end{aligned}$$

where  $p_{\text{B}} = C_F \alpha_s m_t / 2 \simeq 20 \text{ GeV}$ . Thus

$$\left. \frac{F}{G} \right|_{p=p_{\text{peak}}} \simeq 1 - i \frac{p_{\text{B}}}{p_{\text{peak}}} \simeq 1 - i \frac{p_{\text{B}}}{\sqrt{m_t (E + 1 \text{ GeV} + i\Gamma_t)}} .$$

This agrees qualitatively well with Figure 4.10. Note that there is no energy dependence of  $\text{Re}[F/G]$  if  $\Gamma_t = 0$ . Thus this may provide a way to measure the decay width of top quark.

### 4.7.1 Sensitivity

The polarization  $\langle \text{P} \rangle$  projected to certain direction can be measured as

$$\langle \text{P} \rangle \simeq \frac{N_{\uparrow} - N_{\downarrow}}{N_{\uparrow} + N_{\downarrow}} .$$

<sup>20</sup> This can be obtained from  $G = 1/(p_t^2/m_t - (E + i\Gamma_t))$  for  $V \rightarrow 0$ , and  $d\sigma/dp_t \propto p_t^2 |G|^2$ .

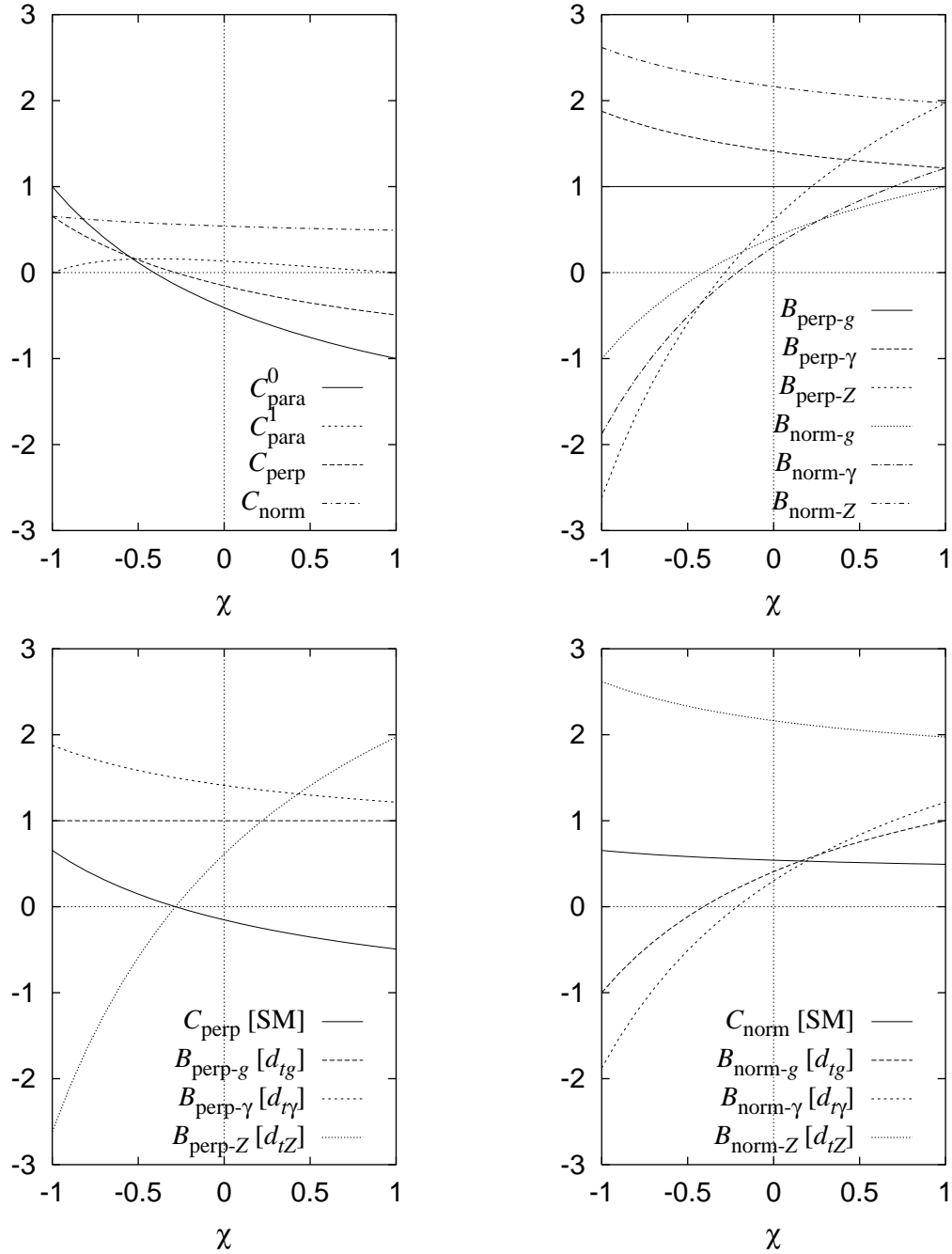


Figure 4.3: Coefficients for polarizations as functions of initial polarization  $\chi$ . In the figures,  $C_{\text{para}} = C_{\parallel}$ ,  $C_{\text{perp}} = C_{\perp}$  and  $C_{\text{norm}} = C_N$ . (Left-top) Coefficients for SM contributions. (Right-top) Coefficients for anomalous EDM couplings. Lines in the lower two figures the same to those in the upper two figures: (Left-bottom) Coefficients for the polarization parallel to  $\mathbf{n}_{\perp}$ . (Right-bottom) Coefficients for the polarization parallel to  $\mathbf{n}_N$ .

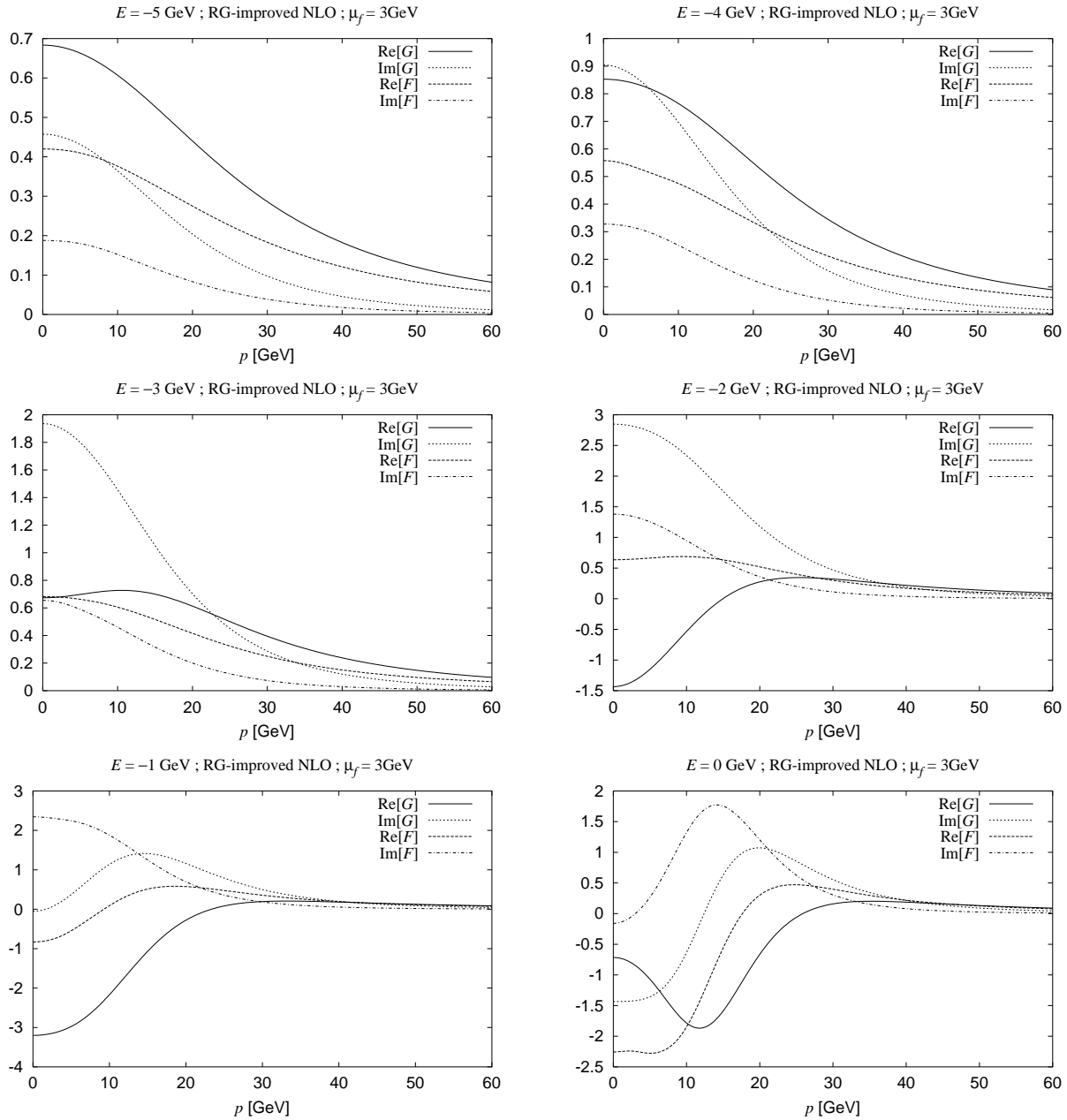


Figure 4.4: Green functions

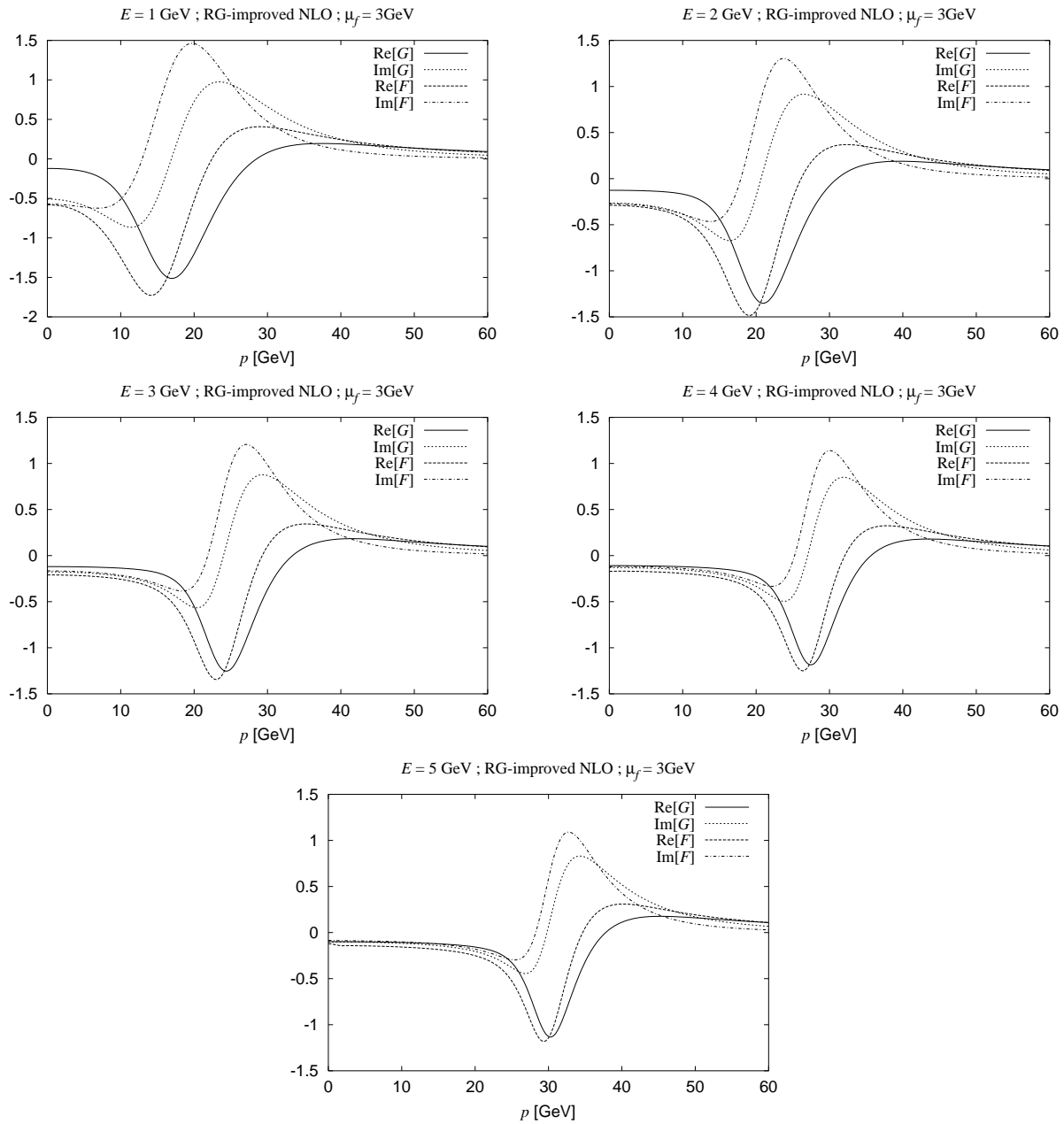


Figure 4.5: Green functions



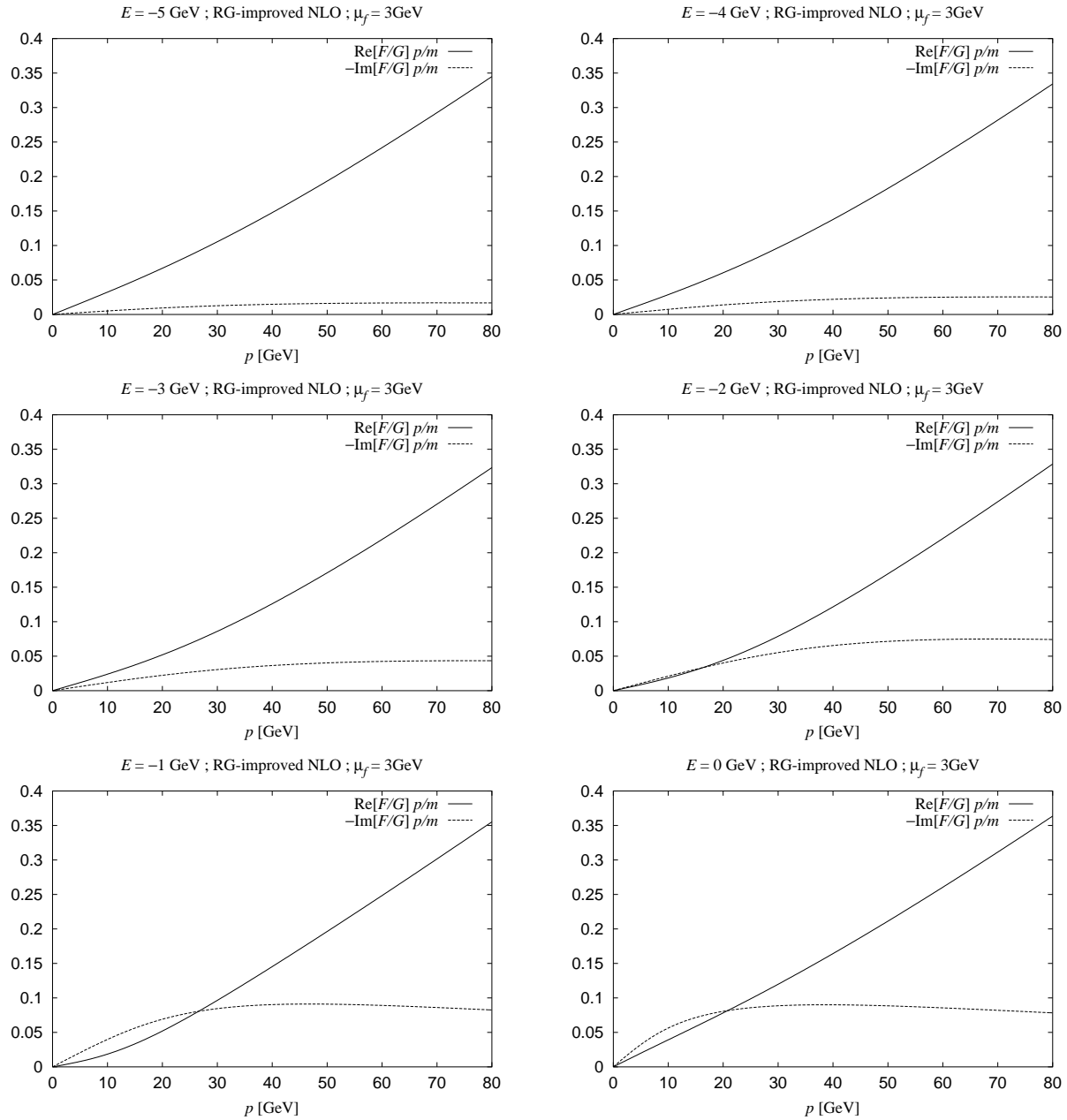


Figure 4.6: Green functions

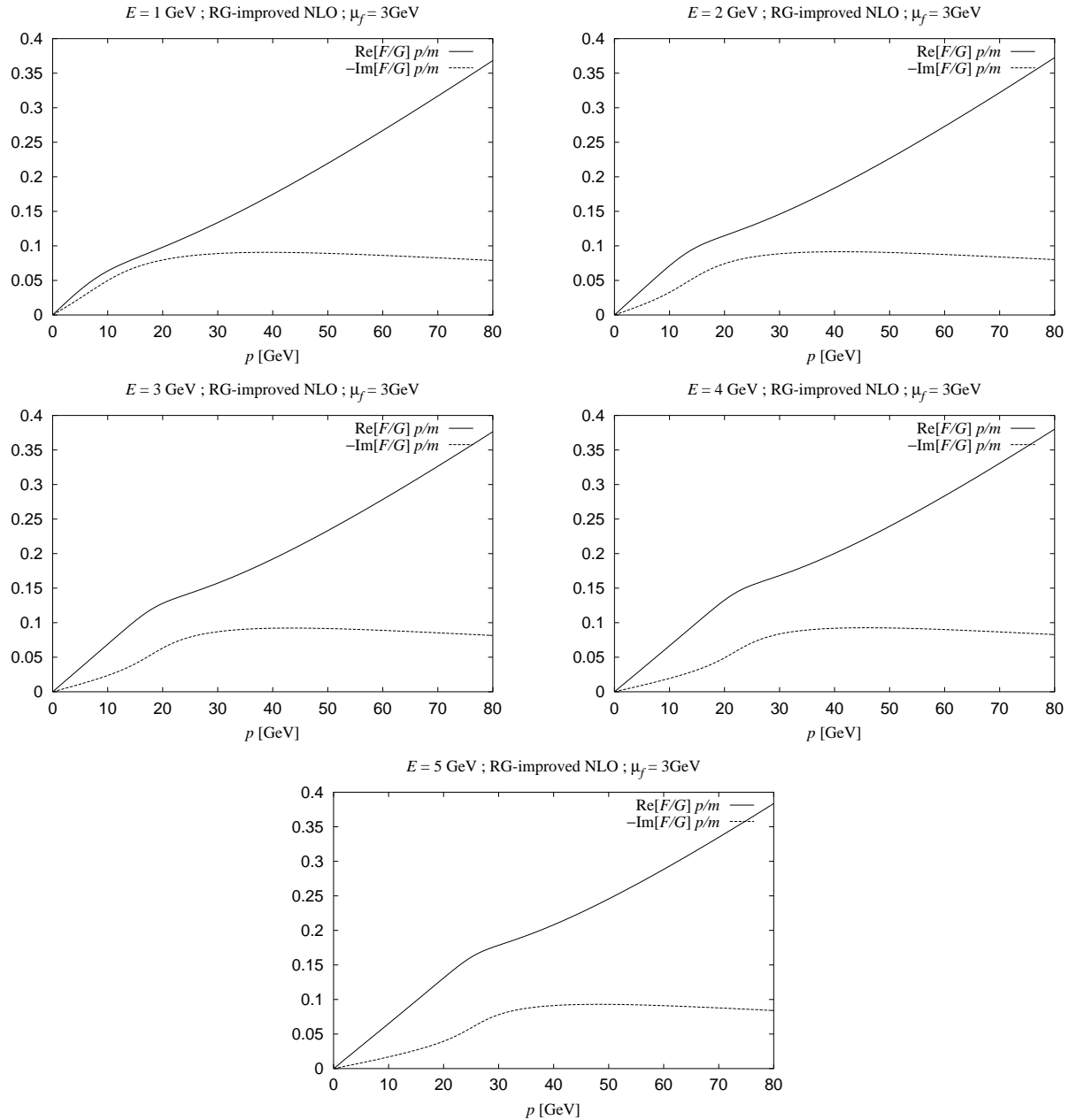


Figure 4.7: Green functions

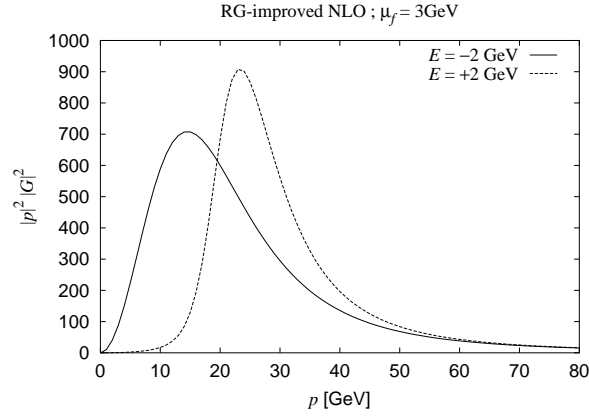


Figure 4.8:  $p^2|G(E, p)|^2 \propto d\sigma/dp$  vs. top quark momentum  $p$  for fixed CM energy.

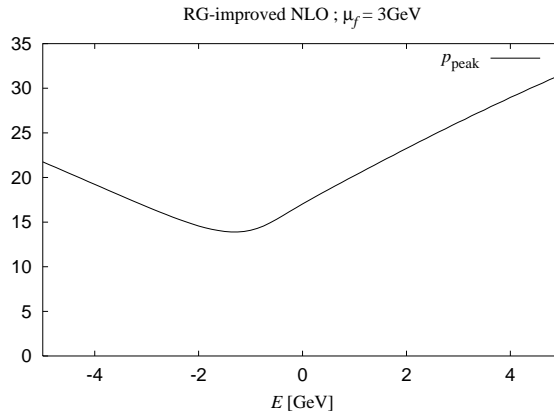


Figure 4.9: Typical momentum of top quark, which is defined by the peak momentum  $p_{\text{peak}}$  of the momentum distribution  $d\sigma/dp \propto |\mathbf{p}|^2|G|^2$ . It is approximately  $p_{\text{peak}} \simeq \left| \sqrt{m_t (E + 1 \text{ GeV} + i\Gamma_t)} \right|$ . Here  $1 \text{ GeV} \simeq 2m_t - M_{1S} = \text{binding energy}$ . Note that if  $\Gamma_t = 0$ , the momentum of  $t$  is uniquely determined.

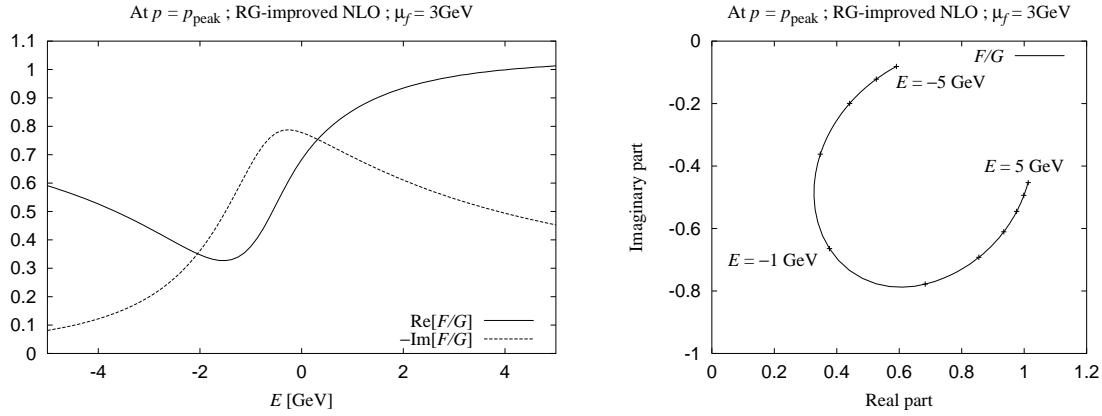


Figure 4.10: The ratio of the Green functions  $F(p)/G(p)$  at the peak momentum  $p_{\text{peak}}$  of the momentum distribution  $d\sigma/dp$ . In operator language,  $G(p) = \langle p|G|r' = 0\rangle$ . In order to avoid the complexity to NNLO ( $= \mathcal{O}(1/c^2)$ ), we use NLO QCD potential with RG improved in momentum space. We also use Potential-Subtracted (PS) mass  $m_{\text{PS}}(\mu_f) = 175 \text{ GeV}$  with  $\mu_f = 3 \text{ GeV}$ . Other inputs are  $\Gamma_t = 1.43 \text{ GeV}$ , and  $\alpha_s(m_Z) = 0.118$ . Two figures are exactly the same: (Left) Real and imaginary parts of the ratio  $F/G$  are plotted with respect to  $E = \sqrt{s} - 2m_{\text{PS}}$ . (Right) The ratio  $F/G$  is plotted in the complex plane.

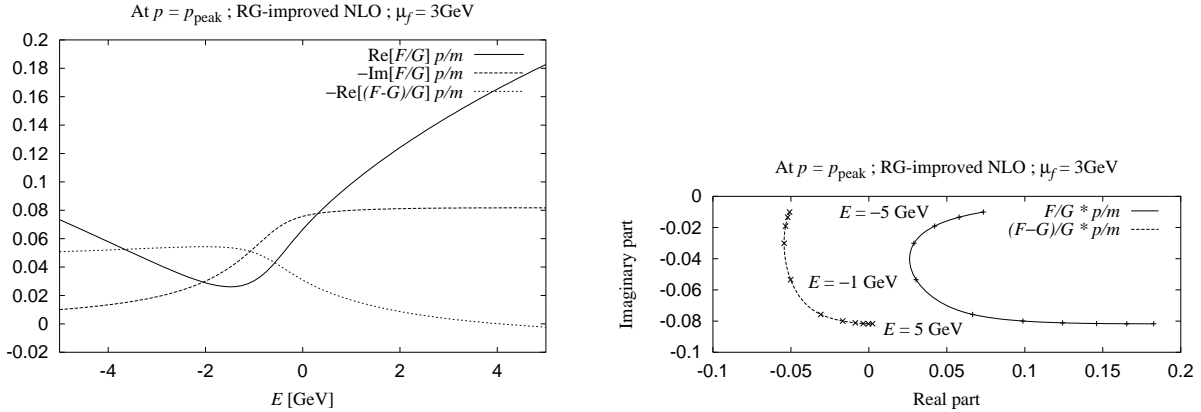


Figure 4.11: The ratios of the Green functions times “velocity” of top quark  $F(p)/G(p) \cdot p/m_t$  and  $(F-G)/G \cdot p/m_t$  at the peak momentum  $p_{\text{peak}}$  of the momentum distribution  $d\sigma/dp$ . Inputs are the same as in Figure 4.10. Two figures are exactly the same: (Left) Real and imaginary parts of the ratios  $F/G \cdot p/m_t$  and  $(F-G)/G \cdot p/m_t$  are plotted with respect to  $E = \sqrt{s} - 2m_{\text{PS}}$ . Note that imaginary part of them coincides each other. (Right) The same ratios are plotted in the complex plane.

Thus the error may be estimated roughly as  $\delta\langle P \rangle \simeq 1/\sqrt{N_{\text{eff}}}$ . Here  $N_{\text{eff}}$  means the number of events used for the analysis:

$$\begin{aligned} N_{\text{eff}} &= \sigma_{t\bar{t}} \times \int \mathcal{L} \times (B_\ell B_h) \times \epsilon \\ &= 0.5 \text{ pb} \times 100 \text{ fb}^{-1} \times \left( \frac{2}{9} \cdot \frac{2}{3} \right) \times 0.6 = 4 \times 10^3 \text{ events}, \end{aligned}$$

which means  $1/\sqrt{N_{\text{eff}}} = 1.5 \times 10^{-2}$ . We used the branching fraction  $B_\ell$  ( $B_h$ ) of  $W^+$  to  $e^+$  or  $\mu^+$  (hadron) is  $2/9$  ( $2/3$ ). We assumed integrated luminosity  $\int \mathcal{L} = 50 \text{ fb}^{-1}$ , and the detection efficiency  $\epsilon = 0.6$ .

For example, with

$$P_N = B_N^g \text{Re} \left( d_{tg} \frac{F-G}{G} \right) \beta_t \sin \theta_{te} ,$$

statistical error for  $d_{tg}$  is

$$\begin{aligned} \delta d_{tg} &\simeq \frac{1}{B_N^g \times \text{Re} \left( d_{tg} \frac{F-G}{G} \right) \beta_t} \times \frac{\int_{-1}^1 d(\cos \theta_{te}) 1}{\int_{-1}^1 d(\cos \theta_{te}) \sin \theta_{te}} \times \frac{1}{\sqrt{N_{\text{eff}}}} \\ &\simeq \frac{1}{1 \times 0.1} \times \frac{4}{\pi} \times 1.5 \times 10^{-2} \\ &\simeq 0.2 \sim \mathcal{O}(10\%) . \end{aligned}$$

From this estimate, we have

$$t\bar{t}g\text{-EDM} = \frac{g_s}{m_t} d_{tg} \lesssim 10^{-17} g_s \text{ cm}$$

for Chromo-EDM. Since all coefficients ( $C_\perp$ ,  $B_N$ , etc.) are similar in magnitude and so are the ratio of Green functions ( $\text{Im}(F/G)$ , etc.), bounds for electroweak EDMs are just the same order:

$$t\bar{t}\gamma\text{-EDM} = \frac{e}{m_t} d_{t\gamma} \lesssim 10^{-17} e \text{ cm} , \quad t\bar{t}Z\text{-EDM} = \frac{g_z}{m_t} d_{tZ} \lesssim 10^{-17} g_z \text{ cm} .$$

A realistic Monte Carlo detector simulation based on the calculation here is also in progress by experimentalists [125]. They show that high detection efficiency is possible with simple event selection criteria and  $b$ -tagging. Up to now, only lepton energy asymmetry  $\langle E_{\ell^+} - E_{\ell^-} \rangle$  for dilepton+dijet event is obtained. Statistical error with  $100 \text{ fb}^{-1}$  is

$$\delta^{(\text{stat})} [\langle E_{\ell^+} - E_{\ell^-} \rangle] = 0.649 \text{ GeV} .$$

Their results for anomalous couplings, based on our calculations, are

$$|\text{Re}[d_{t\gamma}]| < 1.48 , \quad |\text{Re}[d_{tZ}]| < 1.04 , \quad |\text{Re}[d_{tg}]| < 3.93$$

to 95% CL. In fact, lepton energy asymmetry is not a good observable for polarization. This is because the time component of spin 4-vector is suppressed by  $\beta_t \sim 1/10$  compared to the space component. On the other hand event asymmetries are not suppressed in that way, since they can be obtained by integrating 3-momentum asymmetry. Moreover the branching fraction for single-lepton + 4-jets is larger than that for dilepton + dijet. Thus it is expected that the sensitivity for anomalous EDMs is improved by factor 10 or more. This is consistent with the naive estimate we made above.



# Chapter 5

## Summary and Discussions

We study how the  $t\bar{t}$  threshold region serves as a probe of physics at electroweak scale and beyond.

In Chapter 2, we studied the convergence of the perturbative series of the total production cross section  $\sigma_{\text{tot}}$  for  $e^+e^- \rightarrow t\bar{t}$  in the threshold region. Two efforts have been made to improve it. One is to use Potential-Subtracted mass  $m_t^{\text{PS}}(\mu_f)$ , and the other is to resum leading  $\log(q/\mu_s)$ 's of the Coulombic potential  $\tilde{V}_C(q)$  in momentum space using Renormalization Group (RG). The former is to circumvent the (severest) renormalon ambiguity inherent to the pole mass and the coordinate-space potential of an IR-slave interaction. With this prescription, the convergence of the position of  $1S$  resonance becomes better. The latter is to reduce the renormalization scale ( $\mu_s$ ) dependence of  $R$  ratio, where  $\mu_s$  is the scale for the  $t\bar{t}$  potential  $V$ . Among various contributions to the potential  $V = V_C + V_{\text{BF}} + V_{\text{NA}}$ , only the  $\log(q/\mu_s)$ 's in the Coulombic potential  $V_C$  are summed up in this work. RG improvement of the whole  $V$  is a subject of a future study. With these two implementations, we estimate  $(\Delta m_t)^{\text{th}} \sim 0.1 \text{ GeV}$ , where  $(\Delta m_t)^{\text{th}}$  is the theoretical uncertainty for the determination of  $m_t$  using the process  $e^+e^- \rightarrow t\bar{t}$  with  $\sqrt{s} \simeq 2m_t$ . This size is consistent with one of the N<sup>3</sup>LO corrections calculated recently [32]. Lower bound to the CKM element  $|V_{tb}|$  may also be obtained. Note that  $\Gamma_t \propto |V_{tb}|^2$ , and the present bound [2] for  $|V_{tb}|$  is 0.06–0.9993 when the unitarity of CKM matrix within the first three generations is not assumed.

In Chapter 3, we calculated the momentum distributions  $d\sigma/dp$  of top quark near the threshold. Corrections to  $\mathcal{O}(1/c^2)$  are included. However the Final-State Interactions<sup>1</sup> between  $t$  and the decay products of  $\bar{t}$  etc. are not taken into account. The effect of the NNLO correction for  $(1/\sigma_{\text{tot}})d\sigma/dp$  from the rescattering between  $t$  and  $\bar{t}$ , which is calculated here, turns out to be rather small compared to the NNLO correction to  $\sigma_{\text{tot}}$ . In fact the correction is smaller than the effect of the NLO correction from the FSI. Thus the NNLO correction from the FSI may contribute with the similar magnitude to the NNLO correction from  $t\bar{t}$  rescattering.

In Chapter 4, anomalous EDMs of top quark are studied. They can be measured by CP-odd observables. Chromo-EDM modifies  $t\bar{t}$  rescattering, while ElectroWeak-EDMs modify  $t\bar{t}$  production vertex. Thus their effects can be distinguished from the energy dependences, since the latter is enhanced by raising CM energy, while the former is not. On the other hand two EW-EDMs,  $t\bar{t}\gamma$ -EDM and  $t\bar{t}Z$ -EDM, can be distinguished from the dependences on the polarization of the initial  $e^-$  (and  $e^+$ ). We estimate the sensitivity of  $t\bar{t}$  production near the threshold in future  $e^+e^-$  colliders to be  $\sim 10^{-17} g_s \text{ cm}$  ( $e \text{ cm}$ ,  $g_z \text{ cm}$ ) for  $t\bar{t}g$ -EDM ( $t\bar{t}\gamma$ -,  $t\bar{t}Z$ -EDM) with the integrated luminosity  $\simeq 100 \text{ fb}^{-1}$ . It is worth mentioning that a realistic Monte

---

<sup>1</sup>We call this FSI for brevity.

Carlo detector simulation is in progress by experimentalists [125], based on our theoretical calculations. Their first result is already available, and our naive estimate is consistent with it. We note that hadron colliders may be powerful to prove the existence of non-zero EDMs; however precise determination of their values would be difficult. In this respect,  $e^+e^-$  collider is much advantageous.

## Acknowledgment

The author wishes to express his sincere gratitude to Y. Sumino, who is a collaborator of the works, on which the thesis is based. He also would like to thank A. Ota for collaboration, M. Jezabek, K. Fujii, Z. Hioki for useful discussions at the Summer Institute '99 (August 1999, Yamanashi, Japan), M. Yoshimura, K. Hikasa, M. Yamaguchi and M. Tanabashi for several remarks.

Finally the author wishes to express his thanks to the members of High Energy Theory Group at Tohoku University for their kind support while preparing the thesis.



# Appendix A

## A.1 Notes on group theory

### A.1.1 Group theoretic factors

Generators of a Lie group satisfy the following commutation relation:

$$[T^a, T^b] = if^{abc}T^c .$$

Trace normalization  $T_R$  and quadratic Casimir  $C_R$  for a representation  $R$  is defined by

$$\text{tr} [T_R^a T_R^b] = T_R \delta^{ab} , \quad T_R^a T_R^a = C_R \mathbf{1} .$$

For  $SU(N = 3)$

$$T_F = \frac{1}{2} , \quad T_A = C_A = N = 3 , \quad C_F = \frac{N^2 - 1}{2N} = \frac{4}{3} , \quad (\text{A.1})$$

where  $F$  and  $A$  mean fundamental and adjoint representations, respectively.

Coefficients  $\beta_0$  etc. of renormalization group equations are given in Section 2.3.4. When necessary, we use

$$n_f = 5 , \quad n_H = 1 , \quad (\text{A.2})$$

where the former is the number of light quarks and the latter is the number of Higgs bosons.

### A.1.2 Color charge summation for color-singlet state

For a particle-antiparticle pair  $\psi\psi^c$  in color-singlet state, the product of color charge is  $-C_F$ :

$$\langle T^a \bar{T}^a \rangle = -C_F = -\frac{N_C^2 - 1}{2N_C} . \quad (\text{A.3})$$

This corresponds to  $Q_\psi \cdot (-Q_\psi) = -Q_\psi^2$  for Abelian gauge group. Sum over the index  $a$  is implicit. In this section, we show this relation. The relevant Lagrangian is

$$\mathcal{L} = -g_s \bar{\psi} \gamma^\mu T^a \psi G_\mu^a = -g_s \bar{\psi}^c \gamma^\mu \bar{T}^a \psi^c G_\mu^a ,$$

where  $\bar{T}^a = -T^{a\top}$ , and  $\psi^c = C\bar{\psi}^\top$  with  $C\gamma^\mu C^\dagger = -\gamma^\mu$ . Then

$$\begin{aligned}\langle T^a \bar{T}^a \rangle &= \frac{1}{N_C} \sum_{i,j} [\xi^{j\dagger} T^a \xi^i] [\xi^j (-T^{a\top}) \xi^{i\dagger}] \\ &= \frac{-1}{N_C} \sum_{i,j} \text{tr} [\xi^j \xi^{j\dagger} T^a \xi^i \xi^{i\dagger} T^a] \\ &= \frac{-1}{N_C} C_F \text{tr} [\mathbf{1}] = -C_F ,\end{aligned}$$

where

$$\xi^R = \begin{pmatrix} 1 \\ 0 \\ 0 \end{pmatrix}, \quad \xi^G = \begin{pmatrix} 0 \\ 1 \\ 0 \end{pmatrix}, \quad \xi^B = \begin{pmatrix} 0 \\ 0 \\ 1 \end{pmatrix},$$

for example. The indices  $i$  and  $j$  mean the color of initial and final  $\psi$ , respectively.

Although the calculation above is specific to fundamental representation  $F$ , generalization to arbitrary representation  $R$  is obvious;  $\langle T^a \bar{T}^a \rangle = -C_R$ , where  $C_R$  is quadratic Casimir for the representation  $R$ .

## A.2 Notes on non-relativistic quantum mechanics

### A.2.1 Relative coordinate

As is well known, a non-relativistic two-body system can be decomposed into relative and center-of-momentum motions:

$$H = \frac{\mathbf{p}_1^2}{2m_1} + \frac{\mathbf{p}_2^2}{2m_2} = \frac{\mathbf{p}^2}{2\mu} + \frac{\mathbf{P}^2}{2M},$$

where

$$\begin{aligned}\mathbf{R} &\equiv \frac{m_1}{m_1 + m_2} \mathbf{r}_1 + \frac{m_2}{m_1 + m_2} \mathbf{r}_2, & \mathbf{P} &\equiv \mathbf{p}_1 + \mathbf{p}_2, \\ \mathbf{r} &\equiv \mathbf{r}_1 - \mathbf{r}_2, & \mathbf{p} &\equiv \frac{m_2}{m_1 + m_2} \mathbf{p}_1 - \frac{m_1}{m_1 + m_2} \mathbf{p}_2,\end{aligned}$$

and

$$\frac{1}{\mu} \equiv \frac{1}{m_1} + \frac{1}{m_2}, \quad M \equiv m_1 + m_2 \quad (m_1 m_2 = \mu M).$$

One can easily check that those coordinates and momenta satisfy the standard commutation relations  $[R_i, P_j] = i\delta_{ij}$  etc. Thus they are conjugate also in quantum mechanical sense.

### A.2.2 Radial momentum $p_r$

The operator  $p_r$  for radial momentum is defined by the Weyl-ordered product of  $\mathbf{r}/r$  and  $\mathbf{p}$ :

$$p_r \equiv \frac{1}{2} \left( \frac{1}{r} \mathbf{r} \cdot \mathbf{p} + \mathbf{p} \cdot \mathbf{r} \frac{1}{r} \right).$$

Using

$$r \frac{\partial}{\partial r} = r^i \frac{\partial}{\partial r^i}, \quad \frac{\partial}{\partial r^i} \left( \frac{r^i}{r} \right) = \frac{n-1}{r} \quad \text{with } n=3,$$

one obtains

$$ip_r = \frac{\partial}{\partial r} + r = \frac{1}{r} \frac{\partial}{\partial r} r, \quad (ip_r)^2 = \frac{\partial^2}{\partial r^2} + \frac{2}{r} \frac{\partial}{\partial r} = \frac{1}{r} \frac{\partial^2}{\partial r^2} r = \frac{1}{r^2} \frac{\partial}{\partial r} \left( r^2 \frac{\partial}{\partial r} \right).$$

With these relations, one can show that this satisfy  $[r, p_r] = i$ , and  $\langle \psi_1 | p_r \psi_2 \rangle = \langle p_r \psi_1 | \psi_2 \rangle$  for the states of  $\lim_{r \rightarrow 0} r \psi(r) = 0$ . Note that  $\langle \psi_1 | \psi_2 \rangle = \int d\Omega \int r^2 dr \psi_1^*(\mathbf{r}) \psi_2(\mathbf{r})$ . On the other hand, the angular part of  $\mathbf{p}^2$  is given by orbital angular momentum  $\mathbf{L} = \mathbf{r} \times \mathbf{p}$ :

$$\mathbf{p}^2 = p_r^2 + \frac{\mathbf{L}^2}{r^2},$$

where

$$\mathbf{L}^2 = \mathbf{r}^2 \mathbf{p}^2 - \mathbf{r} \cdot (\mathbf{r} \cdot \mathbf{p}) \mathbf{p} + 2i \mathbf{r} \cdot \mathbf{p} = \mathbf{r}^2 \mathbf{p}^2 + \frac{\partial}{\partial r} \left( r^2 \frac{\partial}{\partial r} \right).$$

Since  $[r, L^i] = 0$ ,  $\mathbf{L}^2$  and  $r$  also commutes. The following relations may sometimes be useful:

$$(\mathbf{r} \cdot \mathbf{p})^2 \equiv r^i p^i r^j p^j, \quad \mathbf{r} \cdot (\mathbf{r} \cdot \mathbf{p}) \mathbf{p} \equiv r^i r^j p^j p^i = (\mathbf{r} \cdot \mathbf{p})^2 + i \mathbf{r} \cdot \mathbf{p} = -r^2 \frac{\partial^2}{\partial r^2}.$$

One must be careful for the singularity at the origin  $r = 0$ . For example, with  $-\Delta = \mathbf{p}^2 = p_r^2$  for angle-independent function, naive calculation gives  $\Delta(1/r) = 0$ , while actually

$$\Delta \frac{1}{r} = -4\pi \delta^{(3)}(\mathbf{r}).$$

The contributions of  $\delta$ -functions are easy to miss. They arise from differentiation of functions singular at the origin. It is safer to integrate by parts so that to avoid these subtle points. For example, with functions of well-behaving,

$$\begin{aligned} \langle f | p_r^2 \frac{1}{r} | g \rangle &= \langle p_r^2 f | \frac{1}{r} | g \rangle \\ &= - \int d\Omega \int_0^\infty r^2 dr \left\{ \frac{1}{r} \frac{\partial^2}{\partial r^2} (r f) \right\} \frac{1}{r} g \\ &= 4\pi f(0)g(0) - \int d\Omega \int_0^\infty r^2 dr f \frac{1}{r} \frac{\partial^2}{\partial r^2} g, \end{aligned}$$

or

$$p_r^2 \frac{1}{r} = 4\pi \delta^{(3)}(\mathbf{r}) - \frac{1}{r} \frac{\partial^2}{\partial r^2}.$$

We use following relations in the text:

$$\begin{aligned} [p_r^2, ip_r] &= 4\pi \delta^{(3)}(\mathbf{r}), & [\mathbf{p}^2, ip_r] &= 4\pi \delta^{(3)}(\mathbf{r}) + \frac{2\mathbf{L}^2}{r^3}, \\ [p_r^2, \frac{1}{r}] &= 4\pi \delta^{(3)}(\mathbf{r}) + \frac{2}{r^2} \frac{\partial}{\partial r}, & [\mathbf{p}^2, \frac{1}{r}] &= 4\pi \delta^{(3)}(\mathbf{r}) + \frac{2}{r^2} \frac{\partial}{\partial r}, \\ \{p_r^2, \frac{1}{r}\} &= 4\pi \delta^{(3)}(\mathbf{r}) + \frac{2}{r^2} \frac{\partial}{\partial r} + \frac{2}{r} p_r^2, & \{\mathbf{p}^2, \frac{1}{r}\} &= 4\pi \delta^{(3)}(\mathbf{r}) + \frac{2}{r^2} \frac{\partial}{\partial r} + \frac{2}{r} \mathbf{p}^2, \\ [ip_r, \frac{1}{r}] &= \frac{-1}{r^2}. \end{aligned}$$

The first relation is highly anomalous;  $p_r$  and  $p_r^2$  do not commute.

### A.2.3 Operators in momentum and coordinate space

A momentum independent potential  $V$  is diagonal in coordinate space:

$$\langle \mathbf{x} | V(\hat{\mathbf{x}}) | \mathbf{y} \rangle = V(\mathbf{x}) \delta^{(3)}(\mathbf{x} - \mathbf{y}) ,$$

where hat  $\hat{\phantom{x}}$  means operator. Such an operator in momentum space depends only on momentum transfer:

$$\begin{aligned} \langle \mathbf{p} | V(\hat{\mathbf{x}}) | \mathbf{q} \rangle &= \int d^3x \langle \mathbf{p} | \mathbf{x} \rangle V(\mathbf{x}) \langle \mathbf{x} | \mathbf{q} \rangle \\ &= \int d^3x e^{-i(\vec{p}-\vec{q})\cdot\vec{x}} V(\mathbf{x}) \\ &= \tilde{V}(\mathbf{p} - \mathbf{q}) . \end{aligned}$$

Using

$$\langle \mathbf{x} | \hat{\mathbf{p}} | \rangle = -i \nabla_x \langle \mathbf{x} | \rangle , \quad \langle | \hat{\mathbf{p}} | \mathbf{x} \rangle = +i \nabla_x \langle | \mathbf{x} \rangle , \quad \frac{d}{dy} f(x-y) = -\frac{d}{dx} f(x-y) ,$$

we have

$$\begin{aligned} \langle \mathbf{p} | [\hat{\mathbf{p}}, V(\hat{\mathbf{x}})] | \mathbf{q} \rangle &= (\mathbf{p} - \mathbf{q}) \cdot \tilde{V}(\mathbf{p} - \mathbf{q}) , \\ \langle \mathbf{x} | [\hat{\mathbf{p}}, V(\hat{\mathbf{x}})] | \mathbf{y} \rangle &= (-i \nabla_x V(\mathbf{x})) \delta^{(3)}(\mathbf{x} - \mathbf{y}) . \end{aligned}$$

More generally,

$$\begin{aligned} \langle \mathbf{p} | VG | \rangle &= \int \frac{d^3q}{(2\pi)^3} \tilde{V}(\mathbf{p} - \mathbf{q}) \tilde{G}(\mathbf{q}) , & \langle \mathbf{x} | VG | \rangle &= V(\mathbf{x}) G(\mathbf{x}) , \\ \langle \mathbf{p} | \hat{\mathbf{p}}VG | \rangle &= \int \frac{d^3q}{(2\pi)^3} \mathbf{p} \tilde{V}(\mathbf{p} - \mathbf{q}) \tilde{G}(\mathbf{q}) , & \langle \mathbf{x} | \hat{\mathbf{p}}VG | \rangle &= -i \nabla_x (V(\mathbf{x}) G(\mathbf{x})) , \\ \langle \mathbf{p} | V\hat{\mathbf{p}}G | \rangle &= \int \frac{d^3q}{(2\pi)^3} \tilde{V}(\mathbf{p} - \mathbf{q}) \mathbf{q} \tilde{G}(\mathbf{q}) , & \langle \mathbf{x} | V\hat{\mathbf{p}}G | \rangle &= V(\mathbf{x}) (-i \nabla_x G(\mathbf{x})) , \\ \langle \mathbf{p} | [\hat{\mathbf{p}}, V]G | \rangle &= \int \frac{d^3q}{(2\pi)^3} (\mathbf{p} - \mathbf{q}) \cdot \tilde{V}(\mathbf{p} - \mathbf{q}) \tilde{G}(\mathbf{q}) , & \langle \mathbf{x} | [\hat{\mathbf{p}}, V]G | \rangle &= (-i \nabla_x V(\mathbf{x})) G(\mathbf{x}) , \end{aligned}$$

where

$$\tilde{G}(\mathbf{p}) \equiv \langle \mathbf{p} | G | \rangle , \quad G(\mathbf{x}) \equiv \langle \mathbf{x} | G | \rangle ,$$

Our convention for Fourier transform is

$$\begin{aligned} f(\mathbf{x}) = \langle \mathbf{x} | f \rangle &= \int \frac{d^3p}{(2\pi)^3} \langle \mathbf{x} | \mathbf{p} \rangle \langle \mathbf{p} | f \rangle = \int \frac{d^3p}{(2\pi)^3} e^{i\vec{x}\cdot\vec{p}} \tilde{f}(\mathbf{p}) , \\ \tilde{f}(\mathbf{p}) = \langle \mathbf{p} | f \rangle &= \int d^3x \langle \mathbf{p} | \mathbf{x} \rangle \langle \mathbf{x} | f \rangle = \int d^3x e^{-i\vec{x}\cdot\vec{p}} f(\mathbf{x}) . \end{aligned}$$

For  $\delta$ -functions,

$$\begin{aligned} \delta^{(3)}(\mathbf{x} - \mathbf{y}) = \langle \mathbf{x} | \mathbf{y} \rangle &= \int \frac{d^3p}{(2\pi)^3} e^{i(\vec{x}-\vec{y})\cdot\vec{p}} , \\ (2\pi)^3 \delta^{(3)}(\mathbf{p} - \mathbf{q}) = \langle \mathbf{p} | \mathbf{q} \rangle &= \int d^3x e^{-i\vec{x}\cdot(\vec{p}-\vec{q})} . \end{aligned}$$

### A.2.4 $S$ -wave projection

If a quantity  $f$  depends on a 3-vector, say,  $\mathbf{r}$ , it can be decomposed into “radial part” and “spherical part”. For example, a plain wave of momentum  $\mathbf{p}$  can be written as

Sometimes we use the shorthand notation for  $S$ -wave projection:

$$G \equiv \frac{1}{H - \omega}, \quad \omega \equiv E + i\Gamma_t, \quad (\text{A.4})$$

$$G(\mathbf{r}, \mathbf{r}') \equiv \langle \mathbf{r} | G | \mathbf{r}' \rangle, \quad G(r, r') \equiv \int \frac{d\Omega_r}{4\pi} \frac{d\Omega_{r'}}{4\pi} G(\mathbf{r}, \mathbf{r}').$$

$$\langle r | \equiv \int \frac{d\Omega_r}{4\pi} \langle \mathbf{r} |, \quad \langle p | \equiv \int \frac{d\Omega_p}{4\pi} \langle \mathbf{p} |, \quad \text{etc.}$$

$$L = 0, \quad \mathbf{S}^2 = 2, \quad \overline{r^i r^j} = \delta^{ij} r^2 / 3.$$

In general, partial wave expansion can be defined as follows:

$$f(k, \theta) = \sum_{\ell=0}^{\infty} (2\ell + 1) f_{\ell}(k) P_{\ell}(\cos \theta), \quad f_{\ell}(k) = \int \frac{d\Omega}{4\pi} P_{\ell}(\cos \theta) f(k, \theta).$$

The second relation holds because

$$\int \frac{d\Omega}{4\pi} P_{\ell}(\cos \theta) P_{\ell'}(\cos \theta) = \frac{\delta_{\ell\ell'}}{2\ell + 1}.$$

Here  $P_{\ell}(\cos \theta)$  is Legendre polynomials:

$$P_0(\cos \theta) = 1, \quad P_1(\cos \theta) = \cos \theta, \quad P_2(\cos \theta) = \frac{3}{2} \cos^2 \theta - \frac{1}{2}.$$

Also the following relation holds:

$$\int \frac{d\Omega}{4\pi} |f(k, \theta)|^2 = \sum_{\ell=0}^{\infty} (2\ell + 1) |f_{\ell}(k)|^2.$$

An example may be in order. A plane wave is expanded as follows:

$$e^{i\mathbf{k}\mathbf{r} \cos \theta} = \sum_{\ell=0}^{\infty} (2\ell + 1) i^{\ell} j_{\ell}(kr) P_{\ell}(\cos \theta),$$

where  $j_{\ell}(kr)$  is a spherical Bessel, which is a solution  $R_{\ell}(r) = j_{\ell}(kr)$  of the radial Schrödinger equation:

$$\left[ \frac{d^2}{dr^2} + \frac{2}{r} \frac{d}{dr} - \frac{\ell(\ell + 1)}{r^2} \right] R_{\ell}(r) + k^2 R_{\ell}(r) = 0,$$

where  $k^2/(2m) = E$ . Explicitly,

$$j_0(\rho) = \frac{\sin \rho}{\rho}, \quad j_1(\rho) = \frac{\sin \rho}{\rho^2} - \frac{\cos \rho}{\rho}, \quad j_2(\rho) = \left( \frac{3}{\rho^3} - \frac{1}{\rho} \right) \sin \rho - \frac{3}{\rho^2} \cos \rho.$$

Fourier transform goes as follows:

$$\begin{aligned} f(\mathbf{x}', \mathbf{x}) &= \sum_{\ell=0}^{\infty} (2\ell + 1) f_{\ell}(x', x) P_{\ell}(\cos \theta_{x'x}) , \\ f(\mathbf{p}', \mathbf{x}) &\equiv \int d^3 x' e^{-i\mathbf{p}' \cdot \mathbf{x}'} f(\mathbf{x}', \mathbf{x}) \\ &= \sum_{\ell=0}^{\infty} (2\ell + 1) f_{\ell}(p', x) P_{\ell}(\cos \theta_{p'x}) , \end{aligned}$$

where  $\theta_{x'x}$  is the angle between  $\mathbf{x}'$  and  $\mathbf{x}$ , and

$$\begin{aligned} f_{\ell}(p', x) &\equiv \int_0^{\infty} 4\pi x'^2 dx' (-i)^{\ell} j_{\ell}(p'x') f_{\ell}(x', x) , \\ f_{\ell}(x', x) &= \int_0^{\infty} \frac{4\pi p'^2 dp'}{(2\pi)^3} i^{\ell} j_{\ell}(p'x') f_{\ell}(p', x) . \end{aligned}$$

Here we used

$$\begin{aligned} \int \frac{d\Omega_{x'}}{4\pi} P_{\ell'}(\cos \theta_{p'x'}) P_{\ell}(\cos \theta_{x'x}) &= \frac{\delta_{\ell\ell'}}{2\ell + 1} P_{\ell}(\cos \theta_{p'x}) , \\ \int_0^{\infty} \frac{4\pi p^2 dp}{(2\pi)^3} j_{\ell}(px) j_{\ell}(px') &= \frac{1}{4\pi x^2} \delta^{(1)}(x - x') , \quad \text{for each } \ell . \end{aligned}$$

The following are completeness relations for the angular part:

$$\begin{aligned} \frac{1}{2} \int_{-1}^1 d(\cos \theta) P_{\ell}(\cos \theta) P_{\ell'}(\cos \theta) &= \frac{\delta_{\ell\ell'}}{2\ell + 1} , \\ \frac{1}{2} \sum_{\ell=0}^{\infty} (2\ell + 1) P_{\ell}(\cos \theta) P_{\ell}(\cos \theta') &= \delta^{(1)}(\cos \theta - \cos \theta') , \\ \frac{1}{2\pi} \int_0^{2\pi} d\phi e^{i(m-m')\phi} &= \delta_{mm'} , \\ \frac{1}{2\pi} \sum_{m=-\infty}^{\infty} e^{im(\phi-\phi')} &= \delta^{(1)}(\phi - \phi') . \end{aligned}$$

Since

$$\int d^3 x' \delta^{(3)}(\mathbf{x} - \mathbf{x}') f(x', \cos \theta', \phi') = f(x, \cos \theta, \phi) ,$$

$\delta$ -function in the polar coordinate can be written

$$\begin{aligned} \delta^{(3)}(\mathbf{x} - \mathbf{x}') &= \frac{1}{x^2} \delta^{(1)}(x - x') \delta^{(1)}(\cos \theta_{xz} - \cos \theta_{x'z}) \delta^{(1)}(\phi_x - \phi_{x'}) , \quad \text{for } f = f(x, \cos \theta, \phi) , \\ &= \frac{1}{2\pi x^2} \delta^{(1)}(x - x') \delta^{(1)}(\cos \theta_{xz} - \cos \theta_{x'z}) , \quad \text{for } f = f(x, \cos \theta) , \\ &= \frac{1}{4\pi x^2} \delta^{(1)}(x - x') , \quad \text{for } f = f(x) . \end{aligned}$$

Here  $\theta_{xz}$  is the angle between  $\mathbf{x}$  and certain axis, and likewise for  $\phi_x$ .

## A.3 Formulas for Dirac spinors

References [126] are useful.

### A.3.1 Mode expansions

The anticommutation rules for the creation-annihilation operators  $a_{\mathbf{p}}^s$  and  $b_{\mathbf{p}}^s$ , are

$$\{a_{\mathbf{p}}^r, a_{\mathbf{q}}^{s\dagger}\} = \{b_{\mathbf{p}}^r, b_{\mathbf{q}}^{s\dagger}\} = (2\pi)^3 2E_{\mathbf{p}} \delta^{(3)}(\mathbf{p} - \mathbf{q}) \delta^{rs}, \quad (\text{A.5})$$

and all the others are zero. Here  $a_{\mathbf{p}}^{s\dagger}$  ( $b_{\mathbf{p}}^{s\dagger}$ ) is the creation operator for fermion (anti-fermion) with the momentum  $\mathbf{p}$  and the spin  $s$ . A quantized Dirac field  $\psi(x)$  can be expanded in terms of them:

$$\begin{aligned} \psi(x) &= \int \frac{d^3p}{(2\pi)^3 2E_{\mathbf{p}}} \sum_s (a_{\mathbf{p}}^s u(p, s) e^{-ip \cdot x} + b_{\mathbf{p}}^{s\dagger} v(p, s) e^{+ip \cdot x}), \\ \bar{\psi}(x) &= \int \frac{d^3p}{(2\pi)^3 2E_{\mathbf{p}}} \sum_s (a_{\mathbf{p}}^{s\dagger} \bar{u}(p, s) e^{+ip \cdot x} + b_{\mathbf{p}}^s \bar{v}(p, s) e^{-ip \cdot x}). \end{aligned} \quad (\text{A.6})$$

Since the anticommutator relations above are invariant under the phase rotation  $a \rightarrow e^{i\delta} a$  (and the similar for  $b$ ), the relative phase between  $u$  and  $v$  is not fixed, a priori. Our convention is explained in Section A.3.3.

A one-particle state is  $|\mathbf{p}, s\rangle = a_{\mathbf{p}}^{s\dagger} |0\rangle$ . Note that  $\langle \mathbf{p}, r | \mathbf{q}, s \rangle = (2\pi)^3 2E_{\mathbf{p}} \delta^{(3)}(\mathbf{p} - \mathbf{q}) \delta^{rs}$  is Lorentz invariant.

Note that all flavor-dependence is carried by the creation-annihilation operators  $a_{\mathbf{p}}^s$  and  $b_{\mathbf{p}}^s$ ; c-number spinors  $u(p, s)$  and  $v(p, s)$  is flavor-independent.

### A.3.2 Several conjugations: $\Gamma^\dagger$ , $\bar{\Gamma}$ , $\Gamma^c$ and $\Gamma^b$

There are several conjugations<sup>1</sup> for  $\gamma$ -matrices  $\Gamma$ ; that is, hermitian conjugation  $\Gamma^\dagger$ , Dirac conjugation  $\bar{\Gamma}$ , Charge conjugation  $\Gamma^c$ , and the conjugation related to Time Reversal  $\Gamma^b$ :

$$\bar{\Gamma} \equiv \gamma^0 \Gamma^\dagger \gamma^0, \quad \Gamma^c \equiv C \Gamma^\top C^\dagger, \quad \Gamma^b \equiv B^\dagger \Gamma^\top B, \quad (\text{A.7})$$

where the Charge conjugation matrix  $C$  and the Time Reversal matrix  $B$  are defined by the following properties:

$$C^\dagger = C^{-1}, \quad C^\top = -C, \quad B^\dagger = B^{-1}, \quad B^\top = -B, \quad (\text{A.8})$$

$$C \gamma^{\mu\top} C^\dagger = -\gamma^\mu, \quad B^\dagger \gamma^{0*} B = +\gamma^0, \quad B^\dagger \gamma^{i*} B = -\gamma^i. \quad (\text{A.9})$$

The last two relations can be combined to the single relation  $B^\dagger \gamma^{\mu\top} B = +\gamma^\mu$ . For a product of  $\gamma$ -matrices, one can show that  $\overline{\Gamma_1 \Gamma_2 \cdots \Gamma_n} = \bar{\Gamma}_n \cdots \bar{\Gamma}_2 \bar{\Gamma}_1$  and  $(\Gamma_1 \Gamma_2 \cdots \Gamma_n)^c = \Gamma_n^c \cdots \Gamma_2^c \Gamma_1^c$ . Some of these are collected in Table A.1. By using these conjugations, the operations  $\mathcal{P}$ ,  $\mathcal{C}$  and  $\mathcal{T}$  for a spinor bilinear, which are defined in Eqs. (A.48), (A.49) and (A.50), can be expressed as follows:

$$\gamma^0 \Gamma \gamma^0 = (\bar{\Gamma})^\dagger, \quad C \Gamma^\top C^\dagger = \Gamma^c, \quad B^\dagger \Gamma^* B = (\Gamma^b)^\dagger. \quad (\text{A.10})$$

<sup>1</sup> We limit ourselves to the spinors in 4-dimension.

	1	$i\gamma_5$	$\gamma^\mu$	$\gamma^\mu\gamma_5$	$\sigma^{\mu\nu}$	$i\sigma^{\mu\nu}\gamma_5$	$i$
$\Gamma^\dagger$	+	-	$(-1)^\mu$	$-(-1)^\mu$	$(-1)^\mu(-1)^\nu$	$-(-1)^\mu(-1)^\nu$	-
$\bar{\Gamma}$	+	+	+	+	+	+	-
$\Gamma^c$	+	+	-	+	-	-	+
$\Gamma^b$	+	+	+	-	-	-	+

Table A.1: “Eigenvalues” of  $\gamma$ -matrices under the several conjugations defined in the text:  $\bar{\Gamma} \equiv \gamma^0\Gamma^\dagger\gamma^0$ ,  $\Gamma^c \equiv C\Gamma^\top C^\dagger$ , and  $\Gamma^b \equiv B^\dagger\Gamma^\top B$ . The symbol  $(-1)^\mu$  is defined to be +1 for  $\mu = 0$  and to be -1 for  $\mu = 1, 2, 3$ . The index  $\mu$  on  $(-1)^\mu$  is always not summed; besides there is no distinction whether it is covariant or contravariant. The notations  $\tilde{\gamma}^\mu \equiv (-1)^\mu\gamma^\mu$  and  $\tilde{\sigma}^{\mu\nu} \equiv (-1)^\mu(-1)^\nu\sigma^{\mu\nu}$  may sometimes be convenient.

One can see that “Parity” and “Time Reversal” do not reverse the order of  $\gamma$ -matrices. For successive applications of the conjugations, one can show the following relations:

$$\bar{\Gamma}^c = (\bar{\Gamma})^c, \quad \bar{\Gamma}^b = (\bar{\Gamma})^b.$$

Also one can show  $(CB)\gamma^\mu(CB)^\dagger = -\gamma^\mu$ , which implies  $CB = \gamma_5$  up to phase. Note that  $BC = (CB)^\top$ .

A Dirac conjugated  $\gamma$ -matrix  $\bar{\Gamma}$  appears when one takes the hermitian conjugation of a spinor bilinear:

$$(\bar{\psi}_1\Gamma\psi_2)^\dagger = \bar{\psi}_2\bar{\Gamma}\psi_1, \quad (\text{A.11})$$

for both anti-commuting and commuting spinors.

### A.3.3 Antiparticle field $\psi^c$

The antiparticle field  $\psi^c$  of a Dirac field  $\psi$  is defined by

$$\psi^c(x) \equiv C\bar{\psi}^\top(x), \quad \bar{\psi}^c(x) = -\psi^\top(x)C^\dagger, \quad (\text{A.12})$$

where  $C$  is the charge conjugation matrix defined in Eq. (A.9). It coincides with the charge-conjugated field  $\mathcal{C}\psi\mathcal{C}^\dagger$  up to field-dependent phase. The following relations can be shown:

$$(\psi^c)^c = \psi, \quad (\psi_L)^c = (\psi^c)_R, \quad (\psi_R)^c = (\psi^c)_L, \quad (\text{A.13})$$

where  $\psi_{L/R} \equiv P_{L/R}\psi$  and  $\bar{\psi}_{L/R} = \bar{\psi}P_{R/L}$ , where  $P_{L/R} \equiv (1 \mp \gamma_5)/2$ . Our convention<sup>2</sup> for the relative phase between c-number wave-functions  $u$  and  $v$  are

$$v \equiv u^c = C\bar{u}^\top, \quad \bar{v} = -u^\top C^\dagger, \quad v^\top = -\bar{u}C.$$

<sup>2</sup> In general,  $v = \exp^{i\delta} u^c$ , which means  $u = \exp^{i\delta} v^c$ .



See the next section for details. With this convention, an anti-fermion field  $\psi^c(x)$  is expanded in terms of the creation-annihilation operators as follows:

$$\begin{aligned}\psi^c(x) &= \int \frac{d^3p}{(2\pi)^3 2E_p} \sum_s (b_p^s u(p, s) e^{-ip \cdot x} + a_p^{s\dagger} v(p, s) e^{+ip \cdot x}) , \\ \bar{\psi}^c(x) &= \int \frac{d^3p}{(2\pi)^3 2E_p} \sum_s (b_p^{s\dagger} \bar{u}(p, s) e^{+ip \cdot x} + a_p^s \bar{v}(p, s) e^{-ip \cdot x}) .\end{aligned}\tag{A.14}$$

One can see that  $a$  and  $b$  in  $\psi$  are interchanged in  $\psi^c$ . Thus the role of particle and anti-particle is indeed interchanged.

A spinor bilinear can be rewritten in terms of their anti-particle fields:

$$\bar{\psi}_1 \Gamma \psi_2 = +\bar{\psi}_2^c \Gamma^c \psi_1^c , \quad \text{for anti-commuting spinors.}\tag{A.15}$$

For commuting spinors,  $\bar{u}_1 \Gamma v_2 = -\bar{v}_2^c \Gamma^c u_1^c = -\bar{u}_2 \Gamma^c v_1$ , for example. The second equality holds irrespective of the phase convention between  $u$  and  $v$ , since  $v = e^{i\delta} u^c$  means  $u = e^{i\delta} v^c$ .

### A.3.4 Dirac representation

For an non-relativistic particle, the time component of the 4-momentum is much larger than the space component. Thus it is convenient to choose the representation of  $\gamma$ -matrices such that the time component is “special”. Dirac representation is one of them:

$$\begin{aligned}\gamma^0 &= \begin{pmatrix} 1 & \\ & -1 \end{pmatrix} , \quad \gamma^i = \begin{pmatrix} & \sigma^i \\ -\sigma^i & \end{pmatrix} , \quad \sigma^{\mu\nu} \equiv \frac{i}{2} [\gamma^\mu, \gamma^\nu] , \\ \gamma^5 &\equiv \frac{i}{4!} \epsilon_{\mu\nu\rho\sigma} \gamma^\mu \gamma^\nu \gamma^\rho \gamma^\sigma = i\gamma^0 \gamma^1 \gamma^2 \gamma^3 = \begin{pmatrix} & 1 \\ 1 & \end{pmatrix} ,\end{aligned}\tag{A.16}$$

where  $\sigma^i$  are Pauli matrices:

$$\sigma^1 \equiv \begin{pmatrix} & 1 \\ 1 & \end{pmatrix} , \quad \sigma^2 \equiv \begin{pmatrix} & -i \\ +i & \end{pmatrix} , \quad \sigma^3 \equiv \begin{pmatrix} 1 & \\ & -1 \end{pmatrix} .$$

These satisfy  $\{\gamma^\mu, \gamma^\nu\} = 2g^{\mu\nu}$ , where  $g^{\mu\nu} = \text{diag}(+, -, -, -)$ ; and  $\sigma^i \sigma^j = \delta^{ij} + i\epsilon^{ijk} \sigma^k$ , where  $\epsilon^{123} = +1$ . Our convention for the 4-dimensional totally-antisymmetric tensor is that  $\epsilon_{0123} = +1$ . Note that the phase of  $\gamma_5$  is chosen such that the chirality (= eigenvalue of  $\gamma_5$ ) coincides with the helicity for a massless particle (or  $u$ ); for a massless antiparticle (or  $v$ ), the chirality is the opposite to the helicity [Section A.3.5]. Note also that  $(\gamma_5)^2 = +1$ . Explicit forms of the charge conjugation matrix  $C$  and the time-reversal matrix  $B$  in the Dirac representation are

$$C = i\gamma^2 \gamma^0 = \begin{pmatrix} & -i\sigma^2 \\ -i\sigma^2 & \end{pmatrix} , \quad B = \gamma^1 \gamma^3 = \begin{pmatrix} i\sigma^2 & \\ & i\sigma^2 \end{pmatrix} .\tag{A.17}$$

Overall phases are not fixed by the defining properties in Eq. (A.9). Our convention is such that  $CB = \gamma_5^*$ , which means  $BC = (CB)^\top = \gamma_5^* = \gamma_5^\top$ .

Freely-propagating spinor states are specified by the 4-momentum  $p^\mu = (E, \mathbf{p})$  and the (3 dimensional) spin direction  $\mathbf{s}$  ( $|\mathbf{s}|^2 = 1$ ) at the rest frame. Note that  $\mathbf{s}$  is not the space component of the spin 4-vector  $s^\mu$  that is obtained by boosting  $(0, \mathbf{s})^\mu$  to the “laboratory”

frame. However when the distinction between  $\mathbf{s}$  and  $s^\mu$  is not important, we write simply  $s$ . The c-number wave-functions are as follows:

$$u(p, s) = \sqrt{E+m} \begin{pmatrix} \chi^s \\ \frac{\mathbf{p} \cdot \boldsymbol{\sigma}}{E+m} \chi^s \end{pmatrix}, \quad v(p, s) \equiv u^c(p, s) = \sqrt{E+m} \begin{pmatrix} \frac{\mathbf{p} \cdot \boldsymbol{\sigma}}{E+m} \chi^{-s} \\ \chi^{-s} \end{pmatrix}, \quad (\text{A.18})$$

where  $u^c(p, s) \equiv C\bar{u}^\top(p, s)$ . The second relation defines the relative phase of  $u$  and  $v$ . From this it holds that  $v^c(p, s) = u(p, s)$ . One can see that the upper (lower) two components of  $u$  ( $v$ ) are  $\mathcal{O}(1)$ , while the lower (upper) are  $\mathcal{O}(\beta)$ . This is the reason why the Dirac representation is convenient for non-relativistic particles. The expressions above can be obtained by boosting the expressions at the rest frame of a particle:

$$u(p, s) = \sqrt{2m} \begin{pmatrix} \chi^s \\ 0 \end{pmatrix}, \quad v(p, s) = \sqrt{2m} \begin{pmatrix} 0 \\ \chi^{-s} \end{pmatrix}.$$

Note that the mass-dimension of a spinor field is  $[\psi] = 3/2$ , while that of a scalar field is  $[\phi] = 1$ .

### Other representations

Representations other than the Dirac representation can be obtained by unitary transformation<sup>3</sup>  $U$ . For example, so-called chiral (or Weyl) representation  $\gamma_W^\mu$  can be obtained from the Dirac representation  $\gamma_D^\mu$  as follows:

$$\gamma_W^\mu = U\gamma_D^\mu U^\dagger, \quad U = \begin{pmatrix} 1/\sqrt{2} & -1/\sqrt{2} \\ 1/\sqrt{2} & 1/\sqrt{2} \end{pmatrix}. \quad (\text{A.19})$$

Accordingly  $\psi_W = U\psi_D$  and  $\bar{\psi}_W = \bar{\psi}_D U^\dagger$ . One can see that if  $\gamma_D$  is hermitian (anti-hermitian), then  $\gamma_W$  is also hermitian (anti-hermitian). As for the charge conjugation matrix  $C$  and the time-reversal matrix  $B$

$$C_W = UC_D U^\top, \quad B_W = U^* B_D U^\dagger, \quad (\text{A.20})$$

in general. These follow from the fundamental requirements  $C\gamma^{\mu\top}C^\dagger = -\gamma^\mu$  and  $B^\dagger\gamma^{\mu\top}B = \gamma^\mu$ . Since  $U$  for the Dirac-to-Weyl transformation is real, if one choose  $C_D = i\gamma_D^2\gamma_D^0$  for the Dirac representation, then  $C_W = i\gamma_W^2\gamma_W^0$  also for the Weyl representation. However in general, the representations of  $C$  and  $B$  in terms of  $\gamma$ -matrix depend on the representation of  $\gamma$ -matrix itself. On the other hand, since the fundamental requirement for the parity transformation is  $A\gamma^{\mu\dagger}A^\dagger = \gamma^\mu$  ( $A = \gamma^0$ ), which means  $A_W = UA_D U^\dagger$ , the representation of ‘‘parity matrix’’  $A$  is independent to the representation of  $\gamma$ -matrix. One can also see that the relations  $C^\top = -C$  and  $B^\top = -B$  are representation independent. On the other hand, a relation such as  $C^\dagger = -C$  is representation dependent.

<sup>3</sup> The fundamental relation  $\{\gamma^\mu, \gamma^\nu\} = 2g^{\mu\nu}\mathbf{1}$  remains intact by the transformation  $\gamma \rightarrow U\gamma U^{-1}$  with invertible matrix  $U$  that is not necessarily unitary. However if  $U$  is not unitary,  $\psi^\dagger\psi$  changes when one changes the representation. It may be convenient if  $\gamma^\mu$  is either hermitian or anti-hermitian. Since  $(\gamma^\mu)^2 = 2g^{\mu\mu}$  [no summation],  $\gamma^\mu$  should be hermitian (anti-hermitian) if  $g^{\mu\mu} > 0$  ( $< 0$ ) [no summation].

### A.3.5 Pauli spin spinors $\chi^{\pm s}$ and helicity $h$

#### Spin $s$

Pauli 2-component spinors  $\chi^s$  and  $\chi^{-s}$  for the spin direction<sup>4</sup>  $\mathbf{s}_R = (\cos \phi \sin \theta, \sin \phi \sin \theta, \cos \theta)$  at the rest frame of a particle, is

$$\chi^s = \begin{pmatrix} \cos \frac{\theta}{2} \\ \sin \frac{\theta}{2} e^{i\phi} \end{pmatrix}, \quad \chi^{-s} \equiv (-i\sigma^2)(\chi^s)^* = \begin{pmatrix} -\sin \frac{\theta}{2} e^{-i\phi} \\ \cos \frac{\theta}{2} \end{pmatrix}. \quad (\text{A.21})$$

Note that  $\chi^{-(-s)} \equiv (-i\sigma^2)(\chi^{-s})^* = -\chi^s$ . The  $\chi^s$  and  $\chi^{-s}$  are eigenstates of spin operator for the direction  $\mathbf{s}_R$ :

$$\mathbf{s}_R \cdot \boldsymbol{\sigma} \chi^s = +\chi^s, \quad \mathbf{s}_R \cdot \boldsymbol{\sigma} \chi^{-s} = -\chi^{-s}.$$

Thus  $\chi^{\pm s}$  surely represent the states of spin  $= \pm \mathbf{s}_R$ , and  $(1 \pm \mathbf{s}_R \cdot \boldsymbol{\sigma})/2$  are the spin-projection operators for 2-component spinors.

Spin 4-vector  $s^\mu$  is obtained by boosting  $(0, \mathbf{s}_R)^\mu$  at the rest frame of the particle to the ‘‘laboratory’’ frame:

$$s^\mu = \begin{pmatrix} \gamma (\mathbf{s}_R \cdot \boldsymbol{\beta}) \\ \mathbf{s}_R + \frac{\gamma^2}{\gamma + 1} (\mathbf{s}_R \cdot \boldsymbol{\beta}) \boldsymbol{\beta} \end{pmatrix}, \quad (\text{A.22})$$

where  $\boldsymbol{\beta} = \mathbf{p}/E$ ,  $\beta = |\boldsymbol{\beta}|$ ,  $\gamma = 1/\sqrt{1 - \beta^2}$ . Note that  $(p^\mu, s^\mu) \rightarrow (\tilde{p}^\mu, \mp \tilde{s}^\mu)$  is equivalent to  $(\mathbf{p}, \mathbf{s}_R) \rightarrow (-\mathbf{p}, \pm \mathbf{s}_R)$ , that is, the Parity and Time Reversal transformations.

The following relations are for the process  $e^+(\bar{p}_e) e^-(p_e) \rightarrow t(p_t, s_t) \bar{t}(\bar{p}_t, \bar{s}_t)$  with  $\sqrt{s} = 2m_t \gamma$ , where  $\gamma = 1/\sqrt{1 - \beta^2}$ . We work in the CM frame of  $t\bar{t}$  (and  $e^+e^-$ ). We neglect the electron mass, and dropped  $\mathcal{O}(\beta^2)$  and higher terms. Also note that  $s_t$  and  $\bar{s}_t$  are spin 4-vectors at the ‘‘laboratory frame’’, which is the CM frame of  $t\bar{t}$ , while  $\mathbf{s}_t$  and  $\bar{\mathbf{s}}_t$  are spin 3-vectors at the rest frame of  $t$  and  $\bar{t}$ , respectively. Our convention for the totally antisymmetric tensor is  $\epsilon_{0123} = +1$ . Use  $p_e + \bar{p}_e = p_t + \bar{p}_t$  and  $s_t \cdot p_t = \bar{s}_t \cdot \bar{p}_t = 0$  to obtain other relations.

$$\begin{aligned} s_t \cdot p_e &= +\mathbf{s}_t \cdot (\mathbf{p}_t - \mathbf{p}_e), & \bar{s}_t \cdot p_e &= -\bar{\mathbf{s}}_t \cdot (\mathbf{p}_t + \mathbf{p}_e), \\ s_t \cdot \bar{p}_e &= +\mathbf{s}_t \cdot (\mathbf{p}_t + \mathbf{p}_e), & \bar{s}_t \cdot \bar{p}_e &= -\bar{\mathbf{s}}_t \cdot (\mathbf{p}_t - \mathbf{p}_e), \\ \epsilon_{\mu\nu\rho\sigma} (p_e)^\mu (\bar{p}_e)^\nu (p_t)^\rho (s_t)^\sigma &= -2m_t \mathbf{s}_t \cdot (\mathbf{p}_e \times \mathbf{p}_t), \\ \epsilon_{\mu\nu\rho\sigma} (p_e)^\mu (\bar{p}_e)^\nu (p_t)^\rho (\bar{s}_t)^\sigma &= -2m_t \bar{\mathbf{s}}_t \cdot (\mathbf{p}_e \times \mathbf{p}_t), \\ \epsilon_{\mu\nu\rho\sigma} (p_e)^\mu (\bar{p}_e)^\nu (s_t)^\rho (\bar{s}_t)^\sigma &= -2m_t \mathbf{p}_e \cdot (\mathbf{s}_t \times \bar{\mathbf{s}}_t), \\ \epsilon_{\mu\nu\rho\sigma} (p_e)^\mu (p_t)^\nu (s_t)^\rho (\bar{s}_t)^\sigma &= +m_t (\mathbf{s}_t \times \bar{\mathbf{s}}_t) \cdot (\mathbf{p}_t - \mathbf{p}_e) + \frac{1}{m_t} ((\mathbf{s}_t \cdot \mathbf{p}_t) \bar{\mathbf{s}}_t + (\bar{\mathbf{s}}_t \cdot \mathbf{p}_t) \mathbf{s}_t) \cdot (\mathbf{p}_e \times \mathbf{p}_t), \\ \epsilon_{\mu\nu\rho\sigma} (\bar{p}_e)^\mu (p_t)^\nu (s_t)^\rho (\bar{s}_t)^\sigma &= +m_t (\mathbf{s}_t \times \bar{\mathbf{s}}_t) \cdot (\mathbf{p}_t + \mathbf{p}_e) - \frac{1}{m_t} ((\mathbf{s}_t \cdot \mathbf{p}_t) \bar{\mathbf{s}}_t + (\bar{\mathbf{s}}_t \cdot \mathbf{p}_t) \mathbf{s}_t) \cdot (\mathbf{p}_e \times \mathbf{p}_t). \end{aligned}$$

<sup>4</sup> The subscript  $R$  emphasis that the  $\mathbf{s}_R$  is not the space component of the spin 4-vector  $s^\mu$  in Eq. (A.22). Since we rarely refer only to the space component of  $s^\mu$ , we sometimes write  $\mathbf{s}_R$  simply  $\mathbf{s}$ . In fact, the difference between  $\mathbf{s}$  and the space component of  $s^\mu$  is  $\mathcal{O}(\beta^2)$ , as can be seen in Eq. (A.22). When the distinction between  $\mathbf{s}$  and  $s^\mu$  is not important, we may simply write them  $s$ .

## Helicity $h$

Spin degrees of freedom can also be specified by helicity<sup>5</sup>  $h = \mathbf{s}_R \cdot \mathbf{p}/|\mathbf{p}|$ . The state of  $h = +1$  ( $-1$ ) is called right-handed (left-handed) helicity state, for both particle and anti-particle. Thus the spin for helicity eigenstates are  $\mathbf{s} = \pm \mathbf{p}/|\mathbf{p}| = \pm \boldsymbol{\beta}/|\boldsymbol{\beta}|$  for  $h = \pm$ . Since  $\mathbf{s} \cdot \boldsymbol{\sigma} \chi^{\pm s} = \pm \chi^{\pm s}$ , we have

$$\frac{\mathbf{p} \cdot \boldsymbol{\sigma}}{|\mathbf{p}|} \chi^{\pm} = \pm \chi^{\pm} ,$$

where  $\chi^{\pm} \equiv \chi^{\pm s}$  with  $\mathbf{s}_R = +\mathbf{p}/|\mathbf{p}|$ . By noting  $\chi^{-(\pm)} = \pm \chi^{\mp}$ , Dirac spinors of helicity eigenstates are

$$u(p, h = \pm) = \sqrt{E+m} \begin{pmatrix} \chi^{\pm} \\ \frac{\pm |\mathbf{p}|}{E+m} \chi^{\pm} \end{pmatrix} , \quad v(p, h = \pm) = \sqrt{E+m} \begin{pmatrix} \frac{-|\mathbf{p}|}{E+m} \chi^{\mp} \\ \pm \chi^{\mp} \end{pmatrix} . \quad (\text{A.23})$$

Here  $v(p, h) = u^c(p, h)$ , since charge conjugation do not flip neither momentum nor spin. For a massless state, we have

$$u(p, h = \pm) = \sqrt{E} \begin{pmatrix} \chi^{\pm} \\ h \chi^{\pm} \end{pmatrix} , \quad v(p, h = \pm) = \sqrt{E} \begin{pmatrix} -\chi^{\mp} \\ h \chi^{\mp} \end{pmatrix} .$$

With  $\gamma_5$  in Eq. (A.16), we have

$$\gamma_5 u(p, h) = +h u(p, h) , \quad \gamma_5 v(p, h) = -h v(p, h) \quad \text{for } m = 0 ,$$

which means that our convention for the phase of  $\gamma_5$  is such that its eigenvalue (= chirality) is the same as the helicity for  $u$  ( $\sim$  fermion), while the opposite for  $v$  ( $\sim$  anti-fermion), for a massless case. Note that  $u$  ( $v$ ) can be used also for anti-fermion (fermion), since  $\bar{u}_1 \Gamma v_2 = -\bar{u}_2 \Gamma^c v_1^c$ , etc. [Section A.3.3].

The spin 4-vector  $s^\mu$  for helicity eigenstate is

$$s^\mu(h = \pm) = \frac{\pm 1}{\beta} \begin{pmatrix} \gamma \beta^2 \\ \left(1 + \frac{\gamma^2 \beta^2}{\gamma+1}\right) \boldsymbol{\beta} \end{pmatrix} = \frac{\pm \gamma}{\beta} \begin{pmatrix} \beta^2 \\ \boldsymbol{\beta} \end{pmatrix} , \quad \text{while} \quad \frac{p^\mu}{m\beta} = \frac{\gamma}{\beta} \begin{pmatrix} 1 \\ \boldsymbol{\beta} \end{pmatrix} .$$

Thus  $s^\mu(h = \pm 1) \rightarrow \pm p^\mu/m$  as  $\beta \rightarrow 1$  both for a particle and an anti-particle.

### A.3.6 Lorentz transformation for $\gamma$ -matrices

Parity operation etc. are defined to act on  $\psi$ 's, but in Section A.7.4 we show that equivalent operations can be implemented as manipulations on  $\gamma$ -matrices. Likewise, although Lorentz transformation changes only fields and  $(x^\mu, p^\mu, s^\mu)$ , equivalent manipulations for  $\gamma$ -matrices, which are constant to Lorentz tr., are possible. Consider a Lorentz transformation

$$p^\mu \rightarrow \Lambda^\mu{}_\nu p^\nu , \quad \psi \rightarrow \Lambda_{\frac{1}{2}} \psi .$$

<sup>5</sup> The helicity of massless particles may be defined by the limiting procedure  $m \rightarrow 0$ .

Since  $\bar{\psi}\psi$  is a Lorentz scalar,  $\bar{\psi} \rightarrow \bar{\psi}\Lambda_{\frac{1}{2}}^{-1}$ . Since  $\bar{\psi}p^\mu\gamma_\mu\psi$  is also a scalar, we have  $\Lambda^\mu{}_\nu\Lambda_{\frac{1}{2}}^{-1}\gamma_\mu\Lambda_{\frac{1}{2}} = \gamma_\nu$ , or

$$\Lambda_{\frac{1}{2}}^{-1}\gamma_\mu\Lambda_{\frac{1}{2}} = (\Lambda^{-1})^\nu{}_\mu\gamma_\nu .$$

This means  $\gamma$ -matrices are “transformed backward” by  $\Lambda_{\frac{1}{2}}^{-1}$  and  $\Lambda_{\frac{1}{2}}$ . For example, let us consider the Lorentz transformation  $p^\mu = \Lambda^\mu{}_\nu(m, \vec{0})^\nu$ , or  $(\Lambda^{-1})^\nu{}_\mu p^\mu = (m, \vec{0})^\nu$ . Thus we have

$$\Lambda_{\frac{1}{2}}^{-1}\not{p}\Lambda_{\frac{1}{2}} = (\Lambda^{-1})^\nu{}_\mu p^\mu\gamma_\nu = m\gamma^0 .$$

### A.3.7 Projection operators for energy $\Lambda_\pm(p)$ and spin $\Sigma(s)$

Thus energy projection operators  $\Lambda_\pm(p)$  for positive and negative energy at the rest frame are

$$\begin{aligned} \Lambda_+ &= \begin{pmatrix} 1 & \\ & 0 \end{pmatrix} = \frac{1 + \gamma^0}{2} = \frac{m + m\gamma^0}{2m} \xrightarrow{\text{boost}} \frac{m + \not{p}}{2m} , \\ \Lambda_- &= \begin{pmatrix} 0 & \\ & 1 \end{pmatrix} = \frac{1 - \gamma^0}{2} = \frac{m - m\gamma^0}{2m} \xrightarrow{\text{boost}} \frac{m - \not{p}}{2m} , \end{aligned}$$

or

$$\Lambda_\pm(p) = \frac{\pm\not{p} + m}{2m} . \quad (\text{A.24})$$

It has a following properties:

$$\begin{aligned} \Lambda_+(p)u(p, s) &= u(p, s) , & \Lambda_-(p)v(p, s) &= v(p, s) , \\ \Lambda_-(p)u(p, s) &= \Lambda_+(p)v(p, s) = 0 , \\ \Lambda_\pm(p)\Lambda_\pm(p) &= \Lambda_\pm(p) , & \Lambda_+(p)\Lambda_-(p) &= 0 \quad \text{for } p^2 = m^2 , \\ \Lambda_+(p) + \Lambda_-(p) &= 1 , \\ \not{p}\Lambda_\pm(p) &= \pm m\Lambda_\pm(p) \quad \text{for } p^2 = m^2 . \end{aligned} \quad (\text{A.25})$$

Use the relation  $(\bar{u}_1\Gamma v_2)^\dagger = \bar{v}_2\bar{\Gamma}u_1$  for  $\bar{u}(p, s)$  etc.

Likewise, for the spin-projection operator  $\Sigma(s)$  at the rest frame, and the spin parallel to  $z$ -axis ( $s_z = \pm 1$ ),

$$\Sigma(s) = \begin{pmatrix} \frac{1+s_z\sigma_z}{2} & \\ & \frac{1-s_z\sigma_z}{2} \end{pmatrix} \xrightarrow{\text{rotate}} \begin{pmatrix} \frac{1+\mathbf{s}\cdot\boldsymbol{\sigma}}{2} & \\ & \frac{1-\mathbf{s}\cdot\boldsymbol{\sigma}}{2} \end{pmatrix} = \frac{1 + \mathbf{s}\cdot\boldsymbol{\gamma}\gamma_5}{2} \xrightarrow{\text{boost}} \frac{1 - \not{s}\gamma_5}{2} . \quad (\text{A.26})$$

This has the following properties:

$$\begin{aligned} \Sigma(s)u(p, s) &= u(p, s) , & \Sigma(s)v(p, s) &= v(p, s) , \\ \Sigma(-s)u(p, s) &= \Sigma(-s)v(p, s) = 0 , \\ \Sigma(s)\Sigma(s) &= \Sigma(s) , & \Sigma(s)\Sigma(-s) &= 0 , \\ \Sigma(s) + \Sigma(-s) &= 1 . \end{aligned} \quad (\text{A.27})$$

At the rest frame,  $p^\mu = (m, \vec{0})$  and  $s^\mu = (0, \vec{s})$ . Thus  $p\cdot s = 0$ . From this, projection operators for energy and spin commute:

$$\Lambda_\pm(p)\Sigma(s) = \Sigma(s)\Lambda_\pm(p) . \quad (\text{A.28})$$

Just the same manipulations are possible also for  $\chi^s$  and  $\chi^{-s}$ . We show only the results. These can be verified also by direct calculations. For simplicity we mean  $\mathbf{s}_R$  by  $\mathbf{s}$ , not the space component of  $s^\mu$  in arbitrary frame. They are orthogonal  $\chi^{s\dagger}\chi^{-s} = \chi^{-s\dagger}\chi^s = 0$ .

$$\chi^s\chi^{s\dagger} = \frac{1 + \mathbf{s}\cdot\boldsymbol{\sigma}}{2}, \quad \chi^{-s}\chi^{-s\dagger} = \frac{1 - \mathbf{s}\cdot\boldsymbol{\sigma}}{2}. \quad (\text{A.29})$$

Similarly for  $u$  and  $v$ ,

$$\begin{aligned} u(p, s)\bar{u}(p, s) &= \frac{1 - \not{s}\gamma_5}{2}(\not{p} + m) = 2m\Sigma(s)\Lambda_+(p), \\ v(p, s)\bar{v}(p, s) &= \frac{1 - \not{s}\gamma_5}{2}(\not{p} - m) = -2m\Sigma(s)\Lambda_-(p). \end{aligned} \quad (\text{A.30})$$

As we saw above, at high energy, the spin 4-vector of a particle becomes parallel to the 4-momentum of the particle:  $s^\mu(h = \pm 1) \rightarrow \pm p^\mu/m$  as  $\beta \rightarrow 1$ . Here  $h$  means helicity. Since  $p^\mu(\pm\not{p} + m) = \pm m(\pm\not{p} + m)$  for  $p^2 = m^2$ , we have for  $\beta \simeq 1$ ,

$$u(p, h)\bar{u}(p, h) = \frac{1 + h\gamma_5}{2}\not{p}, \quad v(p, h)\bar{v}(p, h) = \frac{1 - h\gamma_5}{2}\not{p}, \quad (\text{A.31})$$

where  $h = +1$  ( $-1$ ) for right-handed (left-handed) helicity state. One can see that the relation between the helicity and the chirality (= eigenvalue of  $\gamma_5$ ) is opposite between particle and antiparticle, or to be precise,  $u$  and  $v$ .

## A.4 Gordon identities

In this section, we show that the only  $CP$ -odd  $t$ - $\bar{t}$ -gauge boson interaction of dim-5 is that of EDM interaction; others are not independent. We closely follow the Appendix.C of [123]. Let us see  $t\bar{t}Z$  interaction, for example. By integrating by parts, all derivatives on, say,  $Z_\mu$  can be removed. After this manipulation, dim-5 terms of effective Lagrangian can be written as follows:

$$\mathcal{L} = (g_1\bar{\psi}\partial^\mu\psi - g_2\bar{\psi}\gamma_5\partial^\mu\psi + ig_3\bar{\psi}\sigma^{\mu\nu}\partial_\nu\psi + g_4\bar{\psi}i\sigma^{\mu\nu}\gamma_5\partial_\nu\psi)Z_\mu + \text{h.c.}$$

Couplings  $g_{1\sim 4}$  can be complex in general; but should be real in order for those terms are odd under  $CP$ . In interaction picture, where the field operators satisfy equations of motion for free fields

$$(i\not{\partial} - m_t)\psi = 0, \quad (\square + m_Z^2)Z_\mu = 0, \quad \partial^\mu Z_\mu = 0,$$

the following relations hold:

$$\begin{aligned} \partial_\nu(\bar{\psi}\sigma^{\mu\nu}\psi) &= -(\bar{\psi}i\overleftrightarrow{\partial}^\mu\psi) + 2m\bar{\psi}\gamma^\mu\psi, \\ (\bar{\psi}\sigma^{\mu\nu}i\overleftrightarrow{\partial}_\nu\psi) &= \partial^\mu(\bar{\psi}\psi), \\ \partial_\nu(\bar{\psi}i\sigma^{\mu\nu}\gamma_5\psi) &= -(\bar{\psi}i\gamma_5i\overleftrightarrow{\partial}^\mu\psi), \\ (\bar{\psi}i\sigma^{\mu\nu}\gamma_5i\overleftrightarrow{\partial}_\nu\psi) &= -\partial^\mu(\bar{\psi}i\gamma_5\psi) + 2m\bar{\psi}\gamma^\mu\gamma_5\psi. \end{aligned}$$

In these relations, arguments of  $\psi$  and  $\bar{\psi}$  are all  $x$ , and  $\partial_\nu = \partial/\partial x^\nu$ . The first one is the celebrated Gordon decomposition:

$$\bar{\psi}\gamma^\mu\psi = \frac{1}{2m} \left[ (\bar{\psi}i\overleftrightarrow{\partial}^\mu\psi) + \partial_\nu(\bar{\psi}\sigma^{\mu\nu}\psi) \right] .$$

By using these ‘‘Gordon identities’’, the Lagrangian above can be organized as follows:

$$\begin{aligned} \mathcal{L} &= (g'_1\partial^\mu(\bar{\psi}\psi) + g'_2\partial_\nu(\bar{\psi}i\sigma^{\mu\nu}\gamma_5\psi))Z_\mu \\ &= g'_2\bar{\psi}i\sigma^{\mu\nu}\gamma_5\psi\partial_\mu Z_\nu \\ &= -g'_2(\bar{\psi}i\gamma_5i\overleftrightarrow{\partial}^\mu\psi)Z_\mu . \end{aligned}$$

Formulas for  $u(p)$  etc. are obtained from

$$\begin{aligned} \langle p, s | \bar{\psi}(x) &= \langle 0 | \bar{u}(p, s) e^{ip\cdot x} , & \psi(x) | p, s \rangle &= u(p, s) e^{-ip\cdot x} | 0 \rangle , \\ \langle \bar{p}, \bar{s} | \psi(x) &= \langle 0 | v(\bar{p}, \bar{s}) e^{i\bar{p}\cdot x} , & \bar{\psi}(x) | \bar{p}, \bar{s} \rangle &= \bar{v}(\bar{p}, \bar{s}) e^{-i\bar{p}\cdot x} | 0 \rangle . \end{aligned}$$

For example, with the convention  $\langle p, \bar{p} | = (|p, \bar{p}\rangle)^\dagger = (a_p^\dagger a_{\bar{p}}^\dagger | 0 \rangle)^\dagger = \langle 0 | a_{\bar{p}} a_p$ ,

$$\begin{aligned} \langle p, \bar{p} | \bar{\psi}\Gamma i\overleftrightarrow{\partial}^\mu\psi | 0 \rangle &= +(p - \bar{p})^\mu \bar{u}(p)\Gamma v(\bar{p}) e^{i(p+\bar{p})\cdot x} , \\ \langle p' | \bar{\psi}\Gamma i\overleftrightarrow{\partial}^\mu\psi | p \rangle &= +(p' + p)^\mu \bar{u}(p')\Gamma u(p) e^{i(p'-p)\cdot x} , \\ \langle \bar{p}' | \bar{\psi}\Gamma i\overleftrightarrow{\partial}^\mu\psi | \bar{p} \rangle &= +(\bar{p}' + \bar{p})^\mu \bar{v}(\bar{p}')\Gamma v(\bar{p}) e^{i(\bar{p}'-\bar{p})\cdot x} . \end{aligned}$$

Here  $p$  ( $\bar{p}$ ) means the momentum for a particle (anti-particle). Note that the last equation includes the minus sign from the anti-commutativity of fermion. The exponential factor becomes 4-momentum conservation for each vertex:

$$\int d^4x e^{i(p+\bar{p})\cdot x} e^{-iq\cdot x} = (2\pi)^4 \delta^{(4)}(p + \bar{p} - q) .$$

Thus for the process  $\langle p, \bar{p} | \leftarrow | q \rangle$ ,

$$\begin{aligned} iq_\nu \bar{u}(p)\sigma^{\mu\nu}v(\bar{p}) &= -(p - \bar{p})^\mu \bar{u}(p)v(\bar{p}) + 2m \bar{u}(p)\gamma^\mu v(\bar{p}) , \\ (p - \bar{p})_\nu \bar{u}(p)\sigma^{\mu\nu}v(\bar{p}) &= iq^\mu \bar{u}(p)v(\bar{p}) , \\ iq_\nu \bar{u}(p)i\sigma^{\mu\nu}\gamma_5v(\bar{p}) &= -(p - \bar{p})^\mu \bar{u}(p)i\gamma_5v(\bar{p}) , \\ (p - \bar{p})_\nu \bar{u}(p)i\sigma^{\mu\nu}\gamma_5v(\bar{p}) &= -iq^\mu \bar{u}(p)i\gamma_5v(\bar{p}) + 2m \bar{u}(p)\gamma^\mu\gamma_5v(\bar{p}) , \end{aligned}$$

where  $q = p + \bar{p}$ . At the CM-frame of  $q^\mu = (\sqrt{s}, \vec{0})$ ,

$$\begin{aligned} \bar{u}(p)\gamma^i\gamma_5v(\bar{p}) &= \bar{u}(p) i\sigma^{ij}\gamma_5 \frac{-p^j}{m} v(\bar{p}) , \\ i\frac{q_\nu}{2m} \bar{u}(p) i\sigma^{i\nu}\gamma_5v(\bar{p}) &= i\frac{\sqrt{s}}{2m} \bar{u}(p) i\sigma^{i0}\gamma_5v(\bar{p}) = \bar{u}(p) i\gamma_5 \frac{-p^i}{m} v(\bar{p}) , \end{aligned}$$

for example.

## A.5 Merging the effects of $\gamma$ and $Z$ exchange

In  $e^+e^- \rightarrow t\bar{t}$ , both  $\gamma$  and  $Z$  are exchanged in  $s$ -channel. But their effect can be combined to single effective couplings. With the SM vertices

$$\Lambda_{X\mu} = g_X (v^{eX}\gamma_\mu - a^{eX}\gamma_\mu\gamma_5) , \quad \Gamma_X^\mu = g_X (v^{tX}\gamma^\mu - a^{tX}\gamma^\mu\gamma_5) \quad (X = \gamma, Z)$$

where

$$g_\gamma = e = g \sin \theta_W , \quad v^{f\gamma} = Q_f , \quad a^{f\gamma} = 0 , \\ g_Z = \frac{g}{\cos \theta_W} , \quad v^{fZ} = \frac{1}{2}T_{3L} - Q_f \sin^2 \theta_W , \quad a^{fZ} = \frac{1}{2}T_{3L} , \quad (\text{A.32})$$

or

$$v^{e\gamma} = -1 , \quad v^{eZ} = \frac{-1}{4} + \sin^2 \theta_W = -0.01876 , \quad a^{e\gamma} = 0 , \quad a^{eZ} = \frac{-1}{4} , \\ v^{t\gamma} = \frac{+2}{3} , \quad v^{tZ} = \frac{+1}{4} - \frac{2}{3} \sin^2 \theta_W = 0.09584 , \quad a^{t\gamma} = 0 , \quad a^{tZ} = \frac{+1}{4} ,$$

we have

$$\sum_{X=\gamma,Z} \frac{1}{s - m_X^2} (\bar{v}(\bar{p}_e)\Lambda_{X\mu}u(p_e)) (\bar{u}(p_t)\Gamma_X^\mu v(\bar{p}_t)) \\ = \frac{e^2}{s} \left[ [v^e v^t] (\bar{v}(\bar{p}_e)\gamma_\mu u(p_e)) (\bar{u}(p_t)\gamma^\mu v(\bar{p}_t)) \right. \\ - [v^e a^t] (\bar{v}(\bar{p}_e)\gamma_\mu u(p_e)) (\bar{u}(p_t)\gamma^\mu\gamma_5 v(\bar{p}_t)) \\ - [a^e v^t] (\bar{v}(\bar{p}_e)\gamma_\mu\gamma_5 u(p_e)) (\bar{u}(p_t)\gamma^\mu v(\bar{p}_t)) \\ \left. + [a^e a^t] (\bar{v}(\bar{p}_e)\gamma_\mu\gamma_5 u(p_e)) (\bar{u}(p_t)\gamma^\mu\gamma_5 v(\bar{p}_t)) \right] ,$$

where

$$[v^e v^t] = v^{e\gamma}v^{t\gamma} + d(s) v^{eZ}v^{tZ} , \\ [v^e a^t] = v^{e\gamma}a^{t\gamma} + d(s) v^{eZ}a^{tZ} = d(s) v^{eZ}a^{tZ} , \\ [a^e v^t] = a^{e\gamma}v^{t\gamma} + d(s) a^{eZ}v^{tZ} = d(s) a^{eZ}v^{tZ} , \\ [a^e a^t] = a^{e\gamma}a^{t\gamma} + d(s) a^{eZ}a^{tZ} = d(s) a^{eZ}a^{tZ} \quad (\text{A.33})$$

are energy-dependent ‘‘couplings’’, and  $d(s)$  is a ratio of  $Z$ -propagator to  $\gamma$ -propagator:

$$d(s) \equiv \frac{g_Z^2}{e^2} \frac{s}{s - m_Z^2 + im_Z\Gamma_Z} , \quad (\text{A.34})$$

where

$$\frac{g_Z^2}{e^2} = \frac{\left(\frac{g}{\cos \theta_W}\right)^2}{(g \sin \theta_W)^2} = \frac{1}{\cos^2 \theta_W \sin^2 \theta_W} = \frac{1}{(1 - 0.23124) \cdot 0.23124} = 5.625 = (2.372)^2 .$$

Extensions for anomalous vertices should be obvious. The width  $\Gamma_Z$  of  $Z$  introduces absorptive part:  $\Gamma_Z/m_Z = 2.490 \text{ GeV}/91.187 \text{ GeV} = 0.0273$ . For  $\sqrt{s} = 2 \times 175 \text{ GeV}$ , its relative magnitude is typically  $s/(s - m_Z^2 + im_Z\Gamma_Z) = 1.073 - 0.002i$ . Thus for the threshold region, the effect of Coulomb rescattering overwhelms the effect of  $\Gamma_Z$ . Also in the open top region, it is known [90] that the QCD vertex correction is larger than  $\Gamma_Z$ , as far as the normal component  $P_N$  of the polarization of top quark is concerned.



## A.6 Propagators

### A.6.1 Fermion propagator

Let us define the momentum configuration at CM-frame of  $t\bar{t}$  as follows:

$$q^\mu = p_t^\mu + \bar{p}_t^\mu = (2m_t + E, \vec{0}) , \quad p^\mu = (p_t^\mu - \bar{p}_t^\mu)/2 , \quad p_t = \frac{q}{2} + p , \quad -\bar{p}_t = -\frac{q}{2} + p . \quad (\text{A.35})$$

It is sometimes convenient to use  $-\bar{p}_t$  instead of  $+\bar{p}_t$ , since it is the former that enters to the propagators. In other words,

$$\sum_{\text{spin}} u(p_t)\bar{u}(p_t) = \not{p}_t + m_t , \quad -\sum_{\text{spin}} v(\bar{p}_t)\bar{v}(\bar{p}_t) = -\not{\bar{p}}_t + m_t . \quad (\text{A.36})$$

The negative sign for  $v$  reflects anticommuting property of fermion.

$$\begin{aligned} \pm\frac{\not{q}}{2} + \not{p} + m_t &= 2m_t \left[ \frac{1 \pm \gamma^0}{2} - \frac{\vec{p} \cdot \vec{\gamma}}{2m_t c} + \frac{1}{2m_t c^2} \left( \pm\frac{E}{2} + p^0 \right) \gamma^0 \right] \\ \left( \pm\frac{q}{2} + p \right)^2 - m_t^2 + im_t \Gamma_t &= 2m_t \left[ \frac{E}{2} \pm p^0 - \frac{\mathbf{p}^2}{2m_t} + \frac{1}{2m_t c^2} \left( \frac{E^2}{4} \pm E p^0 + (p^0)^2 \right) + i\frac{\Gamma_t}{2} \right] . \end{aligned} \quad (\text{A.37})$$

Thus the Feynman propagators  $S_F(p_t) = i(\not{p}_t + m_t)/(p_t^2 - m_t^2 + im_t \Gamma_t)$  for  $t$  and  $\bar{t}$  are

$$S_F(\pm q/2 + p) = \frac{i \left( \frac{1 \pm \gamma^0}{2} - \frac{\vec{p} \cdot \vec{\gamma}}{2m_t c} \right)}{\left( \frac{E}{2} \pm p^0 + i\frac{\Gamma_t}{2} \right) - \frac{\mathbf{p}^2}{2m_t}} + \mathcal{O}\left(\frac{1}{c^2}\right) .$$

$$\frac{\not{p}_t + m_t}{2m_t} \gamma^i \frac{-\not{\bar{p}}_t + m_t}{2m_t} = \frac{1 + \gamma^0}{2} \gamma^i \frac{1 - \gamma^0}{2} + \mathcal{O}\left(\frac{1}{c}\right) \quad (\text{A.38})$$

$$\frac{\not{p}_t + m_t}{2m_t} \gamma^i \gamma_5 \frac{-\not{\bar{p}}_t + m_t}{2m_t} = \frac{1 + \gamma^0}{2} \left[ i\sigma^{ij} \gamma_5 \frac{-p^j}{m_t c} \right] \frac{1 - \gamma^0}{2} + \mathcal{O}\left(\frac{1}{c^2}\right) \quad (\text{A.39})$$

$$\frac{\not{p}_t + m_t}{2m_t} \sigma^{0i} \gamma_5 \frac{-\not{\bar{p}}_t + m_t}{2m_t} = \frac{1 + \gamma^0}{2} \left[ i\gamma_5 \frac{-p^i}{m_t c} \right] \frac{1 - \gamma^0}{2} + \mathcal{O}\left(\frac{1}{c^2}\right) \quad (\text{A.40})$$

Note that the last two (and Eq. (A.36)) are consistent with ‘‘Gordon identities’’ in Section A.4.

### A.6.2 Gluon propagator

Gluon propagator  $\langle G_\mu^a(q) G_\nu^b(-q) \rangle = D_{\mu\nu} \delta^{ab}$  is given by

$$D_{\mu\nu} = \frac{i}{q^2 + i\epsilon} \left( -g_{\mu\nu} + (1 - \xi) \frac{q_\mu q_\nu}{q^2} \right) \quad (\text{A.41})$$

for covariant gauge, and

$$\begin{aligned} D^{00} &= \frac{i}{|\mathbf{q}|^2 - i\epsilon} , \quad D^{0i} = D^{i0} = 0 , \\ D^{ij} &= \frac{i}{(q^0/c)^2 - |\mathbf{q}|^2 + i\epsilon} \left( \delta^{ij} - \frac{q^i q^j}{|\mathbf{q}|^2} \right) \end{aligned} \quad (\text{A.42})$$

for Coulomb gauge. The later is convenient for non-relativistic calculations.

## A.7 Parity, Charge Conjugation and Time Reversal

Within QFT, Parity operation  $\mathcal{P}$  etc. are defined on creation-annihilation operators. However sometimes it's convenient to consider those operations for c-numbers such as  $\bar{u}(p)\gamma^\mu v(\bar{p})$ .

For explicit calculations, it is convenient to introduce a shorthand notation  $\tilde{\phantom{x}}$  for flipping the sign of space-components of 4-vectors and tensors:

$$\begin{aligned}
p^\mu &= (p^0, p^i), & \gamma^\mu &= (\gamma^0, \gamma^i), & \sigma^{\mu\nu} &= (\sigma^{0i}, \sigma^{ij}), \\
\tilde{p}^\mu &\equiv (p^0, -p^i) & \tilde{\gamma}^\mu &\equiv (\gamma^0, -\gamma^i) & \tilde{\sigma}^{\mu\nu} &\equiv (-\sigma^{0i}, +\sigma^{ij}) \\
&= (-1)^\mu p^\mu, & &= (\gamma^\mu)^\dagger, & &= (\sigma^{\mu\nu})^\dagger.
\end{aligned} \tag{A.43}$$

Relations to another notations are

$$(-1)^\mu \gamma^\mu = \tilde{\gamma}^\mu = \gamma_\mu, \quad (-1)^\mu (-1)^\nu \sigma^{\mu\nu} = \tilde{\sigma}^{\mu\nu} = \sigma_{\mu\nu}.$$

Note that the index on  $(-1)^\mu$  is never summed over. Note also that

$$\begin{aligned}
\tilde{p}^\mu \gamma_\mu &= p^\mu \tilde{\gamma}_\mu = \not{\tilde{p}}, & \tilde{p}^\mu \tilde{\gamma}_\mu &= p^\mu \gamma_\mu = \not{p}, \\
(-1)^\mu (-1)^\nu (-1)^\rho (-1)^\sigma \epsilon_{\mu\nu\rho\sigma} &= -\epsilon_{\mu\nu\rho\sigma}.
\end{aligned}$$

### A.7.1 $\mathcal{P}$ , $\mathcal{C}$ and $\mathcal{T}$ for field operators

Parity operation etc. for a Dirac field operator  $\psi(x)$  [Eq. (A.6)] are

$$\begin{aligned}
\mathcal{P}\bar{\psi}(x)\mathcal{P}^{-1} &= \eta_P^* \eta_P^0 \bar{\psi}(\tilde{x})\gamma^0, & \mathcal{P}\psi(x)\mathcal{P}^{-1} &= \eta_P \eta_P^0 \gamma_0 \psi(\tilde{x}), \\
\mathcal{C}\bar{\psi}(x)\mathcal{C}^{-1} &= \eta_C^* \eta_C^0 \bar{\psi}^c(x), & \mathcal{C}\psi(x)\mathcal{C}^{-1} &= \eta_C \eta_C^0 \psi^c(x), \\
\mathcal{T}\bar{\psi}(x)\mathcal{T}^{-1} &= \eta_T^* \eta_T^0 \bar{\psi}(-\tilde{x})B^\dagger, & \mathcal{T}\psi(x)\mathcal{T}^{-1} &= \eta_T \eta_T^0 B \psi(-\tilde{x}),
\end{aligned} \tag{A.44}$$

where  $\psi^c$  is an antiparticle field defined in Eq. (A.12). The symbol  $\eta_P$  etc. are flavor-dependent phases  $|\eta_P|^2 = 1$ , and  $\eta_P^0$  etc. are flavor-independent ‘‘over-all’’ phases  $|\eta_P^0|^2 = 1$ . In terms of creation-annihilation operators,  $a_p^s$  and  $b_p^s$ , these transformations are

$$\begin{aligned}
\mathcal{P}a_p^s\mathcal{P}^{-1} &= +\eta_P \eta_P^0 a_{-p}^s, & \mathcal{P}b_p^s\mathcal{P}^{-1} &= -\eta_P^* \eta_P^0 b_{-p}^s, \\
\mathcal{C}a_p^s\mathcal{C}^{-1} &= \eta_C \eta_C^0 b_p^s, & \mathcal{C}b_p^s\mathcal{C}^{-1} &= \eta_C^* \eta_C^0 a_p^s, \\
\mathcal{T}a_p^s\mathcal{T}^{-1} &= \eta_T \eta_T^0 a_{-p}^{-s}, & \mathcal{T}b_p^s\mathcal{T}^{-1} &= \eta_T^* \eta_T^0 b_{-p}^{-s}.
\end{aligned} \tag{A.45}$$

Note that c-number spinors  $u(p, s)$  and  $v(p, s)$  are flavor-independent, and

$$\begin{aligned}
\bar{u}(p, s)\gamma^0 &= +\bar{u}(\tilde{p}, s) & \gamma^0 u(p, s) &= +u(\tilde{p}, s) \\
\bar{v}(p, s)\gamma^0 &= -\bar{v}(\tilde{p}, s) & \gamma^0 v(p, s) &= -v(\tilde{p}, s), \\
u(p, s)^\top C^\dagger &= -\bar{v}(p, s) & C\bar{u}(p, s)^\top &= v(p, s) \\
v(p, s)^\top C^\dagger &= -\bar{u}(p, s) & C\bar{v}(p, s)^\top &= u(p, s), \\
(\bar{u}(p, s))^* B &= \bar{u}(\tilde{p}, \tilde{s}) & B^\dagger (u(p, s))^* &= u(\tilde{p}, \tilde{s}) \\
(\bar{v}(p, s))^* B &= \bar{v}(\tilde{p}, \tilde{s}) & B^\dagger (v(p, s))^* &= v(\tilde{p}, \tilde{s}).
\end{aligned} \tag{A.46}$$

In order for  $\mathcal{CPT}$  (and the permutations) to be a symmetry of an action, these phases cannot to be arbitrary:

$$\eta_{P_i} = \pm 1, \quad \eta_{T_i} = \eta_{P_i}^* \eta_{C_i}^*.$$

If one (or more) of fields is Majorana, the reality condition  $\psi = \psi^c$  restricts the “over-all” phases:

$$\eta_P^0 = \pm i, \quad \eta_C^0 = \pm 1, \quad \eta_T^0 = \pm 1.$$

Note that  $\mathcal{C}$  and  $\mathcal{P}$  commutes if and only if  $\eta_{P_i}^* \eta_P^{0*} = -\eta_{P_i} \eta_P^0$ , or<sup>6</sup>  $\eta_P^0 = \pm i$ . Note also that  $\mathcal{T}$  is anti-unitary:

$$\begin{aligned} \langle f | \mathcal{T}^{-1} \mathcal{O} \mathcal{T} | i \rangle &= \langle \mathcal{T}(f) | \mathcal{O} | \mathcal{T}(i) \rangle^* & \mathcal{T}(c\mathcal{O}) \mathcal{T}^{-1} &= c^* \mathcal{T} \mathcal{O} \mathcal{T}^{-1}. \\ &= \langle \mathcal{T}(i) | \mathcal{O}^\dagger | \mathcal{T}(f) \rangle, & & \end{aligned} \quad (\text{A.47})$$

Only spinor-bilinears are relevant for scattering matrices  $\mathcal{M}$ , because they are Lorentz scalars:

$$\begin{aligned} \mathcal{P}[\bar{\psi}_1(x) \Gamma(x) \psi_2(x)] \mathcal{P}^{-1} &= \eta_{P_1}^* \eta_{P_2} \mathcal{P}(\Gamma) \bar{\psi}_1(x) \Gamma(x) \psi_2(x) \Big|_{x=\tilde{x}}, \\ \mathcal{C}[\bar{\psi}_1(x) \Gamma(x) \psi_2(x)] \mathcal{C}^{-1} &= \eta_{C_1}^* \eta_{C_2} \mathcal{C}(\Gamma) \bar{\psi}_2(x) \Gamma(x) \psi_1(x), \\ \mathcal{T}[\bar{\psi}_1(x) \Gamma(x) \psi_2(x)] \mathcal{T}^{-1} &= \eta_{T_1}^* \eta_{T_2} \mathcal{T}(\Gamma) \bar{\psi}_1(x) \Gamma(x) \psi_2(x) \Big|_{x=-\tilde{x}}. \end{aligned} \quad (\text{A.48})$$

Here the parity eigenvalue  $\mathcal{P}(\Gamma)$  for  $\Gamma$  etc. are defined through the following relations:

$$\begin{aligned} \gamma^0 \Gamma(x) \gamma^0 &\equiv \mathcal{P}(\Gamma) \Gamma(\tilde{x}) \\ C \Gamma^\top(x) C^\dagger &\equiv \mathcal{C}(\Gamma) \Gamma(x) \\ B^\dagger \Gamma^*(x) B &\equiv \mathcal{T}(\Gamma) \Gamma(-\tilde{x}) \end{aligned} \quad (\text{A.49})$$

These eigenvalues are summarized in the Table A.2. For example,  $\gamma^0 \gamma^i \gamma^0 = -\gamma^i$  ( $i = 1, 2, 3$ ) means  $\mathcal{P}(\gamma^i) = -1$ , and  $\gamma^0 \frac{\partial}{\partial x^i} \gamma^0 = -\frac{\partial}{\partial(-x^i)}$  means  $\mathcal{P}(\partial_i) = -1$ . Note that, since charge conjugation interchanges fields, even though  $\mathcal{C}(\partial_\mu) = +1$ , be sure that  $\mathcal{C}$  changes  $\vec{\partial}_\mu$  to  $\overleftarrow{\partial}_\mu$ , since  $(\vec{\partial}_\mu)^\top = \overleftarrow{\partial}_\mu$ . Thus  $\mathcal{C}(\vec{\partial}_\mu) = -1$ , where  $A \overleftrightarrow{\partial} B \equiv A(\vec{\partial} - \overleftarrow{\partial})B = A(\partial B) - (\partial A)B$ . Note also that  $\mathcal{T}(i\Gamma) = -\mathcal{T}(\Gamma)$ , or  $\mathcal{T}(e^{i\delta} \Gamma) = e^{-2i\delta} \mathcal{T}(\Gamma)$ , in general.

In the momentum space, eigenvalues for Parity etc. are defined as follows:

$$\begin{aligned} \gamma^0 \Gamma(p, s, \bar{p}, \bar{s}) \gamma^0 &\equiv \mathcal{P}(\Gamma) \Gamma(\tilde{p}, s, \tilde{\bar{p}}, \tilde{\bar{s}}) \\ C \Gamma^\top(p, s, \bar{p}, \bar{s}) C^\dagger &\equiv \mathcal{C}(\Gamma) \Gamma(\bar{p}, \bar{s}, p, s) \\ B^\dagger \Gamma^*(p, s, \bar{p}, \bar{s}) B &\equiv \mathcal{T}(\Gamma) \Gamma(\tilde{p}, \tilde{\bar{s}}, \tilde{\bar{p}}, \tilde{\bar{s}}) \end{aligned} \quad (\text{A.50})$$

For example,  $\gamma^0 (i\gamma_5 (p - \bar{p})^i) \gamma^0 = i\gamma_5 (-(p - \bar{p})^i)$  means  $\mathcal{P}(i\gamma_5 (p - \bar{p})^i) = +1$ . This is in accord with  $\mathcal{P}(i\gamma_5 i \overleftrightarrow{\partial}^i) = +1$ . From the definitions above, we have the following for Dirac conjugates  $\bar{\Gamma} \equiv \gamma^0 \Gamma^\dagger \gamma^0$ :

$$\mathcal{P}(\bar{\Gamma}) = \mathcal{P}(\Gamma)^*, \quad \mathcal{C}(\bar{\Gamma}) = \mathcal{C}(\Gamma)^*, \quad \mathcal{T}(\bar{\Gamma}) = \mathcal{T}(\Gamma)^*.$$

<sup>6</sup> This follows since one can choose  $\eta_{P_i} = +1$  for a certain species  $i$ .

	1	$i\gamma_5$	$\gamma^\mu$	$\gamma^\mu\gamma_5$	$\sigma^{\mu\nu}$	$i\sigma^{\mu\nu}\gamma_5$	$\vec{\partial}_\mu + \overleftarrow{\partial}_\mu$	$i\overleftrightarrow{\partial}_\mu$
P	+	-	$(-1)^\mu$	$-(-1)^\mu$	$(-1)^\mu(-1)^\nu$	$-(-1)^\mu(-1)^\nu$	$(-1)^\mu$	$(-1)^\mu$
C	+	+	-	+	-	-	+	-
T	+	-	$(-1)^\mu$	$(-1)^\mu$	$-(-1)^\mu(-1)^\nu$	$(-1)^\mu(-1)^\nu$	$-(-1)^\mu$	$(-1)^\mu$
CP	+	-	$-(-1)^\mu$	$-(-1)^\mu$	$-(-1)^\mu(-1)^\nu$	$(-1)^\mu(-1)^\nu$	$(-1)^\mu$	$-(-1)^\mu$
CPT	+	+	-	-	+	+	-	-

Table A.2: Eigenvalues of  $\gamma$ -matrices and derivative. They are not transformed under parity  $\mathcal{P}$  etc., which are defined to operate on creation-annihilation operators. It should be understood that they are sandwiched by  $\bar{\psi}$  and  $\psi$ . However, one can define similar transformations for c-numbers. See the text for the definitions. Note that  $i\sigma^{\mu\nu}\gamma_5 = \frac{1}{2}\epsilon^{\mu\nu\rho\sigma}\sigma_{\rho\sigma}$  with  $\epsilon_{0123} = +1$ . Although  $\bar{\psi}(\vec{\partial}_\mu + \overleftarrow{\partial}_\mu)\psi = \partial_\mu(\bar{\psi}\psi)$ , this is listed because each of  $\vec{\partial}$  and  $\overleftarrow{\partial}$  is not the eigenstate of  $\mathcal{C}$ . The symbol  $(-1)^\mu$  is defined to be +1 for  $\mu = 0$  and to be -1 for  $\mu = 1, 2, 3$ . The index on  $(-1)^\mu$  is not summed always; besides there is no distinction whether covariant or contravariant.

	$A_\mu$	$F_{\mu\nu}$	$\mathbf{E}$	$\mathbf{B}$	$j^\mu$
P	$(-1)^\mu$	$(-1)^\mu(-1)^\nu$	-	+	$(-1)^\mu$
C	-	-	-	-	-
T	$(-1)^\mu$	$-(-1)^\mu(-1)^\nu$	+	-	$(-1)^\mu$
CP	$-(-1)^\mu$	$-(-1)^\mu(-1)^\nu$	+	-	$-(-1)^\mu$
CPT	-	+	+	+	-

Table A.3: A gauge connection  $A_\mu$  should transform the same way to  $i\partial_\mu$ . For charge conjugation, extra minus sign comes when changing  $\overleftarrow{\partial}_\mu$  to  $\vec{\partial}_\mu$  by integration by parts. As for time reversal, (seemingly) extra minus sign comes from the anti-unitary nature of  $\mathcal{T}$ .

$\mathbf{P}(\Gamma)$  and  $\mathbf{C}(\Gamma)$  are (usually) real, but  $\mathbf{T}(\Gamma)$  may be complex depending on the choice of the phase of  $\Gamma$ :  $\mathbf{T}(e^{i\delta}\Gamma) = e^{-2i\delta}\mathbf{T}(\Gamma)$ .

All entries in Table A.2 are chosen so that  $\bar{\Gamma} = \Gamma$ . Note  $(\vec{\partial}_\mu)^\dagger = \overleftarrow{\partial}_\mu$ . For a product of  $\gamma$ -matrices,  $\overline{\Gamma_1\Gamma_2\cdots\Gamma_n} = \bar{\Gamma}_n\cdots\bar{\Gamma}_2\bar{\Gamma}_1$ . Likewise for  $\Gamma^c \equiv C\Gamma^T C^\dagger$ ,  $(\Gamma_1\Gamma_2\cdots\Gamma_n)^c = \Gamma_n^c\cdots\Gamma_2^c\Gamma_1^c$ . Thus, be careful to the eigenvalue  $\mathbf{C}$  of a product; it is not just the product of each eigenvalue, in general; however  $\gamma$ -matrices and derivatives commutes, of course. On the other hand,  $\mathcal{P}$  and  $\mathcal{T}$  do not reverse the order of matrices.

We also summarize the transformation properties of gauge fields in Table A.3. For non-Abelian gauge,  $A_\mu = A_\mu^a T^a$  and  $F_{\mu\nu} = F_{\mu\nu}^a T^a$ . For  $\mathcal{P}$  and  $\mathcal{T}$ , the arguments  $x$  of fields change to  $\tilde{x}$  and  $-\tilde{x}$ , respectively. For Charge Conjugation,  $\mathcal{C}A_\mu\mathcal{C}^{-1} = -A_\mu^* = -A_\mu^T$ . In general, field dependent phases should also be considered, as in the case of  $\psi$ . But we do not go into detail here.

### A.7.2 $\mathcal{CPT}$ symmetry

From the Tables A.2 and A.3, one can see that a Lorentz invariant interaction such as  $\bar{\psi}\gamma^\mu\psi A_\mu$  is  $\mathcal{CPT}$ -even:  $\mathcal{CPT} = +1$ . It's easy to remember, since one can assign  $-1$  for each 4-vector index  $\mu$ ; for example,  $\mathcal{CPT}$ -eigenvalue of a tensor such as  $\sigma^{\mu\nu}$  is  $(-1)^2 = +1$ .

### A.7.3 $\mathcal{P}$ , $\mathcal{C}$ and $\mathcal{T}$ for currents

When the topology is the same for all the diagrams contributing to  $\mathcal{M}$ , we can apply  $\mathcal{P}$ ,  $\mathcal{C}$ , or  $\mathcal{CP}$  to, say, an initial current and a final current, independently. A (tree-level) amplitude can be written as

$$\begin{aligned}\mathcal{M} &= \sum_{A,B} \langle t\bar{t} | (\bar{t}\Gamma_A t)(ZZ)(\bar{e}\Lambda_B e) | e\bar{e} \rangle \\ &= \sum_{A,B} \langle t\bar{t} | (\bar{t}\Gamma_A t) | 0 \rangle \langle 0 | (ZZ) | 0 \rangle \langle 0 | (\bar{e}\Lambda_B e) | e\bar{e} \rangle \\ &\sim j_{t\bar{t}}^\dagger j_{e^+e^-}^\dagger .\end{aligned}$$

We can rewrite, say, the final  $t\bar{t}$  current  $j_{t\bar{t}}$  using  $\mathcal{P}$  etc.:

$$\begin{aligned}\langle t\bar{t} | (\bar{t}\Gamma_{\mathcal{P}=\pm t}) | 0 \rangle &= \langle t\bar{t} | (\mathcal{P}^\dagger \mathcal{P})(\bar{t}\Gamma_{\mathcal{P}=\pm t})(\mathcal{P}^\dagger \mathcal{P}) | 0 \rangle \\ &= \pm \langle \mathcal{P}(t\bar{t}) | (\bar{t}\Gamma_{\mathcal{P}=\pm t}) | 0 \rangle , \\ \langle t\bar{t} | (\bar{t}\Gamma_{\mathcal{CP}=\pm t}) | 0 \rangle &= \langle t\bar{t} | ((\mathcal{CP})^\dagger \mathcal{CP})(\bar{t}\Gamma_{\mathcal{CP}=\pm t})((\mathcal{CP})^\dagger \mathcal{CP}) | 0 \rangle \\ &= \pm \langle \mathcal{CP}(t\bar{t}) | (\bar{t}\Gamma_{\mathcal{CP}=\pm t}) | 0 \rangle , \\ \langle t\bar{t} | (\bar{t}\Gamma_{\mathcal{T}=\pm t}) | 0 \rangle &= \langle t\bar{t} | (\mathcal{T}^\dagger \mathcal{T})(\bar{t}\Gamma_{\mathcal{T}=\pm t})(\mathcal{T}^\dagger \mathcal{T}) | 0 \rangle \\ &= \pm \langle \mathcal{T}(t\bar{t}) | (\bar{t}\Gamma_{\mathcal{T}=\pm t}) | 0 \rangle^* ,\end{aligned}$$

where

$$\begin{aligned}|\mathcal{P}(p, s, \bar{p}, \bar{s})\rangle &= -|(\tilde{p}, s, \tilde{\bar{p}}, \bar{s})\rangle , \\ |\mathcal{C}(p, s, \bar{p}, \bar{s})\rangle &= |(\bar{p}, \bar{s}, p, s)\rangle , \\ |\mathcal{T}(p, s, \bar{p}, \bar{s})\rangle &= |(\tilde{p}, \tilde{s}, \tilde{\bar{p}}, \tilde{\bar{s}})\rangle ,\end{aligned}$$

because

$$\begin{aligned}|\mathcal{P}(p, s, \bar{p}, \bar{s})\rangle &= (\mathcal{P}a^\dagger(p, s)\mathcal{P}^\dagger)(\mathcal{P}b^\dagger(\bar{p}, \bar{s})\mathcal{P}^\dagger)(\mathcal{P}|0\rangle) \\ &= (+\eta_P\eta_P^0 a^\dagger(\tilde{p}, s))(-\eta_P^*\eta_P^{0*} b^\dagger(\tilde{\bar{p}}, \bar{s}))|0\rangle \\ &= -|(\tilde{p}, s, \tilde{\bar{p}}, \bar{s})\rangle , \quad \text{etc.}\end{aligned}$$

Due to the complex conjugation for  $\mathcal{T}$ , it's not a good idea to consider only the final or initial current but the whole amplitude.

### A.7.4 $\mathcal{P}$ , $\mathcal{C}$ and $\mathcal{T}$ for amplitudes or currents

Although the parity transformation  $\mathcal{P}$  etc. in the QFT are defined for creation-annihilation operators, the similar manipulations can be applied directly to c-numbers: Combined with the definitions Eq. (A.49) [or Eq. (A.50)] for the transformations of  $\gamma$ -matrices, we can analyze  $\mathcal{P}$  properties etc. of matrix elements  $\mathcal{M}$  solely in terms of c-numbers.

## Parity and Charge Conjugation

We consider a subprocess  $Z^*(q) \rightarrow t(p, s) \bar{t}(\bar{p}, \bar{s})$  for definiteness. Denoted in the parentheses are their momenta and their spins. The relevant vertex  $\Gamma^\mu$  can be decomposed into pieces, so that each of which is an ‘‘eigenstate’’ of parity operation:

$$\Gamma^\mu = \Gamma_A^\mu + \Gamma_B^\mu + \dots$$

where  $\Gamma_A^\mu = A(q^2)\gamma^\mu$ , for example. Here  $A(q^2)$  is a form factor. Hereafter, we consider a part of the  $t\bar{t}$  current  $j_{t\bar{t}}^\mu = j_A^\mu + j_B^\mu + \dots$ :

$$\begin{aligned} j_A^\mu(\mathbf{p}, \mathbf{s}, \bar{\mathbf{p}}, \bar{\mathbf{s}}) &= \bar{u}(p, s) \Gamma_A^\mu v(\bar{p}, \bar{s}) \\ &= (\bar{u}(p, s) \gamma^0) (\gamma^0 \Gamma_A^\mu \gamma^0) (\gamma^0 v(\bar{p}, \bar{s})) \\ &= -\mathbf{P}(\Gamma_A) \cdot j_A^\mu(-\mathbf{p}, \mathbf{s}, -\bar{\mathbf{p}}, \bar{\mathbf{s}}), \end{aligned}$$

where the minus sign can be understood by the fact that the product of the intrinsic parity of a particle and that of its anti-particle is  $-1$ .

From the result above, or

$$j_A^\mu(\mathbf{p}, \bar{\mathbf{p}}) j_B^{\nu*}(\mathbf{p}, \bar{\mathbf{p}}) = \mathbf{P}(\Gamma_A) \mathbf{P}(\Gamma_B)^* \cdot j_A^\mu(-\mathbf{p}, -\bar{\mathbf{p}}) j_B^{\nu*}(-\mathbf{p}, -\bar{\mathbf{p}}),$$

we know that the terms in  $|\mathcal{M}|^2$  that are odd (even) under  $(\mathbf{p}_t, \bar{\mathbf{p}}_t) \rightarrow (-\mathbf{p}_t, -\bar{\mathbf{p}}_t)$  should come from the interference of the  $t\bar{t}$  vertices with the opposite (same) parity,  $\mathbf{P}(\Gamma_A) \mathbf{P}(\Gamma_B)^* = -1$  ( $+1$ ), and vice versa<sup>7</sup>.

We can also see that

$$\int d\Omega j_A^\mu j_B^{\nu*} = 0 \quad \text{for } \mathbf{P}(\Gamma_A) \mathbf{P}(\Gamma_B)^* = -1. \quad (\text{A.51})$$

This can be understood as follows. For a fermion-antifermion system, its parity is  $\mathbf{P} = (-1)^{L+1}$ . Then different parity eigenvalue means different orbital angular momentum  $L$ . And the states with different  $L$  are orthogonal each other:

$$\int \frac{d\Omega}{4\pi} P_L(\cos\theta) P_{L'}(\cos\theta) = \frac{\delta_{LL'}}{2L+1},$$

which means partial waves of different  $L$  are orthogonal each other. Note that an eigenstate of partial wave is a spherical wave, not a plane wave that is a momentum eigenstate  $|\mathbf{p}\rangle$ . In other words,  $|\mathbf{p}\rangle$  is a superposition of the states of definite  $L$ . Thus before phase-space integration, they do not form eigenstates of definite  $L$ , and then need not be diagonal with respect to  $L$ .

We can further operate Charge Conjugation:

$$\begin{aligned} j_A^\mu(\mathbf{p}, \mathbf{s}, \bar{\mathbf{p}}, \bar{\mathbf{s}}) &= -\mathbf{P}(\Gamma_A) \cdot (v(\tilde{\bar{p}}, \tilde{\bar{s}})^\top C^\dagger) (C(\Gamma_A^\mu)^\top C^\dagger) (C\bar{u}(\tilde{p}, s)^\top) \\ &= +\mathbf{P}(\Gamma_A) \mathbf{C}(\Gamma_A) \cdot j_A^\mu(-\bar{\mathbf{p}}, \bar{\mathbf{s}}, -\mathbf{p}, \mathbf{s}) \\ &= \mathbf{C}\mathbf{P}(\Gamma_A) \cdot j_A^\mu(\mathbf{p}, \bar{\mathbf{s}}, \bar{\mathbf{p}}, \mathbf{s}), \end{aligned}$$

or

$$j_A^\mu(\mathbf{s}, \bar{\mathbf{s}}) j_B^{\nu*}(\mathbf{s}, \bar{\mathbf{s}}) = \mathbf{C}\mathbf{P}(\Gamma_A) \mathbf{C}\mathbf{P}(\Gamma_B)^* \cdot j_A^\mu(\bar{\mathbf{s}}, \mathbf{s}) j_B^{\nu*}(\bar{\mathbf{s}}, \mathbf{s}). \quad (\text{A.52})$$

<sup>7</sup> We may sometimes write  $\mathbf{P}(\Gamma_A)$  as  $\mathbf{P}(j)_{t\bar{t}}$ , and  $\mathbf{P}(\Gamma_A) \mathbf{P}(\Gamma_B)^*$  as  $\mathbf{P}(jj^\dagger)_{t\bar{t}}$ .

	$\mathbf{p}$	$\bar{\mathbf{p}}$	$\mathbf{s}$	$\bar{\mathbf{s}}$
P	$-\mathbf{p}$	$-\bar{\mathbf{p}}$	$\mathbf{s}$	$\bar{\mathbf{s}}$
C	$\bar{\mathbf{p}}(-\mathbf{p})$	$\mathbf{p}(-\bar{\mathbf{p}})$	$\bar{\mathbf{s}}$	$\mathbf{s}$
$\tilde{\text{T}}$	$-\mathbf{p}$	$-\bar{\mathbf{p}}$	$-\mathbf{s}$	$-\bar{\mathbf{s}}$
CP	$-\bar{\mathbf{p}}(\mathbf{p})$	$-\mathbf{p}(\bar{\mathbf{p}})$	$\bar{\mathbf{s}}$	$\mathbf{s}$
$\text{CP}\tilde{\text{T}}$	$\bar{\mathbf{p}}(-\mathbf{p})$	$\mathbf{p}(-\bar{\mathbf{p}})$	$-\bar{\mathbf{s}}$	$-\mathbf{s}$

Table A.4: Transformation properties of momentum and spin. Denoted in the parentheses are for when  $\mathbf{p} + \bar{\mathbf{p}} = 0$ .

Thus the terms in  $|\mathcal{M}|^2$  that are odd (even) under  $(\mathbf{s}_t, \bar{\mathbf{s}}_t) \rightarrow (\bar{\mathbf{s}}_t, \mathbf{s}_t)$  should come from the interference of the  $t\bar{t}$  vertices with the opposite (same) CP,  $\text{CP}(\Gamma_A)\text{CP}(\Gamma_B)^* = -1 (+1)$ , and vice versa<sup>8</sup>. We can also see that

$$\sum_{s, \bar{s}} j_A^\mu j_B^{\nu*} = 0 \quad \text{for } \text{CP}(\Gamma_A)\text{CP}(\Gamma_B)^* = -1. \quad (\text{A.53})$$

This can be understood as follows. For a fermion-antifermion pair,  $\text{CP} = (-1)^{S+1}$ , which is a compact expression for the fact that spin-0 (spin-1) state is antisymmetric (symmetric) under the interchange of  $s$  and  $\bar{s}$ . Explicit calculation may be useful:

$$\begin{aligned} \sum_{s, \bar{s}} (\chi^{s\dagger} \chi^{-\bar{s}})^\dagger (\chi^{s\dagger} \sigma^i \chi^{-\bar{s}}) &= \sum_{s, \bar{s}} \text{tr} \left[ (\chi^{-\bar{s}} \chi^{-\bar{s}\dagger}) (\chi^s \chi^{s\dagger}) \sigma^i \right] \\ &= \text{tr} [\sigma^i] = 0, \end{aligned}$$

where we used the completeness relation for spin states:  $\sum_s \chi^s \chi^{s\dagger} = 1$ . They need not be zero before spin-sum over both  $s$  and  $\bar{s}$ . With the definition  $\chi^{-\bar{s}} = -i\sigma^2(\chi^{\bar{s}})^*$  and the explicit calculations, one can easily see that  $\chi^{s\dagger} \chi^{-\bar{s}}$  is a spin-0 state, and  $\chi^{s\dagger} \sigma^i \chi^{-\bar{s}}$  is a spin-1 state.

It is easy to see that these analysis can equally be applied to initial current, say,  $e^+e^- \rightarrow Z^*$ . We may use a term “ $t\bar{t}$ -current” Parity transformation  $\text{P}_{t\bar{t}}$  for  $(\mathbf{p}_t, \bar{\mathbf{p}}_t) \rightarrow (-\mathbf{p}_t, -\bar{\mathbf{p}}_t)$ , “ $e^+e^-$ -current” for  $(\mathbf{p}_e, \bar{\mathbf{p}}_e) \rightarrow (-\mathbf{p}_e, -\bar{\mathbf{p}}_e)$ , and “over-all” for to flip all the momenta; and likewise for CP and C.

The results of this subsection can be summarized as follows. First we express  $\mathcal{M}_i^* \mathcal{M}_j$ , which is a part of  $|\mathcal{M}|^2$ , in terms of momenta  $\mathbf{p}$  and spins  $\mathbf{s}$ . Then let us define Parity operation in terms of  $\mathbf{p}$  and  $\mathbf{s}$  as summarized in Table A.4. Now the results in this subsection reads

$$\begin{aligned} \mathcal{M}_{\mathbf{p}=\pm}^* \mathcal{M}_{\mathbf{p}=\pm} &\dots && \text{P-even}, \\ \mathcal{M}_{\mathbf{p}=\pm}^* \mathcal{M}_{\mathbf{p}=\mp} &\dots && \text{P-odd}, \\ \mathcal{M}_{\text{CP}=\pm}^* \mathcal{M}_{\text{CP}=\pm} &\dots && \text{CP-even}, \\ \mathcal{M}_{\text{CP}=\pm}^* \mathcal{M}_{\text{CP}=\mp} &\dots && \text{CP-odd}. \end{aligned}$$

These results are very plausible. One might think that the same situation holds also for Time-Reversal. However in the next subsection, we shall see that this is not the case.

<sup>8</sup> We may sometimes write  $\text{CP}(\Gamma_A)$  as  $\text{CP}(j)_{t\bar{t}}$ , and  $\text{CP}(\Gamma_A)\text{CP}(\Gamma_B)^*$  as  $\text{CP}(jj^\dagger)_{t\bar{t}}$ .

## Time reversal and $\tilde{\mathbf{T}}$

As we saw, an initial current and a final current can separately be rewritten using either Parity and/or Charge Conjugation operations. This is because Charge Conjugation operation invokes transpose in the spinor space, while each current is  $1 \times 1$  in that space, which is invariant under transpose. As for Time Reversal, it is convenient to consider whole  $\mathcal{M}$ , because each current is not real. Of course  $\mathcal{M}$  itself is not real, in general. We mention to this point later.

For definiteness, we consider the process  $e^-(p_e, r) e^+(\bar{p}_e, \bar{r}) \rightarrow Z^*(q) \rightarrow t(p_t, s) \bar{t}(\bar{p}_t, \bar{s})$  at the tree level, and decompose the final vertex  $\Gamma^\mu$  and the initial vertex  $\Lambda_\mu$  into pieces that are ‘‘eigenstates’’ of Time Reversal. Let  $A(q^2)$  and  $B(q^2)$  be the form factors for the final vertex, and  $C(q^2)$  and  $D(q^2)$  for the initial vertex:

$$\Gamma_A^\mu \equiv A \cdot \hat{\Gamma}_A^\mu, \quad \Lambda_{C\mu} \equiv C \cdot \hat{\Lambda}_{C\mu},$$

and

$$\begin{aligned} \mathcal{M}_{AC} &\equiv AC \cdot \hat{\mathcal{M}}_{AC} \\ &= AC \cdot \bar{u}(p_t, s) \hat{\Gamma}_A^\mu v(\bar{p}, \bar{s}) \bar{v}(\bar{p}_e, \bar{r}) \hat{\Lambda}_{C\mu} u(p_e, r), \end{aligned} \tag{A.54}$$

up to factors  $e^2$  etc. Then

$$\begin{aligned} \hat{\mathcal{M}}_{AC}^*(\mathbf{p}, \mathbf{s}) &= (\bar{u}(p_t, s)^* B) (B^\dagger \hat{\Gamma}_A^{\mu*} B) (B^\dagger v(\bar{p}, \bar{s})^*) \\ &\quad \times (\bar{v}(\bar{p}_e, \bar{r})^* B) (B^\dagger \hat{\Lambda}_{C\mu}^* B) (B^\dagger u(p_e, r)) \\ &= \mathsf{T}(\hat{\Gamma}_A) \mathsf{T}(\hat{\Lambda}_C) \cdot \hat{\mathcal{M}}_{AC}(-\mathbf{p}, -\mathbf{s}), \end{aligned}$$

or

$$\begin{aligned} &\mathcal{M}_{AC}^*(\mathbf{p}, \mathbf{s}) \mathcal{M}_{BD}(\mathbf{p}, \mathbf{s}) \\ &= \mathsf{T}(\hat{\Gamma}_A) \mathsf{T}(\hat{\Gamma}_B)^* \mathsf{T}(\hat{\Lambda}_C) \mathsf{T}(\hat{\Lambda}_D)^* \cdot \mathcal{M}_{AC}(-\mathbf{p}, -\mathbf{s}) \mathcal{M}_{BD}^*(-\mathbf{p}, -\mathbf{s}). \end{aligned}$$

Here  $(-\mathbf{p}, -\mathbf{s})$  means to flip all the momenta and the spins. Now

$$\begin{aligned} |\mathcal{M}|^2 &= |\mathcal{M}_{AC} + \mathcal{M}_{BD} + \dots|^2 \\ &= \dots + \mathcal{M}_{AC} \mathcal{M}_{BD}^* + \mathcal{M}_{AC}^* \mathcal{M}_{BD} + \dots \\ &= \dots + \text{Re}(AB^*CD^*) [\hat{\mathcal{M}}_{AC} \hat{\mathcal{M}}_{BD}^* + \hat{\mathcal{M}}_{AC}^* \hat{\mathcal{M}}_{BD}] \\ &\quad + i \text{Im}(AB^*CD^*) [\hat{\mathcal{M}}_{AC} \hat{\mathcal{M}}_{BD}^* - \hat{\mathcal{M}}_{AC}^* \hat{\mathcal{M}}_{BD}] + \dots \end{aligned}$$

means that the terms in  $|\mathcal{M}|^2$  that are even (odd) under  $(\mathbf{p}, \mathbf{s}) \rightarrow (-\mathbf{p}, -\mathbf{s})$  should be accompanied by  $\text{Re}(AB^*CD^*)$  when  $\mathsf{T}(\hat{\Gamma}_A) \mathsf{T}(\hat{\Gamma}_B)^* \mathsf{T}(\hat{\Lambda}_C) \mathsf{T}(\hat{\Lambda}_D)^* = +1$  ( $-1$ ), or by  $\text{Im}(AB^*CD^*)$  when  $\mathsf{T}(\hat{\Gamma}_A) \mathsf{T}(\hat{\Gamma}_B)^* \mathsf{T}(\hat{\Lambda}_C) \mathsf{T}(\hat{\Lambda}_D)^* = -1$  ( $+1$ ). Note that one can always adjust the phases of  $\hat{\Gamma}$ 's and  $\hat{\Lambda}$ 's so that  $\mathsf{T}(\hat{\Gamma}_A) \mathsf{T}(\hat{\Gamma}_B)^* \mathsf{T}(\hat{\Lambda}_C) \mathsf{T}(\hat{\Lambda}_D)^* = \pm 1$ . Correspondingly, the phase of  $AB^*CD^*$  changes counterwise.

The statement above can be simplified as follows. First let us write  $\mathsf{T}(\hat{\Gamma}_A) \mathsf{T}(\hat{\Gamma}_B)^* \mathsf{T}(\hat{\Lambda}_C) \mathsf{T}(\hat{\Lambda}_D)^*$  as  $\mathsf{T}(\mathcal{M}\mathcal{M}^*)$ . Since  $\mathcal{M}\mathcal{M}^*$  is Lorentz scalar,  $\text{CPT}(\mathcal{M}\mathcal{M}^*) = +1$  [Section A.7.2], which means  $\mathsf{T}(\mathcal{M}\mathcal{M}^*) = \text{CP}(\mathcal{M}\mathcal{M}^*)$ . As we saw in the previous subsection,  $\text{CP}(\mathcal{M}\mathcal{M}^*)$  is equivalent to the eigenvalue under CP-transformation  $(\mathbf{s}, \bar{\mathbf{s}}) \rightarrow (\bar{\mathbf{s}}, \mathbf{s})$  [Table A.4]. Thus the result in this subsection is that

$$\begin{aligned} (\mathcal{M}\mathcal{M}^*)_{\text{CPT}=+} &\propto \text{Re}(\text{product of relevant form factors}), \\ (\mathcal{M}\mathcal{M}^*)_{\text{CPT}=-} &\propto \text{Im}(\text{product of relevant form factors}), \end{aligned}$$



where  $\tilde{T}$ -transformation is also defined in Table A.4. Note that  $\tilde{T}$  do NOT interchange initial- and final-states, while the genuine  $\mathcal{T}$ -transformation do.

In fact, the argument above holds only for tree-level diagrams. This is because we neglected  $i\epsilon$  in propagators at Eq. (A.54). The sign of this imaginary part becomes relevant once we across a physical threshold in a loop:  $\log(-x \pm i\epsilon) = \log(x) \pm i\pi$ , for example. Thus, to be precise, the argument above holds when there is no absorptive part. As we shall see below, the sources for absorptive part are rescattering and physical threshold, which are absent to tree level<sup>9</sup>. If there is an absorptive part,  $\text{Re}(AB^*CD^*)$  and  $\text{Im}$  above are replaced by  $\text{Re}(AB^*CD^* e^{i\delta})$  etc., where  $e^{i\delta}$  is an effect of absorptive parts.

Symmetry considerations for  $|\mathcal{M}|^2$  continue to Section 4.3.1.

### A.7.5 Absorptive parts and $\text{CPT}$

Transformation properties of  $S$ -matrix and  $T$ -matrix,  $S = 1 + iT$ , is as follows:

$$\begin{array}{llll}
\mathcal{P}S\mathcal{P}^{-1} = S & \mathcal{P}T\mathcal{P}^{-1} = T & \text{if} & \mathcal{P}H\mathcal{P}^{-1} = H \\
(\mathcal{C}\mathcal{P})S(\mathcal{C}\mathcal{P})^{-1} = S & (\mathcal{C}\mathcal{P})T(\mathcal{C}\mathcal{P})^{-1} = T & \text{if} & (\mathcal{C}\mathcal{P})H(\mathcal{C}\mathcal{P})^{-1} = H \\
\mathcal{T}S\mathcal{T}^{-1} = S^\dagger & \mathcal{T}T\mathcal{T}^{-1} = T^\dagger & \text{if} & \mathcal{T}H\mathcal{T}^{-1} = H \\
(\mathcal{C}\mathcal{P}\mathcal{T})S(\mathcal{C}\mathcal{P}\mathcal{T})^{-1} = S^\dagger & (\mathcal{C}\mathcal{P}\mathcal{T})T(\mathcal{C}\mathcal{P}\mathcal{T})^{-1} = T^\dagger & \text{if} & (\mathcal{C}\mathcal{P}\mathcal{T})H(\mathcal{C}\mathcal{P}\mathcal{T})^{-1} = H
\end{array}$$

The last two rows can be understood by  $S \simeq e^{-iHt}$  and  $\mathcal{T}$  is anti-unitary.

In terms of matrix element,  $\text{CPT}$  invariance can be written as

$$\begin{aligned}
T_{fi} &= \langle f | T | i \rangle \\
&= \langle f | (\mathcal{C}\mathcal{P}\mathcal{T})^{-1} (\mathcal{C}\mathcal{P}\mathcal{T}) T (\mathcal{C}\mathcal{P}\mathcal{T})^{-1} (\mathcal{C}\mathcal{P}\mathcal{T}) | i \rangle \\
&= \langle \mathcal{C}\mathcal{P}\mathcal{T}(f) | T^\dagger | \mathcal{C}\mathcal{P}\mathcal{T}(i) \rangle^* \\
&= \langle \mathcal{C}\mathcal{P}\mathcal{T}(i) | T | \mathcal{C}\mathcal{P}\mathcal{T}(f) \rangle \\
&= T_{\hat{i}\hat{f}} ,
\end{aligned}$$

where  $\hat{i}$  ( $\hat{f}$ ) denotes  $\text{CPT}$ -conjugate state of a state  $i$  ( $f$ ).  $\text{CPT}$  is defined in Eq. (4.5). Thus

$$\begin{aligned}
T_{\hat{f}\hat{i}}^* &= T_{\hat{i}\hat{f}}^\dagger = T_{fi}^\dagger , & \text{from } \text{CPT} \text{ invariance,} \\
&= T_{fi} , & \text{if there is no absorptive part,}
\end{aligned}$$

where the absorptive part of a  $T$ -matrix is defined by its anti-hermitian part<sup>10</sup>  $T - T^\dagger$  (or times  $-i$  or something). The relation above  $T_{\hat{f}\hat{i}}^* = T_{fi}$ , or  $|T_{\hat{f}\hat{i}}|^2 = |T_{fi}|^2$ , for the case of no absorptive part has the following consequences: an expectation value of a  $\text{CPT}$ -odd observable is zero, unless there is an absorptive part, while that of  $\text{CPT}$ -even observable can be non-zero without an absorptive part. This is the basis of the classification of observables based on  $\text{CPT}$  transformation [89, 93]. In fact, as we saw in the previous subsection,  $\text{CPT}$ -even (-odd) term  $\mathcal{M}\mathcal{M}^*$  is proportional to the real- (imaginary-) part of the relevant product of couplings.

<sup>9</sup>Decay width is a part of physical threshold effect, but can be treated to the tree level. Likewise, the imaginary part of form factors originate from physical thresholds, but those are treated by effective vertices here.

<sup>10</sup> Hermitian may be called ‘‘dispersive part’’.

The dagger  $\dagger$  on  $T$  (and  $S$ ) for  $\mathcal{T}$  complicates symmetry arguments. However  $T$  is hermitian to tree level; that is, no absorptive part. This can be shown as follows. Unitarity  $S^\dagger S = 1$  in terms of  $T$ -matrix is  $-i(T - T^\dagger) = T^\dagger T$ , or

$$-i(T_{fi} - T_{fi}^\dagger) = \sum_n T_{fn}^\dagger T_{ni} . \quad (\text{A.55})$$

This is a celebrated formula, which relates the absorptive part of an amplitude and the ‘‘cut diagrams’’ of the amplitude. If an intermediate state  $n$  is a two- (or more) particle state, the RHS is loop effect. If  $n$  is a one-particle state, it hits the pole of the propagator for  $n$ :

$$\left. \frac{i}{p^2 - m_n^2 + im_n \Gamma_n} \right|_{p^2=m_n^2} = \frac{1}{m_n \Gamma_n} ,$$

while  $\Gamma_n \simeq \text{Im}[\text{self-energy of } n]$  is again loop effect. Thus anyway, absorptive part ( $T - T^\dagger$ ) comes from loop effect.

A source of absorptive part can be traced back to the boundary condition for Green functions: a positive energy particle propagates forward in time, while a negative, backward. This boundary condition is embodied by the Feynman prescription for the position of the pole of a propagator:

$$\frac{i}{p^2 - m^2 + i\epsilon} .$$

If one choose principal-value prescription

$$\text{P} \frac{1}{x} \equiv \frac{1}{2} \left( \frac{1}{x + i\epsilon} + \frac{1}{x - i\epsilon} \right)$$

instead, there would be no absorptive part. We can see this by analyticity of an amplitude  $\mathcal{M}(s)$  as a function of CM energy  $\sqrt{s}$ . Below the threshold, there is no absorptive part, and thus  $\mathcal{M}(s)$  is real:

$$\mathcal{M}(s) = [\mathcal{M}(s^*)]^* .$$

Analyticity requires this to hold also above thresholds:

$$\text{Im}[\mathcal{M}(s + i\epsilon)] = -\text{Im}[\mathcal{M}(s - i\epsilon)] .$$

Thus, no absorptive part for principal-value prescription. We know by experience that the sign of  $i\epsilon$  in propagators are irrelevant to tree-level. This is in accord with the observation above that no absorptive part to tree-level.

A word may be in order for ‘‘tree-level’’. Higher order effects can be treated by effective interactions, and so are absorptive parts. They can effectively introduced as anti-hermitian parts of Lagrangian. For example, a decay width  $\Gamma$  can be introduced to ‘‘tree’’ level:

$$\mathcal{L} = \dots - \left( m - i\frac{\Gamma}{2} \right) \bar{\psi}\psi + \dots , \quad (\text{A.56})$$

which is consistent with  $s - m^2 + im\Gamma \simeq s - (m - i\Gamma/2)^2$ . Thus in the statement ‘‘no absorptive part to tree-level’’, anti-hermitian parts of Lagrangian are counted as higher order. It’s interesting that it seems QFT with the Feynman prescription specifies the direction of time-flow:

$$|\psi|^2 \sim |e^{-Et}|^2 \sim |e^{-i(m-i\Gamma/2)t}|^2 \sim e^{-\Gamma t} .$$

That is, simple time reversal  $t \rightarrow -t$  may not be a symmetry, if absorptive part is finite. This may be a ‘‘conjugate statement’’ to that  $\text{CP}\tilde{\text{T}}$  and  $\mathcal{CPT}$  differs when absorptive part is finite.

### A.7.6 $\mathcal{CP}$ violation

Roughly speaking,  $\mathcal{CP}$  transformation changes an operator to its hermitian conjugate, while the coupling intact [Eq. (A.57)].  $\mathcal{T}$  changes the coupling to its complex conjugate. Thus  $\mathcal{CPT}$  changes a term in Lagrangian to its hermitian conjugate.

There two kinds of complex phase in  $\mathcal{M}$ : one is weak phase  $\epsilon$  and the other is strong phase  $\delta$ . Non-zero  $\sin \delta$  means non-zero absorptive part. In this sense,  $\delta$  can also be called “absorptive phase”. On the other hand,  $\epsilon$  is related to the hermitian contribution; thus it might also be called “dispersive phase”; it is also sometimes called “ $\mathcal{CP}$  phase”. Both of these phases are important for  $\mathcal{CP}$ -violating phenomena. For example, let us consider the amplitude  $A_f$  for a certain process with a final state  $f$ , and its  $\mathcal{CP}$ -conjugated amplitude  $\bar{A}_{\bar{f}}$ :

$$\begin{aligned} A_f &= A_1 e^{i\delta_1} + A_2 e^{i\delta_2} \\ &= |A_1| e^{i\epsilon_1} e^{i\delta_1} + |A_2| e^{i\epsilon_2} e^{i\delta_2} , \\ \bar{A}_{\bar{f}} &= A_1^* e^{i\delta_1} + A_2^* e^{i\delta_2} \\ &= |A_1| e^{-i\epsilon_1} e^{i\delta_1} + |A_2| e^{-i\epsilon_2} e^{i\delta_2} . \end{aligned}$$

Here  $\bar{A}_{\bar{f}}$  is determined up to overall phase, which is irrelevant to  $|\mathcal{M}|^2$ . Now one can calculate the following  $\mathcal{CP}$ -odd quantity:

$$\begin{aligned} \frac{|A_f|^2 - |\bar{A}_{\bar{f}}|^2}{|A_f|^2 + |\bar{A}_{\bar{f}}|^2} &= \frac{2 \operatorname{Im}(A_1^* A_2) \sin(\delta_1 - \delta_2)}{|A_1|^2 + |A_2|^2 + 2 \operatorname{Re}(A_1^* A_2) \cos(\delta_1 - \delta_2)} \\ &= \frac{-2 |A_1| |A_2| \sin(\epsilon_1 - \epsilon_2) \sin(\delta_1 - \delta_2)}{|A_1|^2 + |A_2|^2 + 2 |A_1| |A_2| \cos(\epsilon_1 - \epsilon_2) \cos(\delta_1 - \delta_2)} . \end{aligned}$$

One can clearly see that one needs both of two independent  $\mathcal{CP}$  phases and two independent absorptive phases.

The fact above that one needs an absorptive part, is well known from  $K$  physics. However before sum-over final state momenta and/or spins, one do not need an absorptive part for  $\mathcal{CP}$  violating observables.

In general, one can not say that a certain interaction  $\mathcal{L}_{\text{int}}$  violates  $\mathcal{CP}$ . This is because of the degrees of freedom to redefine  $\mathcal{CP}$  by flavor-dependent complex phases. For flavor-off-diagonal interaction, vector-like phase transformation changes  $\mathcal{CP}$ -property; while for flavor-diagonal interaction, chiral phase transformation does. A simple example is a Dirac mass term written in terms of two chiral fermions:

$$-\mathcal{L}_m = m \bar{\psi} \psi = m \overline{\psi_R} \psi_L + m \overline{\psi_L} \psi_R .$$

Here non-zero imaginary part of  $m$  means (effective) absorptive part, not  $\mathcal{CP}$ -violation. In terms of Dirac fermion, this is flavor-diagonal; while in terms of chiral fermion, this is flavor-off-diagonal. One can easily see that this term is  $\mathcal{CP}$ -even. Now we make chiral rotation, which is a symmetry of the Lagrangian if it's anomaly-free:

$$\psi \rightarrow e^{i(\alpha/2)\gamma_5} \psi , \quad \text{or} \quad \begin{cases} \psi_L \rightarrow e^{-i\alpha/2} \psi_L \\ \psi_R \rightarrow e^{+i\alpha/2} \psi_R \end{cases} .$$

Accordingly the mass term above changes its form:

$$\begin{aligned} -\mathcal{L}_m &\rightarrow m \bar{\psi} e^{i\alpha\gamma_5} \psi = m \cos \alpha \bar{\psi} \psi + m \sin \alpha \bar{\psi} i\gamma_5 \psi \\ &= m e^{-i\alpha} \overline{\psi_R} \psi_L + m e^{+i\alpha} \overline{\psi_L} \psi_R . \end{aligned}$$

Now the term  $\bar{\psi} i\gamma_5 \psi$  is  $\mathcal{CP}$ -odd, while  $\bar{\psi}\psi$  is even. Thus the mass term above violates  $\mathcal{CP}$  symmetry, although the original one do not. In terms of chiral fermions,  $\mathcal{CP}$  interchanges  $\bar{\psi}_R \psi_L$  and  $\bar{\psi}_L \psi_R$  with the transformation [Eq. (A.44)]

$$(\mathcal{CP})\psi_{L/R}(\mathcal{CP})^{-1} = \eta_{CP} \gamma^0 (\psi_{L/R})^c ,$$

with<sup>11</sup>  $\eta_{CP} \equiv \eta_P \eta_C = 1$ . With  $\bar{\psi}_1 \Gamma \psi_2 = \bar{\psi}_2^c \Gamma^c \psi_1^c$  and  $(\bar{\psi}_1 \Gamma \psi_2)^\dagger = \bar{\psi}_2 \bar{\Gamma} \psi_1$ , one can see that the non-zero complex phase  $\alpha$  seems to mean  $\mathcal{CP}$  violation. In fact, as can be expected from the context, this can be cured by taken into account of the degrees of freedom to choose the field-dependent phases  $\eta_{CP}$  in the definition of  $\mathcal{CP}$  transformation:

$$(\mathcal{CP})\psi_L(\mathcal{CP})^{-1} = e^{+i\alpha} \gamma^0 (\psi_L)^c , \quad (\mathcal{CP})\psi_R(\mathcal{CP})^{-1} = e^{-i\alpha} \gamma^0 (\psi_R)^c .$$

One can see that  $\mathcal{L}_m$  can indeed be a  $\mathcal{CP}$  eigenstate. Usually one redefines the field to include the phase  $(\eta_{CP})^{-1/2}$ . For the case above,

$$(\mathcal{CP}) e^{-i\alpha/2} \psi_L (\mathcal{CP})^{-1} = \gamma^0 (e^{-i\alpha/2} \psi_L)^c , \quad (\mathcal{CP}) e^{+i\alpha/2} \psi_R (\mathcal{CP})^{-1} = \gamma^0 (e^{+i\alpha/2} \psi_R)^c .$$

Note that  $\psi^c$  contains  $\psi^\dagger$ . The redefinition  $(e^{-i\alpha/2} \psi_L, e^{+i\alpha/2} \psi_R) \rightarrow (\psi_L, \psi_R)$  takes the Lagrangian back to the original form, where the  $\mathcal{CP}$  property is transparent. To summarize, non-zero imaginary part in the coupling for a flavor-off-diagonal interaction may or may not be a source of  $\mathcal{CP}$  violation; it depends on how many explicitly broken U(1) symmetries are there<sup>12</sup>.

While for flavor-diagonal such as

$$\bar{\psi} i\cancel{\partial}\psi = \bar{\psi}_L i\cancel{\partial}\psi_L + \bar{\psi}_R i\cancel{\partial}\psi_R ,$$

their  $\mathcal{CP}$  property is definite, since the flavor-dependent phases  $\eta_{CP}$  cancel in each term. One can unambiguously say that a certain flavor-diagonal interaction is whether  $\mathcal{CP}$ -even or odd.

Some more examples may be useful. Let us consider the following  $S - P$  interaction:

$$(\bar{\psi}\psi - \bar{\psi} i\gamma_5 \psi)\phi .$$

From Table A.2, one can see that  $\bar{\psi}\psi$  is  $\mathcal{CP}$ -even, while  $\bar{\psi} i\gamma_5 \psi$  is odd. Thus one can not define the  $\mathcal{CP}$  property of  $\phi$  so as to preserve  $\mathcal{CP}$ . The situation is similar for the  $V - A$  interaction, which violates both  $\mathcal{C}$  and  $\mathcal{P}$  maximally. However there is a difference:  $S - P$  interaction is off-diagonal in terms of chiral fermion, while  $V - A$  is diagonal (and conserves  $\mathcal{CP}$ ). Thus in principle, there is a possibility to “rotate”  $\psi$  so that the interaction above preserves  $\mathcal{CP}$ . However such a degree of freedom may already be used to rewrite the mass term, as we did just above. Thus if  $\phi$  is the Higgs that gives mass to  $\psi$ , the above  $S - P$  interaction may be “rotated” to the  $\mathcal{CP}$ -even interaction  $\bar{\psi}\psi\phi$  at the same time. On the other hand, if  $\phi$  is not the Higgs that gives mass to  $\psi$ , the interaction of  $\phi$  may violates  $\mathcal{CP}$ , in general.

Likewise, MDM and EDM interaction are also flavor-off-diagonal in terms of chiral fermion:

$$\bar{t} (\sigma^{\mu\nu} F_2(q^2) + i\sigma^{\mu\nu} \gamma_5 d(q^2)) t \partial_\mu A_\nu .$$

<sup>11</sup>Here we dropped field-independent phases  $\eta_P^0 \eta_C^0$  which do not contribute to any fermion bilinears.

<sup>12</sup> Unbroken U(1) symmetries, such as fermion-number or electric charge, can not be used to redefine the phase of couplings, since those symmetry do not alter the form of Lagrangians. On the other hand, axial U(1) symmetry is explicitly broken by a fermion mass, thus can be used to absorb the phase of the fermion mass.

Since chiral rotation of  $t$  is already fixed by the mass term of  $t$ , non-zero  $d$  means  $\mathcal{CP}$  violation. Non-zero imaginary part of  $d$  means (effective) absorptive part, in this case.

Hermitian conjugation of a flavor-off-diagonal interaction is closely related to the  $\mathcal{CP}$  operation. For example,

$$\begin{aligned}
\mathcal{L} &= \frac{-g}{\sqrt{2}} V_{tb} \cdot \bar{t} \gamma^\mu \frac{1 - \gamma_5}{2} b \cdot W_\mu^+ + \text{h.c.} + \dots, \\
(\mathcal{CP})\mathcal{L}(\mathcal{CP})^\dagger &= \frac{-g}{\sqrt{2}} V_{tb} \cdot (-1) \bar{b} \tilde{\gamma}^\mu \frac{1 - \gamma_5}{2} t \cdot (-1) \widetilde{W}_\mu^{+*} + \text{h.c.} + \dots \\
&= + \frac{-g}{\sqrt{2}} V_{tb} \cdot \bar{b} \gamma^\mu \frac{1 - \gamma_5}{2} t \cdot W_\mu^- + \text{h.c.} + \dots \\
&= \left[ \left( \frac{-g}{\sqrt{2}} V_{tb} \right)^* \bar{t} \gamma^\mu \frac{1 - \gamma_5}{2} b \cdot W_\mu^+ \right]^\dagger + \text{h.c.} + \dots,
\end{aligned} \tag{A.57}$$

where tilde~ means to flip space components [Eq. (A.43)]. Since the gauge coupling  $g$  is real, the term above is invariant under  $\mathcal{CP}$  with the phase convention that  $V_{tb}$  is real.  $\mathcal{CP}$  transformation of gauge bosons are summarized in Table A.3.

### Effect of rephasing

We saw that  $\mathcal{CP}$  transformation of  $\mathcal{L}_{\text{int}}$  looks different for the different choice of the phase of fields. Let us consider how  $\mathcal{M}$  changes under the phase transformation of the fields. The key observation is that  $\mathcal{L}_{\text{int}}$  remains intact under field-redefinitions, since couplings are also redefined to absorb the difference. Since  $\mathcal{M} \simeq \left\langle f \left| \left( \exp(i \int \mathcal{L}_{\text{int}}) - 1 \right) \right| i \right\rangle$ , rephasing affects only  $\langle f |$  and  $|i\rangle = a^\dagger \cdots a^\dagger |0\rangle$ . This means each term in  $\mathcal{M}$  changes with the same phase. Thus each term in  $\mathcal{M}\mathcal{M}^*$  is rephasing invariant; thus it is sensible to consider the real or imaginary part of the product of the couplings in  $\text{CPT}\tilde{\text{T}}$ -argument.



# Appendix B

## B.1 Top quark decay width $\Gamma_t$

Decay width of top quark is calculated in [6, 7]:

$$\Gamma(t \rightarrow bW^+) = \Gamma_{\text{Born}} \cdot \left(1 - \frac{2}{3} \frac{\alpha_s}{\pi} f\right),$$

where

$$\begin{aligned} \Gamma_{\text{Born}} &= |V_{tb}|^2 \frac{G_F m_t^3}{8\pi\sqrt{2}} \frac{2p_W}{m_t} \left\{ \left[1 - \left(\frac{m_b}{m_t}\right)^2\right]^2 + \left[1 + \left(\frac{m_b}{m_t}\right)^2\right]^2 \left(\frac{m_W}{m_t}\right)^2 - 2 \left(\frac{m_W}{m_t}\right)^4 \right\} \\ &\simeq \frac{G_F m_t^3}{8\pi\sqrt{2}} \left(1 - \frac{m_W^2}{m_t^2}\right)^2 \left(1 + 2\frac{m_W^2}{m_t^2}\right), \quad \text{where} \end{aligned}$$

$p_W = W$  momentum in the  $t$  rest frame

$$= \sqrt{m_t^2 - (m_W + m_b)^2} \sqrt{m_t^2 - (m_W - m_b)^2} / (2m_t)$$

and

$$\begin{aligned} f &= [\pi^2 + 2\text{Li}_2(y) - 2\text{Li}_2(1-y)] + [4y(1-y-2y^2)\ln y + 2(1-y)^2(5+4y)\ln(1-y) \\ &\quad - (1-y)(5+9y-6y^2)] / 2(1-y)^2(1+2y), \end{aligned}$$

where  $y = m_W^2/m_t^2$ .

## B.2 Coulomb plus $1/r^2$ potential: explicit calculation

**Confluent hypergeometric function  $F(\alpha, \gamma; z)$**

Confluent hypergeometric function  $F(\alpha, \gamma; z)$ , or Kummer's function, is defined by

$$F(\alpha, \gamma; z) = \sum_{k=0}^{\infty} \frac{(\alpha)_k}{k!(\gamma)_k} z^k = 1 + \frac{\alpha}{\gamma} z + \frac{\alpha(\alpha+1)}{2!\gamma(\gamma+1)} z^2 + \dots,$$

where  $(\alpha)_k \equiv \alpha(\alpha+1)\cdots(\alpha+k-1)$ ,  $(\alpha)_0 \equiv 1$ . This is one of the solutions of

$$\frac{d^2 w}{dz^2} + \left(-1 + \frac{\gamma}{z}\right) \frac{dw}{dz} - \frac{\alpha}{z} w = 0.$$

Its asymptotic behavior is

$$\begin{aligned} F(\alpha, \gamma; \zeta) &\rightarrow 1, & \text{for } \zeta \rightarrow 0, \\ F(\alpha, \gamma; \zeta) &\sim \frac{\Gamma(\gamma)}{\Gamma(\gamma - \alpha)} (-\zeta)^{-\alpha} + \frac{\Gamma(\gamma)}{\Gamma(\alpha)} e^\zeta \zeta^{\alpha - \gamma}, & \text{for } |\zeta| \rightarrow \infty \end{aligned} \quad (\text{B.1})$$

Note also that  $F(\alpha, \gamma; \zeta) = e^{-\zeta} F(\gamma - \alpha, \gamma; -\zeta)$ .

Whittaker's differential equation is

$$\frac{d^2 W}{d\zeta^2} + \left( -\frac{1}{4} + \frac{k}{\zeta} + \frac{\mu^2 - 1/4}{\zeta^2} \right) W = 0.$$

One of the solution can be written by  $F$ :

$$W = \zeta^{\mu+1/2} e^{-\zeta/2} F(\mu - k + \frac{1}{2}, 2\mu + 1; \zeta).$$

### Coulomb plus $1/r^2$ potential: explicit calculation

This section is continued from Section 2.4.2.

Let us consider the case  $E < 0$  for the moment. The case when  $E > 0$  can be obtained from analytic continuation. The parameter  $\nu$  is pure imaginary for  $E < 0$ , thus we introduce another variable  $\zeta$ :

$$\zeta = \frac{iz}{\nu}$$

By multiplying Eq. (2.36) by  $(-\nu^2)$ , one obtains

$$\left( \frac{d^2}{d\zeta^2} - \frac{1}{4} - \frac{i\nu}{\zeta} + \frac{\kappa}{\zeta^2} \right) g(\zeta) = 0 \quad (\text{B.2})$$

By comparing this and Whittaker's differential equation, one can see the correspondence  $k = -i\nu$ ,  $\mu^2 - 1/4 = -\kappa$ , or  $\mu = \pm \sqrt{1/4 - \kappa} = d_\pm - \frac{1}{2}$ . Thus the solution<sup>1</sup> is

$$g(\zeta) = \zeta^{d_\pm} e^{-\zeta/2} F(d_\pm + i\nu, 2d_\pm; \zeta), \quad (\text{B.3})$$

or

$$g_\pm(z) \equiv z^{d_\pm} e^{z/(2\rho)} F(d_\pm + \rho, 2d_\pm; -z/\rho), \quad \rho \equiv i\nu, \quad z \equiv -\rho\zeta.$$

Any solution of Eq. (B.2) is expressed as a linear combination of  $g_\pm$ , and so are  $g_>(z)$  and  $g_<(z)$ . Since  $F(\alpha, \gamma; \zeta) \rightarrow 1$  for  $\zeta \rightarrow 0$ , we have

$$g_<(z) = g_+(z). \quad (\text{B.4})$$

<sup>1</sup> For Coulomb ( $\kappa = 0$ ), these two degenerate, and independent solutions are

$$\zeta e^{-\zeta/2} F(1 + i\nu, 2; \zeta), \quad \zeta e^{-\zeta/2} [F(1 + i\nu, 2; \zeta) \ln \zeta + F^*(1 + i\nu, 2; \zeta)]$$

where  $F^*$  is some other function. Thus it may not a good idea to let  $\kappa = 0$  at this stage. However, wave function etc. can be obtained with this method.



While the limit  $\zeta \rightarrow \infty$  is more complicated. For  $E < 0$ ,  $\text{Re} \zeta < 0$ , since

$$\nu = -\frac{C_F \alpha_s}{2} \sqrt{\frac{m}{E + i\epsilon}} \simeq -i|\nu| + \epsilon, \quad \text{or} \quad \rho \simeq |\nu| + i\epsilon.$$

Thus one can see the the first term in Eq. (B.1) dominates:

$$g_{\pm}(z) \stackrel{z \rightarrow \infty}{\sim} z^{d_{\pm}} e^{z/(2\rho)} \frac{\Gamma(2d_{\pm})}{\Gamma(d_{\pm} - \rho)} \left(\frac{z}{\rho}\right)^{-d_{\pm} - \rho} = \rho^{d_{\pm} + \rho} z^{-\rho} e^{z/(2\rho)} \frac{\Gamma(2d_{\pm})}{\Gamma(d_{\pm} - \rho)}.$$

With this expression, we have

$$g_{>}(z) = g_{-}(z) - \rho^{d_{-} - d_{+}} \frac{\Gamma(2d_{-})\Gamma(d_{+} - \rho)}{\Gamma(2d_{+})\Gamma(d_{-} - \rho)} g_{+}(z). \quad (\text{B.5})$$

The Wronskian  $W$  can be calculated from  $g_{\pm}(z) \simeq z^{d_{\pm}}$  for  $z \rightarrow 0$ :

$$W = 1 - 2d_{-} = \sqrt{1 - 4\kappa}, \quad (\text{B.6})$$

Now all ingredients for the Green function in Section 2.4.2 are obtained.

Next we want to obtain the location of pole and its residue  $F(\alpha, \gamma; \zeta)$  diverges when  $\gamma$  is zero or negative integer. However since  $d_{\pm} > 0$ ,  $g_{\pm}$  do not diverge. Thus the divergence of the Green function comes solely from  $\Gamma(d_{+} - \rho)$ . The poles sit at  $d_{+} - \rho = -(n-1)$  ( $n = 1, 2, 3, \dots$ ), or

$$\begin{aligned} \rho^2 &= (n - d_{-})^2, \quad \text{while} \\ &= -\frac{(C_F \alpha_s)^2}{4} \frac{m}{E + i\epsilon}. \end{aligned}$$

Thus

$$E_n = -\frac{(C_F \alpha_s)^2 m}{4(n - d_{-})^2} - i\epsilon \quad (n = 1, 2, 3, \dots).$$

Especially with  $\kappa \rightarrow 0$  or  $d_{-} \rightarrow 0$ , we have energy levels for Coulomb potential

$$E_n = -\frac{(C_F \alpha_s)^2 m}{4n^2} = -\frac{(C_F \alpha_s m/2)^2}{m} \frac{1}{n^2} \quad (n = 1, 2, 3, \dots).$$

One can also read off energy eigenfunctions from the residue of the pole, since

$$G(\mathbf{r}, \mathbf{r}') = \langle \mathbf{r} | \frac{1}{H - (E + i\Gamma)} | \mathbf{r}' \rangle = \sum_n \frac{\psi_n(\mathbf{r}) \psi_n^*(\mathbf{r}')}{E_n - (E + i\Gamma)},$$

where the wave function for bound states are properly normalized:  $\langle \psi_n | \psi_m \rangle = \delta_{nm}$ . With  $n' = n - 1$  ( $d_{+} + n' = n - d_{-}$ )

$$\Gamma(d_{+} - \rho) \sim \frac{1}{d_{+} - \rho + n'} \frac{(-1)^{n'}}{n'!} \simeq -\frac{(-1)^{n'}}{n'!} \frac{(C_F \alpha_s)^2 m}{2(n - d_{-})^3} \frac{1}{E - E_n + i\epsilon}, \quad \text{near the pole,}$$

since with  $\rho(E) = \frac{C_F \alpha_s}{2} \sqrt{\frac{m}{|E|}}$ ,

$$\frac{\partial \rho}{\partial |E|} \simeq -\frac{2(n - d_{-})^3}{(C_F \alpha_s)^2 m}, \quad \text{near the pole.}$$

Thus

$$g_{>}(z) \sim \frac{(-1)^{n'}}{n!} \frac{(C_F \alpha_s)^2 m}{2} \frac{1}{(n-d_-)^{4-2d_-}} \frac{\Gamma(2d_-)}{\Gamma(2-2d_-)\Gamma(2d_- - n)} \frac{1}{E - E_n + i\epsilon} g_+(z)$$

or

$$\begin{aligned} g(z, z') &\sim \frac{1}{4\pi(1-2d_-)} \frac{(-1)^{n'}}{n!} \frac{C_F \alpha_s m}{2} \frac{1}{(n-d_-)^{4-2d_-}} \frac{\Gamma(2d_-)}{\Gamma(2-2d_-)\Gamma(2d_- - n)} \times \\ &\quad \times \frac{1}{E - E_n + i\epsilon} g_+(z) g_+(z'), \quad \text{while,} \\ = rr' G(r, r') &\sim -\frac{r\psi_n(r) r'\psi_n^*(r')}{E - E_n + i\epsilon}, \end{aligned}$$

which means

$$\begin{aligned} r\psi_n(r) &= \left[ \frac{C_F \alpha_s m}{8\pi} \frac{(-1)^n}{(n-1)!} \frac{1}{(1-2d_-)(n-d_-)^{4-2d_-}} \frac{\Gamma(2d_-)}{\Gamma(2-2d_-)\Gamma(2d_- - n)} \right]^{1/2} g_+(z), \\ g_+(z) &= z^{d_+} e^{-z/(2\rho)} F(1-n, 2d_+; z/\rho), \quad \rho = n - d_-, \quad d_+ = 1 - d_-. \end{aligned}$$

Here we used  $F(\alpha, \gamma; \zeta) = e^{-\zeta} F(\gamma - \alpha, \gamma; -\zeta)$ . For Coulomb, using  $\Gamma(\epsilon - n) = \frac{1}{\epsilon} \frac{(-1)^n}{n!}$ , we have

$$\begin{aligned} r\psi_n(r) &= r\psi_n(0) e^{-z/(2n)} F(1-n, 2; z/n) \\ &= r\psi_n(0) \left[ 1 - \frac{z}{2} + \frac{z^2}{12} \left( 1 + \frac{1}{2n^2} \right) + \mathcal{O}(z^3) \right], \end{aligned}$$

where

$$|\psi_n(0)|^2 = \frac{(C_F \alpha_s m/2)^3}{\pi} \frac{1}{n^3}.$$

These are for  $E < 0$ . For  $E > 0$ , one obtains

$$\begin{aligned} \text{Im } G(r, r') &= \frac{m^2 u}{4\pi} |\psi_u(0)|^2 [\mathcal{O}(\kappa^0) + \mathcal{O}(\kappa^1) + \mathcal{O}(\kappa^2)], \quad \text{where} \\ \mathcal{O}(\kappa^0) &= 1 - \frac{1}{2} C_F a_s m (r + r') + \mathcal{O}(r^2), \\ \mathcal{O}(\kappa^1) &= 2\kappa \left[ -\frac{1}{2} \left\{ \ln \left( \frac{ur}{r_0^{(\text{ref})}} \right) + \ln \left( \frac{ur'}{r_0^{(\text{ref})}} \right) \right\} + f \left( \frac{z_u}{2\pi} \right) + \mathcal{O}(r) \right], \end{aligned}$$

where

$$f(x) = \text{Re} [\psi(ix) + \gamma_E] = \sum_{n=1}^{\infty} \zeta(2n+1) (-x^2)^n, \quad x \in \mathbb{R},$$

and  $r_0^{(\text{ref})}$  is given in Eq. (2.45). Note  $\text{Im } G_0(0, 0) = m^2 u / (4\pi)$ . The factor  $|\psi_u(0)|^2$

$$|\psi_u(0)|^2 \equiv \frac{z_u}{1 - e^{-z_u}} = 1 + \frac{z_u}{2} + \frac{z_u^2}{12} + \mathcal{O}(z_u^4), \quad z_u \equiv \frac{\pi C_F \alpha_s}{u}$$

is called Sommerfeld-Sakharov factor. One can see that for both  $E < 0$  and  $E > 0$  case,

$$\text{Im } G_C(r, r') \propto 1 - \frac{1}{2} C_F \alpha_s m (r + r') + \mathcal{O}(r^2 \text{ etc.}) ,$$

irrespective of  $E$ .

The Sommerfeld-Sakharov factor is derived as follows. Consider  $\text{Im } G(0, 0)$  for Coulomb. By expanding to Taylor series, one have

$$g_{<}(z') = z' \left( 1 - \frac{1}{2} z' \right) + \mathcal{O}(z'^3, \kappa) ,$$

$$g_{>}(z) = 1 - z \ln z + \left[ 1 - 2\gamma_E + \frac{1}{2\rho} + \ln \rho - \psi(-\rho) \right] z + \mathcal{O}(z^2, \kappa) ,$$

where  $\psi(z) \equiv \Gamma'(z)/\Gamma(z)$  is digamma function. Thus

$$G(r, r') = \frac{C_F \alpha_s m^2}{4\pi} \left\{ \frac{1}{z} - \ln z + \left[ -\frac{1}{2} \frac{z'}{z} + 1 - 2\gamma_E + \ln \rho + \frac{1}{2\rho} - \psi(-\rho) \right] + \mathcal{O}(z) \right\} ,$$

or

$$\text{Im } G(0, 0) = \frac{C_F \alpha_s m^2}{4\pi} \text{Im} \left[ \ln \rho + \frac{1}{2\rho} - \psi(-\rho) \right] .$$

This can be reduced more. Let us concentrate for  $E > 0$ . Using

$$\rho^2 = -\frac{(C_F \alpha_s)^2}{4} \frac{m}{E + i\epsilon} , \quad \text{or} \quad \rho = \frac{i}{2\pi} \frac{\pi C_F \alpha_s}{u} + \epsilon , \quad \text{where} \quad u = \sqrt{\frac{E}{m}}$$

and

$$-\frac{1}{2z} - \psi(z) = \gamma_E + \frac{\pi}{2} \cot(\pi z) + \sum_{n=1}^{\infty} \zeta(2n+1) z^{2n} ,$$

one obtains

$$\text{Im} \ln \rho = \frac{\pi}{2} , \quad \frac{1}{2\rho} - \psi(-\rho) = i \frac{\pi}{2} \frac{1 + e^{-z_u}}{1 - e^{-z_u}} + \text{real} .$$

Thus we obtain

$$\text{Im } G(0, 0) = \frac{C_F \alpha_s m^2}{4} \frac{1}{1 - e^{-z_u}} = \frac{m^2 u}{4\pi} \frac{z_u}{1 - e^{-z_u}} \quad \text{for} \quad E > 0 .$$

The second factor in the last expression is the Sommerfeld-Sakharov factor.

## B.3 Results for Coulomb potential

Here we summarize some results for Coulomb potential  $-C_F \alpha_s / r$ . Noting that the reduced mass  $\mu$  is  $m/2$ , we define

$$\begin{aligned} \text{Bohr momentum} & \cdots p_B \equiv C_F \alpha_s m / 2 , \\ \text{Bohr radius} & \cdots r_B \equiv 1 / p_B , \\ \text{Bohr energy} & \cdots E_B \equiv p_B^2 / m . \end{aligned} \tag{B.7}$$

Bohr energy may also be called Rydberg energy. Typically  $p_B \simeq 20 \text{ GeV}$ . See Figure 2.4. For  $E < 0$  ( $n = 1, 2, 3, \dots$ ),

$$E_n = -E_B \frac{1}{n^2}, \quad |\psi_n(0)|^2 = \frac{p_B^3}{\pi} \frac{1}{n^3},$$

and

$$G_C(r, r') \simeq -\frac{\psi_n(r) \psi_n^*(r')}{E - E_n + i\epsilon}, \quad \text{near } E = E_n,$$

where

$$\begin{aligned} \psi_n(r) &= \psi_n(0) e^{-r/(r_B n)} F(1 - n, 2; 2r/(r_B n)) \\ &= \psi_n(0) \left[ 1 - \frac{r}{r_B} + \frac{1}{3} \left( \frac{r}{r_B} \right)^2 \left( 1 + \frac{1}{2n^2} \right) + \mathcal{O}(r^3) \right]. \end{aligned}$$

While for  $E > 0$ ,

$$\begin{aligned} \text{Im } G_C(r, r') &= \frac{m^2}{4\pi} \sqrt{\frac{E}{m}} |\psi_E(0)|^2 \left[ 1 - \left( \frac{r}{r_B} + \frac{r'}{r_B} \right) + \mathcal{O}(r^2 \text{ etc.}) \right], \\ |\psi_E(0)|^2 &= \frac{z_E}{1 - e^{-z_E}}, \quad z_E = \pi C_F \alpha_s \sqrt{\frac{m}{E}}. \end{aligned} \tag{B.8}$$

Thus irrespective of energy  $E$ ,

$$\text{Im } G_C(r, r') \propto 1 - \left( \frac{r}{r_B} + \frac{r'}{r_B} \right) + \mathcal{O}(r^2 \text{ etc.})$$

With this relation, we have

$$\frac{1}{m a_s r} \frac{d}{dr} r G_C(r) = \left( \frac{1}{m a_s r} - \frac{C_F}{2} \right) G_C(r) + \mathcal{O}\left(r, \frac{1}{c}\right) \tag{B.9}$$

where  $G_C(r)$  may either be  $G_C(r, r')$  or  $G_C(r, p)$ .

## B.4 Expressions needed for matching

As was explained in Section 2.5, perturbative expansions with respect to  $\alpha_s$  and with respect to  $\alpha_s/\beta$  are both valid when  $\alpha_s \ll \beta \ll 1$ . Here we collect both of them. These are used to determine the matching coefficients for NRQCD calculations. In the following, we use the quantity  $u$  that is equal to  $\beta$  to the leading order. Relation between them are as follows:

$$\begin{aligned} \frac{u}{c} &\equiv \sqrt{\frac{E}{m_t c^2}} = \sqrt{\frac{\sqrt{s} - 2m_t}{m_t}} \\ &= \sqrt{2(\gamma - 1)} = \beta \left( 1 + \frac{3}{8} \beta^2 + \mathcal{O}(\beta^4) \right), \end{aligned}$$

$$\frac{4m^2}{s} = \frac{1}{\gamma^2} = 1 - \beta^2, \quad \gamma = \frac{1}{\sqrt{1 - \beta^2}} = 1 + \frac{u^2}{2},$$

$$\begin{aligned} \frac{p^2}{m^2} &= \gamma^2 \beta^2 = \frac{\beta^2}{1 - \beta^2} = \beta^2(1 + \beta^2 + \beta^4 + \dots) \\ &= \gamma^2 - 1 = u^2 \left(1 + \frac{u^2}{4}\right). \end{aligned}$$

#### B.4.1 NRQCD calculation of $R$ ratio

When  $\alpha_s \ll \beta \ll 1$ , the Green function  $G$  defined in Eq. (2.26) can be expanded perturbatively:

$$\text{Im } G(r, r') = \sum_{i=0}^{10} \text{Im } G_i(r, r'),$$

where with

$$G_0 \equiv \frac{1}{\frac{p^2}{m} - E - i\epsilon},$$

$$\begin{aligned}
\text{Im } G_0(r_0, r_0) &= \text{Im} \langle r_0 | G_0 | r_0 \rangle \\
&= \frac{m^2 u}{4\pi} + \mathcal{O}(r_0^2) , \\
\text{Im } G_1(r_0, r_0) &= \text{Im} \langle r_0 | G_0 \frac{C_{F a_s}}{r} \left[ 1 + \frac{a_s}{4\pi c} \{ 2\beta_0 \ln(\mu' r) + a_1 \} \right] G_0 | r_0 \rangle \\
&= \frac{m^2 u}{4\pi} \cdot \frac{C_{F a_s}}{u} \frac{\pi}{2} \left[ 1 - \frac{2}{\pi} m r_0 u + \frac{a_s}{c} \frac{1}{4\pi} \left\{ a_1 - 2\beta_0 \ln \left( \frac{2mu}{\mu} \right) \right\} \right] + \mathcal{O}(r_0) , \\
\text{Im } G_2(r_0, r_0) &= \text{Im} \langle r_0 | G_0 \frac{p^4}{4m^3 c^2} G_0 | r_0 \rangle \\
&= \frac{m^2 u}{4\pi} \cdot \left( \frac{u}{c} \right)^2 \frac{5}{8} + \mathcal{O}(r_0) , \\
\text{Im } G_3(r_0, r_0) &= \text{Im} \langle r_0 | G_0 \left[ \frac{-11\pi C_{F a_s}}{3m^2 c^2} \delta^{(3)}(\mathbf{r}) \right] G_0 | r_0 \rangle \\
&= \frac{m^2 u}{4\pi} \cdot \frac{C_{F a_s}}{c} \frac{-11}{6m r_0 c} + \mathcal{O}(r_0) , \\
\text{Im } G_4(r_0, r_0) &= \text{Im} \langle r_0 | G_0 \frac{C_{F a_s}}{2m^2 c^2} \left\{ p^2, \frac{1}{r} \right\} G_0 | r_0 \rangle \\
&= \frac{m^2 u}{4\pi} \cdot \frac{C_{F a_s}}{c} \left( \frac{1}{m r_0 c} + \frac{u \pi}{c 2} \right) + \mathcal{O}(r_0) , \\
\text{Im } G_5(r_0, r_0) &= \text{Im} \langle r_0 | G_0 \frac{C_A C_{F a_s}^2}{2m r^2 c^2} G_0 | r_0 \rangle \\
&= \frac{m^2 u}{4\pi} \cdot \frac{C_A C_{F a_s}^2}{c^2} \left\{ -\ln \left( \frac{2m u r_0}{e^{2-\gamma_E}} \right) \right\} + \mathcal{O}(r_0) , \\
\text{Im } G_6(r_0, r_0) &= \text{Im} \langle r_0 | G_0 \frac{C_{F a_s}}{r} G_0 \frac{C_{F a_s}}{r} G_0 | r_0 \rangle \\
&= \frac{m^2 u}{4\pi} \cdot \frac{(C_{F a_s})^2 \pi^2}{u^2 12} + \mathcal{O}(r_0) , \\
\text{Im } G_7(r_0, r_0) &= \text{Im} \langle r_0 | G_0 \frac{C_{F a_s}}{r} G_0 \frac{C_{F a_s}}{r} G_0 \frac{p^4}{4m^3 c^2} G_0 | r_0 \rangle + 2 \text{ permutations} \\
&= \frac{m^2 u}{4\pi} \cdot \frac{(C_{F a_s})^2}{c u} \left[ \frac{\pi}{4m r_0 c} + \frac{u}{c} \left\{ \frac{11}{96} \pi^2 - \frac{1}{2} - \frac{1}{2} \ln \left( \frac{2m u r_0}{e^{2-\gamma_E}} \right) \right\} \right] + \mathcal{O}(r_0) , \\
\text{Im } G_8(r_0, r_0) &= \text{Im} \langle r_0 | G_0 \frac{C_{F a_s}}{r} G_0 \left[ \frac{-11\pi C_{F a_s}}{3m^2 c^2} \delta^{(3)}(\mathbf{r}) \right] G_0 | r_0 \rangle + \left[ \frac{1}{r} \leftrightarrow \delta^{(3)}(\mathbf{r}) \right] \\
&= \frac{m^2 u}{4\pi} \cdot \frac{(C_{F a_s})^2}{c u} \left[ \frac{-11\pi}{12m r_0 c} + \frac{u}{c} \left\{ \frac{11}{4} + \frac{11}{6} \ln \left( \frac{2m u r_0}{e^{2-\gamma_E}} \right) \right\} \right] + \mathcal{O}(r_0) , \\
\text{Im } G_9(r_0, r_0) &= \text{Im} \langle r_0 | G_0 \frac{C_{F a_s}}{r} G_0 \frac{C_{F a_s}}{2m^2 c^2} \left\{ p^2, \frac{1}{r} \right\} G_0 | r_0 \rangle + \left[ \frac{1}{r} \leftrightarrow \left\{ p^2, \frac{1}{r} \right\} \right] \\
&= \frac{m^2 u}{4\pi} \cdot \frac{(C_{F a_s})^2}{c u} \left[ \frac{\pi}{2m r_0 c} + \frac{u}{c} \left\{ \frac{\pi^2}{6} - 1 - 2 \ln \left( \frac{2m u r_0}{e^{2-\gamma_E}} \right) \right\} \right] + \mathcal{O}(r_0) , \\
\text{Im } G_{10}(r_0, r_0) &= \text{Im} \langle r_0 | G_0 \frac{C_{F a_s}}{r} G_0 \frac{p^4}{4m^3 c^2} G_0 | r_0 \rangle + \left[ \frac{1}{r} \leftrightarrow p^4 \right] \\
&= \frac{m^2 u}{4\pi} \cdot \frac{C_{F a_s}}{c} \left[ \frac{1}{2m r_0 c} + \frac{u \pi}{c 2} \right] + \mathcal{O}(r_0) .
\end{aligned}$$

Thus we have

$$\begin{aligned}
& \frac{4\pi}{m^2 c} \text{Im} G(r_0, r_0) / \left(\frac{u}{c}\right) \\
&= \left\{ 1 + \frac{a_s}{u} C_F \frac{\pi}{2} - C_F a_s m r_0 + \left(\frac{a_s}{u}\right)^2 C_F^2 \frac{\pi^2}{12} \right\} \\
&+ \frac{a_s}{c} \left\{ \frac{a_s}{u} C_F \frac{1}{8} \left[ a_1 - 2\beta_0 \ln \left( \frac{2mu}{\mu} \right) \right] \right\} \\
&+ \left(\frac{a_s}{c}\right)^2 \left\{ \left(\frac{u}{a_s}\right)^2 \frac{5}{8} + \frac{u}{a_s} C_F \pi - C_F \left( C_A + \frac{2}{3} C_F \right) \ln \left( \frac{2mur_0}{e^{2-\gamma_E}} \right) \right. \\
&\quad \left. + C_F^2 \left( \frac{9}{32} \pi^2 + \frac{5}{4} \right) + C_F \frac{1}{a_s m r_0} \left( \frac{-1}{3} \right) + \frac{a_s}{u} C_F^2 \frac{\pi}{a_s m r_0} \left( \frac{-1}{6} \right) \right\} \\
&+ \mathcal{O}\left(\frac{1}{c^3}\right) \\
&= \left\{ 1 + \left(\frac{u}{c}\right)^2 \frac{5}{8} \right\} + C_F \frac{a_s}{c} \left\{ \frac{c}{u} \frac{\pi}{2} \left[ 1 - \frac{2}{\pi} m r_0 u \right] - \frac{1}{3 m r_0 c} + \frac{u}{c} \pi \right\} \\
&+ C_F \left(\frac{a_s}{c}\right)^2 \left\{ \left(\frac{c}{u}\right)^2 C_F \frac{\pi^2}{12} + \frac{c}{u} \frac{1}{8} \left[ a_1 - 2\beta_0 \ln \left( \frac{2mu}{\mu} \right) \right] + \frac{c}{u} C_F \frac{\pi}{m r_0 c} \left( \frac{-1}{6} \right) \right. \\
&\quad \left. - \left( C_A + \frac{2}{3} C_F \right) \ln \left( \frac{2mur_0}{e^{2-\gamma_E}} \right) + C_F \left( \frac{9}{32} \pi^2 + \frac{5}{4} \right) \right\} \\
&+ \mathcal{O}(a_s^3) . \tag{B.10}
\end{aligned}$$

The two expressions above are exactly the same each other. The  $R$  ratio and  $\text{Im} G$  is related in Eq. (2.8). By comparing the result in this section and that in the next section, one can determine the matching coefficients  $C_1^{(\text{cur})}$  and  $C_2^{(\text{cur})}$ . For this purpose, it is convenient to rewrite  $u$  with  $\beta$ . To each order in  $\alpha_s$ , their relations are

$$\begin{aligned}
u \left( 1 + \frac{5}{8} u^2 \right) &= \beta (1 + \beta^2 + \mathcal{O}(\beta^4)) , \\
u \left( \frac{\pi}{2u} + \pi u \right) &= \beta \left( \frac{\pi}{2\beta} + \pi \beta + \mathcal{O}(\beta^3) \right) , \\
u \left( \frac{\pi^2}{12u^2} + \frac{9}{32} \pi^2 \right) &= \beta \left( \frac{\pi}{12\beta^2} + \frac{\pi^2}{4} + \mathcal{O}(\beta^2) \right) .
\end{aligned}$$

One can just substitute  $\beta$  for  $u$  in other cases, since their difference is  $\mathcal{O}(\beta^3)$  and higher.

### B.4.2 Perturbative QCD calculation of $R$ ratio

Perturbative calculation of  $R$  ratio for  $e^+e^- \rightarrow \gamma^* \rightarrow \bar{q}q$  was done in [40]. Here we summarize the result for reference:

$$R = \frac{3}{2} N_C Q_q^2 \beta \left( 1 - \frac{\beta^2}{3} \right) \left[ 1 + C_F \left( \frac{\alpha_s(\mu_h)}{\pi} \right) \Delta^{(1)} + C_F \left( \frac{\alpha_s(\mu_h)}{\pi} \right)^2 \Delta^{(2)} + \mathcal{O}(\alpha_s^3) \right]$$

where  $m$  is mass of  $q$ , and

$$\begin{aligned}\Delta^{(1)} &= \frac{\pi^2}{2\beta} - 4 + \frac{\pi^2}{2}\beta + \mathcal{O}(\beta^2) , \\ \Delta^{(2)} &= C_F\Delta_A^{(2)} + C_A\Delta_{NA}^{(2)} + T_F n_f \Delta_L^{(2)} + T_F n_H \Delta_H^{(2)} + \Delta_{\ln 2\beta}^{(2)} + \Delta_{\mu_h}^{(2)} + \mathcal{O}(\beta) ,\end{aligned}$$

where

$$\begin{aligned}\Delta_A^{(2)} &= \frac{\pi^4}{12\beta^2} - 2\frac{\pi^2}{\beta} + \frac{\pi^4}{6} + \pi^2 \left( -\frac{35}{18} - \frac{2}{3}\ln\beta + \frac{4}{3}\ln 2 \right) + \frac{39}{4} - \zeta_3 , \\ \Delta_{NA}^{(2)} &= -\frac{31\pi^2}{72\beta} + \pi^2 \left( \frac{179}{72} - \ln\beta - \frac{8}{3}\ln 2 \right) - \frac{151}{36} - \frac{13}{2}\zeta_3 , \\ \Delta_L^{(2)} &= -\frac{5\pi^2}{18\beta} + \frac{11}{9} , \\ \Delta_H^{(2)} &= \frac{44}{9} - \frac{4\pi^2}{9} , \\ \Delta_{\ln 2\beta}^{(2)} &= -\frac{\pi^2}{4\beta}\beta_0 \ln 2\beta , \\ \Delta_{\mu_h}^{(2)} &= \left( -\frac{\pi^2}{4\beta} + 2 \right) \beta_0 \ln \frac{m}{\mu_h} = -\Delta^{(1)} \frac{\beta_0}{4} \ln \frac{m^2}{\mu_h^2} .\end{aligned}$$

## B.5 Top quark polarization

Neglecting  $\mathcal{O}(\beta_t)$  and higher, the production cross section for  $t\bar{t}$  pair can be written as follows:

$$\frac{d\sigma}{d^3\mathbf{p}_t} = \frac{N_C\alpha^2\Gamma_t}{2\pi m_t^4} \frac{1 - P_{e^+}P_{e^-}}{2} \times |G|^2(a_1 + \chi a_2) \quad (\text{B.11})$$

Here we sum over the spins of  $t$  and  $\bar{t}$ .

$$D = G - F \quad (\text{B.12})$$

$$\begin{aligned}|G|^2(a_1 + \chi a_2) &\rightarrow \frac{1}{4} \left( [\text{no } \mathbf{s}_t, \bar{\mathbf{s}}_t \text{ dependence}] + [\mathbf{s}_t \text{ dependent}] \right. \\ &\quad \left. + [\bar{\mathbf{s}}_t \text{ dependent}] + [\mathbf{s}_t, \bar{\mathbf{s}}_t \text{ dependent}] \right) \quad (\text{B.13})\end{aligned}$$

$$\begin{aligned}&[\text{no } \mathbf{s}_t, \bar{\mathbf{s}}_t \text{ dependence}] \\ &= |G|^2(a_1 + \chi a_2) + 2 \text{Re} [G^* F(a_3 + \chi a_4)] \frac{\mathbf{p}_e \cdot \mathbf{p}_t}{m_t^2} \\ &= |G|^2(a_1 + \chi a_2) \left\{ 1 + 2 \text{Re} \left( C_{\text{FB}} \frac{F}{G} \right) \beta_t \cos \theta_{te} \right\} \quad (\text{B.14})\end{aligned}$$



$$\begin{aligned}
& [\mathbf{s}_t \text{ dependent}] \\
& = -|G|^2(a_2 + \chi a_1) \frac{\mathbf{s}_t \cdot \mathbf{p}_e}{m_t} \\
& \quad - \text{Re} [G^* F(a_4 + \chi a_3)] \left[ \frac{\mathbf{s}_t \cdot \mathbf{p}_t}{m_t} + \frac{\mathbf{s}_t \cdot \mathbf{p}_e}{m_t} \frac{\mathbf{p}_e \cdot \mathbf{p}_t}{m_t^2} \right] \\
& \quad + \text{Im} [G^* F(a_3 + \chi a_4)] \frac{\mathbf{s}_t \cdot (\mathbf{p}_e \times \mathbf{p}_t)}{m_t^2} \\
& \quad + [ - \text{Im}(d_{tg} G^* D)(a_1 + \chi a_2) + \text{Im} [G^* F(a_5 + \chi a_6)] ] \left[ \frac{\mathbf{s}_t \cdot \mathbf{p}_t}{m_t} - \frac{\mathbf{s}_t \cdot \mathbf{p}_e}{m_t} \frac{\mathbf{p}_e \cdot \mathbf{p}_t}{m_t^2} \right] \\
& \quad + [ - \text{Re}(d_{tg} G^* D)(a_2 + \chi a_1) + \text{Re} [G^* F(a_6 + \chi a_5)] ] \frac{\mathbf{s}_t \cdot (\mathbf{p}_e \times \mathbf{p}_t)}{m_t^2} \\
& = |G|^2(a_1 + \chi a_2) \left\{ C_{//}^0 s_{//} + 2 \text{Re} \left( C_{\perp} \frac{F}{G} \right) s_{//} \beta_t \cos \theta_{te} \right. \\
& \quad + \text{Re} \left( C_{\perp} \frac{F}{G} \right) s_{\perp} \beta_t \sin \theta_{te} + \text{Im} \left( C_{\text{N}} \frac{F}{G} \right) s_{\text{N}} \beta_t \sin \theta_{te} \\
& \quad + \left[ B_{\perp}^g \text{Im} \left( d_{tg} \frac{D}{G} \right) + \text{Im} \left( B_{\perp} \frac{F}{G} \right) \right] s_{\perp} \beta_t \sin \theta_{te} \\
& \quad \left. + \left[ B_{\text{N}}^g \text{Re} \left( d_{tg} \frac{D}{G} \right) + \text{Re} \left( B_{\text{N}} \frac{F}{G} \right) \right] s_{\text{N}} \beta_t \sin \theta_{te} \right\} \tag{B.15}
\end{aligned}$$

$$[\bar{\mathbf{s}}_t \text{ dependent}] = \left( \mathbf{s}_t \rightarrow \bar{\mathbf{s}}_t, d_{tg} \rightarrow -d_{tg}, d_{t\gamma} \rightarrow -d_{t\gamma}, d_{tZ} \rightarrow -d_{tZ} \text{ at } [\mathbf{s}_t \text{ dependent}] \right) \tag{B.16}$$

Note that  $d_{t\gamma} \rightarrow -d_{t\gamma}$  and  $d_{tZ} \rightarrow -d_{tZ}$  mean  $B_{\perp}^{\gamma/Z} \rightarrow -B_{\perp}^{\gamma/Z}$  and  $B_{\text{N}}^{\gamma/Z} \rightarrow -B_{\text{N}}^{\gamma/Z}$ .

$$\begin{aligned}
& [\mathbf{s}_t, \bar{\mathbf{s}}_t \text{ dependent}] \\
& = |G|^2 (a_1 + \chi a_2) \frac{\mathbf{s}_t \cdot \mathbf{p}_e}{m_t} \frac{\bar{\mathbf{s}}_t \cdot \mathbf{p}_e}{m_t} \\
& \quad + \text{Re} [G^* F (a_3 + \chi a_4)] \left[ \frac{\mathbf{s}_t \cdot \mathbf{p}_e}{m_t} \frac{\bar{\mathbf{s}}_t \cdot \mathbf{p}_t}{m_t} + \frac{\bar{\mathbf{s}}_t \cdot \mathbf{p}_e}{m_t} \frac{\mathbf{s}_t \cdot \mathbf{p}_t}{m_t} \right] \\
& \quad - \text{Im} [G^* F (a_4 + \chi a_3)] \left[ \frac{\mathbf{s}_t \cdot \mathbf{p}_e}{m_t} \frac{\bar{\mathbf{s}}_t \cdot (\mathbf{p}_e \times \mathbf{p}_t)}{m_t^2} + \frac{\bar{\mathbf{s}}_t \cdot \mathbf{p}_e}{m_t} \frac{\mathbf{s}_t \cdot (\mathbf{p}_e \times \mathbf{p}_t)}{m_t^2} \right] \\
& \quad + [ - \text{Im} (d_{tg} G^* D) (a_2 + \chi a_1) + \text{Im} [G^* F (a_6 + \chi a_5)] ] \\
& \quad \quad \times \left[ \frac{\mathbf{s}_t \cdot \mathbf{p}_e}{m_t} \frac{\bar{\mathbf{s}}_t \cdot \mathbf{p}_t}{m_t} - \frac{\bar{\mathbf{s}}_t \cdot \mathbf{p}_e}{m_t} \frac{\mathbf{s}_t \cdot \mathbf{p}_t}{m_t} \right] \\
& \quad + [ - \text{Re} (d_{tg} G^* D) (a_1 + \chi a_2) + \text{Re} [G^* F (a_5 + \chi a_6)] ] \\
& \quad \quad \times \left[ \frac{\mathbf{s}_t \cdot \mathbf{p}_e}{m_t} \frac{\bar{\mathbf{s}}_t \cdot (\mathbf{p}_e \times \mathbf{p}_t)}{m_t^2} - \frac{\bar{\mathbf{s}}_t \cdot \mathbf{p}_e}{m_t} \frac{\mathbf{s}_t \cdot (\mathbf{p}_e \times \mathbf{p}_t)}{m_t^2} \right] \\
& = |G|^2 (a_1 + \chi a_2) \left\{ s_{//} \bar{s}_{//} + 2 \text{Re} \left( C_{\text{N}} \frac{F}{G} \right) s_{//} \bar{s}_{//} \beta_t \cos \theta_{te} \right. \\
& \quad + \text{Re} \left( C_{\text{N}} \frac{F}{G} \right) (s_{//} \bar{s}_{\perp} + \bar{s}_{//} s_{\perp}) \beta_t \sin \theta_{te} \\
& \quad + \text{Im} \left( C_{\perp} \frac{F}{G} \right) (s_{//} \bar{s}_{\text{N}} + \bar{s}_{//} s_{\text{N}}) \beta_t \sin \theta_{te} \\
& \quad + \left[ B_{\text{N}}^g \text{Im} \left( d_{tg} \frac{D}{G} \right) + \text{Im} \left( B_{\text{N}} \frac{F}{G} \right) \right] (s_{//} \bar{s}_{\perp} - s_{\perp} \bar{s}_{//}) \beta_t \sin \theta_{te} \\
& \quad \left. + \left[ B_{\perp}^g \text{Re} \left( d_{tg} \frac{D}{G} \right) + \text{Re} \left( B_{\perp} \frac{F}{G} \right) \right] (s_{//} \bar{s}_{\text{N}} - s_{\text{N}} \bar{s}_{//}) \beta_t \sin \theta_{te} \right. \tag{B.17}
\end{aligned}$$

In general,

$$(\mathbf{s}_t \cdot \mathbf{p}_e) (\bar{\mathbf{s}}_t \cdot \mathbf{p}_t) - (\bar{\mathbf{s}}_t \cdot \mathbf{p}_e) (\mathbf{s}_t \cdot \mathbf{p}_t) = (\mathbf{s}_t \times \bar{\mathbf{s}}_t) \cdot (\mathbf{p}_e \times \mathbf{p}_t) \tag{B.18}$$

By replacing  $\mathbf{p}_t$  with  $(\mathbf{p}_e \times \mathbf{p}_t)$  we have

$$\begin{aligned}
& (\mathbf{s}_t \cdot \mathbf{p}_e) [\bar{\mathbf{s}}_t \cdot (\mathbf{p}_e \times \mathbf{p}_t)] - (\bar{\mathbf{s}}_t \cdot \mathbf{p}_e) [\mathbf{s}_t \cdot (\mathbf{p}_e \times \mathbf{p}_t)] \\
& \quad + (\mathbf{s}_t \times \bar{\mathbf{s}}_t) \cdot [\mathbf{p}_t |\mathbf{p}_e|^2 - \mathbf{p}_e (\mathbf{p}_e \cdot \mathbf{p}_t)] \\
& = (p_e)_i (p_e)_j (p_t)_k (s_t)_l (\bar{s}_t)_m \cdot \frac{1}{4!} \delta_{i[j} \epsilon_{klm]} = 0 \tag{B.19}
\end{aligned}$$

Thus one can see that the anomalous contributions to the  $[\mathbf{s}_t, \bar{\mathbf{s}}_t \text{ dependent}]$ -part is proportional to  $\mathbf{s}_t \times \bar{\mathbf{s}}_t$ .

# References

- [1] F. Abe *et al.*, The CDF Collaboration, *Phys. Rev. D* **50**, 2966 (1994); *Phys. Rev. Lett.* **74**, 2626 (1995);  
S. Abachi *et al.*, The D0 Collaboration, *Phys. Rev. Lett.* **74**, 2632 (1995).
- [2] C. Caso *et al.* (Particle Data Group), *Euro. Phys. Jour. C* **3**, 1 (1998) and 1999 off-year partial update for the 2000 edition (URL: <http://pdg.lbl.gov/>).
- [3] K. Fujii, in Y. Sumino, *Acta Phys. Polo.* **B25**, 1837 (1994).
- [4] E. Accomando *et al.*, *Phys. Rept.* **299**, 1 (1998).
- [5] V. A. Miransky, M. Tanabashi, and K. Yamawaki, *Phys. Lett.* **B221**, 177 (1989); *Mod. Phys. Lett.* **A4**, 1043 (1989).
- [6] I. Bigi, Y. L. Dokshitzer, V. Khoze, J. Kühn and P. Zerwas, *Phys. Lett.* **B181**, 157 (1986).
- [7] J. H. Kühn, *Acta Phys. Pol.* **B12**, 347 (1981); *Acta Phys. Austr. Suppl.* **XXIV**, 203 (1982);  
M. Jeżabek and J. H. Kühn, *Nucl. Phys.* **B314**, 1 (1989);  
A. Denner and T. Sack, *Nucl. Phys.* **B358**, 46 (1991);  
C. S. Li, R. J. Oakes and T. C. Yuan, *Phys. Rev. D* **43**, 3759 (1991);  
A. Czarnecki, *Phys. Lett.* **B252**, 467 (1990);  
J. H. Kühn, in “*QCD–20 Years Later*” Vol. 1, eds. P. M. Zerwas and H. A. Kastrup (World Scientific, 1993);  
A. Czarnecki and K. Melnikov, *Nucl. Phys.* **B544**, 520 (1999).
- [8] J. L. Richardson, *Phys. Lett.* **82B**, 272 (1979);  
W. Buchmüller, G. Grunberg and S.-H. H. Tye, *Phys. Rev. Lett.* **45**, 103 (1980); (E) *ibid.* **45**, 587 (1980);  
W. Buchmüller and S.-H. H. Tye, *Phys. Rev. D* **24**, 132 (1981);  
J. Pantaleone and S.-H. H. Tye, *Phys. Rev. D* **33**, 777 (1986);  
K. Hagiwara, A. D. Martin and A. W. Peacock, *Z. Phys. C* **33**, 135 (1986).
- [9] V. S. Fadin and V. A. Khoze, *Pis'ma Zh. Éksp. Theo. Fiz.* **46**, 417 (1987) [*JETP Lett.* **46**, 525 (1987)]; *Yad. Fiz.* **48**, 487 (1988) [*Sov. J. Nucl. Phys.* **48**, 309 (1988)].
- [10] V. S. Fadin and V. A. Khoze, *Yad. Fiz.* **53**, 1118 (1991) [*Sov. J. Nucl. Phys.* **53**, 692 (1991)].
- [11] M. J. Strassler and M. E. Peskin, *Phys. Rev. D* **43**, 1500 (1991).

- [12] V. S. Fadin and O. I. Yakovlev, *Yad. Fiz.* **53**, 1111 (1991) [*Sov. J. Nucl. Phys.* **53**, 688 (1991)].
- [13] M. Jezabek, J. H. Kühn, and T. Teubner, *Z. Phys. C* **56**, 653 (1992).
- [14] Y. Sumino, K. Fujii, K. Hagiwara, H. Murayama, and C.-K. Ng, *Phys. Rev. D* **47**, 56 (1993).
- [15] H. Murayama and Y. Sumino, *Phys. Rev. D* **47**, 82 (1993).
- [16] Y. Sumino, Ph. D. Thesis, University of Tokyo, 1993.
- [17] K. Melnikov and O. Yakovlev, *Phys. Lett. B* **324**, 217 (1994);  
V. S. Fadin, V. A. Khoze, and A. D. Martin, *Phys. Rev. D* **49**, 2247 (1994); *Phys. Lett. B* **320**, 141 (1994).
- [18] K. Fujii, T. Matsui, and Y. Sumino, *Phys. Rev. D* **50**, 4341 (1994).
- [19] W. Mödritsch and W. Kummer, *Nucl. Phys.* **B430**, 3 (1994);  
W. Kummer and W. Mödritsch, *Z. Phys. C* **66**, 225 (1995).
- [20] M. Jezabek, in *Physics at LEP200 and Beyond*, edited by T. Riemann and J. Blumlein [*Nucl. Phys. B (Proc. Suppl.)* **37**, 197 (1994)].
- [21] R. Harlander, M. Jezabek, J. H. Kühn and T. Teubner, *Phys. Lett. B* **346**, 137 (1995).
- [22] V. S. Fadin, V. A. Khoze, A. D. Martin and A. Chapovsky, *Phys. Rev. D* **52**, 1377 (1995).
- [23] W. Mödritsch, *Nucl. Phys.* **B475**, 507 (1996).
- [24] R. Harlander, M. Jezabek, J. H. Kühn and M. Peter, *Z. Phys. C* **73**, 477 (1997).
- [25] M. Peter and Y. Sumino, *Phys. Rev. D* **57**, 6912 (1998).
- [26] A. H. Hoang and T. Teubner, *Phys. Rev. D* **58**, 114023 (1998).
- [27] K. Melnikov and A. Yelkhovsky, *Nucl. Phys.* **B528**, 59 (1998).
- [28] O. Yakovlev, *Phys. Lett. B* **457**, 170 (1999).
- [29] T. Nagano, A. Ota, and Y. Sumino, *Phys. Rev. D* **60**, 114014 (1999).
- [30] M. Beneke, A. Signer, and V. A. Smirnov, *Phys. Lett. B* **454**, 137 (1999).
- [31] A. H. Hoang and T. Teubner, *Phys. Rev. D* **60**, 114027 (1999).
- [32] B. A. Kniehl and A. A. Penin, hep-ph/9911414.
- [33] A. H. Hoang, *et al.*, hep-ph/0001286.
- [34] W. E. Caswell and G. P. Lepage, *Phys. Lett.* **167B**, 437 (1986).
- [35] G. T. Bodwin, E. Braaten, and G. P. Lepage, *Phys. Rev. D* **51**, 1125 (1995); (E) *ibid.* **55**, 5853 (1997).

- [36] A. Pineda and J. Soto, *Nucl. Phys. (Proc. Suppl.)* **64**, 428 (1998).
- [37] N. Brambilla, A. Pineda, J. Soto and A. Vairo, hep-ph/9907240.
- [38] A. Pineda and J. Soto, *Phys. Lett. B* **420**, 391 (1998); *Phys. Rev. D* **59**, 016005 (1999).
- [39] A. H. Hoang, *Phys. Rev. D* **56**, 5851 (1997).
- [40] A. Czarnecki and K. Melnikov, *Phys. Rev. Lett.* **80**, 2531 (1998);  
M. Beneke, A. Signer, and V. A. Smirnov, *Phys. Rev. Lett.* **80**, 2535 (1998).
- [41] V. B. Berestetskii, E. M. Lifshitz and L. P. Pitaevskii, “*Relativistic Quantum Theory*”  
part 1 (Pergamon, 1974).
- [42] S. N. Gupta and S. F. Radford, *Phys. Rev. D* **24**, 2309 (1981); (E) *ibid.* **25**, 3430 (1982);  
S. N. Gupta, S. F. Radford, and W. W. Repko, *Phys. Rev. D* **26**, 3305 (1982).
- [43] W. Fischler, *Nucl. Phys.* **B129**, 157 (1977);  
A. Billoire, *Phys. Lett.* **92B**, 343 (1980).
- [44] M. Peter, *Phys. Rev. Lett.* **78**, 602 (1997); *Nucl. Phys.* **B501**, 471 (1997).
- [45] Y. Schröder, *Phys. Lett. B* **447**, 321 (1999).
- [46] M. Ježabek, J. H. Kühn, M. Peter, Y. Sumino, and T. Teubner, *Phys. Rev. D* **58**, 014006  
(1998).
- [47] W. Lucha, F. F. Schöberl, and D. Gromes, *Phys. Rept.* **200**, 127 (1991).
- [48] R. Karplus and A. Klein, *Phys. Rev.* **87**, 848 (1952);  
R. Barbieri, R. Gatto, R. Kögerler, and Z. Kunszt, *Phys. Lett.* **57B**, 455 (1975);  
W. Buchmüller and S.-H. H. Tye, *Phys. Rev. D* **24**, 132 (1981).
- [49] P. Gambino and A. Sirlin, *Phys. Lett.* **B355**, 295 (1995).
- [50] B. A. Kniehl and M. Steinhauser, *Nucl. Phys.* **B454**, 485 (1995); *Phys. Lett.* **B365**, 297  
(1996).
- [51] M. Beneke and V. M. Braun, *Nucl. Phys.* **B426**, 301 (1994).
- [52] I. I. Bigi, M. A. Shifman, N. G. Uraltsev and A. I. Vainshtein, *Phys. Rev. D* **50**, 2234  
(1994).
- [53] M. Beneke, *Phys. Lett.* **B344**, 341 (1995).
- [54] M. C. Smith and S. S. Willenbrock, *Phys. Rev. D* **79**, 3825 (1997).
- [55] G. 't Hooft, in *Erice Subnucl.*, 943 (1977), (Reprinted in “*The Whys of Subnuclear  
Physics*”, ed. A. Zichichi (Plenum, 1979), and in “*Under the Spell of the Gauge Principle*”,  
ed. G. 't Hooft (World Scientific, 1994)).
- [56] A. H. Mueller, in “*QCD–20 Years Later*”, eds. P. M. Zerwas and H. A. Kastrup (World  
Scientific, 1993).

- [57] V. I. Zakharov, *Prog. Theor. Phys. Suppl.* **131**, 107 (1998).
- [58] M. Beneke, *Phys. Rept.* **317**, 1 (1999).
- [59] M. Beneke, *Phys. Lett.* **B434**, 115 (1998).
- [60] A. H. Hoang, M. C. Smith, T. Stelzer, and S. Willenbrock, *Phys. Rev. D* **59**, 114014 (1999).
- [61] A. H. Hoang, Z. Ligeti and A. V. Manohar, *Phys. Rev. Lett.* **82**, 277 (1999); *Phys. Rev. D* **59**, 074017 (1999).
- [62] I. I. Bigi, M. A. Shifman and N. G. Uraltsev, *Ann. Rev. Nucl. Part. Sci.* **47**, 591 (1997).
- [63] K. G. Chetyrkin and M. Steinhauser, hep-ph/9911434;  
K. Melnikov and T. van Ritbergen, hep-ph/9912391.
- [64] K. G. Chetyrkin and M. Steinhauser, *Phys. Rev. Lett.* **83**, 4001 (1999); hep-ph/9911434.
- [65] For the theoretical developments on heavy quark-antiquark systems in 1997–1999, see, for example,  
M. Beneke, hep-ph/9911490.
- [66] M. Jezabek, T. Nagano and Y. Sumino, to appear in PRD; hep-ph/0001322.
- [67] S. M. Barr and W. J. Marciano, in “*CP VIOLATION*”, ed. C. Jarlskog (World Scientific, 1989);  
W. Bernreuther and M. Suzuki, *Rev. Mod. Phys.* **63**, 313 (1991); (E) *ibid.* **64**, 633 (1992).
- [68] C.-P. Yuan, *Mod. Phys. Lett.* **A10**, 627 (1995);  
J. Bernabéu, G. A. González-Sprinberg, and J. Vidal, hep-ph/9505223;  
W. Bernreuther, hep-ph/9808453;  
S. Bar-Shalom and G. Eilam, hep-ph/9810234.
- [69] J. F. Donoghue, *Phys. Rev. D* **18**, 1632 (1978);  
E. P. Shabalin, *Yad. Fiz.* **28**, 151 (1978) [*Sov. J. Nucl. Phys.* **28**, 75 (1978)];  
E. P. Shabalin, *Yad. Fiz.* **31**, 1665 (1980) [*Sov. J. Nucl. Phys.* **31**, 864 (1980)];  
I. B. Khriplovich, *Yad. Fiz.* **44**, 1019 (1986) [*Sov. J. Nucl. Phys.* **44**, 659 (1986)]; *Phys. Lett.* **B173**, 193 (1986);  
C. Jarlskog, *Phys. Rev. D* **35**, 1685 (1987);  
F. Hoogeveen, *Nucl. Phys.* **B341**, 322 (1990).
- [70] A. Czarnecki and B. Krause, *Acta Phys. Polon.* **B28**, 829 (1997); *Phys. Rev. Lett.* **78**, 4339 (1997).
- [71] W. Bernreuther, T. Schröder and T. N. Pham, *Phys. Lett.* **B279**, 389 (1992).
- [72] A. Soni and R. M. Xu, *Phys. Rev. Lett.* **69**, 33 (1992).

- [73] A. Bartl, E. Christova, T. Gajdosik and W. Majerotto, *Nucl. Phys.* **B507**, 35 (1997);  
(E) *ibid.* **B531**, 653 (1998);  
A. Pilaftsis, hep-ph/9909485;  
W. Hollik, J. I. Illana, S. Rigolin, C. Schappacher, and D. Stöckinger, *Nucl. Phys.* **B551**,  
3 (1999).
- [74] M. Dugan, B. Grinstein and L. Hall, *Nucl. Phys.* **B255**, 413 (1985).
- [75] C.-S. Huang and T.-J. Li, *Z. Phys. C* **68**, 319 (1995).
- [76] C. R. Schmidt and M. E. Peskin, *Phys. Rev. Lett.* **69**, 410 (1992);  
C. R. Schmidt, *Phys. Lett.* **B293**, 111 (1992).
- [77] T. D. Lee, *Phys. Rev. D* **8**, 1226 (1973);  
S. Weinberg, *Phys. Rev. Lett.* **37**, 657 (1976); Weinberg's model is not viable [67].
- [78] S. Weinberg, *Phys. Rev. Lett.* **63**, 2333 (1989); *Phys. Rev. D* **42**, 860 (1990).
- [79] G. Boyd, A. K. Gupta, S. P. Trivedi and M. B. Wise, *Phys. Lett.* **B241**, 584 (1990).
- [80] D. Chang, W.-Y. Keung, C. S. Li and T. C. Yuan, *Phys. Lett.* **B241**, 589 (1990);  
D. Chang, T. W. Kephart, W.-Y. Keung and T. C. Yuan, *Phys. Rev. Lett.* **68**, 439  
(1992); *Nucl. Phys.* **B384**, 147 (1992).
- [81] W. Buchmüller and D. Wyler, *Phys. Lett.* **B121**, 321 (1983);  
J. Polchinski and M. B. Wise, *Phys. Lett.* **B125**, 393 (1983);  
F. del Aguila, M. B. Gavela, J. A. Grifols, and A. Méndez, *Phys. Lett.* **B126**, 71 (1983);  
(E) *ibid.* **B129**, 473 (1983);  
J. M. Gerard, W. Grimus, A. Masiero, D. V. Nanopoulos, and Amitava Raychaudhuri,  
*Nucl. Phys.* **B253**, 93 (1985);  
Y. Kizukuri and N. Oshimo, *Phys. Rev. D* **45**, 1806 (1992); *Phys. Rev. D* **46**, 3025 (1992);  
S. Bertolini and F. Vissani, *Phys. Lett.* **B324**, 164 (1994);  
W. Hollik, J. I. Illana, S. Rigolin, D. Stöckinger, *Phys. Lett.* **B425**, 322 (1998);  
R. M. Godbole, S. Pakvasa, S. D. Rindani, and X. Tata, hep-ph/9912315;  
S. A. Abel, A. Dedes, and H. K. Dreiner, hep-ph/9912429.
- [82] U. Mahanta, *Phys. Rev. D* **54**, 3377 (1996);  
W. Bernreuther, A. Brandenburg, and P. Overmann, *Phys. Lett.* **B391**, 413 (1997).
- [83] A. De Rújula, M. B. Gavela, O. Pène and F. J. Vegas, *Phys. Lett.* **B245**, 640 (1990);  
*Nucl. Phys.* **B357**, 311 (1991).
- [84] P. Haberl, O. Nachtmann and A. Wilch, *Phys. Rev. D* **53**, 4875 (1996).
- [85] K. Cheung and D. Silverman, *Phys. Rev. D* **55**, 2724 (1997).
- [86] J. L. Hewett, T. Takeuchi, and S. Thomas, hep-ph/9603391;  
J. L. Hewett, *Int. J. Mod. Phys.* **A13**, 2389 (1998).
- [87] S. Dawson and G. Valencia, *Phys. Rev. D* **53**, 1721 (1996).

- [88] OPAL Collaboration (K. Ackerstaff *et al.*), *Z. Phys. C* **74**, 413 (1997);  
L3 Collaboration (M. Acciarri *et al.*), *Phys. Lett.* **B426**, 207 (1998).
- [89] A. De Rújula, J. M. Kaplan and E. de Rafael, *Nucl. Phys.* **B35**, 365 (1971);  
K. Hagiwara, K. Hikasa and N. Kai, *Phys. Rev. D* **27**, 84 (1983);  
K. Hagiwara, R. D. Peccei, D. Zeppenfeld and K. Hikasa, *Nucl. Phys.* **B282**, 253 (1987).
- [90] J. H. Kühn, *Nucl. Phys.* **B237**, 77 (1984);  
J. H. Kühn, A. Reiter and P. M. Zerwas, *Nucl. Phys.* **B272**, 560 (1986);  
M. Jezabek and J. H. Kühn, *Nucl. Phys.* **B320**, 20 (1989);  
C. A. Nelson, *Phys. Rev. D* **41**, 2805 (1990);  
A. Czarnecki, M. Jezabek and J. H. Kühn, *Nucl. Phys.* **B351**, 70 (1991);  
C.-P. Yuan, *Phys. Rev. D* **45**, 782 (1992);  
R. H. Dalitz and G. R. Goldstein, *Phys. Rev. D* **45**, 1531 (1992);  
T. Arens and L. M. Sehgal, *Nucl. Phys.* **B393**, 46 (1993); *Phys. Lett.* **B302**, 501 (1993);  
*Phys. Rev. D* **50**, 4372 (1994);  
E. Christova and D. Draganov, *Phys. Lett.* **B434**, 373 (1998).
- [91] D. Atwood and A. Soni, *Phys. Rev. D* **45**, 2405 (1992).
- [92] M. S. Baek, S. Y. Choi and C. S. Kim, *Phys. Rev. D* **56**, 6835 (1997).
- [93] D. Chang, W.-Y. Keung, I. Phillips, *Nucl. Phys.* **B408**, 286 (1993); (E) *ibid.* **B429**, 255 (1994).
- [94] D. Chang, W.-Y. Keung, I. Phillips, *Phys. Rev. D* **48**, 3225 (1993);  
A. Pilaftsis and M. Nowakowski, *Int. J. Mod. Phys.* **A9**, 1097 (1994); (E) *ibid.* **A9**, 5849 (1994).
- [95] G. A. Ladinsky and C.-P. Yuan, *Phys. Rev. D* **49**, 4415 (1994).
- [96] F. Cuypers and S. D. Rindani, *Phys. Lett.* **B343**, 333 (1995).
- [97] P. Poulouze and S. D. Rindani, *Phys. Lett.* **B349**, 379 (1995); *Phys. Rev. D* **54**, 4326 (1996); *Phys. Lett.* **B383**, 212 (1996).
- [98] C. R. Schmidt, *Phys. Rev. D* **54**, 3250 (1996).
- [99] W. Bernreuther, A. Brandenburg and P. Overmann, hep-ph/9602273.
- [100] H. Anlauf, W. Bernreuther, and A. Brandenburg, *Phys. Rev. D* **52**, 3803 (1995); (E) *ibid.* **53**, 1725 (1996);  
S. Y. Choi and K. Hagiwara, *Phys. Lett.* **B359**, 369 (1995);  
P. Poulouze and S. D. Rindani, *Phys. Rev. D* **57**, 5444 (1998); *Phys. Lett.* **B452**, 347 (1999).
- [101] T. G. Rizzo, hep-ph/9610373.
- [102] S. D. Rindani and M. M. Tung, *Phys. Lett.* **B424**, 125 (1998); *Eur. Phys. J.* **C11**, 485 (1999).
- [103] D. Atwood, A. Aeppli and A. Soni, *Phys. Rev. Lett.* **69**, 2754 (1992).



- [104] S. Y. Choi, C. S. Kim and Jake Lee, *Phys. Lett. B* **415**, 67 (1997).
- [105] E. L. Berger and J. Qiu, *Phys. Rev. D* **40**, 778 (1989).
- [106] K. Cheung, *Phys. Rev. D* **53**, 3604 (1996); *Phys. Rev. D* **55**, 4430 (1997).
- [107] T. G. Rizzo, *Phys. Rev. D* **53**, 6218 (1996).
- [108] W. Bernreuther and A. Brandenburg, *Phys. Lett.* **B314**, 104 (1993); *Phys. Rev. D* **49**, 4481 (1994);  
W. Bernreuther, A. Brandenburg and M. Flesch, hep-ph/9812387.
- [109] J. P. Ma and A. Brandenburg, *Z. Phys. C* **56**, 97 (1992);  
G. L. Kane, G. A. Ladinsky and C.-P. Yuan, *Phys. Rev. D* **45**, 124 (1992);  
D. Atwood, S. Bar-Shalom, G. Eilam and A. Soni, *Phys. Rev. D* **54**, 5412 (1996).
- [110] B. Grz̧dkowski and J. F. Gunion, *Phys. Lett.* **B287**, 237 (1992).
- [111] B. Grz̧dkowski and W.-Y. Keung, *Phys. Lett.* **B316**, 137 (1993); *Phys. Lett.* **B319**, 526 (1993).
- [112] D. Atwood, G. Eilam, A. Soni, R. R. Mendel and R. Migneron, *Phys. Rev. Lett.* **70**, 1364 (1993);  
D. Atwood, G. Eilam and A. Soni, *Phys. Rev. Lett.* **71**, 492 (1993).
- [113] R. Frey, hep-ph/9606201;  
R. Frey *et al.*, hep-ph/9704243.
- [114] E. Christova, *Int. J. Mod. Phys.* **A14**, 1 (1999).
- [115] W. Bernreuther, O. Nachtmann, P. Overmann and T. Schröder, *Nucl. Phys.* **388**, 53 (1992); (E) *ibid.* **406**, 516 (1993).
- [116] B. Grz̧dkowski and Z. Hioki, *Nucl. Phys.* **B484**, 17 (1997); *Phys. Lett.* **B391**, 172 (1997); hep-ph/9805318;  
L. Brzezinski, B. Grz̧dkowski, and Z. Hioki, *Int. J. Mod. Phys.* **A14**, 126 (1999).
- [117] A. Bartl, E. Christova, T. Gajdosik and W. Majerotto, *Phys. Rev. D* **58**, 074007 (1998).
- [118] W. Bernreuther and P. Overmann, *Z. Phys. C* **61**, 599 (1994); *ibid.* **72**, 461 (1996).
- [119] B. Grz̧dkowski, *Phys. Lett.* **B305**, 384 (1993);  
A. Bartl, E. Christova and W. Majerotto, *Nucl. Phys.* **B460**, 235 (1996); (E) *ibid.* **B465**, 365 (1996);  
A. Bartl, E. Christova, T. Gajdosik and W. Majerotto, *Phys. Rev. D* **59**, 077503 (1999).
- [120] A. Brandenburg and J. P. Ma, *Phys. Lett.* **B298**, 211 (1993).
- [121] A. Pilaftsis, *Z. Phys. C* **47**, 95 (1990);  
W. Bernreuther, J. P. Ma and T. Schröder, *Phys. Lett.* **B297**, 318 (1992);  
W. Bernreuther, J. P. Ma and B. H. J. McKellar, *Phys. Rev. D* **51**, 2475 (1995);  
G. Eilam, J. L. Hewett and A. Soni, *Phys. Rev. Lett.* **67**, 1979 (1991); *Phys. Rev.*

- Lett.* **68**, 2102ff (1992);  
R. Cruz, B. Grzadkowski and J. F. Gunion, *Phys. Lett.* **B289**, 440 (1992);  
B. Grzadkowski, *Phys. Lett.* **B338**, 71 (1994);  
D. Chang and W.-Y. Keung, *Phys. Lett.* **B305**, 261 (1993);  
J. L. Diaz-Cruz and G. Lopez Castro, *Phys. Lett.* **B301**, 405 (1993);  
A. Ilakovac, B. A. Kniehl and A. Pilaftsis, *Phys. Lett.* **B320**, 329 (1994);  
E. Christova and M. Fabbrichesi, *Phys. Lett.* **B315**, 113 (1993); *ibid.* **B315**, 338 (1993);  
*ibid.* **B320**, 299 (1994). J. M. Yang and B.-L. Young, *Phys. Rev. D* **56**, 5907 (1997).
- [122] W. Bernreuther and O. Nachtmann, *Phys. Rev. Lett.* **63**, 2787 (1989); (E) *ibid.* **64**, 1072 (1990).
- [123] W. Bernreuther, U. Löw, J. P. Ma and O. Nachtmann, *Z. Phys. C* **43**, 117 (1989).
- [124] F. Hoogeveen and L. Stodolsky, *Phys. Lett.* **212B**, 505 (1988);  
J. F. Donoghue and G. Valencia, *Phys. Rev. Lett.* **58**, 451 (1987); (E) *ibid.* **60**, 243 (1988);  
G. Valencia and A. Soni, *Phys. Lett.* **B263**, 517 (1991);  
A. Aeppli and A. Soni, *Phys. Rev. D* **46**, 315 (1992);  
W. Bernreuther, U. Löw, J. P. Ma and O. Nachtmann, *Z. Phys. C* **41**, 143 (1988);  
W. Bernreuther and O. Nachtmann, *Phys. Lett.* **B268**, 424 (1991);  
J. Körner, J. P. Ma, R. Münch, O. Nachtmann and R. Schöpf, *Z. Phys. C* **49**, 447 (1991);  
A. Brandenburg, J. P. Ma, R. Münch and O. Nachtmann *Z. Phys. C* **51**, 225 (1991);  
W. Bernreuther, G. W. Botz, O. Nachtmann and P. Overmann, *Z. Phys. C* **52**, 567 (1991);  
A. Brandenburg, J. P. Ma and O. Nachtmann, *Z. Phys. C* **55**, 115 (1992);  
C. J.-C. Im, G. L. Kane and P. J. Malde, *Phys. Lett.* **B317**, 454 (1993);  
J. Liu, *Phys. Rev. D* **47**, R1741 (1993);
- [125] K. Ikematsu, talk given at the 2nd ACFA Workshop (Seoul, 5 Nov 1999).
- [126] J. J. Sakurai, *Invariance Principles and Elementary Particles* (Princeton Univ. Press, 1964);  
J. D. Bjorken and S. D. Drell, *Relativistic Quantum Mechanics* (McGraw-Hill, 1964);  
*Relativistic Quantum Fields* (McGraw-Hill, 1965);  
K. Hikasa, unpublished;  
M. E. Peskin and D. V. Schroeder, *An Introduction to Quantum Field Theory* (Addison-Wesley, 1995).